UNIVERSIDAD DE CÓRDOBA

DEPARTAMENTO DE BIOQUÍMICA Y BIOLOGÍA MOLECULAR

DIVERSITY OF REGULATORY MECHANISMS IN THE C/N METABOLISMS OF THE MARINE CYANOBACTERIA *PROCHLOROCOCCUS* AND *SYNECHOCOCCUS*

Mª Agustina Domínguez Martín

Diciembre 2014

TITULO: *Diversity of regulatory mechanisms in the C/N metabolism of the marine cyanobacteria Prochlorococcus and synechococcus*

AUTOR: *Maria Agustina Domínguez Martín*

Campus de Rabanales
Ctra. Nacional IV, Km. 396 A
14071 Córdoba

www.uco.es/publicaciones
publicaciones@uco.es

DIVERSITY OF REGULATORY MECHANISMS IN THE C/N METABOLISMS OF THE MARINE CYANOBACTERIA *PROCHLOROCOCCUS* AND *SYNECHOCOCCUS*

Trabajo realizado en el departamento de Bioquímica y Biología Molecular de la Universidad de Córdoba, para optar al grado de Doctor en Bioquímica y por la licenciada

María Agustina Domínguez Martín

DIRECTORES

JESÚS DÍEZ DAPENA

Dr. en Ciencias Biológicas y Catedrático del Departamento de Bioquímica y Biología Molecular de la Universidad de Córdoba

JOSÉ MANUEL GARCÍA FERNÁNDEZ

Dr. en Ciencias Biológicas y Profesor titular del Departamento de Bioquímica y Biología Molecular de la Universidad de Córdoba

Córdoba, Diciembre de 2014

Abstract

Marine picocyanobacteria are the most abundant photosynthetic organisms on Earth, with only two genera, *Prochlorococcus* (Johnson *et al.*, 2006, Olson *et al.*, 1990, Partensky *et al.*, 1999) and *Synechococcus* (Scanlan, 2003, Scanlan & West, 2002) numerically dominating most oceanic waters. During this research project our main goal was to study the diversity of the regulatory mechanisms in the C/N metabolism of these cyanobacteria. Recent advances in the knowledge of nitrogen metabolism of *Prochlorococcus* have shown that it has fine regulatory systems to optimize nitrogen assimilation (Rocap *et al.*, 2003, García-Fernández *et al.*, 2004, Lindell *et al.*, 2002). Thus, we have studied the role of 2-oxoglutarate in the control of the C/N balance in order to check whether there exist differences with respect to other model cyanobacteria and among strains of *Prochlorococcus*. The comparative study performed show that 2-oxoglutarate is the molecule responsible in *Prochlorococcus* to control the balance between carbon and nitrogen metabolism and there are differences among strains in sensing this metabolite. These results could be an explanation for its adaptation to different ecological niches in the ocean. Besides, we wanted to know how *Synechococcus* is able to successfully coexist with *Prochlorococcus*. For that, the hypothesis was that *Synechococcus* could be more efficient at the utilization of low concentration of nitrate. The results showed that when concentrations of nitrate in the range of nanomolar are present, the genes related with the assimilation of that source are up-regulated in *Synechococcus* WH7803. Therefore, these facts suggest that the machinery is working at transcriptional level in order to uptake the nitrate. This could be an evolutionary advantage against *Prochlorococcus* in the real field.

Resumen

Las picocianobacterias marinas son los organismos fotosintéticos más abundantes en la Tierra, con sólo dos géneros, *Prochlorococcus* (Johnson *et al.*, 2006, Olson *et al.*, 1990, Partensky *et al.*, 1999) y *Synechococcus* (Scanlan, 2003, Scanlan & West, 2002) dominando la mayor parte de los océanos. El principal objetivo durante este proyecto de investigación ha sido estudiar la diversidad de mecanismos regulatorios del metabolismo del C/N en estas cianobacterias. Recientes avances en la regulación del metabolismo del nitrógeno en *Prochlorococcus* muestran que tienen una fina regulación para optimizar la asimilación del nitrógeno (Rocap *et al.*, 2003, García-Fernández & Diez, 2004, Lindell *et al.*, 2002). Por lo tanto, hemos estudiado el papel del 2-oxoglutarato en el control del balance C/N con el fin de comprobar si existen diferencias con respecto a otras cianobacterias modelos, e incluso si estas diferencias se encuentran entre estirpes. Lo resultados obtenidos del estudio comparativo mostraron que el 2-oxoglutarato es la molécula responsable del control del balance C/N en *Prochlorococcus* y que existen diferencias entre estirpes en la detección de este metabolito. Esto pueden ser una explicación de la adaptación a diferentes nichos ecológicos en el océano. Además, nosotros queríamos responder a la pregunta de cómo *Synechococcus* es capaz de coexistir con éxito con *Prochlorococcus*. Para ello, la hipótesis era que *Synechococcus* puede ser más eficaz en la utilización de concentraciones bajas de nitrato. Los resultados mostraron que cuando hay concentraciones de nitrato en el rango de nanomolar, se sobreexpresan los genes relacionados con la asimilación de esta fuente en *Synechococcus* WH7803. Estos hechos sugieren que hay una regulación a nivel transcripcional con el objetivo de absorber el nitrato a concentraciones bajas. Esto podría ser una ventaja evolutiva respecto a *Prochlorococcus* en los ecosistemas donde conviven.

“Far from being tedious, studying this extraordinary little cell is like opening a present every day. It is a gift, and a responsibility ”

Sallie W. Chisholm,

Unveiling *Prochlorococcus*, 2011

“There is, one knows not what sweet mystery about the sea, whose gentle awful stirrings seem to speak of some hidden soul beneath”

Herman Melville

A mis padres

A mi hermano

TABLES OF CONTENTS

Introduction

1. **The role of 2-OG in the control of C/N balance in *Prochlorococcus marinus***
   1.1 The effect of key nutrients absence on the level of 2-OG
   1.2 The effect of nitrogen assimilation inhibitors on the level of 2-OG

2. **Effect of azaserine addition on the metabolism of *Prochlorococcus* SS120, MIT9313 and PCC 9511**
   2.1 Changes on key enzymes
   2.2 Changes on the expression of genes related to nitrogen metabolism
   2.3 Changes on the proteome of *Prochlorococcus* SS120

3**. Study of the interaction NtcA-*glnA* promoter of *Prochlorococcus* SS120 and MIT9313**
   3.1 Purification of heterologous regulatory proteins from *Prochlorococcus* SS120 and MIT9313

Summary of figures

Summary of tables

Summary of Supplemantary data

Supplementary Table S1: Proteins up-regulated

Supplementary Table S2: Proteins down-regulated

Supplementary Table S3: Proteins from the extract of NtcA MIT9313 and possible candidates for protein-protein interactions

Supplementary Table S4: Absolute quantification (electronic format)

Supplementary Figure S1: Supplementary data for proteomics approach

INTRODUCTION

1. THE MARINE ECOSYSTEM

The ocean covers 71 % of the surface of the Earth and contains 97 % of the water of the planet, the total volume is 1.3 billion Km^3 (1.3 sextillion L) and sea surface plus seabed over 354 million Km^2 (Costello *et al.*, 2010). Most of the ocean is cold, dark and deep, although it is important to realize that there are some zones containing an abundance of ocean life because sunlight is available for photosynthesis. This process occurs only down to about 100 or 200 m and sunlight disappears around 1,000 m while the ocean descends to a maximum depth of 11,000 m (Mariana Trench).

1.1 Geophysics structure of the ocean

The oceans are divided into two broad realms, the pelagic and the benthic zone (figure 1). Pelagic refers to the open water in which swimming and floating organisms live. Organisms living there are called the pelagos. Pelagic ecosystems support a significant and vital component of the productivity and biodiversity of the ocean (Grantham et al., 2011). The pelagic zone is divided into neritic zone (the nearest to the coast) and oceanic zone. Likewise, the oceanic zone is divided into: epipelagic, less than 200 meters depth, where there can be photosynthesis; mesopelagic: 200-1,000 meters, the "twilight" zone with faint sunlight but no photosynthesis; bathypelagic: 1,000-4,000 meters; abyssopelagic: 4,000-6,000 meters and hadopelagic: the deep trenches below 6,000 meters to about 11,000. The last three zones have no sunlight at all.

Benthic zones are defined as the bottom sediments of water such as an ocean or a lake. Organisms living in this zone are called *benthos*. They live in a close relationship with the bottom of the sea, with many of them permanently attached to it, some burrowed in it, others swimming just above it. In oceanic environments, benthic habitats are zoned by depth, generally corresponding to the comparable pelagic zones: intertidial: where sea meets land, with no pelagic equivalent; subtidal: the continental shelves, to about 200 m; bathyal: generally the continental slopes to 4,000 m; abyssal: most of the deep ocean seafloor, 4,000 - 6,000 m and hadal: the deep trenches 6,000 to 11,000 m.

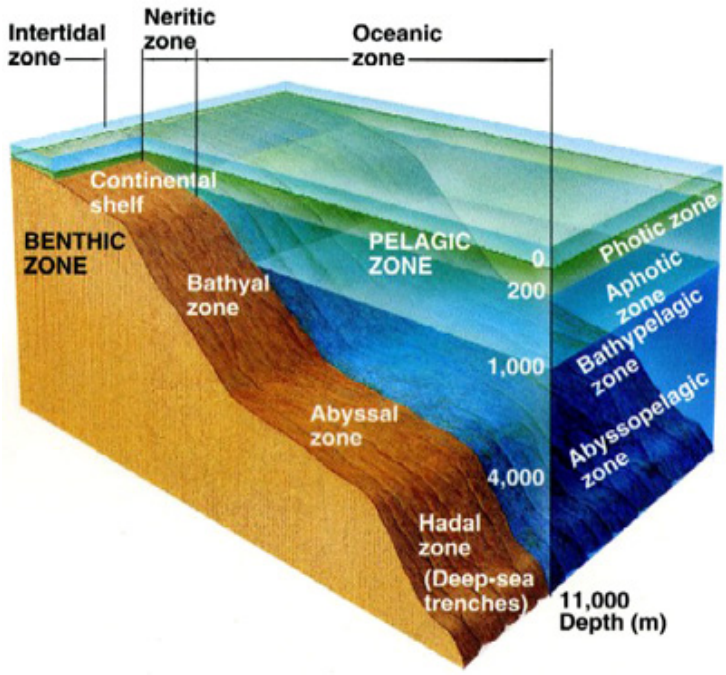

Figure 1: Divisions of the marine environment. Obtained from www.faculty.scf.edu.

The state of oceans depends on temperature (warm on the upper ocean, cold in the deeper ocean), salinity (variations determined by evaporation, precipitation, sea-ice formation and melt, and river runoff) and density (small in the upper ocean, large in the deeper ocean).

1.2 The ocean and the temperature

From the knowledge of the temperature profiles in global ocean basins, it is convenient to divide the oceanic column into three regions:

1. Surface layer (SL): It is the portion of the ocean column, which experiences seasonal changes in response to the exchange of energy with the atmosphere and the absorption of solar radiation. Usually SL is 10-200 m thick layer except in winters. Stirring of surface waters by the wind produces a well-mixed layer of uniform or nearly uniform density, for this reason, the ocean surface is called the mixed layer. Constant salinity and temperature is usually found.

2. Thermocline (pycnocline): this region is below the mixed layer and extends approximately down to a depth of 1000 m where temperatures are in the range

of 2 - 4 ºC. It is the region where most rapid decrease in temperature (density) occurs with depth. The thermocline region is strongly stable.

3. Deep water (DW) layer: is below the permanent thermocline and there is a gradual decrease in temperature and salinity with depth. Deep waters are found below a depth of 1000-2000 meters. Deep-water temperatures are below 4 ºC. This layer is cold, salty and with high nutrients concentration.

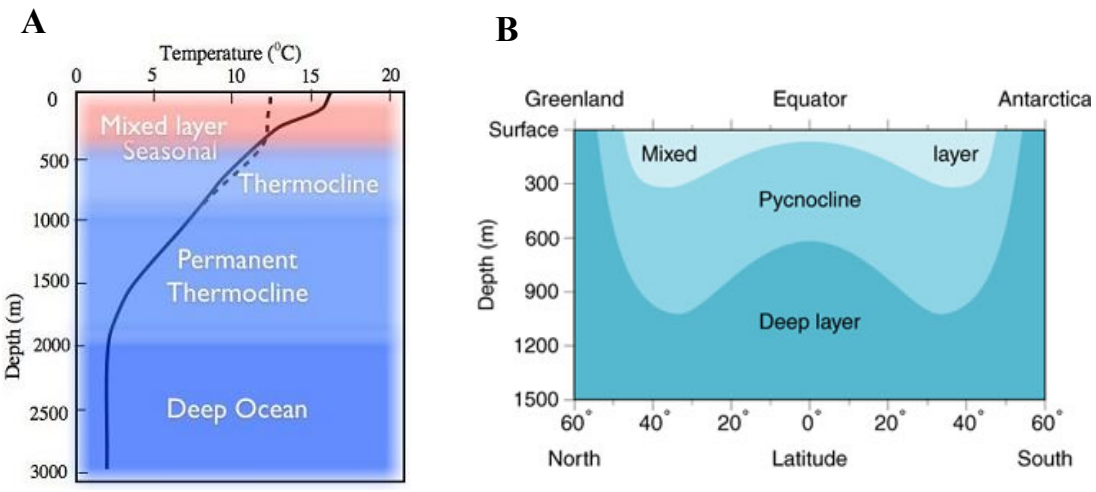

Figure 2: A. Vertical profile of the different layers respect to the temperature. **B. Cross-sectional longitudinal profile of the Atlantic Ocean** from 60 degrees N to 60 degrees S showing the location of the mixed layer, pycnocline, and deep layer. Adapted from *DataStreme Ocean.*

1.3 The ocean and the light

Sunlight in the ocean is important for many reasons: it heats sea water, warming the surface layers; it provides energy required by phytoplankton; it is used for navigation by animals near the surface; and reflected subsurface light is used for mapping chlorophyll concentration from space. Because light travels slower in water than in air, some light is reflected at the sea surface, ca. 2%. Hence most sunlight reaching the sea surface is transmitted into the sea. Blue light is absorbed least and red light is absorbed most strongly (Stewart, 2008).

Two zones can be distinguished in oceans respect to the light:

1. The **photic zone, euphotic zone** or **sunlight zone** is the region of the well-lit upper ocean that sustains the net production of organic matter. Often defined by the depth of penetration of sunlight, typically the depth to which 1% of the light intensity that is observed at the surface ocean penetrates. In clear, open ocean ecosystems, the euphotic zone can extend to 200 m (Karl & Church, 2014). The zone that extends from the base of the euphotic zone to about 200 m is sometimes called the disphotic zone. While there is some light, it is insufficient for photosynthesis.
2. The **aphotic zone** is the portion of the ocean where there is little or no sunlight. It is formally defined as the depths beyond which less than 1% of sunlight penetrates. Consequently, bioluminescence is essentially the only light found in this zone.

Water absorbs certain wavelengths of visible light. The long wavelengths of the light spectrum (red, yellow and orange) can penetrate to approximately 15, 30 and 50 meters respectively, while the short wavelengths of the light spectrum (violet, blue and green) can penetrate further, to the lower limits of the euphotic zone, blue penetrates the deepest (figure 3).

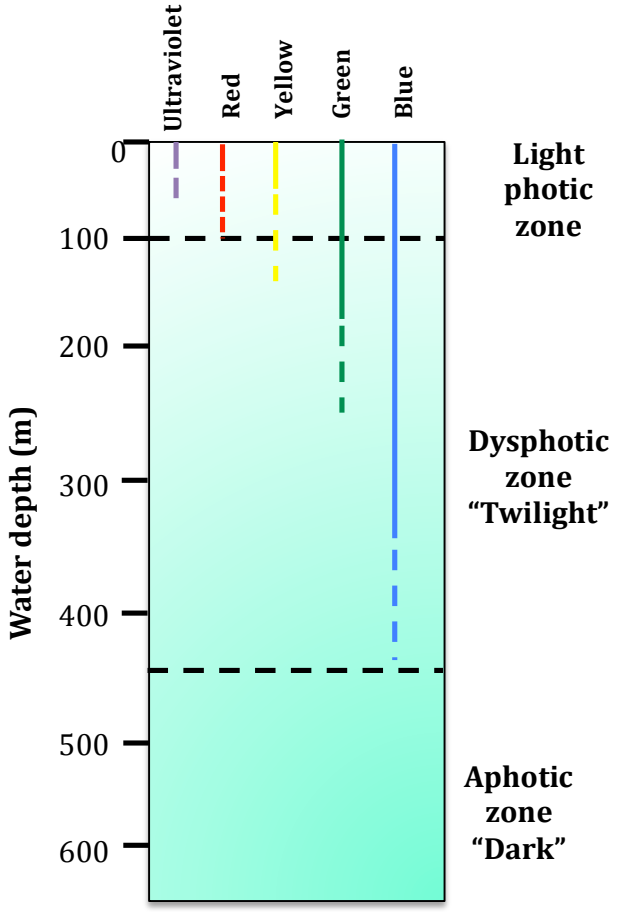

Figure 3: Light zones through the column water. Diagram offers a basic illustration of the depth at which different colours of light penetrate into the ocean waters. Adapted from www.alex.state.al.us.

1.4. Oceanic distribution of the nutrients

Biological and physical processes move nutrients in the oceans. In the euphotic zone of the open oceans, nutrients are utilized by phytoplankton and cyanobacteria. Respiration and the decomposition of marine organisms cause nutrients to be released back into the seawater, mostly in the deep waters. As a result, nutrient concentrations are generally low near surface but high in deeper waters, except in Polar Regions where intensive upwelling brings cold, nutrient-rich seawater back to the surface.

The key nutrients for the development of marine plankton are carbon (C), nitrogen (N), phosphorus (P) and iron (Fe), although the concentration of each element is different. More than half a century ago, Redfield recognized that the dissolved nutrient ratios in the deep sea corresponded remarkably to the ratios of particulate organic matter in surface waters (Redfield, 1934). He attributed this correlation to the

fact that organic matter (phytoplankton biomass) is produced, on average, in a ratio that is determined by biochemical needs, and that his material is subsequently remineralized in the deep ocean, releasing inorganic nutrients in the same proportions (Sohm *et al.*, 2011). This ratio is 106 C:16 N:1 P, and it links three major biogeochemical cycles through the activities of marine phytoplankton (Arrigo, 2005). But different results show that the canonical Redfield N:P ratio of 16 is not a universal biochemical optimum, but instead represents an average of species-specific N:P ratios (Klausmeier *et al.*, 2004, Arrigo, 2005).

It is difficult to imagine life without nitrogen and carbon. Carbon and nitrogen offer remarkable contrasts with regard to both their abundances and distribution. Carbon resides primarily in the lithosphere with less than 0.05% being cycled through the biosphere, hydrosphere and atmosphere. The quantity of carbon on the oceans is approximately 38,400 Gt. The concentration of total dissolved inorganic carbon in the ocean increases markedly under 300 m. Biological processes also contribute to the absorption of atmospheric CO_2 in the ocean. In addition, several phytoplankton and zooplankton species form $CaCO_3$ shells that sink into the interior of the ocean, where some fraction dissolves (Falkowski & Scholes, 2000).

Nitrogen is generally accepted as the most common nutrient limiting primary production for phytoplankton throughout much of the world´s upper ocean. Nitrogen occurs in a variety of inorganic and organic forms (Table 1). The largest reservoir of nitrogen in the sea is dissolved dinitrogen gas (N_2), which occurs in concentrations of about 1 mM (Capone, 2000).

Table 1: Primary pools and concentrations of nitrogen in the ocean (Capone, 2000)

Form	Oceanic concentrations (µM)	Coastal concentrations (µM)	Global marine pools (Pg)
GASEOUS			
Dinitrogen (N_2)	900-1100	900-1100	22-23 x 10^3
Nitrous oxide (N_2O)	0.006-0.07	0-0.25	0.2-0.8
Nitric oxide (NO)	?	?	?
INORGANIC			
Nitrate (NO_3^-)	<0.03 - >40	<0.1-200	570-677
Nitrite (NO_2^-)	<0.03-0.1	<0.03-10	?
Ammonium (NH_4^+)	<0.03-1	<0.03->100	7-8
ORGANIC			
Dissolved organic (DON)	3-7	3-20	63-530
Particulate organic (PON)	0.07-0.5	0.1-30	3-24
Amino acids	0.15-1.5	0.12-6.6	

Most microorganisms can use inorganic nitrogen in the form of nitrate, nitrite and ammonium (DIN= dissolved inorganic nitrogen). Particularly in the oligotrophic open ocean gyres, low concentration of these compounds (<0.03 µM to 0.1) can limit the rate of productivity in the surface layer (0-200 m depth) (Capone, 2000). But nitrogen can regulate productivity even in coastal upwelling regions (Kudela & Dugdale, 2000). Anyway, there are large geographical variations in the sources and fluxes of nitrate and ammonium (Zehr & Ward, 2002). The dissolved organic nitrogen (DON) can be a large pool in the oceans (3 to 7 µm) (Capone, 2000) and even larger in coastal waters (Sharp, 1983). DON is also important, which are amino acids (free or oligopeptides), urea and other heterotrophic compounds (Zehr & Ward, 2002).

Nitrogen has a complex cycle (figure 4), it is composed of multiple transformations of nitrogenous compounds, catalysed primarily by microbes. The nitrogen cycle controls the availability of nitrogenous nutrients and biological productivity in marine systems (Ryther & Dunstan, 1971) and thus is linked to the fixation of atmospheric CO_2 and export of carbon from the ocean´s surface (Falkowski *et al.*, 1998).

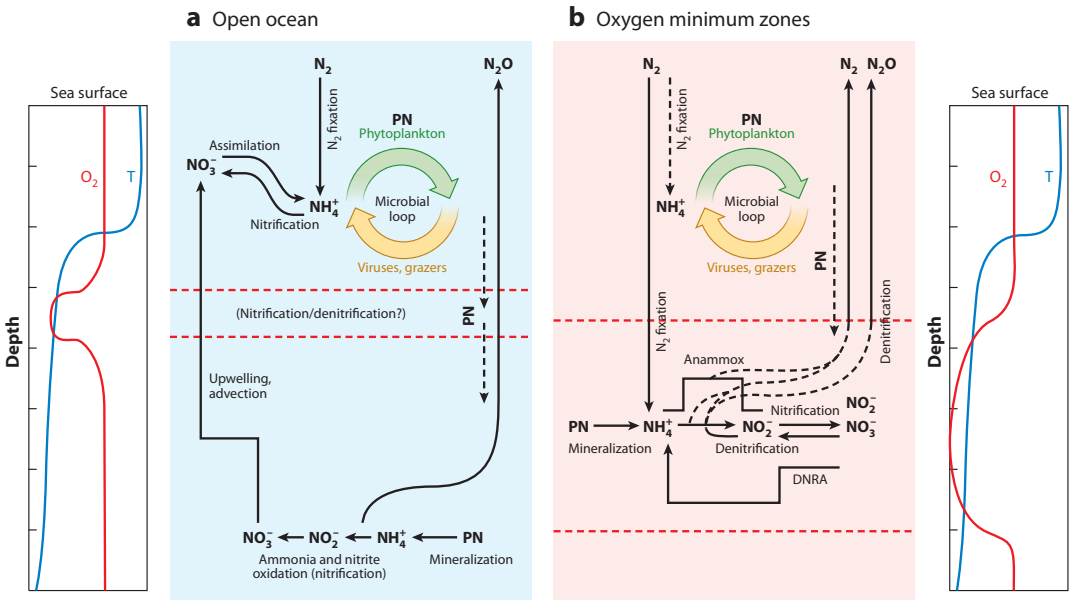

Figure 4: Conceptual diagram highlighting and comparing the major nitrogen-cycle components in (a) the typical oceanic water column and in (b) OMS (oxygen minimum zones). DNRA: dissimilatory nitrate reduction to ammonia, PN: particulate nitrogen. (Zehr & Kudela, 2011).

Phytoplankton (eukaryotes and cyanobacteria) in general prefers ammonium to nitrate, presumably due to the additional energy and reductant necessary to reduce nitrate to ammonium (García-Fernández & Diez, 2004, Luque & Forchhammer, 2008, Flores & Herrero, 2005, García-Fernández *et al.*, 2004).

Nitrate assimilation was assumed universal by photosynthetic picoplankton and now it is known absent in many, likewise it was ignored in heterotrophic bacteria and now it is recognized that they perform nitrate assimilation (Zehr & Ward, 2002). Bacteria can take up DIN while simultaneously liberating ammonium in decomposition. Thus, bacteria in the ocean can be competing for ammonium, regenerating ammonium or both.

N_2 fixation is an integral component of the global nitrogen cycle, providing the link between the largest reservoir of nitrogen on earth, gaseous N_2, and the pool of biochemically fixed nitrogen (Capone, 2008). Microbial N_2 fixation in the ocean is globally important for the inputs of the new nitrogen to surface waters, it controls the export of organic matter to the deep ocean in many regions, a process commonly referred to as the "biological pump" (Longhurst & Harrison, 1989, Sohm *et al.*, 2011).

N_2 fixation is carried out by several types of diazotrophs. *Trichodesmium* spp. is a marine cyanobacterium able to fix N_2 and take up combined nitrogen (ammonium, nitrate) simultaneously (Mulholland & Capone, 2000). The occurrence of N_2 fixation and the diversity of diazotroph species in the < 10 μm plankton fraction was only recognized about a decade ago (Zehr *et al.*, 2001). These unicellular diazotrophs are divided into three groups: *Crocosphaera watsonii* (Webb et al., 2009), UCYN-A an uncultured cyanobacterium (Zehr *et al.*, 2001) and often the more abundant of the unicellular diazotrophs in oligotrophic waters and UCYN-C (Sohm *et al.*, 2011). The amount of marine N_2 fixation was small compared with overall phytoplankton nitrogen demand (Mulholland & Capone, 2000).

The availability of fixed inorganic nitrogen (nitrate, nitrite and ammonium) limits primary productivity in many ocean regions. Denitrification by heterotrophic bacteria is believed to be the only important sink for fixed inorganic nitrogen in the ocean. *Anammox* bacteria, in anaerobic conditions oxidize ammonium with nitrite to N_2 in the black sea (figure 4,b). *Annamox* is important in the oceanic nitrogen cycle (Kuypers *et al.*, 2003, Kuypers *et al.*, 2005, Hu *et al.*, 2011, Lamp & Kuypers, 2011).

It is important to point that there are large geographical variations in the sources and fluxes of nitrate and ammonium (Zehr & Ward, 2002). For instance, the oligotrophic waters of the subtropical gyres cover > 60% of the total ocean surface and contribute > 30% of the global marine carbon fixation, there NO_3^- was undetectable (< 0.05 μM) in the upper 70 to 80 m of the water column (Marañón *et al.*, 2003). On the other hand, NO_2 is an intermediate redox position between ammonium and nitrate, it is an useful indicator of the equilibrium state of the oxidative and reductive pathways of the marine nitrogen cycle because it is derived from the reduction of nitrate during assimilation of phytoplankton. In the upper 200 m of the water column the NO_2^- concentration was between 0.1 nM and 2 nM. Into deep waters, 2 peaks with different concentration of nitrite were found, one associated with the nitracline which concentration was 60-200 nM and the other at 200 m with 10-25 nM of NO_2 (Dore & Karl, 1996).

It has been described in detail that nitrogen is the most often limiting nutrient although it is now recognized large areas of the ocean that are iron and phosphorus limited (Martin, 1992, Sohm *et al.*, 2011). In oligotrophic regions at the upper mixed

layer the concentration of phosphate is 0.01-0.02 μM and the average of phosphorus in the North Pacific subtropical gyre is 50 nM (Bjorkman *et al.*, 2000). Iron in the open ocean derives from the deposition of dust from adjacent desert areas, the oceans in the Northern hemisphere receive greater dust inputs than the southern oceans (table 2) (Sohm *et al.*, 2011). The average of iron concentrations at the upper mixed layer was > 0.6 nM (Marañón *et al.*, 2003). Marine phytoplankton are generally thought to be nitrogen limited through much of the tropical and subtropical oceans, whereas diazotrophs by definition are not. This suggests that other nutrients control diazotrophs in the ocean, the most likely candidates being iron and phosphorus.

Table 2: Iron and phosphorus concentration at different oceans (Sohm *et al.*, 2011)

Location	Dust deposition	Fe (nM)	DIP (nM)
North Atlantic Ocean	Very high	0.2-1.2	0.2-5
South Atlantic Ocean	Very low	0.1-0.4	Ca. 200
North Pacific Ocean	Low	0.1-0.3	10-100
South Pacific Ocean	Very low	0.1-0.2	110-240
Arabian Sea	High	0.5-1	BD-1,000
Mediterranean Sea	High	0.2-1.2	BD-70
Baltic Sea	Low	3-7	BD-800

BD: below detectable limits; DIP: dissolved inorganic phosphorus.

1.5 Marine microorganisms

Marine microbes are capable of flourishing in all oceanic habitats, from several kilometers below the seafloor to the top of the ocean surface. They thrive in environmental conditions where other organisms cannot, ranging from super cooled brine channels of Arctic ice floes to near-boiling waters of hydrothermal vents. Consequently, marine microbes are the most numerous group of organisms on the planet. In addition to being abundant, the many different types of marine microbes carry out many different types of metabolism. As a consequence of this diversity, marine microbes are involved in virtually all geochemical reactions occurring in the oceans (table 3).

Microbes or microorganisms include all the organisms smaller than about 100 μm, which can be seen only with a microscope. These organisms include bacteria, archaea, and protists (single cell eukaryotes).

Table 3: Functional groups of microbes in the oceans (Kirchman, 2008)

Functional group	Function	Type of microbe
Primary producers	Fix CO_2 to produce organic material using light energy	Eukaryotes and cyanobacteria
Photoheterotrophs	Use organic material, aided by light energy	Cyanobacteria and other bacteria
Heterotrophic prokaryotes	Mineralize and oxidize dissolved organic matter (DOM) to produce biomass and inorganic byproducts	Bacteria and archaea
Grazers	Control prey populations and release dissolved material	Eukaryotes
Viruses	Control prey populations, release dissolved material, and mediate genetic exchange	Not applicable
N_2 fixers (diazotrophs)	Reduce N_2 to ammonium	Cyanobacteria
Nitrifiers	Oxidization of ammonium to nitrate	Bacteria and archaea
Denitrifiers	Release of N_2 or N_2O during oxidation of ammonium or reduction of nitrate	Bacteria and archaea

1.5.1 Response of ocean phytoplankton community structure to climate change

The oceans have an important role in the climate change, as they are a major sink for carbon dioxide: marine life consumes CO_2 to transform it into organic material through photosynthesis. Therefore, the abundance of phytoplankton in the ocean renders it an important organic sink of CO_2. Ubiquitous phytoplankton communities in the ocean are responsible for nearly half of the planetary photosynthesis (Goericke, 2011). Much of the marine life crucially depends on phytoplankton, which receives nutrients from deeper layers of the ocean.

The climate change promotes variations in nutrients and light, that situation have a stronger impact on small phytoplankton than on diatom growth rate (Marinov *et al.*, 2010). Another study showed an increment in cell numbers of example of 29% and 14% for *Prochlorococcus* and *Synechococcus*, respectively due to the concentration of greenhouse gases at the end of the 21st century. Thus, that suggested that oceanic microbial communities will experience complex changes as a result of projected future climate conditions (Flombaum *et al.*, 2013).

2. CYANOBACTERIA

The oxygenic photoautotrophic prokaryotes, cyanobacteria, are one of the main lineages of the domain *Bacteria* (Giovannoni & Rappé, 2000, Rippka *et al.*, 1979, Rippka, 1972, Pelroy *et al.*, 1972, Waterbury & Rippka, 1989, Stanier & Cohen-Bazire, 1977, Stanier, 1977).

The role of cyanobacteria in the original oxygenation of the atmosphere about $2.4x10^9$ billion years ago is generally accepted (Capone, 2001, Falkowski & Knoll, 2007). Nowadays, marine cyanobacteria still play important roles, especially in tropical ecosystems, where they have a high biodiversity, are widespread, and may sometimes occur in striking abundance (Moore *et al.*, 1995, Hoffman, 1999, Partensky *et al.*, 1999a, Scanlan *et al.*, 2009, Scanlan, 2003, Flombaum *et al.*, 2013). They occupy a wide range of niches in marine ecosystems in tropical regions where they occur along maritime coasts as well as in the open ocean.

Cyanobacteria are classified into α- and β-cyanobacteria (Badger *et al.*, 2002), based on the content of Rubisco and carboxysomes. The α-group are marine cyanobacteria, *Prochlorococcus* and *Synechococcus* (Ohashi *et al.*, 2011).

2.1 Marine picocyanobacteria

Marine picocyanobacteria are the most abundant photosynthetic organisms on Earth, with only two genera, *Prochlorococcus* (Heywood *et al.*, 2006, Johnson *et al.*, 2006, Olson *et al.*, 1990, Partensky *et al.*, 1999b, Chisholm *et al.*, 1988, Partensky & Garczarek, 2010, Biller *et al.*, 2014b) and *Synechococcus* (Scanlan, 2003, Scanlan & West, 2002, Waterbury *et al.*, 1979) numerically dominating most oceanic waters. These genera share a common ancestor (Waterbury *et al.*, 1979, Urbach *et al.*, 1998, Dufresne *et al.*, 2008) and they occupy complementary though overlapping niches in the ocean.

They dominate the photosynthetic picoplankton over vast tracts of the ocean of the world oceans (figure 5) and contribute significantly to the primary production (García-Pichel *et al.*, 2003, Heywood *et al.*, 2006, Partensky *et al.*, 1999a, Tarran *et al.*, 2001).

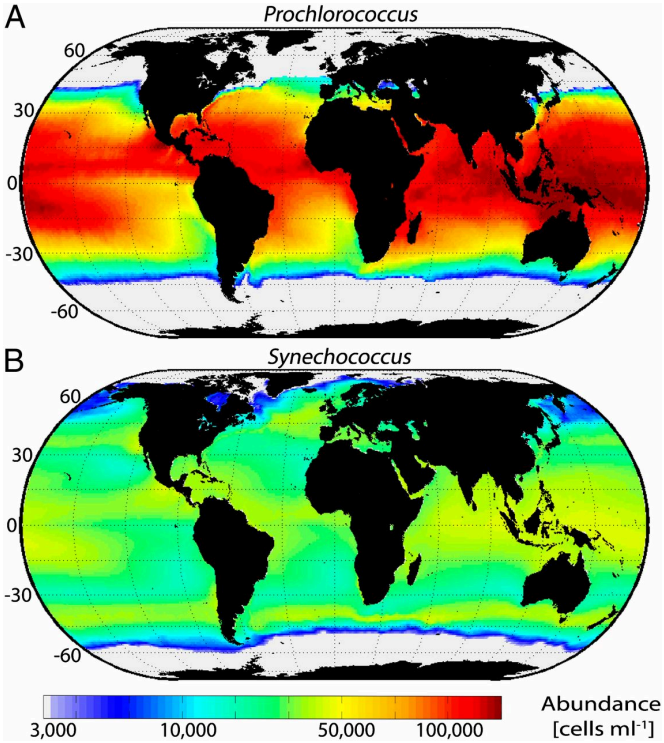

Figure 5: Present global distribution of *Prochlorococcus* and *Synechococcus* abundance. (A) *Prochlorococcus* and (B) *Synechococcus* mean annual abundances at the sea surface (Flombaum *et al.*, 2013).

These two cell types have adopted alternative strategies to occupy the oceanic ecosystem, which encompasses a range of water bodies from turbid, estuarine waters to transparent oligotrophic waters and delineates a complex light environment.

2.1.1 *Prochlorococcus marinus*

Since the discovery of *Prochlorococcus* in 1988 (Chisholm *et al.*, 1988), its major importance in the ecology of the oceans has become evident, leading to a large number of studies (Partensky *et al.*, 1999b, Biller *et al.*, 2014a, Coleman & Chisholm, 2007) and to the sequencing of the genomes of members from the different ecotypes (www.proportal.mit.edu), making *Prochlorococcus* one of the most studied microorganism from a genomic and ecological point of view. It is the smallest oxygenic phototroph described to date.

2.1.1.1 Size and ultrastructure

The best estimates made on cultures give a range of 0.5 to 0.8 µm for length and 0.4 to 0.6 µm for width (Lichtle *et al.*, 1995, Morel *et al.*, 1993). The cell size appears to vary

with environmental conditions. For example, it was shown to increase form 0.45 to 0.75 µm between the surface and a depth of 150 m in the Sargasso Sea (Sieracki *et al.*, 1995).

Transmission electron microscopy reveals typical cyanobacterial architecture that is similar to the other abundant oceanic photosynthetic prokaryote, *Synechococcus*. However, *Prochlorococcus* cell is distinctly elongated whereas the *Synechococcus* cell is much more spherical.

The cytoplasm contains DNA fibrils, carboxysomes and glycogen granules, located near or between thylakoids. In cross-sections, there are generally between two and four thylakoids, and there are sometimes up to six (figure 6).

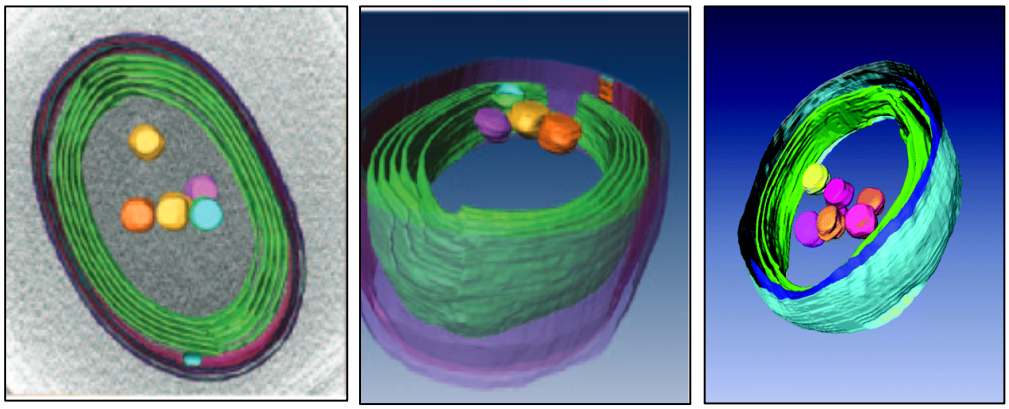

Figure 6: Cellular model of *Prochlorococcus* MIT9313. They were obtained by cryo-electron tomography. Structures include the cell wall (purple, pink, blue), extensive intracytoplasmic membrane system (green), and carboxysomes (yellow, pink, orange, blue). Images obtained by Claire S. Ting (Ting *et al.*, 2007).

2.1.1.2 Oceanic distribution

Prochlorococcus appears to have a very wide oceanic distribution. *Prochlorococcus* is virtually ubiquitous in the latitudinal band extending from 40 ºN to 40 ºS (Partensky *et al.*, 1999b). This oceanic distribution suggests that low temperatures are lethal to *Prochlorococcus*, contrasting strongly with that for *Synechococcus*, that can thrive in habitats with temperature as low as 2ºC (Shapiro & Haugen, 1988, Pittera *et al.*, 2014). Although *Prochlorococcus* is most abundant in oligotrophic waters, both in absolute terms and relative to the other photosynthetic populations, it can be found in coastal areas or the Mediterranean Sea.

Vertical plots of the available measurements of *Prochlorococcus* and *Synechococcus* concentration by flow cytometry reveal the broad features that distinguish these two photosynthetic prokaryotes (Partensky *et al.*, 1999b, Saito *et al.*, 2014). On average *Synechococcus* concentrations are about 1 order of magnitude lower than *Prochlorococcus* concentrations, although they divide once per day, which is equivalent to a population growth rate of 0.5 to 0.6 day^{-1}. Clearly, *Prochlorococcus* extends much deeper than *Synechococcus*, since the latter disappears virtually beyond 100 m deep (Partensky & Garczarek, 2010, Ting *et al.*, 2002).

The ability of *Prochlorococcus* to colonize the entire euphotic zone is due to the presence and differential distribution of specific High-Light (HL-) and Low-Light (LL-) adapted ecotypes, i.e., genetically and physiologically distinct populations, that partition themselves vertically down the water column in accordance with incident light levels (Johnson *et al.*, 2006, Moore *et al.*, 1998, Scanlan & West, 2002, West & Scanlan, 1999). The HL group comprises the HLI and HLII, while the LL group consists of clades LLI to LLIV (table 4).

Table 4: Summary of ecological conditions where *Prochlorococcus* ecotypes are most frequent Adapted (Scanlan *et al.*, 2009)

Clade	Ecological conditions of largest abundance
HLI	More weakly stratified surface waters, particularly between 35º and 48 ºN and 35º and 40 ºS
HLII	Strongly stratified surface waters, particularly tropical and subtropical regions between 30 ºN and 30 ºS
LLI	Occupies an intermediate position in the water column in stratified waters; at high latitude these cells can be found throughout the euphotic zone up to the surface
LLIV	Widely distributed within the 40 ºN to 35 ºS latitudinal range but largely restricted to the deep euphotic zone
LLII and LLIII	Present in deep waters at very low concentrations

2.1.1.3 Genomic features

It seems that *Prochlorococcus* possesses the smallest genome of all prokaryotes evolving oxygen. In contrast to marine *Synechococcus*, characterized by a high G+C

content (47.7 to 69.5%) (Watson & Tabita, 1996), most *Prochlorococcus* strains have a low G+C content (table 5).

Table 5: *Prochlorococcus* genomes sequenced to date (Biller *et al.*, 2014a)

Prochlorococcus	Subcluster or ecotype	Clade no.[a]	Genome size (Mb)	No. of protein-coding genes	GC (%)
MED4	HL	HLI	1.66	1,716	31
MIT9515	HL	HLI	1.7	1,908	31
MIT9301	HL	HLII	1.64	1,907	31
AS9601	HL	HLII	1.67	1,926	31
MIT9215	HL	HLII	1.74	1,989	31
MIT9312	HL	HLII	1.71	1,962	31
NATL1A	LL	LLI	1.86	2,201	35
NATL2A	LL	LLI	1.84	2,158	35
SS120	LL	LLII	1.75	1,884	36
MIT9211	LL	LLIII	1.69	1,855	38
MIT9303	LL	LLIV	2.68	3,022	50
MIT9313	LL	LLIV	2.41	2,275	51
EQPAC1	HL	HLI	1.65	1,954	30.8
GP2	HL	HLII	1.62	1,884	31.2
MIT0604	HL	HLII	1.78	2,085	31.2
MIT9107	HL	HLII	1.69	1,991	31
MIT9116	HL	HLII	1.68	1,972	31
MIT9123	HL	HLII	1.69	2,005	31
MIT9201	HL	HLII	1.67	1,989	31.3
MIT9302	HL	HLII	1.74	2,015	31.1
MIT9311	HL	HLII	1.71	1,983	31.2
MIT9314	HL	HLII	1.69	1,990	31.2
MIT9321	HL	HLII	1.65	1,956	31.2
MIT9322	HL	HLII	1.65	1,959	31.2
MIT9401	HL	HLII	1.66	1,972	31.2
SB	HL	HLII	1.66	1,933	31.5
MIT0801	LL	LLI	1.93	2,287	34.9
PAC1	LL	LLI	1.84	2,264	35.1
LG	LL	LLII,III	1.75	1,973	36.4
MIT0601	LL	LLII,III	1.7	1,934	37
MIT0602	LL	LLII,III	1.75	1,998	36.3
MIT0603	LL	LLII,III	1.75	2,015	36.3
SS2	LL	LLII,III	1.75	1,989	36.4

SS35	LL	LLII,III	1.75	1,977	36.4
SS51	LL	LLII,III	1.74	1,974	36.4
SS52	LL	LLII,III	1.75	1,987	36.4
MIT0701	LL	LLIV	2.59	3,079	50.6
MIT0702	LL	LLIV	2.58	3,066	50.6
MIT0703	LL	LLIV	2.57	3,054	50.6
UH18301	HL	HLII	1.65	1,947	31.2
MIT9202	HL	HLII	1.69	2,000	31.1
[b]W6	HL	HLII	0.38	646	31.3
HNCL2	HL	HLIII	1.4	1,701	30.3
[b]W3	HL	HLIII	0.33	529	30.7
[b]W5	HL	HLIII	0.099	212	29.8
[b]W7	HL	HLIII	0.9	989	30.7
[b]W8	HL	HLIII	0.84	917	31.4
[b]W9	HL	HLIII	0.42	638	30.7
HNCL1	HL	HLIV	1.56	1,830	29.8
[b]W10	HL	HLIV	0.56	892	30.8
[b]W11	HL	HLIV	0.76	929	30.6
[b]W12	HL	HLIV	0.42	602	29.6
[b]W2	HL	HLIV	1.26	1,374	30.5
[b]W4	HL	HLIV	0.76	819	29.9

[a] Ecotype as defined in reference (Kettler *et al.*, 2007)

[b] Single cell genomes

The genomes are composed of a single circular chromosome with no plasmids. The genome sizes ranges from 1.62 to 2.7 Mb in *Prochlorococcus*. GP2 has the smallest cyanobacterial genome sequenced to date (1.62 Mb). This small size, a result of a genome reduction process during evolution of the *Prochlorococcus* genus, occurred with a sharp drop in G+C content (Dufresne *et al.*, 2005).

2.1.1.4 Photosynthetic apparatus

Prochlorococcus have adopted different strategies with respect to light harvesting with respect to the other cyanobacteria. They have a much simple pigmentation specifically adapted to collect the blue light predominant at depth in oceanic waters.

Prochlorococcus is an atypical cyanobacterium, since its main antenna complexes comprise thylakoid membrane proteins binding unique divinyl derivatives of Chl *a* and *b* (so called Chl a_2 and b_2) (Goericke & Repeta, 1992, La Roche *et al.*, 1996, Partensky

& Garczarek, 2003, Steglich *et al.*, 2003). Both Chl a_2 and Chl b_2 have absorption and fluorescence excitation maxima in the blue part of the visible spectrum red-shifted by 8 to 10 nm compared to their monovinyl counterparts.

In both HL and LL *Prochlorococcus* ecotypes, these phycobilisome genes are expressed at a low level, giving rise to only a very small amount of phycoerythrin per cell (Hess *et al.*, 1996, Steglich *et al.*, 2005).

The major light-harvesting complexes of *Prochlorococcus* comprise pigment binding (Pcb) proteins possessing six transmembrane helices. The PSII antenna comprises two series of 4-Pcb subunits located on each side of PSII dimers, whereas the PSI antenna is an 18-Pcb ring surrounding PSI trimmers. PSII antenna is likely constitutive in all *Prochlorococcus* strains, the presence of the PSI antenna is much more variable (Garczarek *et al.*, 2000, Scanlan *et al.*, 2009).

One notable peculiarity of *Prochlorococcus* is the dramatic difference in pigment ratios among different isolates. For example, several isolates, notably SS120, have a Chl b_2/Chl a_2 ratio equal to or higher than 1 whereas other isolates display much lower ratios, with the MED4 strain exhibiting the lowest, 0.13 (Moore, 1997, Moore & Chisholm, 1999, Moore *et al.*, 1995, Partensky *et al.*, 1993).

A study confirmed that differences in pigmentation among isolates correlate with differing photosynthetic efficiencies: when grown at 9 µmol quanta m^{-2} s^{1}, two *Prochlorococcus* isolates (MIT9303 and MIT9313) with high ratios of Chl b_2 to Chl a_2 (> 1.1) had a significantly higher photosynthetic efficiency than did two other isolates (MIT9302 and MIT9312) with Chl b_2/Chl a_2 ratios lower by a factor of 2 (2.4 and 1.8 fg of C fg Chl^{-1} h^{-1}) (Moore, 1997).

Some of its photosynthetic properties may give *Prochlorococcus* a definite selective advantage for growth at depth in oligotrophic areas, particularly respect to *Synechococcus.*

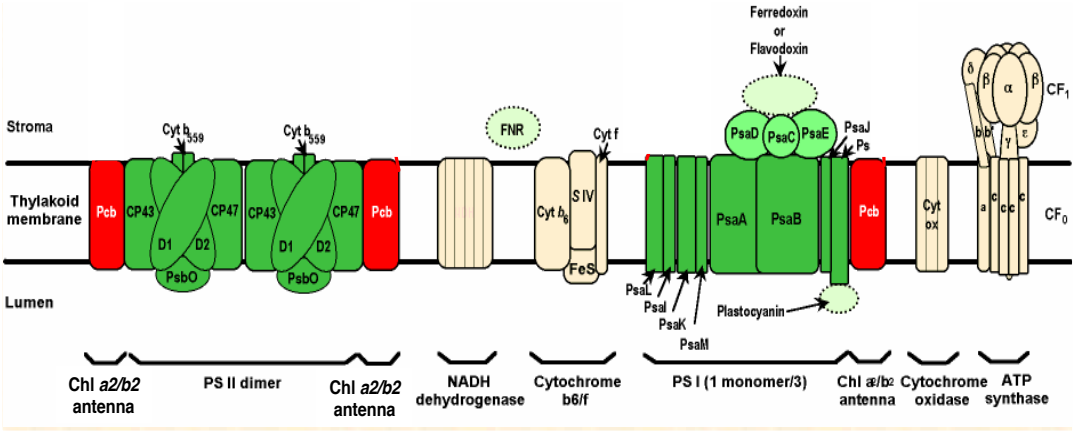

Figure 7: Scheme of the photosynthetic apparatus of *Prochlorococcus* (Bibby et al., 2003).

2.1.1.5 Nutrient assimilation

One of the most intriguing ecological characteristics of *Prochlorococcus*, besides its capacity to grow over a very wide range of irradiances in nature, is its ability to colonize extremely oligotrophic areas.

Although nitrogen is the primary limiting nutrient in many oceanic areas, recent evidence points to phosphorus as an important limiting nutrient, *Prochlorococcus* is well represented in areas with low phosphorus concentration, suggesting that it also has the ability to thrive under very low phosphorus concentrations (Parpais *et al.*, 1996, Zubkov *et al.*, 2007, Krumhardt *et al.*, 2013, Saito *et al.*, 2014).

Iron is the third major nutrient implicated in the limitation of primary productivity in remote areas of the ocean not subjected to eolian inputs, such as the equatorial pacific, as well as in more coastal areas (La Roche *et al.*, 1995). The low iron requirement of *Prochlorococcus* could be a key factor in its success in central oceanic areas.

In *Prochlorococcus* is likely that the loss of genes for utilising nitrate and nitrite reflects the niche occupied by this ecotype, surface waters where oxidised forms of nitrogen are extremely scarce, providing a relatively strong selection for gene loss and ultimately contributing to a compact genome for this ecotype. In spite of that occurs in the major proportion of *Prochlorococcu,* there are LL strains as MIT9313, NATL1A and NATL2A, that in addition to utilising ammonium and urea, are able to utilise nitrite, reflecting the often found nitrite maxima at the bottom of the euphotic zone. Recently, nitrate utilization has been demonstrated in isolated strains of *Prochlorococcus*, as had

been proposed previously on base of lab and field studies (Scanlan & West, 2002, Martiny *et al.*, 2009, Moore *et al.*, 2002, Rocap *et al.*, 2003, Berube *et al.*, 2014).

2.1.2 Marine *Synechococcus*

Synechococcus was detected earlier than *Prochlorococcus* by virtue of their intense orange phycoerythrin fluorescence (Waterbury *et al.*, 1979). The *Synechococcus* cells are the dominant phycobilisome containing cyanobacteria in the world´s ocans. Marine *Synechococcus* isolated comprise a complex taxon and have been classified by their major light-harvesting accessory pigment profiles, growth requirements, and their ability to carry out swimming motility (Waterbury *et al.*, 1986, Partensky *et al.*, 1999a, Urbach *et al.*, 1998, Scanlan *et al.*, 2009, Six *et al.*, 2007, Scanlan, 2001). Known physiological differences between strains include their response to nitrogen depletion, preference for nitrate or urea for growth and cell cycle behaviour (Scanlan & West, 2002).

2.1.2.1 Size and ultrastructure

Marine *Synechococcus* size is a coccoid organism about 1 μM of diameter. They divide by binary fission into equal halves in one plane. They contain photosynthetic thylakoid membranes located peripherally and lack structure sheaths (Waterbury & Rippka, 1989, Scanlan, 2003).

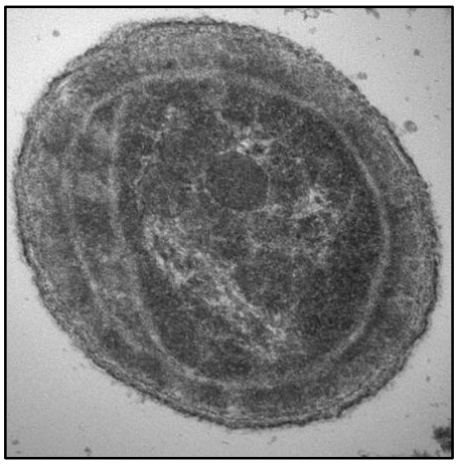

Figure 8: Cellular model of *Synechococcus* WH8102. Photo by Dawn Moran, Woods Hole Oceanographic Insitution.

2.1.2.2 Oceanic distribution

Synechococcus is virtually ubiquitous in all marine environments with concentrations ranging from $5x10^2$ to $1.5x10^6$ cell ml^{-1}. It is much more abundant in nutrient-rich than in oligotrophic areas and its distribution is generally restricted to the upper well-lit layer. They are important contributors to global marine carbon fixation, e.g. contributing up to 20% of fixed carbon in some areas (Li, 1994, Li *et al.*, 1992).

Table 6: Summary of ecological conditions where *Synechococcus* ecotypes are most frequent Adapted (Scanlan *et al.*, 2009)

Clade	Ecological conditions of largest abundance
I	Coastal and/or temperate mesotrophic open ocean waters largely above 30 ºN and below 30 ºS
II	Offshore, continent shelf, oligotrophic tropical or subtropical waters between 30 ºN and 30 ºS
III	Ultraoligotrophic open-ocean waters
IV	Coastal and/or temperate mesotrophic open ocean waters largely above 30 ºN and below 30 ºS
V/VI/VII	Relatively wide distribution but in low abundance in various oceanic waters

2.1.2.3 Genomic features

The genome is composed of a single circular chromosome with no plasmids. Genome size average is ca. 2.86 Mb. *Synechococcus* gene number ranges from 2,358 to 3,224 (table 7). There are more marine *Synechococcus* genomes that are currently sequencing, besides the table 7 shows some *Synechococcus* that the information is not yet complete.

Table 7: *Synechococcus* genomes sequenced to date

Synechococcus	Subcluster or ecotype[a]	Clade no.[b]	Genome size (Mb)	No. of protein-coding genes	GC (%)
CC9311	5.1B	I	2.61	2,892	52
CC9605	5.1A	II	2.51	2,645	59
WH8102	5.1A	III	2.43	2,519	59
CC9902	5.1A	IV	2.23	2,358	54
BL107	5.1A	IV	2.28	2,553	54
WH7803	5.1B	V	2.37	2,586	60
WH7805	5.1B	VI	2.62	2,934	57
RS9917	5.1B	VIII	2.58	2,820	65
RS9916	5.1B	IX	2.66	3,099	60
WH5701	5.2		2.86	3,129	66
RCC307	5.3		2.22	2,583	61

WH8109	II	2.11	2,644	60
PCC7002		3.4	3,186	49
CB0205		2.42		63
CB101		2.68		63
PCC7336		5.68		54
WH8016		2.69	2,992	54
KORDI-49		2.58	2,734	61
KORDI-52		2.57	2,820	59
KORDI-100		2.79	3,061	57
NKBG15041C		3.18	3,224	49.3

[a] 5.1A and 5.1B, subcluster number as defined (Dufresne *et al.*, 2008)

[b]Ecotype as defined in reference (Kettler *et al.*, 2007, Fuller *et al.*, 2003)

2.1.2.4 Photosynthetic apparatus

The structure of the main components of the photosynthetic apparatus from marine *Synechococcus* strains are similar to that of model freshwater cyanobacteria (figure 9).

Synechococcus have adopted completely different adaptation strategies with respect to light harvesting than *Prochlorococcus*. Members of *Synechococcus* genus have developed a variety of pigmentations (Waterbury *et al.*, 1986, Pittera *et al.*, 2014, Shukla *et al.*, 2012, Garczarek *et al.*, 2008, Six *et al.*, 2007), allowing the genus as a whole to cope with the wide range in light quality naturally occurring in subsurface waters over horizontal gradients.

Synechococcus strains possess phycobilisomes, which are large antennae located in the stromatic space between thylakoid membranes (figure 9) and comprising different combinations of phycobiliproteins, each binding one or several chromophore (phycobilin) types: phycocyanobilin (PCB), phycoerythrobilin (PEB) and phycourobilin (PUB) (Ong & Glazer, 1991).

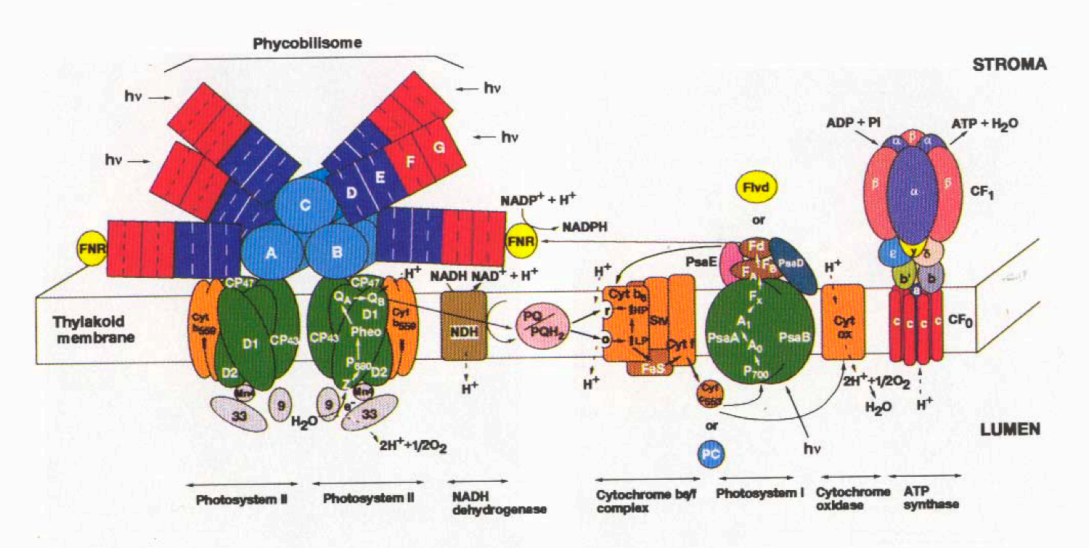

Figure 9: Scheme of the photosynthetic apparatus of *Synechococcus.* Adapted (Bryant, 1995)

The phycobilisome core, made of allophycocyanin, is connected to the photosystems and is thought to be surrounded by six to eight rods, the latter comprising phycocyanin and/or phycoerythrin. Three main *Synechococcus* pigment types (pigment types 1, 2 3 respectively) have been defined based on the absence (pigment type 1) or presence of one (pigment 2) or two (pigment 3) phycoerythrins (I and II). Furthermore, pigment type 3 has been subdivided into four subtypes (3a to 3d). depending on the ratio of PUB to PEB chromophores bound to phycoerythrins (figure 10).

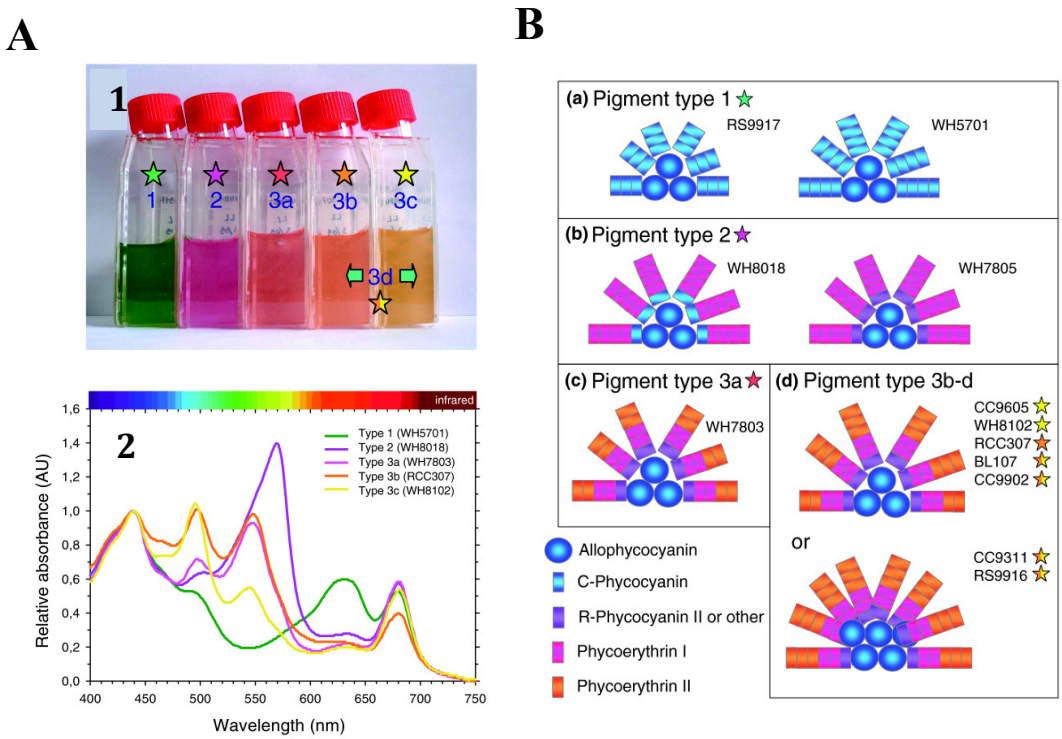

Figure 10: Diversity of pigment in marine *Synechococcus*. A. (1) Photograph of cultures representative of the three main pigment types (1 to 3) and subtypes (3a to 3c). 3d is the pigment type that modify their pigmentation from 3b to 3c**. (2)** Absorption properties of each pigment**. B.** Models of phycobilisome structure from the different pigments types (a-d) (Six et al., 2007).

2.1.2.5 Nitrogen assimilation

Marine *Synechococcus* strains appear to show a relatively broad utilisation of nitrogen sources for growth. Ammonium, nitrate, nitrite and urea are capable of acting as the sole nitrogen source for growth in one or more strains (Glibert & Ray, 1990, Lindell *et al.*, 1998, Collier *et al.*, 1999). Further, strains WH7803 and WH8101 can assimilate amino acids (Paerl, 1991), whilst others e.g. WH8102, WH8103, WH8112 and WH7803 have been shown to express aminopeptidase activity (Martinez & Azam, 1993), suggesting that hydrolysis of dissolved organic nitrogen may also be important in the nitrogen nutrition of these organisms, it is likely that the ability to utilise amino acids is also widespread in members of the genus. However, some differences in nitrogen resource utilisation among strains are known. Thus, although most strains are capable of consuming urea a few exceptions have also been noted (Waterbury *et al.*, 1986), for instance, WH7803 lack urease gene (Collier *et al.*, 1999).

Most marine *Synechococcus* strains that have been isolated so far are capable of utilising nitrate as a nitrogen source for growth with the exception of strain RS9917, which lacks the nitrate assimilation genes (Scanlan *et al.*, 2009). Nitrate uptake is carried out by a permease NrtP of the major facilitator super family (instead of nrtABCD encoding typical ABC transporter freshwater) (Sakamoto *et al.*, 1999, Ohashi *et al.*, 2011).

This difference in nitrate utilisation between *Synechococcus* and *Prochlorococcus* populations is reflected in observations made in situ, where natural populations of *Synechococcus* have been reported to respond rapidly to periodic nitrate input, and bloom, whilst *Prochlorococcus* is absent in nitrate well-mixed winter waters (Moore, 1997, Martiny *et al.*, 2009).

3. NITROGEN METABOLISM

Synechococcus and *Prochlorococcus* strains require nitrogen as an essential nutrient, but they differ in key aspects of nitrogen metabolism reflecting properties of the ocean niches they occupy. Nitrogen is potentially a limiting factor for phytoplankton in general and for the picocyanobacteria in particular. Despite the low ambient nitrogen concentrations, picocyanobacteria maintain high cell numbers and biomass while lacking the ability to fix molecular dinitrogen, as do other, less abundant, *Crocosphaera*, *Trichodesmium* and the endosymiotic *Richelia*. The dimensions of their oceanic niches, the spatial and temporal gradients of nitrogen availability and regeneration, and the low concentrations in which they occur have all affected the genomic properties of *Synechococcus* and *Prochlorococcus* (Scanlan *et al.*, 2009).

Central to nitrogen metabolism is the assimilation of ammonium into organic nitrogen compounds. As in other cyanobacteria, marine *Synechococcus* and *Prochlorococcus* strains assimilate ammonium via the glutamine synthetase-glutamate synthase pathway (GS-GOGAT pathway) (figure 11).

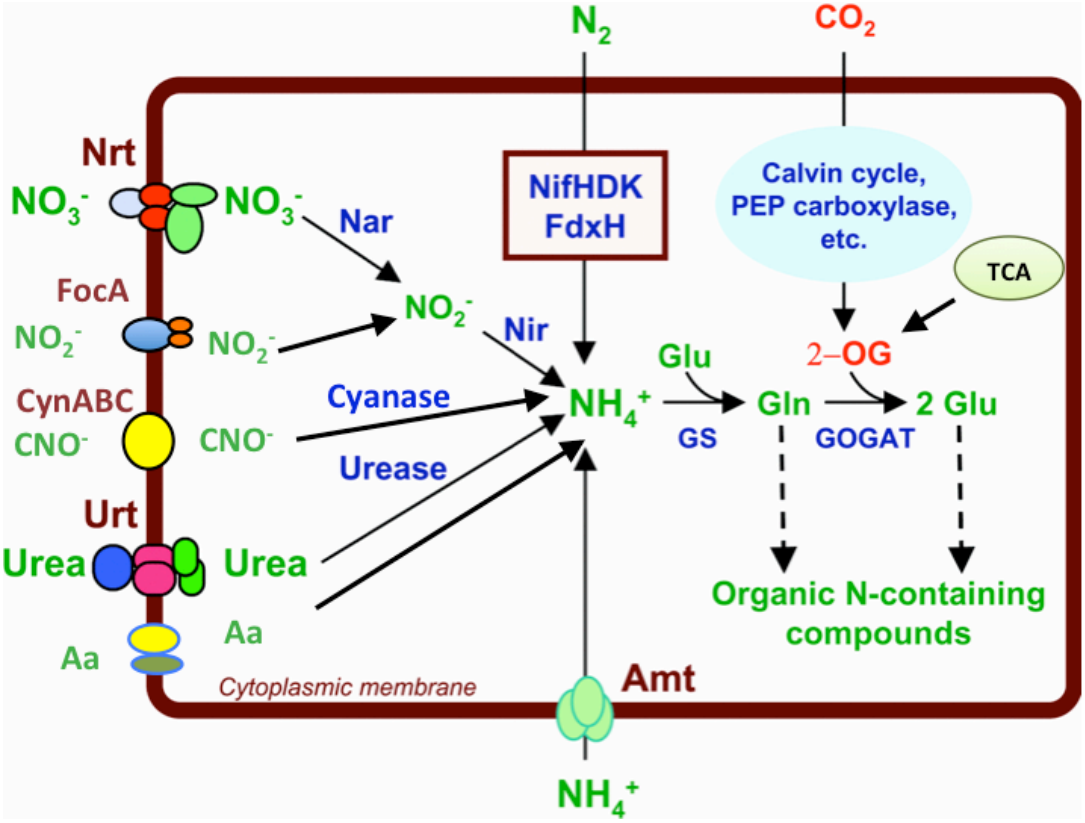

Figure 11: Main nitrogen assimilation pathways in cyanobacteria. Different nitrogen sources are taken up through permeases and transporters and metabolized to ammonium, which is incorporated into carbon skeletons through the GS-GOGAT pathway. Nitrogen is then distributed from glutamine or glutamate to other nitrogen-containing organic compounds. Nrt: NO_3^-/NO_2^- transporter; FocA: NO_2^- transporter; CynABC: cyanate transporter; Urt: ABC type urea transporter; Amt: ammonium permease; Nar: nitrate reductase; Nir: nitrite reductase; NifHDK: nitrogenase complex; FdxH: heterocyst-specific ferredoxin. Adapted (Flores & Herrero, 2005).

The table 8 shows a summary of the genes involved in nitrogen metabolism in cyanobacteria that are presented or not in the strains used during this work. This table help us to know the genetic diversity between these strains.

Table 8: Summary of N metabolism gene content on the strains studied in this work

Proteins	Genes	MIT9313[a]	SS120[a]	MED4[a]	WH7803[b]
Transporters					
NO_3^-/NO_2^-	*nrtP*	-	-	-	+
NO_2^-	*focA*	+	-	-	+
Cyanate	*cynABD*	-	-	+	-
Ammonium	*amt1*	+	+	+	+
Enzymes					
NR	*narB*	-	-	-	+
NiR	*nirA*	+	-	-	+
GDH	*gdhA*	+	-	-	+
GSIII	*glnN*	-	-	-	+
GS	*glnA*	+	+	+	+
GOGAT	*glsF*	+	+	+	+
ICDH	*icd*	+	+	+	+
Cyanasa	*cynS*	-	-	+	+
Urease	*ure*	+	-	+	-
Regulatory proteins					
NtcA	*ntcA*	+	+	+	+
P_{II}	*glnB*	+	+	+	+
PipX	*pipX*	+	+	+	+

[a] ***Prochlorococcus*** **marinus**

[b] **Marine** ***Synechococcus***

3.1 TCA cycle in cyanobacteria

Since 1967, it has become common knowledge that cyanobacteria have an incomplete TCA cycle (Smith *et al.*, 1967, Pearce *et al.*, 1969, Ohashi *et al.*, 2011) lacking the enzyme 2-oxoglutarate dehydrogenase (2-OGDH). There were no sequenced cyanobacterial genomes showing the genes for 2-OGDH (Wood *et al.*, 2004) and this absence has frequently been discussed as a factor to explain why most cyanobacteria are obligate photolithoautotrophs (Stanier & Cohen-Bazire, 1977). However, two genes that encode a novel 2-oxoglutarate decarboxylase (2-OGDC) and succinic semialdehyde dehydrogenase (SSADH) in *Synechococcus* sp. PCC 7002 have been recently reported (Zhang & Bryant, 2011). These two enzymes convert the 2-OG to succinate replacing 2-OG dehydrogenase and succinyl-CoA synthetase (figure 12).

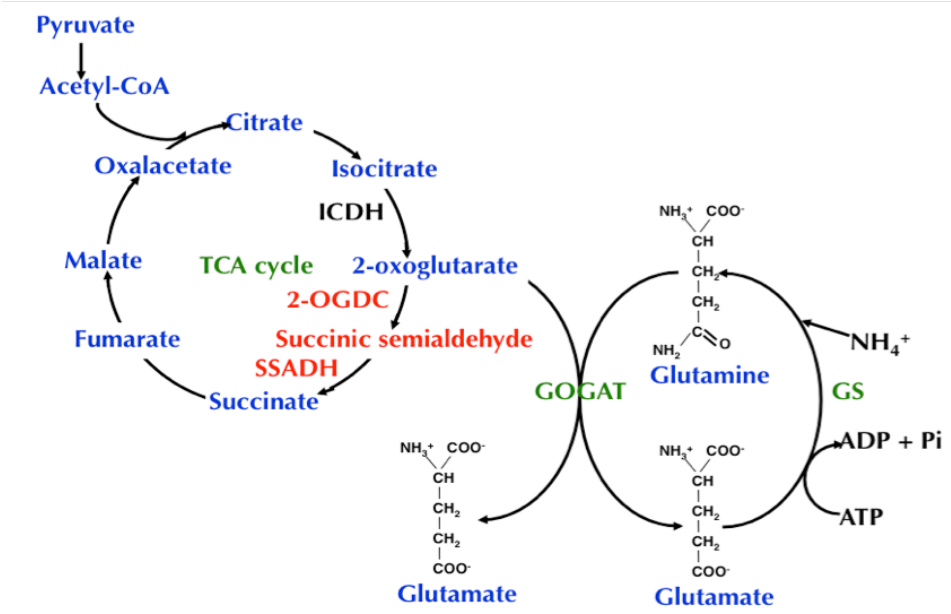

Figure 12: Outline of the pathways for 2-OG metabolism in cyanobacteria. 2-OG produced from isocitrate in the TCA cycle can be used by all cyanobacteria as backbone to incorporate ammonium, through the GS/GOGAT pathway. Alternatively, the majority of cyanobacteria can transform 2-OG to succinic semialdehyde and later to succinate using 2-OGDC and SSADH enzymes. These enzymes are highlighted in red and they are absent in *Prochlorococcus* and marine *Synechococcus*.

These two genes are present in all cyanobacterial genomes except those of *Prochlorococcus* and marine *Synechococcus* species giving a different background respect to the rest of cyanobacteria described to date, because the only way that 2-OG could be further oxidized is by the GS-GOGAT pathway.

Furthermore, recent reports from Vermaas and coworkers suggest that there is another alternate way of closing the TCA cycle in cyanobacteria, by means of the γ-aminobutyric acid shunt, which according to them is the major contributor to flux from 2-OG and glutamate to succinate in *Synechocystis* sp. PCC 6803 (Xiong *et al.*, 2014).

3.2 Assimilation of nitrogen

Ammonium is the preferred nitrogen source of cyanobacteria. The assimilation of ammonium by most microorganisms occurs through the sequential action of two enzymes: glutamine synthetase (GS) and glutamate synthase (GOGAT). This pathway

represents the connecting step between carbon and nitrogen metabolism. Ammonia diffuses through membranes whereas the ammonium ion cannot. Cyanobacteria possess ammonium transporters of the widely distributed Amt family (Montesinos *et al.*, 1998, Muro-Pastor *et al.*, 2005). Genes encoding ammonium permeases*, amt1*, *amt2* and *amt3* have been described.

Nitrate is the most abundant source of combined nitrogen in many environments. Accordingly, most investigated cyanobacteria have the capability to utilize this source. Most isolated *Prochlorococcus* strains have been found to lack the nitrate assimilation genes (López-Lozano *et al.*, 2002, Rocap *et al.*, 2003, Dufresne *et al.*, 2003, Biller *et al.*, 2014a, Berube *et al.*, 2014). However, there are interesting cases, that is *Prochlorococcus* sp. MIT9313, NATL2A and NATL1A which has been shown to carry a nitrite reductase gene but no gene encoding a nitrate reductase, thus suggesting the capability of this cyanobacterium to assimilate nitrite but not nitrate (Rocap *et al.*, 2003, Martiny *et al.*, 2009, Lomas & Lipschultz, 2006). Recently, it has been described several *Prochlorococcus* strains able to growth on nitrate (Berube *et al.*, 2014). Nitrate uptake and reduction to nitrite and ammonium are driven in cyanobacteria by photosynthetically generated assimilatory power (ATP and reduced ferredoxin). High-affinity nitrate and nitrite uptake takes place in different cyanobacteria through either an ABC-type transporter or a permease from the major facilitator super family (MFS).

Synechococcus WH7803 carries a single nitrate transport gene, *nrtP*. It is part of the major facilitator superfamily of proteins (MFS) (Forde, 2000). NrtP likely contains 12 transmembrane segments in the form of α-helices. Its mechanism has not yet been determined, although Na^+ or H^+ symport has been suggested (Sakamoto *et al.*, 1999). It is commonly found in marine cyanobacteria (Sakamoto *et al.*, 1999, Bird & Wyman, 2003).

3.3 Key enzymes in nitrogen metabolism in cyanobacteria

3.3.1 Glutamine synthetase

The glutamine synthetase (GS) (EC 6.3.1.2) catalyzes the synthesis of glutamine from glutamate and ammonium in the presence of divalent cations (Mg^{2+} or Mn^{2+}) and using the energy of ATP hydrolysis.

Most cyanobacteria strains have only one GS (known as GS type I, GSI), encoded by the *glnA* gene. This is the typical prokaryotic GS composed of 12 identical subunits of about 50 kDa, disposed in two hexagonal rings. Some cyanobacterial strains have in addition to GSI a hexameric GS (known as GS type III, GSIII), encoded by *glnN* gene (Reyes & Florencio, 1994, Florencio & Reyes, 2002). The case of cyanobacterium *Pseudanabaena sp*. PCC 6903 is particularly relevant, because this strain is the only one, up to date, that lacks GSI harbouring only GSIII (Crespo *et al.*, 1998).

These two types of GS are quite different in amino acid sequence, however they share five domains of homology that can be identified among all known GS (Reyes & Florencio, 1994).

GSI has been characterized in a number of cyanobacterial strains including *Anabaena* sp. PCC 7120, *Anabaena azollae*, *Anacystis nidulans*, *Synechocystis*, *Calothrix* sp. PCC 7601 and *Phormidium laminosum*. In all the cases GSI were similar to each other in size and subunit composition. Km for the different substrates of GSI ranges from 20 to 170 μM for ammonium, from 0.35 to 5 mM for glutamate, and from 0.3 to 0.7 mM for ATP. The GS from *Prochlorococcus* has a stimated molecular mass of each subunit of 48.3 kDa; the apparent K_m constants for the biosynthetic activity were 0.3 mM for ammonium, 1.29 mM for glutamate and 1.35 mM for ATP and the optimum pH was 8.0 (El Alaoui *et al.*, 2003).

It has been described the important role of the metal-catalyzed oxidation (MCO) in the control of the biological activity and the turnover of the GS enzyme (Gómez-Baena *et al.*, 2006, Gómez-Baena *et al.*, 2001, Martin *et al.*, 1997, Gómez-Baena *et al.*, 2014).

Studies carried out with *Synechocystis glnA* mutant led to discover GSIII encoded by the *glnN* gene in cyanobacteria. This GSIII present homology with GSIII from *Bacteroides fragilis* (44% identity) and *Butyrivibrio fibrisolvens* (41%). This enzyme is composed of 6 identical subunits about 75 kDa. Biosynthetic activity of GSIII requires the same substrates and cofactors as the GSI enzyme. Apparent Km values for ATP, glutamate and ammonium are also similar to those of the Synechocystis GSI. Induction of GSIII only under conditions of nitrogen deficiency is found in several

different cyanobacterial strains where GSIII coexists with GSI (Reyes & Florencio, 1994, García-Domínguez *et al.*, 1997).

3.3.2 Glutamate synthase

The glutamate synthase (GOGAT) (EC 1.4.7.1) is the enzyme that synthesizes glutamate from glutamine, by the transfer of its amide group to the carbon skeleton 2-OG, in a reductive step that involves two electrons. Three different types of GOGAT have been described, depending on the electron donor used to reduce the iminoglutarate formed upon transfer of ammonia to 2-OG.

In photosynthetic oxygenic organisms two types of GOGAT have been found, one using ferredoxin and a second type using NADH as electron donors. A third type of GOGAT using NADPH for reduction is present in other bacterial groups (Temple *et al.*, 1998).

The enzyme is a monomer of about 170 kDa. The gene encoding Fd-GOGAT is *glsF*. Every GOGAT sequence shows about 40-45% amino acid sequence identity with all other GOGAT (Muro-Pastor *et al.*, 2005).

3.3.3 Isocitrate dehydrogenase

The enzyme isocitrate dehydrogenase (ICDH) (EC 1.1.1.42) catalyzes the oxidative decarboxylation of isocitrate, to produce 2-OG. ICDH reaction represents the connection between carbon and nitrogen metabolisms and the incompleteness of the tricarboxylic acids cycle in marine cyanobacteria confers a special importance to this enzyme in the C/N balance. This enzyme is encoded by the gene *icd*.

Attempts to completely segregate *Synechocystis* or *Anabaena* sp. PCC7120 *icd* mutants have been unsuccessful, indicating that *icd* is an essential gene for these cyanobacteria (Muro-Pastor & Florencio, 1994, Muro-Pastor *et al.*, 1996).

3.3.4 Glutamate dehydrogenase

An alternative route for ammonium assimilation in bacteria is mediated via glutamate dehydrogenase (GDH) activity (Hayden *et al.*, 2002, Florencio *et al.*, 1987, Sallala & Nimera, 1990, Chávez *et al.*, 1995). All marine *Synechococcus* genomes except strain WH5701, but only 4 of the *Prochlorococcus* genomes, carry a *gdhA* gene. The observation of the genomes suggests that GDH was lost in most *Prochlorococcus*

strains. A recent study has characterized GDH activity in *Prochlorococcus* sp. strain MIT9313 and suggested that its main role is in amino acid recycling via glutamate (Rangel *et al.*, 2009, Zubkov & Tarran, 2005).

3.3.5 Ferredoxin-nitrate reductase

Cyanobacterial nitrate reductases are enzymes that catalyze the 2-electron reduction of nitrate to nitrite for assimilatory purposes. They are monomers of the product of the *narB* gene with a molecular weight of about 80 kDa, which contain a [4Fe-4S] cluster and Mo-cofactor (Mikami & Ida, 1984, Rubio *et al.*, 2002).

Cyanobacterial nitrate reductase is partially associated with the thylakoid membrane and can use photosynthetically reduced ferredoxin or flavodoxin as physiological electron donor (Candau *et al.*, 1976, Manzano *et al.*, 1976).

3.3.6 Ferredoxin-nitrite reductase

Cyanobacterial nitrite reductases catalyze the assimilatory 6-electron reduction of nitrite to ammonium. They are monomers of the *nir* gene product with a molecular weight of 52-56 kDa, which contain a [4Fe-4S] cluster and a siroheme as prosthetic groups. The physiological electron donor to nitrite reductase is the photosynthetically reduced ferredoxin or flavodoxin (Manzano *et al.*, 1976).

4. REGULATORY PROTEINS IN NITROGEN METABOLISM IN CYANOBACTERIA

In order to adapt to changes in nitrogen source and availability, leading to an appropriate balance between carbon and nitrogen metabolisms, cyanobacteria require adequate mechanisms for sensing and response. This involves diverse global regulators, including NtcA, P_{II} and PipX, which monitor the C/N balance through the intracellular concentration of 2-oxoglutarate.

4.1 The molecule responsible for the control of the C/N balance: 2-OG

To maintain their metabolic homeostasis, bacteria must coordinate the flow rates of carbon and nitrogen assimilation. This coordination is achieved by signal transduction

systems that integrate signals from the status of the carbon and nitrogen metabolism and regulate the level of glutamine synthetase (GS) activity and the transcription of genes involved in the utilization of different nitrogen sources (Muro-Pastor *et al.*, 2001).

In cyanobacteria, it was demonstrated long ago that the ammonium-promoted repression of nitrate or dinitrogen utilization does not occur in the presence of inhibitors of the GS-GOGAT pathway (Herrero *et al.*, 1981), suggesting that metabolites related to the GS-GOGAT cycle are involved in signalling.

The molecule responsible to control of the C/N balance in cyanobacteria is 2-OG (Forchhammer, 2004, Herrero *et al.*, 2004, Muro-Pastor *et al.*, 2001, Forchhammer, 1999, Tanigawa *et al.*, 2002, Vazquez-Bermudez *et al.*, 2002). Due to the absence of 2-OG dehydrogenase in marine *Synechococcus* and *Prochlorococcus*, 2-OG serves only as the acceptor for the newly assimilated nitrogen to form glutamate, with its concentration changing according to the nitrogen status of the cell (Ohashi *et al.*, 2011).

4.2 The master nitrogen regulator: NtcA

In cyanobacteria, transcription of nitrogen-regulated genes is under the control of the DNA-binding protein NtcA (Luque *et al.*, 1994, Herrero *et al.*, 2001). NtcA belongs to the CRP (catabolic repressor protein) family of bacterial transcription factors. There is another transcription factor involved in regulation of that nitrate assimilation, NtcB (a LysR type transcriptional regulator), acts as sensor of nitrite (Aichi & Omata, 1997).

The regulatory gene *ntcA* encodes a protein of the Crp-FNR family of transcriptional regulators that includes more than 369 family members widely distributed in bacteria (Korner *et al.*, 2003). NtcA binds to and controls the promoters of genes subjected to metabolic control by ammonium including, for instance, *glnA* encoding GS, the *nir* operon and its own gene (Wei *et al.*, 1993, Luque *et al.*, 1994). The gene *ntcA* is ubiquitous in cyanobacteria and exclusive of this taxonomic group.

NtcA regulates transcription acting either as an activator or as repressor. Its activity has been described to respond to 2-OG, the key molecule signalling C/N status (Vazquez-Bermudez *et al.*, 2002, Tanigawa *et al.*, 2002, Muro-Pastor *et al.*, 2001).

NtcA is a dimeric protein of ca. 50 kDa, composed of two identical monomers each about 220 amino acids long. The C-terminal domain is formed by three short α-helices, the two C-terminal forming a helix-turn-helix (HTH) motif involved in DNA binding. This HTH motif is almost identical in the NtcA proteins whose whole sequence is available. The palindromic sequence $GTAN_8TAC$ is the consensus DNA sites for NtcA (Luque *et al.*, 1994). The most important nucleotides for NtcA binding seem to be the two external nucleotides (underlined) of the GTA and TAC triplets, their mutation increasing largely the K_d for NtcA binding (Vázquez-Bermúdez *et al.*, 2002a).

Activated NtcA enhances transcription of *ntcA*, *glnB, amt1*, *glnA* and *nir*. Furthemore, NtcA stimulates expression of the alternative sigma factor gene *rpoD*, and of the alternative glutamine synthetase *glnN*, exhibiting a non-canonical NtcA-binding promoter sequence. There is a repressive effect of activated NtcA on *rbcLS* (Schwarz & Forchhammer, 2005, Vázquez-Bermúdez *et al.*, 2002b). NtcA has also a repressive role on the regulation of the transcription of the inactivating factors of GS, IF7 and IF17, encoded by the genes *gifA* and *gifB* respectively (García-Domínguez *et al.*, 2000, García-Domínguez *et al.*, 1999).

The structure of the NtcA-activated promoter was first described for some NtcA-dependent genes in *S. elongatus*. The canonical NtcA-activated promoter is composed of an NtcA-binding box centered around -40.5 with respect to the transcription start point and a -10 Pribnow-like box with the consensus sequence TAN_3T located about 22 bp downstream (Luque *et al.*, 1994, Luque & Forchhammer, 2008).

4.3 P_{II}

The P_{II}-like signalling proteins constitute one of the most widely distributed families of signal transduction proteins, whose members are found in bacteria, archaea and plants (Arcondéguy *et al.*, 2001, Forchhammer, 2004, Ninfa & Jiang, 2005, Forchhammer & Tandeau de Marsac, 1994).

P_{II} proteins are pivotal regulators in bacterial nitrogen assimilatory processes, where they are engaged in sensing and integrating signals of the central metabolic state of the cells.

The P_{II} proteins are trimers of 12-13 kDa subunits with a highly conserved three-dimensional structure. The three subunits form a squat barrel made up of a central core of antiparallel bet-sheets and laterally arranged α-helices and loop structures. The largest of these loops (termed T-loop) protrudes from the protein. It seems to be flexible in solution and is of particular importance for P_{II}-receptor interactions (Xu *et al.*, 2003).

There are two basics modes of signal perception by P_{II}. The first one involves the binding of the effector molecules ATP (ADP) and 2-OG to P_{II}. A second mode of signal perception occurs by covalent modification of P_{II} proteins at the apex of the exposed T-loop (Jiang & Ninfa, 1999, Forchhammer & Hedler, 1997) .

In the case of proteobacteria, modification of P_{II} proteins occurs by reversible uridylylation of a conserved tyrosyl-residue (Tyr51). A distinct type of P_{II} modification has been demonstrated in unicellular cyanobacteria, where a P_{II} protein is phosphorylated and dephosphorylated in a seryl residue (Ser49) located in the vicinity of the conserved Tyr51 (Forchhammer & Tandeau de Marsac, 1994).

4.4 PipX

Studies aimed at the identification of potential P_{II} targets revealed the protein PipX (P_{II}-interacting protein X) (Burillo *et al.*, 2004), which is able to interact with both, P_{II} and NtcA. PipX is a small monomeric protein of 89 amino acids, conserved in all cyanobacterial genomes but lacking homologues outside the cyanobacterial phylum.

PipX interaction with P_{II} or NtcA is antagonistically regulated by 2-OG: in the presence of low 2-OG, it binds preferentially to P_{II}, whereas increased 2-OG levels favour binding to NtcA (Espinosa *et al.*, 2006, Llácer *et al.*, 2010).

A recent study showed that PipX is involved in NtcA-independent regulatory pathways. It has been demonstrated by a combination of genetic, transcriptomic, and multivariate analyses that PipX is involved in a much wider interaction network affecting nitrogen assimilation, translation and photosynthesis (Espinosa *et al.*, 2014).

4.5 Sigma factors

The RNA polymerase holoenzyme is considered to play a key role in global changes in gene expression patterns *via* the rapid modulation of its promoter selectivity. One major mechanism by which RNA polymerase controls promoter selectivity is the replacement of a sigma factor on a common core enzyme. Each sigma factor is activated in response to corresponding environmental or internal physiological conditions and recognizes a specific subset of promoters to coordinate cellular processes (Ishihama, 1993, Lonetto *et al.*, 1992).

The σ factors of *E. coli* can be classified into two major groups, the σ^{70} and σ^{54} families. In all cyanobacterial genomes sequenced to date only members of the σ^{70} family were found (Imamura & Asayama, 2009).

The different σ^{70} factors are frequently subdivided into three groups according to sequence similarity, structural and functional properties. Group 1 σ factors are also named principal σ factors, they are essential for cell viability. Group 2 are similar to the group 1 types in molecular structure, they are non-essential for cell viability. Finally, group 3 are structurally different from group 1 and 2 and not much is known about the sets of genes they regulate, SigF is the best investigated of this group in the cyanobacterium *Synechocystis* PCC 6803 (Imamura *et al.*, 2003).

To summarize, not much is known about the promoter recognition of group 3 σ factors and nothing at all about their function within species belonging to the clade of marine picocyanobacteria.

5. INTERACTION BETWEEN REGULATORY PROTEINS

Although the P_{II} protein (the product of the *glnB* gene in cyanobacteria) is regarded as having a central role in the post-translational regulation of nitrogen assimilation and allocation (Forchhammer, 2004), recent studies on PipX, a small P_{II}-binding protein, have revealed its essential roles in the regulation of the activity of NtcA (Espinosa *et al.*, 2006, Espinosa *et al.*, 2007, Espinosa *et al.*, 2009). PipX was first identified as a P_{II}-binding protein and then shown to bind NtcA as well (Espinosa *et al.*, 2006).

The binding of PipX to P_{II} and NtcA is influenced by 2-OG in opposite ways: When 2-OG concentrations are low, PipX preferentially binds to P_{II}. At higher concentrations, 2-OG interferes with the binding of PipX to P_{II} and it binds to NtcA (figure 12).

In vivo evidences for the involvement of PipX in the enhancement of NtcA activity have been presented (Espinosa *et al.*, 2006, Espinosa *et al.*, 2007). X-ray crystallographic structures of a PipX-NtcA complex suggest that PipX enhances the activity of NtcA in the promotion of transcription by stabilizing the active conformation of NtcA rather than increasing the interaction with DNA (Llácer *et al.*, 2010). From the interaction of PipX with P_{II} and NtcA, it is deduced that P_{II} negatively regulates the activity of NtcA via PipX.

The presence of *glnB* and *pipX* in all the cyanobacterial strains examined to date indicates that enhancement of NtcA regulon expression is essential, but needs to be tightly regulated by P_{II} according to the changes in cellular nitrogen status. The critical importance of the regulation by P_{II} of NtcA activity would account for the difficulties experienced by researchers in the construction and maintenance of P_{II}-deficient mutants from cyanobacteria (Espinosa *et al.*, 2009).

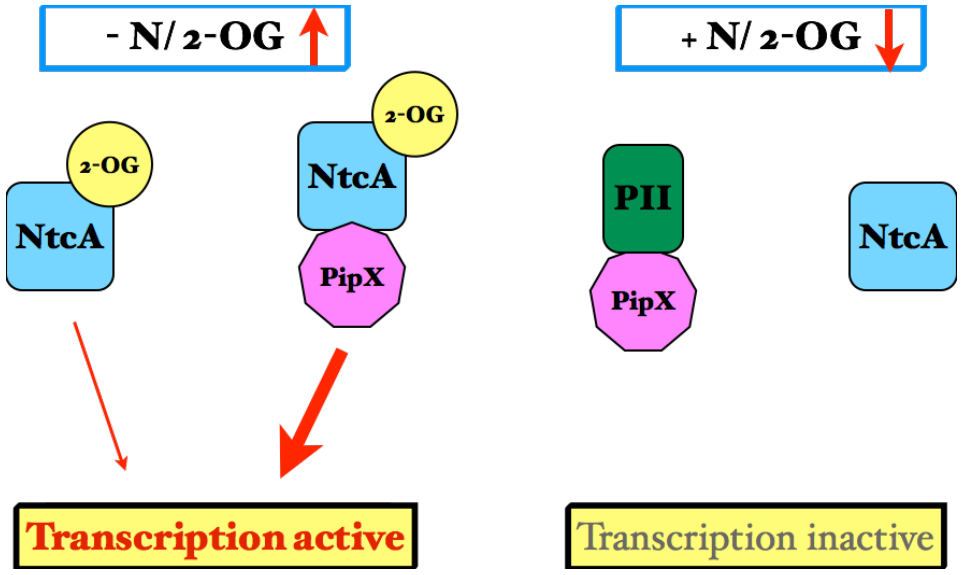

Figure 13: Schematic model of the proposed mode of action of PipX, NtcA and P_{II}. Left panel shows the situation of nitrogen deprivation where the level of 2-OG increased. Right panel shows the situation with nitrogen where the level of 2-OG is not increased.

OBJECTIVES

The aim of the work described in this thesis was to further understand in the diversity of adaptations related with nitrogen metabolism in the marine picocyanobacteria *Prochlorococcus* and *Synechococcus*. The thesis can be divided three main parts corresponding to each chapters:

1. Diversity of the N/C balance regulation in three different strains of *Prochlorococcus marinus* (MIT9313, SS120 and PCC 9511). It has been specified in the following objectives:

    a. Role of the 2-oxoglutarate: determination of the intracellular concentration
    b. Effect of azaserine addition on the metabolism of *Prochlorococcus*
    c. Comparative study of the interaction NtcA-*glnA* promoter of *Prochlorococcus*

2. Physiological characterization of glutamine synthetase from *Synechococcus* WH7803.

3. Effect of nanomolar concentration of different nitrogen sources on nitrogen metabolism of *Synechococcus* WH7803.

MATERIALS AND METHODS

1. STRAINS AND CULTURING OF CYANOBACTERIA

1.1. *Prochlorococcus marinus*

The *Prochlorococcus marinus* strains PCC 9511 (high-irradiance-adapted, HL, axenic and genetically identical to MED4), SS120 (low-irradiance-adapted, LL) and MIT9313 (low-irradiance-adapted, LL) were used in this study. The strains were provided by the *Roscoff Culture Collection* (*Station Biologique de Roscoff*, France), the *Pasteur Culture Collection* (*Institute Pasteur*, Paris, France) and the *Cyanobacteria Culture Collection* of *Massachusetts Institute of Technology* (Cambridge, United States).

Table 9: Characteristics of the *Prochlorococcus* strains used in this work

Strain	Ecotype	Origin	Depth	Remarks
PCC 9511	HL	NW Mediterranean	5 m	First axenic strain
SS120	LL	Sargasso Sea	120 m	
MIT9313	LL	North Atlantic	135 m	

1.1.1. Culturing

Prochlorococcus strains were routinely cultured in polycarbonate Nalgene flasks (50 mL) using PCR-S11 medium as described (Rippka *et al.*, 2000). The seawater used as the basis for this medium was kindly provided by the Instituto Español de Oceanografía (Spain). The medium was prepared as follows: the seawater was filtered using a bracket with an stainless steel 90 mm diameter filter from *Millipore,* pre-filter of fiberglass (*Millipore*) and a 0.22 μm filter (*Millipore*). The result was sterilized at 121 ºC, and 1 atm of pressure for 20 min. When the sterilized seawater reached the room temperature, the enrichment nutrients solution (table 10) was added. After that, the medium was filtered again under a sterile laminar flow hood with the filter previously sterilized. The PCR-S11 medium was stored at room temperature.

Table 10: Composition of the PCR-S11 medium (Final volume 1 L)

Enrichment solution	Volume	Final concentration
Hepes-NaOH 1M pH 7.5	1 mL	1 mM
EDTA-Na_2/$FeCl_3$ 2 mM *	1 mL	2 µM
$(NH_4)_2SO_4$ 400 mM	1 mL	400 µM
Phosphate buffer 50 mM pH 7.5	1 mL	50 µM
Trace metals (Gaffron + Se) **	0.1 mL	-

*** EDTA-Na_2/$FeCl_3$ 2 mM was prepared as follows: 0.54 g of $FeCl_3 \cdot 6\ H_2O$ in 20 mL of HCl 0.1 N and 0.744 g of Na_2-EDTA in 20 mL of NaOH 0.1 N. Mix them and complete the volume until 1 L.**

**** See Table 11.**

Table 11: Composition of Gaffron + Se Solution

Trace Metals	Stock Concentration	Final Concentration (nM)
$MnSO_4 \cdot H_2O$	0.6 mM	30
SeO_2	30 µM	1.5
$KAI(SO_4)_2 \cdot 12\ H_2O$	60 µM	3
$VSO_5 \cdot 5\ H_2O$	6 µM	0.3
H_3BO_3	3 mM	150
$Na_2WO_4 \cdot 2\ H_2O$	6 µM	0.3
$Cr(NO_3)_3 \cdot 9\ H_2O$	6 µM	0.3
$NiCl_2 \cdot 6\ H_2O$	30 µM	1.5
$(NH_4)_6Mo_7O_{24} \cdot 4\ H_2O$	4.2 µM	1.45
$CuSO_4 \cdot 5\ H_2O$	30 µM	1.5
KBr	60 µM	3
KI	30 µM	1.5
$ZnSO_4 \cdot 7\ H_2O$	60 µM	3
$Cd(NO_3)_2 \cdot 4\ H_2O$	30 µM	1.5
$Co(NO_3)_2 \cdot 6\ H_2O$	30 µM	1.5

Cultures were grown in a culture room set at 24 ºC under blue irradiances: 40 µE/m^2/s for high-light adapted ecotypes and 4 µE/m^2/s for low-light adapted ecotypes using neon *Sylvania* F18W/154-ST *Daylight*, covered with a filter *Moonlight blue L183* from *Lee Filters*. The strains were conserved in liquid culture in flasks of 50 mL *Nunclon Δ Surface* and all of them were refreshed every 5 days with a 1/5 dilution using PCR-S11 medium.

Figure 14: Culture room for *Prochlorococcus* and *Synechococcus.*

1.1.2. Cryopreservation

Cryopreservation was carried out according to ---. At the end of the exponential phase of culture, 50 mL were transferred to a sterilized centrifuge tube and centrifuged at 7,700 *g* for 15 min and 24 ºC. The supernatant was poured and the pellet resuspended with 1 mL of medium PCR-S11. This volume was transferred to a new *eppendorf* tube. 7.5% DMSO (dimethyl sulfoxide) added, mixed and stored at -80 ºC. To revitalise the culture the eppendorf was taken from -80 ºC to a sterile laminar flow hood, using low light in the room. Small amount of cells were scraped and transferred them into 25 mL of PCR-S11 medium and then incubated at 24 ºC in the culture room.

1.2 *Synechococcus marinus*

Synechococcus WH7803 (high-irradiance-adapted, axenic) and a SigF mutant derived from that strain were kindly provided by Prof. Wolfgang Hess (University of Freiburg, Germany).

Table 12: *Synechococcus* strain used in this work

Strain	Ecotype	Origin	Depth	Remarks
WH7803	HL	Mesotrophic waters		
WH7803 ΔSigF	HL	Mesotrophic waters		Provided by Prof. W.R. Hess

1.2.1. Culturing

Cultures of *Synechococcus* WH7803 and *Synechococcus* WH7803 ΔSigF were grown in a chemically defined artificial seawater medium (ASW) (Table 13) (Moore *et al.*, 2007). Cells were grown in a culture room under continuous blue light conditions at 40 μE/m^2/s and 24 ºC. Cultures were routinely cultured in polycarbonate Nalgene flasks (50 mL) and diluted every one or two weeks with 1/10 parts of fresh media.

Table 13: ASW composition

Components	Final Concentration
Turk´s Island Salt Mix (1)(5):	
NaCl	481 mM
$MgSO_4 \bullet 7\ H_2O$	28 mM
$MgCl_2 \bullet 6\ H_2O$	27 mM
$CaCl_2 \bullet 2\ H_2O$	10 mM
KCl	9 mM
Macronutrients (5):	
NaH_2PO_4 (2)	50 μM
$(NH_4)_2SO4$	400 μM
Buffers (5):	
$NaHCO_3$ (3)	6 mM
HEPES (4)	1 mM
Trace metals (5):	
$Na_2EDTA \bullet 2\ H_2O$	0.1170 μM
$FeCl_3 \bullet 6\ H_2O$	0.1180 μM
$ZnSO_4 \bullet 7\ H_2O$	0.0008 μM
$CoCl_2 \bullet 6\ H_2O$	0.0005 μM

(1) Turk´s Island salts were prepared by dissolving each salt in order into ultrapure water and sterilizing in autoclave. The filter-sterilized macronutrients, HEPES and $NaHCO_3$ buffers, and trace metal mix were added to sterilized salt mix and stored up to one month at room temperature.

(2) The NaH_2PO_4 solution should be adjusted to pH 7.5 with NaOH before sterilizing.

(3) The $NaHCO_3$ should only be stored for up to one month.

(4) The HEPES solution should be adjusted to pH 7.5 with NaOH before sterilizing.

(5) The macronutrient stock, the trace metals and buffers were prepared using chemicals of highest grade to avoid trace metals contamination. The chemicals were dissolved with ultrapure water and filter-sterilized through 0.2 μm syringe filter. All of them in separate containers stored at 4 ºC.

1.2.2. Cryopreservation

200 mL of cultures were centrifuged for 10 min at room temperature at 10,000 *g* using a JA-14 rotor. The pellet was resuspended in 5,78 mL of ASW with 7.5% DMSO. The solution was transferred into a 10 mL falcon tube. The vial was immediately placed into liquid nitrogen and stored at -80 ºC. Frozen cells were thawed in a water bath at 37 ºC until the half was liquid and transferred into sterile medium to revitalise the culture.

2. CELL COLLECTION

2.1. *Prochlorococcus*

When cultures reached 0.05 at A_{674}, cells were centrifuged at 26,000 *g* for 8 min at 4 ºC using an *Avanti J-25 Beckman* centrifuge equipped with a JA-14 rotor. After pouring most of the supernatant and carefully pipetting out the remaining medium, the pellet was directly resuspended in the corresponding volume of buffer (generally 1 mL per litre of culture of its corresponding solution; table 14). For western blotting the proportion was 0.5 mL per litre of culture and for proteomic studies 10 L of culture were resuspended in 2 mL of buffer. For protein assays (enzymatic and western blotting) the solution was Tris-HCl 50 mM pH 7.5 and for RNA analysis the pellet was resuspended in 10 mM of sodium acetate (pH 4.5), 200 mM sucrose and 5 mM EDTA. For proteomic approaches we used a specific cold buffer (25 mM ammonium bicarbonate including 1 mM of a cocktail of proteases inhibitors (*Sigma*)).

Table 14: Buffer using for cell collection

ASSAY	BUFFER COMPOSITION
Protein assays	Tris-HCl 50 mM pH 7.5
RNA analysis	10 mm sodium acetate (pH 4.5); 200 mM sucrose and 5 mM EDTA
Proteomic analysis	25 mM ammonium bicarbonate and 1 mM cocktail of proteases inhibitor

In the experiments studying nutrient starvation, cultures were centrifuged as described above. The pellets were then washed with PCR-S11 medium limited of the corresponding nutrient and finally diluted with the same original volume of medium, using standard PCR-S11 for controls, or medium without the addition of the corresponding nutrient supplementation (either nitrogen, iron or phosphorus); therefore, the media were under limited nutrient condition, but not completely deprived of it,

because they were made with natural seawater, except for *Synechococcus* WH7803 which used ASW, that is an artificial medium.

For experiments requiring darkness, culture bottles were completely covered with two layers of aluminium foil. For experiments with inhibitors, 0.06 µM DBMIB (2,5-dibromo-3-methyl-6-isopropyl-*p*-benzoquinone) was dissolved in ethanol prior to addition to the cultures. 0.3 µM DCMU [diuron, 3-(3-4-dichlorophenyl)-1,1-dimethylurea], 1, 5, 20, 50 and 100 µM of azaserine and 100 µM of MSX (L-metionine sulfoximine) were dissolved in culture media.

2.2 *Synechococcus*

When cultures reached between 0.1-0.12 at A_{550}, cells were centrifuged at 26,000 *g* for 8 min at 4 ºC using an *Avanti J-25 Beckman* centrifuge equipped with a JA-14 rotor. To analyze the addition of different sources of nitrogen, the pellet was washed with ASW medium without nitrogen and then resuspended in ASW medium without nitrogen and supplemented with different nitrogen sources (from nM to µM of nitrite and nitrate). For the experiments requiring darkness, the process was the same as described in 2.1 for *Prochlorococcus*. Finally, the cells were resuspended in the same buffer shown in table 14.

3. PREPARATION OF CELL EXTRACTS

3.1. French Press

After thawing, the cell suspensions were broken in a French pressure cell (*SLM/Aminco model FA-079*) at 16,000 psi; the obtained extracts were centrifuged for 10 min at 16,900 *g* and 4 ºC in an *Eppendorf* microfuge *5418R*. The supernatant was transferred to a new tube.

3.2. Freezing/thawing

Cells were centrifuged using a *Avanti J-25 Beckman* centrifuge with the JA-14 or JA-20 rotor. The pellet obtained was resuspended in its corresponding solution and frozen at 80 ºC. After thawing in ice, the extract was centrifuged for 10 min at 16,900 *g* and 4 ºC in an *Eppendorf* microfuge *5418R*. The supernatant was used for activity assay and the pellet was used to measure chlorophyll concentration.

3.3 Glass beads

We used two different protocols, depending on the organism:

3.3.1. *Prochlorococcus*

320 µL of the cell suspension were mixed with 180 mg of glass beads *B. Braun Melsungen AG* (0.10- 0.11 mm of diameter). Then, the mix was subjected to 7 cycles of 1 min vortex-1 min ice. It was centrifuged at 16,900 *g* for 5 min and 4 ºC with an *Eppendorf* microfuge *5418R*. The supernatant was used immediately.

3.3.2. *Synechococcus*

After thawing, the samples were centrifuged at 16,900g for 10 min and 4 ºC in an *eppendorf* microfuge *5418R*. The supernatants were poured and the pellets were resuspended in 250 µL of 50 mM Tris-HCl pH 7.5. These suspensions were mixed with 140.6 mg of glass beads *B. Braun Melsungen AG* (0.10 - 0.11 mm of diameter). After that, 5 cycles of 3 min vortex-3 min ice were done. The mixtures were centrifuged at 16,900 *g* for 5 min at 4ºC. Finally the supernatants were used for enzymatic activities. For western blotting some changes were introduced in the protocol in order to increase the concentration of the sample: the pellet was resuspended in 50 µL of 50 mM Tris-HCl pH 7.5 and mixed with 28.125 mg of glass beads *B. Braun Melsungen AG* (0.10-0.11 mm of diameter).

4. ANALYTICAL DETERMINATION

4.1. Growth of cyanobacteria

Growth of *Prochlorococcus* samples was determined by measuring the absorbance of aliquots of cultures at 674 nm (El Alaoui *et al.*, 1999). For *Synechococcus* WH7803 a wavelength scan was made using the spectrophotometer *Beckman DU 640* from 350 nm to 800 nm**.** Finally, the growth of *Synechococcus* WH7803 was determined by measuring the absorbance of aliquots of cultures at 550 nm.

4.2. Determination of the purity of *Prochlorococcus* and *Synechococcus* strains

The purity of the cultures was checked as follow: petri dishes were filled with PCR-S11 medium or ASW medium with 8 g per L of agar and enriched with 1 g D+ glucose and 0.2 g of casein acid hydrolysate per litre of medium. Two different inoculums volumes were tested, 50 and 200 mL. The absence of bacterial colonies on plates after 6 days of inoculation were compared with a positive control consisting in a similar volume of non-bacteria-free *Prochlorococcus* culture.

4.3. Determination of the fluorescence spectra of *Prochlorococcus*

Prochlorococcus marinus has chlorophyll a_2 and b_2, exhibiting big differences in their proportion among strains (Morel *et al.*, 1993, Partensky *et al.*, 1993), leading to a fluorescence emission spectrum that differs between surface and depth ecotypes (figure 15). This is a classical method to realize a phenotypic analysis between strains.

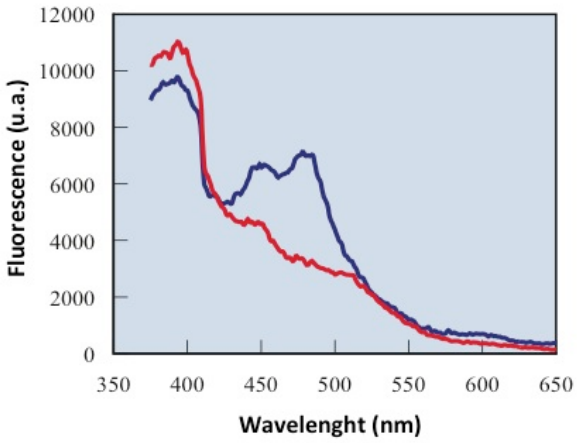

Figure 15: Spectrum of fluorescence from *Prochlorococcus* high-light-adapted (Red) and low-light-adapted (blue).

Routinely, aliquots from cultures were measured in a *Pelkin-Elmer LS50B* fluorimeter with a quartz cuvette 101-OS 10 mm (*Hellma*). The fluorescence excitation spectrum from 375 nm to 650 nm was measured with the fixed emission wavelength at 680 nm.

4.4. Determination of chlorophyll and phycoerythrin

Chlorophyll from *Prochlorococcus* was determined using the method described by Mackinney (Mackinney, 1941). The samples were centrifuged at 16,900 *g* for 5 min

at room temperature. The pellet was resuspended in 1 mL of 100% ethanol and centrifuged again at 16,900 *g* for 5 min at room temperature. Finally, the absorbance from the supernatant was measured at 665 nm. For the calculation of the concentration of chlorophyll we used the following equation:

$$Abs_{665\ nm} = 0.074069 \times -2.996 \cdot 10^{-4}$$

Phycoerythrin (PE) from *Synechococcus* WH7803 was measured as described (Wyman, 1992). PE was extracted as explained in 3.3.2. PE concentration was determined by measuring absorption at 542 nm with a molar extinction coefficient for the hexamer of $2.15 \times 10^6\ cm^{-1}\ M^{-1}$. The equation used was:

$$PE\ in\ \mu g/mL = 106 \times A_{542}$$

4.5. Determination of photosynthetic capacity

250 mL of culture were centrifuged at 26,000 *g*, for 8 min at 4 ºC. The pellet was resuspended in 2 mL of PCR-S11 medium and used to fill a 24 well culture plate (*Biofil*). Then, the fluorescence of the chlorophyll was measured using a system imaging-PAM *WALZ IMAG-K5*. The photosynthetic radiations used were 11 and 36 µE. The parameters Fo, Fo´(minimal fluorescence from dark- and light-adapted respectively), Fm, Fm´(maximal fluorescence from dark- and light-adapted respectively) F and F´ (fluorescence emission from dark- or light-adapted respectively) were determined.

4.6. Determination of protein concentration

Protein concentration of soluble fractions was determined by the *Bio-Rad Protein assay* according with the Bradford method (Bradford, 1976). The samples were diluted 1:1000 and the *Bio-Rad Protein assay* was diluted 1:5. After that, we mixed 100 µL of the reagent and 100 µL of diluted sample in a 96 well plate. The reaction was measured at 595 nm using a *Multiskan* system from *Thermo Fischer*. A standard curve was made in all determinations in order to avoid the variability of the reagent by preparing a serial dilution of 1 mg/mL of bovine seroalbumin.

4.7. Quantification of concentration and quality of nucleic acids

Nucleic acid samples (DNA and RNA) were checked for concentration and quality using the *NanoDrop ND-1000* spectrophotometer (*NanoDrop Technologies*, Inc. Wilmington, USA). To measure nucleic acid samples the "Nucleic Acid" application module was selected. 2 µl of the sample were pipetted onto the lower measurement pedestal and 2 µl of *milliQ* water were used as blank. Sample concentration was determined in ng/µL based on absorbance at 260 nm. To assess the purity of the nucleic acids the ratios 260/280 and 260/230 were used. The value of the ratio 260/280 had to be between 1.8-2.0; if it was appreciably lower, it may indicate the presence of protein, phenol or other contaminants that absorb at or near 280 nm. The ratio 260/230 is a secondary measure of nucleic acid purity. It is commonly in the range of 1.8-2.2. If the ratio is appreciably lower, this may indicate the presence of copurified contaminants.

4.8. Determination of intracellular concentration of 2-OG

An enzymatic method based on the oxidation of NADPH in the reaction catalyzed by the glutamate dehydrogenase was used (Senior, 1975). This enzyme catalyzes the production of glutamate from ammonium and 2-OG using NADPH as reducing power with a stoichiometry of 1:1. The reaction was optimized for *Prochlorococcus* samples. The extracts of *Prochlorococcus* were obtained as explained in 3.2. The reaction mixture content is shown in table 15. The NADPH consumption was monitorized by measuring the absorbance at 340 nm by using a *Beckman DU-640* for 10 min, in 104-QS 10 mm (*Hellma)* quartz cuvettes thermostatized at 35ºC.

Table 15: Composition of the reaction mixture

Composition of the mixture	Concentration of the stock solution	Volume (µL)	Final concentration
Tris-HCl pH 8.0	1 M	85	0.085 M
NADPH	2 mM	100	0.2 mM
GDH (*Fluka*)	1 mg/ mL	5	5 µg/1000 µL (ca. 0.15 UI)
NH_4Cl	0.5 M	200	0.1 M
***Prochlorococcus* extract**	-	200	-
H_2O	-	610 (up to 1000)	-

For the quantification of the intracellular concentration of 2-OG a standard curve was calculated (figure 16) with different known concentrations (from 10 to 100 µM) of 2-OG (*Sigma*).

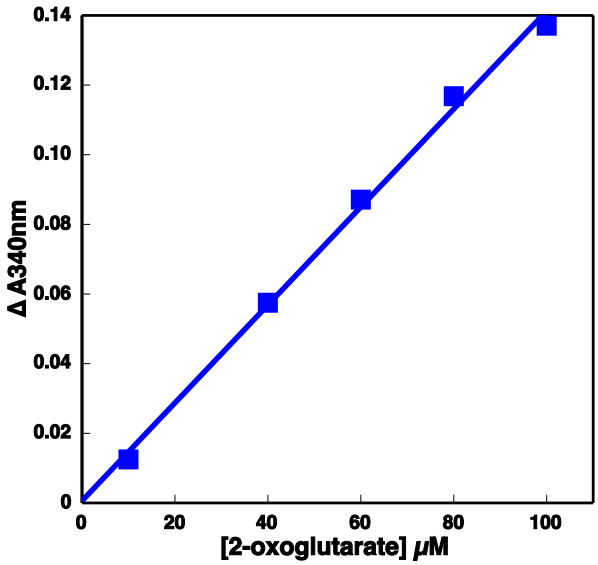

Figure 16: Standard curve for quantification of 2-OG.
The equation is: f(x) = 0.0014 x + 0.000598 and R^2 = 0.9958

4.9. Oxidative modification of NADP-isocitrate dehydrogenase

For the inactivation of ICDH by the Fe^{3+}/ascorbate system (Gómez-Baena *et al.*, 2001), incubations were carried out at 4°C in a solution containing 50 mM Tris-HCl buffer pH 7.6, 0.2 mM $FeCl_3$ and variable concentrations of ascorbate (1, 5 or 10 mM).

The ascorbate solution was prepared as follows: 100 µL of 20 mM dithiothreitol was added to 9 mL of 100 mM ascorbate, in order to keep ascorbate under reduced conditions; after carefully neutralizing this solution with 1 mM NaOH, the volume was adjusted to 10 mL.

The inactivation reactions were initiated by the addition of ascorbate. Distilled water further purified with a *Millipore MilliQ* system was used in the preparation of the inactivation reaction mixtures to avoid the effect of metal traces. After the treatment, ICDH activity was determined following 4.10.2.

4.10. Determination of enzymatic activities

4.10.1. Determination of the glutamine synthetase transferase activity from *Prochlorococcus* and *Synechococcus*

The glutamine synthetase transferase activity was measured in both organisms by using different methods to extract the enzyme. *Prochlorococcus* cells were frozen/thawed and then centrifuged at 16,900 *g* for 10 min and the supernatant collected; for *Synechococcus* the cells were disrupted using glass beads (3.3.2).

Glutamine synthetase transferase activity was determined as previously described (Sampaio *et al.*, 1979). The composition of the reaction mixture was 500 µl of solution A (table 16), 200 µL of water, 50 µL of sample and 250 µL of solution B (table 16). The reaction mixture was incubated for 30 min at 37ºC shaking at 40 u.m. After that, 3 mL of iron solution (table 16) was added to 1 mL of reaction mixture, it was incubated for 10 min and the complex produced (γ-glutamyl hydroxamate) was measured by determining the absorbance at 510 nm. One unit of activity is the amount of enzyme that transforms 1 µmol of substrate per min.

Table 16: Composition of the solutions for GS activity

Solution A (*)	Amount (for 100 mL)	Final concentration
MOPS 0.25 M pH 7.0	40 mL	0.1 M
Glutamine	2.92 g	200 mM
$MnCl_2 \cdot 2\ H_2O$	1.97 mg	100 µM
$NH_2OH \cdot HCl$	0.138 g	20 mM
H_2O	60 mL	-

Solution B (*)	Amount (for 100 mL)	Final concentration
MOPS 0.25 M pH 7.0	50 mL	40 µM
ADP	1.7 mg	200 mM
$Na_2AsO_4H \cdot 7\ H_2O$	6.24 mg	0.125 M
H_2O	50 mL	-

Iron solution (**)	Amount (for 1 L)	Final concentration
HCl concentrated	7.73 g	0.27 % (v/v)
Trichloroacetic acid	12.04 g	1.2 % (p/v)
$FeCl_3 \cdot 6\ H_2O$	33.33 g	123.3 mM

(*) Solution A and B stored at 4º C. (**) Iron solution stored at room temperature.

4.10.2. Determination of the NADP-isocitrate dehydrogenase activity from *Prochlorococcus marinus*

For measuring the NADP-isocitrate dehydrogenase activity the cell extracts were obtained using a French press as mentioned in 3.1.

Isocitrate dehydrogenase (ICDH) activity was determined as previously described (López-Lozano, 2007) with modifications. The reaction mixture is shown in table 17. Isocitrate was added last to start the reaction. 1 mL of 50 mM Tris-HCl pH 7.5 was used as a blank for the spectrophotometer. NADPH production was monitorized by determining absorbance at 340 nm for 10 min, in thermostatized cuvettes at 40 ºC. Blank without isocitrate was measured at the same time that the samples, and the result was substracted from the average of the samples. The slope of the curve between 6 and 10 min was used to calculate the ICDH activity. For all enzymatic activities, one unit of activity is the amount of the enzyme that transforms 1 µmol of substrate per min.

Table 17: Composition of the reaction mixture for NADP-IDH activity

Reaction mixture	Volume (µL)	Final concentration (mM)
Tris-HCl 50 mM pH 7.5	840	50
$MnSO_4$	20	2
Cell extract	100	-
$NADP^+$ 10 mM	20	0.2
Isocitrate 100 mM	20	2

4.10.3. Determination of aminating glutamate dehydrogenase activity from *Prochlorococcus marinus*

For the determination of aminating glutamate dehydrogenase activity (GDH activity), cells were disrupted by using glass beads as described in section 3.3.1.

Aminating glutamate dehydrogenase was determined *in vitro* as described for the enterobacteria *Klebsiella pneumonia* (Kim *et al., 2002*) and the cyanobacterium *Synechocystis* PCC 6803 (Florencio *et al.*, 1987, Chávez & Candau, 1991). The GDH activity was determined by following the oxidation of NADPH at 340 nm for 10 min using a spectrophotometer *Beckman DU 640* thermostatized at 35 ºC. The reaction mixture is shown in table 18. The same mixture without ammonium chloride was used as blank for the reaction.

One unit of activity NAD(P)H-GDH is the amount of enzyme that transforms 1 µmol of NADPH per min.

Table 18: Composition of the reaction mixture for NADPH-GDH dehydrogenase

Reaction mixture	Volume (µL)	Final concentration (mM)
Tris-HCl 1M pH 8	85	85
2-OG 0.1 M	100	10
NH_4Cl 0.5 M	200	100
Cell extract	40	-
NADPH 2 mM	100	0.2
H_2O	Up to 1000	-

4.10.4. Determination of the nitrate reductase activity from *Synechococcus*

The method used to determine the nitrate reductase (NR) was described (Paneque *et al.*, 1965). The assay mixture (table 19) was incubated at 30ºC for 10-30 min. The reaction was stopped shaking vigorously in a vortex until the dithionite ($Na_2S_2O_4$) was completely oxidized (the blue-violet colour disappeared). After that, 500 µL of water, 1 mL of sulphanilamide (4-aminobenzenesulfonamide, dissolved in HCl, stored in opaque bottles) and 1 mL of NNEDA (N-(1-naphthyl)ethylenediamine, stored in opaque bottles) were added to the assay mixture to determine the formation of nitrite. After 10 min to allow the appearance of the pink colour, absorbance at 540 nm was determined in a *Beckman DU-640* spectrophotometer, to calculate nitrite concentration.

One unit of nitrate reductase was defined as the amount of enzyme that will catalyse the formation of 1 µmol of NO_2^- per min under the conditions of the standard assay.

Table 19: Composition of the reaction mixture

Composition	Volume (µL)
NR mix (table 20)	250
Sample	200
Dithionite 46 mM (*)	50

(*) Dithionite 46 mM was dissolved in Tris-HCl 500 mM pH 7.5, freshly prepared.

Table 20: Composition of NR Mix

Composition	Volume (mL)
Tris-HCl pH 7.5 50 mM	40
KNO_3^- 100 mM	20
Methyl viologen 2 mM	20
H_2O	20

(*) This NR mix could be stored up 2 months at 4ºC.

For the calculation a standard curve with different known concentration of NO_2 is required (figure 17).

During the determination of NR activity we had the problem that the colour of *Synechococcus* pigments interfered in the measurement. We followed different

strategies to avoid it: one of them was adding 50 µL of 2 M of $ZnSO_4$ and 50 µL of 2 M of NaOH to the mixture to remove pink debris (absorbing at 550 nm). The other strategy was using different combinations of blank assay mixtures, for instance: blank without nitrate, blank without sample, blank without dithionite and blank with methyl viologen and dithionite, then vortex until the colour disappeared and the sample was added.

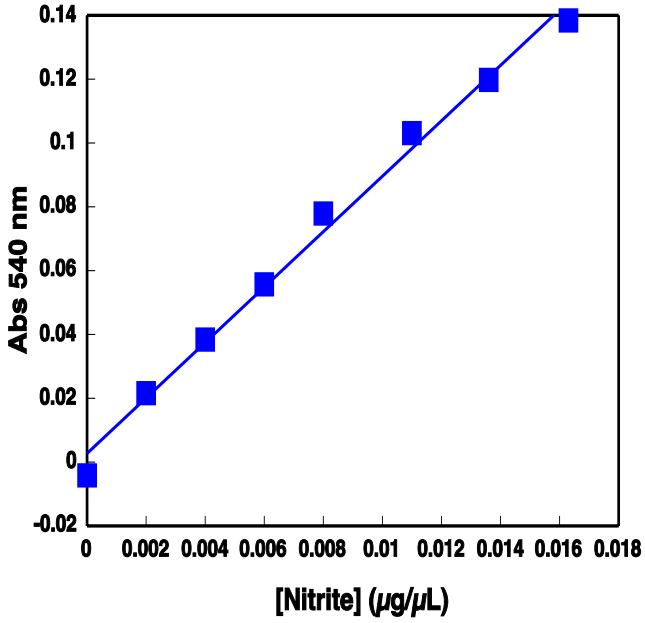

Figure 17: Standard curve for nitrate reductase activity.
f(x) = 8.6861 x + 0.0027; R^2 = 0.9918

5. ANALYSIS OF NUCLEIC ACIDS

5.1. Extraction of genomic DNA

50 mL from *Prochlorococcus* or *Synechococcus* cultures were centrifuged at 27,200 *g* for 10 min. After pouring the supernatant, the pellet was resuspended in 400 µL of the buffer TE (table 21). The mix was transferred to a 1.5 mL eppendorf tube with 150 µL of glass beads *B. Braun Melsungen AG* (0.10 - 0.11 mm of diameter), 20 µL of 10% SDS, 225 µL of phenol (pH 6.0) and 225 µL of chloroform:isoamyl alcohol (24:1). The following cycle was repeated 4 times: 1 min vortex- 1 min on ice. The mixture was centrifuged at 15,700 *g*, at 4ºC for 15 min. The upper phase was transferred to a new 1.5 mL eppendorf tube, then 250 µL of phenol (pH 6.6) and 250 µL of chloroform: isoamyl alcohol (24:1) were added, mixed and centrifuged at 15,700 *g* for 10 min at 4ºC. The upper phase was transferred to a new 2 mL eppendorf, the

volume was completed up 2 mL with cold ethanol and kept at -20 ºC between 2-3 hours. Then centrifuged at 15,700 *g*, at 4 ºC for 30 min. The supernatant was taken and the pellet was dried, resuspended with 50 µL of *milliQ* sterilized water and kept at 4 ºC. The resulting material was quantified using *NanoDrop* system and visualized in an agarose gels.

Table 21: Composition of TE buffer

Composition	Volume (µL)
Tris-HCl 50 mM pH 7.5	200
EDTA 100 mM pH 8	1
Distilled H_20	800

5.2. RNA extraction

RNA from *Prochlorococcus* and *Synechococcus* was extracted using the following methods: the RNA from *Prochlorococcus* was routinely extracted using the *Aurum* kit, while the RNA from *Synechococcus* was obtained using the *Trisure* method (since after testing different methods this one was proved to give the best result).

5.2.1 RNA extraction with the *Aurum* kit (*Bio-Rad*)

RNA was extracted by using the *Aurum Kit* (*Bio-Rad*), according to the manufacture instructions. This kit includes a DNase step to remove any remaining genomic DNA from RNA samples, thus ensuring that all cDNA was produced by reverse transcription from mRNA.

5.2.2 RNA extraction using the *Trisure* kit (*Bioline*)

250 µL of sample were centrifuged at 16,900 *g* for 1 min at 4ºC. 100 µL of lysozyme (50 µg/µL) were added to the pellet and then resuspended and incubated for 5 min. Then the homogenization step was done: 800 µL of *Trisure* (*Bioline*) were added and mixed vigorously. Samples were incubated for 5-10 min at room temperature. Centrifuged at 16,900 *g*, for 5 min at 4 ºC, the supernatant taken into a new clean *eppendorf* and 0.2 ml of chloroform was added. The tubes were capped securely and shaked vigorously manually for 15 s. Samples were incubated for 10 min at room temperature and then centrifuged at 16,900 *g* for 10 min and 4 ºC. The samples were separated into a pale green, phenol-chloroform phase, an interphase, and a colourless

upper aqueous phase, which contains the RNA. The aqueous phase was transferred very carefully, without disturbing the interphase to another tube. The RNA was precipitated by mix with cold 100% isopropanol (ca. 500 µL). The samples were incubated for 15 min at room temperature and then centrifuge at 16,900 g for 20 min at 4 ºC. The supernatants were removed. The pellet were washed once with 750 µL of 75% cold ethanol, mixed by vortex and centrifuged at 7,500 *g* for 5 min at 4 ºC. An additional LiCl 8 M precipitation step was included at the end of the procedure to improve the RNA quality. After overnight, 750 µL of 75% cold ethanol were added, samples centrifuged at 7,500 *g*, 5 min at 4 ºC and pellet resuspended in 20 µL of sterilized *milliQ* water. RNA was stored at -80 ºC.

Treatment with DNAase I

After the extraction of RNA with the *Trisure* kit, a step with DNase I (RNase-free) (*Ambion*) was required to degrade DNA in the presence of RNA when the absence of RNase is critical to maintain the integrity of the RNA. The procedure to remove contaminating genomic DNA from RNA samples was: 2 µL of 10x DNase I Buffer and 1 µL of rDNase I were added to 400 ng – 1 µg of RNA and mixed gently. Then, the samples were incubated at 37 ºC for 30 min. 2 µL of resuspended *DNase Inactivation Reagent* were added and mixed well, and the samples incubated for 10 min at room temperature. Then, centrifuged at 16,900 *g,* for 5 min at 4 ºC and transferred the RNA to a new tube. 1 µL of RNA treated was used for PCR test.

5.2.3. Determination of concentration and quality of RNA

After the extraction, RNA was quantified using a *NanoDrop* system (4.7) spectrophotometer and its quality visualized by electrophoresis on a 1% agarose gel in order to check if there was any degradation.

5.3. Design and production of oligonucleotides

The sequences of cyanobacterial genes were obtained from CYORF (Cyanobacteria gene annotation database, http://cyano.genome.ad.jp/). The oligonucleotides used in this work were designed using the program *Oligo v4.05* (National Biosciences Inc. Plymouth), *Primer3* (University of Massachusetts Medical School) (http://biotools.umassmed.edu/bioapps/primer3_www.cgi) and refined manually.

The criteria used to design the oligonucleotides that were taken into account were: similar Tm (melting temperature) for each primer of the same pair, absence of secondary structures (self dimers, hairpins and cross dimers), similar percentage of G+C, and an approximate length of ca. 20 nucleotides.

Sigma and *Invitrogen* provided the oligonucleotides.

5.3.1. Oligonucleotides used for cloning

The oligonucleotides used for amplifying the different genes from *Prochlorococcus* are shown in the following sections. The optimal Tm of each pair of primers was selected doing a temperature gradient PCR.

***ntcA* MIT9313**

Oligonucleotides	Sequence 5´- 3´	Function
FNTC	TCATATTTCTGCCGTTTGCT	Amplification of *ntcA* (796 bp)
RNTC	AACCCGTTTCACCATCCT	
FNNM2	CATATGATGGCCAACTCGCCTGCT	Introduction of NdeI-BamHI restriction sites
RBNM2	GGATCCTCAGTTGAATTTTTTAGCAAGGGC	

***ntcA* SS120**

Oligonucleotides	Sequence 5´- 3´	Function
FSNTC1	AATCTAGCGGGACTTGGAA	Amplification of *ntcA* (1036 bp)
RSNTC1	CCTCCCAAAAGAAGCAAAA	
FNNS2	CATATGATGACAGGTTCTGCTAACTC	Introduction of NdeI-BamHI restriction sites
RBNS2	GGATCCTTAGTTAAAACGTTTAGCAAG	

glnB MIT9313

Oligonucleotides	Sequence 5´- 3´	Function
FP2M	CCGTTTCTGACACACTTCCT	Amplification of *glnB* (468 bp)
RP2M	ATGAATACCTGCTCTGGCTG	
FN2PM2	GGCATATGATGAAGAAAGTCGAGGCGATT	Introduction of NdeI-BamHI restriction sites
RB2PM2	GGATCCCTAGAGGGCCTTGCTGTCAC	

glnB SS120

Oligonucleotides	Sequence 5´- 3´	Function
FSP22	CTAATGATGCGATGGAAGC	Amplification of *glnB* (557 bp)
RSP22	TCAAAGGTCCAGCAGGTAA	
FNP2S2	CCATATGATGAAAAAGATAGAAGCAATTATC	Introduction of NdeI-BamHI restriction sites
RBP2S2	GGATCCTTAAAGAGCTGAATCGTCAG	

pipX MIT9313

Oligonucleotides	Sequence 5´- 3´	Function
FMPX1	TTGCTGCTATTTGTGCTTG	Amplification of *pipX* (570 bp)
RMPX1	CACCTTGTTCGCCTGTAGA	
FNXM2	CATATGGTGAGCGCCGAGCGCTAT	Introduction of NdeI-BamHI restriction sites
RBXM2	GGGATCCTCAGATAAAGGTCTGAGCAA	

***pipX* SS120**

Oligonucleotides	Sequence 5´- 3´	Function
FSPX1	GCTGAACAAGGTGCTGATT	Amplification of *pipX* (619 bp)
RSPX1	TTGACGCCATTAGGAAGAG	
FNXS2	CATATGTTGAGCTCAGGTTCAGAGCG	Introduction of NdeI-BamHI restriction sites
RBXS2	GGATCCTTAAAGAGCTGAATCGTCAG	

5.3.1.1 Generic oligonucleotides

Table 22 shows the oligonucleotides that were used for checking the ligation and for sequencing each step during the cloning process. SP6 and T7 were used for checking pGEM-T and pSPARK vectors and T7/T7 terminator for checking pET-15b.

Table 22: Generic Oligonucleotides

Oligonucleotides	Sequence 5´- 3´
T7	TAATACGACTCACTATAGGG
SP6	TATTTAGGTGACACTTATAG
T7 Terminator	GCTAGTTATTGCTCAGCGG

5.3.2. Oligonucleotides for qRT-PCR

The oligonucleotides used for qRT-PCR have the same properties that the oligonucleotides for cloning, however the product amplified had to be ca. 120 nucleotides. The Tm for oligonucleotides for RT-PCR was 58 ºC (for *Prochlorococcus*) and 56 ºC (for *Synechococcus*). All the oligonucleotides used are shown in the following sections.

***Prochlorococcus* SS120**

Oligonucleotides	Sequence 5´- 3´	Gene
SGF	CGCTCTTGTTCCTGGCTTC	*glnA*
SGR	AGCATCTCCTGACCTGAACTC	
FALL-3	CGTGGGAGTTGGGCTTG	*glsF*
RALL-3	TTAAACCTCCATCTGCTCTAAG	
SIF	AATTGTTGGAGGATTAGGAATGG	*icd*
SIR	ACTGAACCTGGATTAATTCTATCG	
FALL-1	AGCTCCTGCTGGCTCAGTTA	*ntcA*
RALL-1	GAGAAGTAGCCCAACCCCAC	
FALL-2	TTTGGGCGACAAAAAGGA	*glnB*
RALL-2	TCAACACTTTCATCAGCAACAA	
RT-FPS	CCACTTTTGGGATGCTTTAT	*pipX*
RT-RPS	ACTTCAAAATCTGCACCTCG	
SRF	CTCTCGGTTGAGGAAAGTC	*rnpB*
SRR	CCTTGCCTGTGCTCTATG	

***Prochlorococcus* MIT9313**

Oligonucleotides	Sequence 5´- 3´	Gene
RT-FGLM	CGTTGGAGGCGTTGTTATTT	*glsF*
RT-RGLM	CCGCAAAAGAAACCTCAAAG	
RT-FMI	CAACATGCTCTTCGGCTAAA	*icd*
RT-RMI	AGTTCATAGCCCCAGTCACG	
RT-FEGA	TTTTATTCTTTCCAACCGTG	*gdh*
RT-REGA	CATCGGCAGACCAGTAAGAC	
RT-FP2M	CGACGACGACAAGGTGGA	*glnB*
RT-RP2M	CTTGCTGTCACGCTCGCC	
RT-FTCA	GCGTGGGGTTACTTCTGC	*ntcA*
RT-RTCA	CGATGGACTGATGTGAGAGG	
RT-FPXM	TTACGCCACGCTCTATGC	*pipX*
RT-RPXM	AACAACTGCTGCCAACTCTC	
FRPM	CTATCTAGGACCGCCGTTAC	*rnpB*
RRPM	GAGAGTGCCACAGAAAAACA	

***Prochlorococcus* PCC 9511**

Oligonucleotides	Sequence 5´- 3´	Gene
RT-FNP	CCTGGAGATCCTGCTGAAAG	*ntcA*
RT-RNP	CAATTGCTCTCAAAACAGAA	
FG	AGACTGCATTACGGAAAGAGAAAGC	*icd*
RGH	CAGCAGCAGCATCAGAAACATAATC	
MGF4	TCCTAATGACACCGCACAAG	*glnA*
MGR4	CATGATGATGCTTCTCAGTTGG	
RT-FFPCC	TATCTCCACCCCCACATCAT	*glsF*
RT-RFPCC	GCATTCGCTTTGCTAACTCC	
FE	ACAGAAACATACCGCCTAAT	*rnpB*
RE	ACCTAGCCAACACTTCTCAA	
RT-FBP	TTGAGGCAATCATACGTCCA	*glnB*
RT-RBP	TCCAAATCCCCTGACTTCAC	

***Synechococcus* WH7803**

Oligonucleotides	Sequence 5´- 3	Gene
RT-FRNSY	TGAGGAGAGTGCACAGAAA	*rnpB*
RT-RRNSY	GTTTACCGAGCCAGCACCT	
RT-FNISY	AATTTGCTGAAATCGGTTGG	*nirA*
RT-RNISY	CAGTTGTTGTGCCGAAAGAA	
RT-FGS1SY	ATTTATCTGGCAGCGGTTTG	*glnAI*
RT-RGS1SY	TTCAATGGTGTCAACGCTGT	
RT-FGS3SY	AGGTGTGGGGGATTGAAAAT	*glnAIII*
RT-RGS3SY	AAGCAACAGGTAGGGATTGG	
RT-FGNSY	CTCCGGAAAGCATGTGAACT	*glnN*
RT-RGNSY	GCAGCACAGAACAACAGGAA	
RT-FNBSY	CTGATCCGTTTGAAGCCATT	*narB*
RT-RNBSY	AATCCTCGGTGTGAAACTGG	
RT-FSTN	TGATTTCTGGGGACTTCTGG	*nrtP*
RT-RSTN	CCCCAGGTTTGAAAGACAAA	

5.3.3. PCR (Polymerase Chain Reaction)

The standard PCR was done in 0.2 mL PCR tubes (*Sarstedt*), using two thermal cyclers: *GeneAmp PCR System 2400* (*Perkim-Elmer*) and *iCycler iQ Multicolor Real Time PCR Detection System* (*Bio-Rad*). The standard mix for PCR was 2.5 μL of 10x

buffer *(Biotools),* 0.2 mM of dNTP´s (*Biotools*), 0.8 ng/µL of primers and 0.5 U of polymerase (*Biotools*) and the final volume was completed up to 25 µL with *milliQ* water. For DNA template we used either genomic DNA, cDNA, plasmid or directly cells. 2 mL of cells were centrifuged at 16,900 *g,* for 10 min at 4 ºC. The pellet was resuspended in 15 µL of sterilized distilled water, after carefully removing all the PCR-S11 medium (that contains high salt concentration, and could therefore inhibit the polymerase).

The standard thermal program was 95 ºC for 5 min (denaturation), followed by 35 cycles of: 95 ºC for 30 s (denaturation), Tm for 30 s (annealing) and 72 ºC for 30 s (extension); an additional step of extension, 72 ºC for 5 min; and finally hold on at 4 ºC.

A high fidelity polymerase (*Fermentas*) was used for cloning in order to avoid mutations. The buffer was *10x High-fidelity PCR buffer*, with addition of 15 mM $MgCl_2$. The thermal program used was: 94 ºC for 3 min, followed by 30 cycles of: 94 ºC for 30 s, Tm for 30 s and 72 ºC for 1 min; then extra extension step of 72 ºC for 10 min.

5.3.4. Electrophoresis of nucleic acids in agarose gel

The DNA was subjected to electrophoresis on 1% or 1.7% agarose gel depending of the size of the fragment amplified, using either ethidium bromide (*Fluka*) or GelRed (*Biotium*) for visualization on UV light. The samples were prepared with 10 % (v/v) loading buffer (0.25% (p/v), bromophenol blue, 0.25% (p/v), Xylene cyanol and 30% (v/v) glycerol). The electrophoresis was performed in a *BioRad* system (7x10 cm *Mini-Sub Cell GT* and 15x10 cm *Wide Mini-Sub Cell GT*) using TBE 0.5x diluted 10 fold from TBE 5x (Table 23) for 30 min at 100 V. The size markers were 100-1000 pb (*gTPbio*) and 250-10.000 pb (*gTPbio*). For small fragments of DNA (ca. 26 nucleotides) polyacrylamide gel was used (9.1.1).

Table 23: Composition of TBE 5x

Components	Amount for 1 L
Tris base	54 g
Boric Acid	27.5 g
EDTA 0.5 M pH 8	20 mL

To better purify DNA fragments from agarose gel, low-melting point agarose (*Invitrogen*) in TAE buffer (table 24) was used.

Table 24: Composition of TAE 50x

Components	Amount for 1 L
Tris base	242 g
Acetic acid glacial	571 mL
EDTA 0.5 M pH 8	100 mL

To visualize the image from agarose gels, a *Molecular Imager ChemiDoc XRS + Imaging System* from *Bio Rad* (equipped with UV illumination at 302 nm) was used. The obtained image was analyzed with *Quantity One 1-D Analysis Software (Bio-Rad).*

5.4. Cloning

For cloning the *ntcA*, *glnB* and *pipX* genes from *Prochlorococcus* strains SS120 and MIT9313 to overexpress the corresponding proteins, the following methods were used.

5.4.1. Bacteria and culture conditions

Several strains of *E. coli* (table 25) were used in the different cloning steps (table 25).

E. coli HB101 and DH5α were transformed with the vectors pGEMT and pSPARK to conserve the clone. The strain BL21 (DE3) was used to overexpress the protein. The *Rosetta* strain was used in order to improve the overexpression providing six rare codon tRNAs (AUA, AGG, AGA, CUA, CCC and GGA), facilitating the expression of proteins that encode rare codons for *E. coli*.

Table 25: Strains of *E. coli* used in this work

Strain	Genotype
HB101	F^- mcrB mrr hsdS20 (r_B^- m_B^-) recA13 leuB6 ara-14 proA2 lacY1 galK2 xyl-5 mtl-1 rpsL20 (Sm^R) glnV44 λ^-
DH5α	F^- endA1 glnV44 thi-1 recA1 relA1 gyrA96 deoR nupG Φ80d*lacZ*ΔM15 Δ (*lacZYA-argF*)U169, hsdR17(r_K^- m_K^+), λ–
BL21(DE3)	F^- ompT gal dcm lon $hsdS_B$(r_B^- m_B^-) λ(DE3 [lacI lacUV5-T7 gene 1 ind1 sam7 nin5])
***Rosetta*(DE3)**	F^- *ompT* $hsdS_B$(r_B^- m_B^-) *gal dcm* (DE3) pRARE (Cam^R)

E. coli was cultured in *Falcon* tubes at 37 ºC with 200 rpm shaking overnight. The medium used was LB (Luria-Bertani) prepared liquid or solid (with agar). Both of them were sterilized in autoclave at 100 ºC for 20 min. Petri dishes were filled with LB agar under a laminar flow hood. The antibiotics used were filtered with 0.22 µm of *Millipore* filter and added at the required concentration.

5.4.2. Long time storage of *E. coli*

E. coli cultures were long term stored at -80 ºC, by mixing 0.75 mL of culture samples with 0.25 mL sterilized 60% glycerol (15% final concentration).

5.4.3. Plasmids

The plasmids used during this work are shown in table 26 with their main features.

Table 26: Plasmid used in this work

Plasmid	Description	Resistence	Reference/Source
pGEM-T System I *pGEM-T easy vector*	A linearized vector with a single 3´- terminal thymidine at both ends. The T overhangs at the insertion site greatly improve the efficiency of ligation of PCR products by preventing recircularization of the vector and providing a compatible overhang for PCR products generated by certain thermostable polymerases.	Amp	*Promega*
pET15b	The pET system is for cloning and expression of recombinant proteins in *E. coli*. It carries a N-terminal His-Tag sequence followed by a thrombin site and three cloning sites.	Amp Cam	*Novagen*
pSPARK	Highly efficient DNA cloning of PCR products amplified with proofreading DNA polymerases	Amp	*Canvax*

- **Amp = Ampicillin**
- **Cam = Chloramphenicol**

5.4.4. Minipreps

The commercial kit *GenElute Plasmid Miniprep* (*Sigma*) was used for isolating plasmid DNA from 2-5 mL of a recombinant culture of *E. coli* cultures, following the instructions from the manufacturer. For efficient recovery, 20 µL of 5 mM Tris-HCl, pH 8.0 was used as eluent.

5.4.5. Gel extraction

The *GenElute Gel Extraction Kit* (*Sigma*) was used for the purification of 50 pb to 10 Kb linear DNA fragments and plasmids from standard or low-melting agarose gels following the instruction from the manufacture. To increase the concentration of the eluted DNA, 25 µL of the elute solution (preheated at 65 ºC) was used.

5.4.6. Enzymatic manipulation of DNA

5.4.6.1 Digestion with restriction enzymes

The digestion was performed in a total volume of 20 µL. 500 ng of DNA were digested with 0.5 µL (10 U) of BamHI (*New England BioLabs*) and 0.5 µL (10 U) of NdeI (*New England BioLabs),* the buffer optimal was R 10x. The digestion was incubated for 90 min at 37 ºC. The result was visualized in a 1% TAE low-melting point agarose gel (5.3.4).

5.4.6.2. Ligation

DNA fragments were ligated with T4 DNA ligase (*dominion MBL*) in the following reaction: 50 ng of linear vector, 3:1 molar relation insert:vector, 1 µL of 10x Buffer T4 DNA ligase, 1 µL of T4 DNA ligase (5 U Weiss/µL) and *milliQ* water up to 10 µL. Incubate at 22 ºC overnight. A negative control, without DNA template, was used.

When DNA fragments were ligated with *pGEM-T* or *pSpark* vectors, the reaction was carried out by following the manufacturer instructions.

5.4.7. Methods for DNA transfer

5.4.7.1. Competent cells

The method used was described in (Inoue *et al.*, 1990). 3 mL of culture were grown overnight in LB broth at 37 ºC. 500 µL of this culture were used to inoculate 50 mL of LB in a 250 mL flask. The flask was incubated at 18 ºC with shaking (200 rpm) until A_{600} was about 0.5 (between 0.4-0.6), it took around 30 h. Cells and all solutions were incubated on ice for 10 min. Cells were centrifuged at 3,800 *g* for 10 min at 4 ºC. The pellet cells were resuspended in TB (table 27) (32 mL/ 100 mL culture) and chilled on ice for 10 min. Then, centrifuged at 1,000 *g* for 10 min at 4 ºC and the pellet were

resuspended in TB (8 mL/100 mL culture), then high grade DMSO (600 µL/100 mL culture) was added at 7% final concentration and then, incubated on ice 20 min. Cells were aliquoted (100 µL/tube), snapped freeze in liquid nitrogen and then stored at -80 ºC until use.

Table 27: Composition of TB buffer

Components	Amount for 1 Liter	Final concentration
Hepes (*)	3 g	10 mM
KCl 2M (*)	125 mL	250 mM
$CaCl_2$ 1M (*)	15 mL	15 mM
$MnCl_2$ 1M	55 mL	55 mM

(*) pH 6.7 was adjusted with KOH and then $MnCl_2$ was added.

For the calculation of the efficiency of the competent cells obtained, the following equation was used:

Efficiency = cfu on control plates/ ng of competent cells control DNA plate × $1 \cdot 10^3$ng/1 µg

5.4.7.2. Transformation of *E. coli*

The transformation was performed after the inactivation of the ligase enzyme at 65 ºC for 10 min. 2-5 µL of the ligation mixture was mixed with 200 µL of competent *E. coli* cells. The mix was incubated on ice for 30 min, then for 2 min at 42 ºC and finally 2-3 min on ice. 700 µL of SOC medium (table 28) were added followed by incubation for 45 min at 37 ºC with shaking (200 rpm). Then it was plated on ampicillin LB agar plates and incubated at 37 ºC overnight.

Table 28: Composition of SOC medium

Components	Amount for 100 mL
Bacto tryptone	2 g
Bacto Yeast Extract	0.5 g
NaCl 1 M	1 mL
KCl 1 M	0.250 mL
97 mL of distilled H_2O were added. Sterilized by autoclave. Cooled down and the following solutions were added:	
Stock 2 M Mg^{2+} filter-sterilized (*)	1 mL
Stock 2 M glucose, filtered-sterelized	1 mL

(*) 2 M Mg^{2+} stock: 20.33 g $MgCl_2 \cdot 6\ H_20$ and 24.65 g $MgSO_4 \cdot 7\ H_2O$, final volume 100 mL. SOC Medium was stored at -80 ºC to avoid contamination at room temperature.

5.4.8. DNA sequencing

The cloning procedure was checked by sequencing the DNA inserts at different steps. We used the DNA sequencing service from the SCAI (Servicio Central de Apoyo a la Investigación) at the University of Córdoba. The samples were prepared as follows: 15-20 ng per 100 bp when they are PCR products or 400 ng of plasmid (maximum volume up to 7 µL). The results were analyzed using the *SeqMan* (*Lasergene*) software to visualize the quality of the chromatogram. The sequences were revised by using the *Sequence Analysis* (*Lasergene*) software.

5.5. Quantitation of gene expression by qRT-PCR

5.5.1. Synthesis of cDNA

cDNA synthesis from a broad range of RNA (free of DNA) concentrations (from 400 ng to 1 µg) was done using the *qScript cDNA Synthesis Kit* (*Quanta*). The reaction was performed in a total volume of 20 µL in 0.2 mL PCR tubes following the manufacturer instructions. The thermal program used was: 1 cycle 22 ºC for 5 min, 1 cycle 42 ºC for 30 min and 1 cycle 85 ºC for 5 min. After completion of cDNA synthesis, 1 µL of product was checked with a PCR test to amplify the housekeeping gene (*rnpB*).

5.5.2. Optimization of the qRT-PCR amplification

During the optimization of qRT-PCR reactions, products were checked for single amplification of DNA fragments of the expected size by agarose gel electrophoresis. The efficiency of amplifications for each couple of primers was analysed by preparing serial dilutions of samples and three different concentrations of oligonucleotides to test qRT-PCR reactions, in order to reach optimal, linear amplification. The samples used for optimization were the amplified product cloned in a TA vector. Previously, the cloned vector was sequenced to ensure that the amplified product corresponded to our gene of interest.

The standard curve is constructed by plotting the log of the starting quantity of template against the C_t value obtained during amplification of each dilution. Amplification efficiency, E, was calculated from the slope of the standard curve using the following formula:

$$E = (10^{-1/slope} - 1) \cdot 100$$

The amplification efficiency has to be between 90-105%. Low reaction efficiencies may be caused by poor primer design or by suboptimal reaction conditions. Reaction efficiencies >100% may indicate pipetting error in serial dilutions or coamplification of nonspecific products, such as primer dimers.

5.5.3. qRT-PCR reaction

qRT-PCR was carried out with an *iCycler iQ System* (*Bio-Rad*) using an *EvaGreen*-fluorescence dye (*EvaGreen* dye is a fluorescent nucleic acid dye with spectral properties similar to *SYBR Green I* and fluorescein) based procedure with reagents purchased from *Bio-Rad.* The thermal program consisted of 95°C for 2 min (denaturation), followed by 50 cycles of: 95 ºC for 15 s (denaturation), 58 °C (*Prochlorococcus*) or 56 ºC (*Synechococcus*) for 30 s (annealing) and 72 ºC for 30 s (extension). After the final cycle, a melting curve analysis was performed over a temperature range of 65–100 °C by increments of 0.5 °C each 10 s in order to verify the reaction specificity.

5.5.4. Analysis

Measurements were carried out in triplicate from at least three different biological samples subjected to identical culture conditions. The results obtained from the *iCycler iQ System* were analysed using the software *iCycler iQ v3.0* from *Bio-Rad*.

The relative change in gene expression was endogenously normalized to that of the *rnpB* gene (encoding RNase P) (Holtzendorff *et al.*, 2001), calculated using the $2^{-\Delta\Delta Ct}$ method (Pfaffl, 2001), where Ct is the point at which the fluorescence rises appreciably above the fluorescence background.

$$\text{Ratio} = 2\ \Delta Ct \text{ target (calibrator – test)}/\ 2\Delta Ct \text{ ref (calibrator – test)}$$

$$= 2^{-[(Ct,\ \text{target (test)} - Ct \text{ target (calibrator)})] - [(Ct,\ \text{ref (test)} - Ct \text{ ref (calibrator)})]} = 2^{-\Delta\Delta Ct}$$

6. METHODS FOR PROTEIN ANALYSIS

6.1. Polyacrylamide gel electrophoresis (PAGE)

6.1.1. Sodium dodecyl sulphate polyacrylamide gel electrophoresis (SDS PAGE)

The gels were run using a *Mini Protean III* system (*Bio-Rad*) and 1.5 mm thick gels. The composition of the gels is shown in table 29.

Table 29: Composition of gels for SDS-PAGE:

RESOLVING GEL (12%)	VOLUME
H_2O	1.7 mL
Tris-HCl pH 8.8, 1.5 M	1.25 mL
Polyacrilamide	2 mL
SDS 10%	50 µL
APS 10%	35 µL
TEMED	5 µL

STACKING GEL (4%)	VOLUME
H_2O	1.75 mL
Tris-HCl pH 6.8, 0.5 M	625 µL
Polyacrilamide	325 µL
SDS 10%	25 µL
APS 10%	15 µL
TEMED	2.5 µL

The samples were prepared using loading buffer with β-mercaptoethanol (5%) (table 30) final concentration 1x and heated for 5 min at 100 ºC.

Table 30: Composition of loading buffer 4x

Components	Amount for 8 mL
1 M Tris-HCl pH 6.8	1.25 mL
Glycerol	3 mL
20% SDS	1 mL
Bromophenol blue	5 mg
Distilled water	Up to 8 mL

The electrophoresis was performed in a buffer which composition was 38 mM glycine, 50 mM Tris base and SDS 1% (p/v), pH 8.3 at 200 V during 45 min using the power supplies *Power Pac 1000* and *Power Pac 300* from *Bio-Rad.*

6.1.2. Native PAGE

The native PAGE gels were run using a *Mini Protean III* system (*Bio-Rad*) and 1.5 mm thick gels. The composition of the gels is shown in table 31.

Table 31: Composition of separation gel

Components	Amount (1 gel)	Final concentration
Acrylamide (39:1)	1.88 mL	7.5 % (v/v)
85 mM Tris-HCl pH 8.8	850 µL	85 mM
100 mM Tris-Boric acid pH 8.8	2 mL	100 mM
APS 10%	200 µL	
TEMED	5 µL	
Millipore	6.1 mL	

The samples were prepared with 1x native protein loading dye (5x native protein loading dye: 50% (v/v) glycerol and 1.5 % (v/v) bromophenol blue). The electrophoresis was performed with 1x native protein PAGE buffer (10x native protein PAGE buffer: 1.92 M glycine and 0.5 M Tris-HCl pH 8.8).

6.1.3. Staining of gels

6.1.3.1. Coomassie Blue stain

The gels were stained with an aqueous solution composed of 40% (v/v) methanol, 10% (v/v) acetic acid and 0.1% (p/v) of *Coomassie Brilliant Blue R-250* (*Sigma*). A solution containing 40% (v/v) methanol and 10% (v/v) of acetic acid was used to destain the gels.

6.1.3.2. Silver stain

The silver stain method was used when high sensitivity was required to detect protein. All the solutions used in this method are shown in table 32. The protocol for silver stain was as follows: the gel was incubated overnight with fixer buffer. Then washed threefold for 20 min in 50% EtOH, incubated 1 min with sensitizing buffer and then washed again threefold with *Millipore* water for 20 s. Then incubated for 15-20 min with silver stain buffer and then washed threefold with *MilliQ* water for 20 s. Then, the gel was developed with developer buffer until the desired band appeared. The development was finished with stopped solution ca. 10 min and washed with *MilliQ* water.

Table 32: Buffer for silver stain

Buffer	Components for 100 mL
Fixer	50 mL 100 % EtOH; 12 mL 100% acetic acid and 100 µL formaldehyde
Wash	50 % EtOH
Sensitizing	20 mg Na_2SO_3
Developer	6 g Na_2CO_3; 2 mL silver stain; 50 mL formaldehyde
Stop solution	1.86 g EDTA
Silver stain	200 mg $AgNO_3$; 100 µL formaldehyde

6.2. WESTERN BLOTTING

6.2.1. Semidry transfer of proteins to nitrocellulose membrane

Crude extracts from *Prochlorococcus* and *Synechococcus* WH7803 (10-40 µg of protein) were loaded in each lane. SDS electrophoresis was performed as described in 6.1.2.

Proteins were transferred to a nitrocellulose membrane (*Sigma*) utilizing a semidry *Trans-Blot SD System* (*Bio-Rad*). Transfer was performed for 90 min at 100 mA. After transfer the membrane was stained using Ponceau S (0.2%) in 5% acetic acid to check for equivalent protein loading and transfer efficiency.

6.2.2. Incubation with primary antibody

The membranes were washed threefold for 15 min with TBS-T (20 mM Tris-HCl pH 7.4, 150 mM NaCl and 0.1% Tween 20). Then, blocked with TBS-T containing

1% bovine seroalbumin for 2-3 hours and washed threefold for 15 min with TBS-T buffers. The incubation with primary antibody (table 33) was performed shaking at 4 ºC overnight.

Table 33: Antibodies used in this work

Antibody	Dilution used	Source
(*) Anti-GSI	1: 5000 (v/v) in TBS-T 1% BSA	*Synechocystis* PCC6803 produced in rabbit
(*) Anti-GSIII	1: 4000 (v/v) in TBS-T 1% BSA	*Synechocystis* PCC6803 produced in rabbit
(*) Anti-ICDH	1: 4000 (v/v) in TBS-T 1% BSA	*Synechocystis* PCC6803 produced in rabbit
Anti-GDH	1: 5000 (v/v) in TBS-T 1% BSA	*Prochlorococcus* produced in rabbit
Anti-HisTag	1: 2000 (v/v) in TBS-T 1% milk	*Sigma*

(*) These antibodies were kindly provided by Dr. Maribel Muro-Pastor and Prof. Javier Florencio.

6.2.3. Detection with chemiluminiscence

The membranes were washed threefold for 15 min with TBS-T buffer; and then incubated with secondary antibody (anti-immunoglobulin from rabbit produced in goat, linked with peroxidase, *Sigma*) diluted 1:4000 or 1:2000 (v/v) in TBS-T or in TBS-T in the presence of 1% milk, for 30 min was performed with shaking at room temperature. Then, the membranes were washed threefold for 15 min with TBS-T buffer. The immunoreacting material was detected by addition to the membrane of *ECL Plus Western Blotting Detection System* (*Amersham*), mixed with the proportion 1:1 of solution A and solution B.

6.2.4. Imaging

Chemiluminescent signal was detected using a *LAS-3000* camera (*Fujifulm*) or *ChemiDoc* (*Bio-Rad*) system. Images were analysed using *Multi-Gauge V3.0* (*Fujifulm*) for images obtained with *LAS-3000* or *Quantity One 1-D Analysis* Software *(Bio-rad)* for images obtained with *ChemiDoc*.

6.2.5. Stripping and reprobing membranes

When it was necessary to reuse the same membrane, it was washed threefold again with TBS-T for 30 min and then incubated with primary antibody to continue the protocol (from section 6.2.2).

6.2.6. Quantitation of bands

The gel scanning images were saved as TIFF, and then we used the *Quantity One 1-D Analysis* software (*Bio-Rad*) to quantify the intensity of every band, assigning 100% to the control condition band.

6.3. Detection of carbonylation

We followed a method adapted from that previously described by Conrad and coworkers (Conrad *et al.*, 2001). Proteins were first derivatized with 10 mM 2,4-dinitrophenylhydrazine (DNPH) in 10% trifluoroacetic acid for 15 min, followed by neutralization in 2 M Tris-base/30% glycerol for 15 min. The samples were cold acetone precipitated, and centrifuged at 12,000 *g*, for 5 min at 4ºC. The pellet was resuspended in 52 µL of a solution (8 M urea, 2 mM EDTA, 4% CHAPS (p/v)) and the concentration of protein was determined. 20 µg of protein were loaded on gels and the inmunoblotting was made. The primary antibody used (anti-dinitrophenyl (DNP) from rabbit) was dilluted 1: 2000 (v/v) in TBS-T 1% BSA.

6.4. Determination of glutathionylation

To detect glutathionylated proteins under different experimental conditions, 40 µg of proteins and 1X loading buffer without reducer were run in a SDS-PAGE. Then the protein transfer was made and the membrane was blocked for 1 hour with TBS-T containing 1% BSA and incubated with monoclonal anti-GSH antibody from *Virogen* (Watertown, MA, USA). Glutathionylated proteins were detected as explained in 6.2.3.

7. PURIFICATION OF HETEROLOGOUS PROTEINS

7.1. Overexpression test

The overexpression of the proteins NtcA$(His)_6$, $P_{II}(His)_6$ and PipX$(His)_6$ from *Prochlorococcus* SS120 and MIT9313 was examined after inducing their expression in the corresponding *E. coli* strains, as described in section 5.4.1. Before induction, 90 min and 240 min after induction 5 O.D. equivalents were taken, harvested by centrifugation at 5,000 *g* at 4°C for 10 min and the pellets were stored at -20°C. The cells were adjusted at 20 OD/mL with HisA buffer, disrupted by sonication and the supernatant was removed. To discover misfolded proteins in inclusion bodies, the pellets containing the cell debris was treated as follows: they were resuspended again in the same volume of HisA buffer with 2 % Triton X 100, incubated on ice for 30 min and centrifuged for 20 min at 13,000 *g* for 4°C. The supernatant was removed and the pellets were washed twice with SBT buffer (50 mM Tris-HCl pH 7.5, 200 mM NaCl). Finally the pellets were resuspended in HisA buffer containing 8 M urea to solve the pellet. The samples were heated at 37 °C and mixed with SDS PAGE loading buffer. 0.25 O.D. equivalents of supernatant and pellet fraction were analyzed by SDS PAGE.

7.2. Purification of heterologous protein NtcA from *Prochlorococcus* SS120 and MIT9313

The purification of heterologous NtcA was done using two different steps in order to get a high purity preparation, as required for interaction assays.

7.2.1. Growth of culture

100 mL of *E. coli* BL21(DE3) were grown overnight at 37 ºC, in the presence of ampicillin, to overexpress NtcA from *Prochlorococcus* SS120 and MIT9313. This culture was added to 6 L of LB and ampicillin. They were incubated with shaking at 37 ºC until A_{600} was 0.5-0.6. After 4 h of induction using 0.5 mM of IPTG, the culture was centrifuged at 3,800 *g* for 5 min at room temperature. The pellet was stored at -80 ºC. Control samples were obtained as well, with equal cell number, taking 5 O.D. equivalents before induction and 4 h after induction.

7.2.2. Buffers

All buffers used for chromatography were filter-sterilized (0.22 µm pore size) and stored at 4°C.

Table 34: Buffers for Ni-NTA affinity chromatography

Buffers	Composition
HisA	50 mM NaH_2PO_4, 300 mM NaCl, 30-80 mM imidazole
HisB	50 mM NaH_2PO_4, 300 mM NaCl, 500 mM imidazole
Stripping buffer	20 mM NaH_2PO_4, 500 mM NaCl, 50 mM EDTA, pH 7.4
Recharging the column	100 mM $NiSO_4$

Table 35: Buffers for size exclusion chromatography

Buffers	Composition
HBS-E	150 mM NaCl, 3 mM EDTA, 10 mM HEPES (pH 7.4)
Column regeneration	0.5 mM NaOH

7.2.3. Bacterial cell lysate

After the collected pellet thawed, 30 mL of HisA buffer pH 7.4 (table 34) with 1.2 mL of *Complete C* protease inhibitor (1 tablet in 2 mL of *MilliQ* water) were added. The cells resuspended on ice were sonicated with 3 times 30 s bursts at 30% of intensity with 2 min cooling period between each burst. After that, 30 µL of DNAseI (10 mg/mL diluted in *MilliQ* water) and 30 µL of RNase (5 mg/mL diluted in *MilliQ* water) were added and incubated on ice for 20 min. The lysate was centrifuged at 48,000 *g* (rotor JA-25.50), for 40 min at 4 ºC to precipitate the cellular debris. The supernatant was transferred to a fresh tube. 5 µL of the lysate was removed for SDS-PAGE analysis. The remaining lysate could be stored on ice or freeze at -20 ºC.

7.2.4. Ni-NTA chromatography

The purification was carried out with an *Äkta Prime* chromatography system (*GE Healthcare*). The first purification step was a chromatography on a 5 ml Ni-NTA column, following the manufacturer instructions. After a washing step with 15 column volumes (CV) of HisA buffer, the protein was eluted with a linear gradient of 10 %, 20 %, 30 %, 50 % and finally 100 % HisB buffer. Protein containing fractions were

analyzed by SDS-PAGE and merged afterwards.

To recharge the column the following procedure was followed: first the nickel was removed from the column with EDTA, for that the stripping buffer was used with a flow rate of 1 mL/min loading 5 column volumes. The column turned white. Then, it was necessary to remove all the EDTA from the column, therefore the column was washed with *MilliQ* water at flow rate of 1 mL/min and then recharged using a solution 100 mM of $NiSO_4$ a at flow rate of 0.5 mL/min. Finally, to remove all the nickel not bound, the column was washed using *MilliQ* water. The profile of the chromatogram obtained after recharge the column is shown in figure 18.

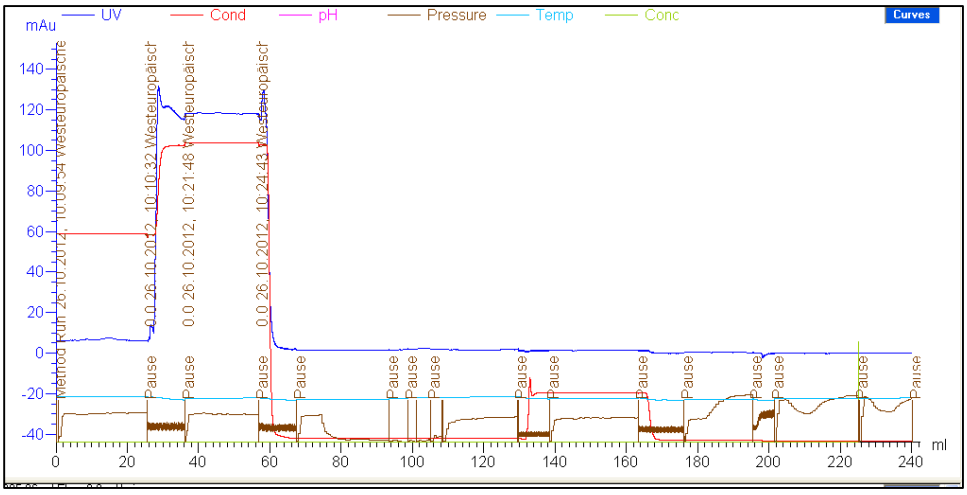

Figure 18: Representative chromatograms of recharge of the Ni-NTA column process

7.2.5. Molecular size exclusion chromatography

The protein solution was concentrated to a volume of 5 mL by centrifugation with *Centriprep* filters (MWCO 10 or 30 kDa) (*Millipore*) at 1,500 *g* and 4°C. The concentrated sample was loaded on the *Sephadex 75* size exclusion chromatography column for further purification and transferred to the HBS-E storage buffer. Pure protein fractions were further concentrated and stored in HBS-E buffer at 4°C for approximately 4 weeks or in HBS-E with 50 %(v/v) glycerol at -20°C.

Regeneration of *Sephadex 75* columns

The column was regenerated with 0.5 M NaOH at flow rate of 40 mL/min for approximately 16 h. The chromatogram after generation is shown in figure 19.

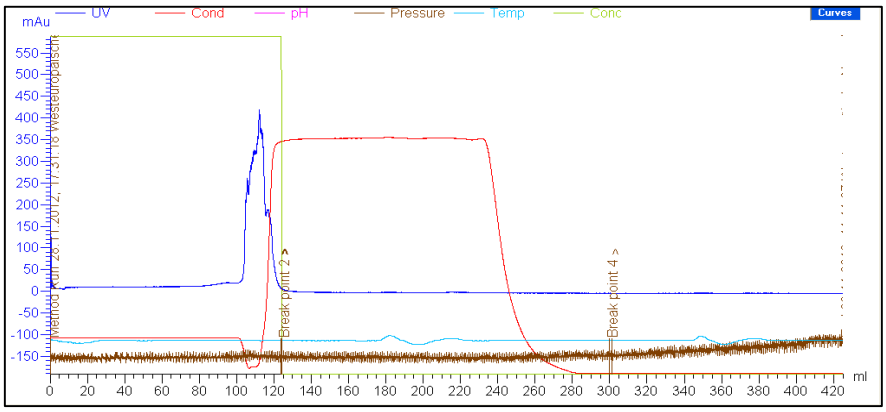

Figure 19: Representative chromatogram of the regeneration of the *Sephadex 75* column

7.3. Purification of heterologous protein PII and PipX from *Prochlorococcus* SS120 and MIT9313

7.3.1. Growth of cultures

10 mL of *E. coli* BL21(DE3) were grown with 100 µg/µL ampillicin overnight at 37 ºC to overexpress PII and PipX from *Prochlorococcus* SS120 and MIT9313 overnight at 37 ºC. This culture was added to 500 mL of LB and ampillicin. The culture was incubated with shaking at 37 ºC until A_{600} reached 0.5-0.6. After 4 hours of induction with 0.5 mM of IPTG the culture was centrifuged at 3,800 *g* for 5 min at room temperature. The pellet was stored at -80 ºC until used.

7.3.2. Buffer

All the buffers used for the purification process are shown in this section.

Table 36: 5x Native Purification Buffer

Components	Amount
NaH_2PO_4	7 g
NaCl	29.2 g
Deionized water	Up to 200 mL

Well mixed and the pH adjusted with NaOH to pH 8.0. Stored at room temperature.

Table 37: Native Binding Buffer

Components	Amount for 30 mL
1X Native purification buffer	29.8 mL
3 M imidazole pH 6.0	200 µL

Well mixed and the pH adjusted with NaOH to pH 8.0

Table 38: Native washing buffer (50 mM of imidazole)

Components	Amount for 50 mL
1X Native purification buffer	49.163 mL
3 M imidazole pH 6.0	837.5 µL

Well mixed and the pH adjusted with NaOH to pH 8.0

Table 39: Native elution buffer (250 mM of imidazole)

Components	Amount for 15 mL
1X Native purification buffer	13.75 mL
3 M imidazole pH 6.0	1.25 mL

Well mixed and the pH adjusted with NaOH to pH 8.0

7.3.3. Bacterial cell lysate for native conditions

The cells were resuspended in 8 mL of native binding buffer (table 37). 8 mg of lysozyme were added and incubated on ice for 30 min. The solution was sonicated with a sonicator equipped with a microtip using six cycles of 10 s bursts with a 10 s cooling period between each burst. The lysate was centrifuged at 3,000 *g*, 15 min to precipitate the cellular debris. The supernatant was transferred to a fresh tube. 5 µL of the lysate were removed for SDS-PAGE analysis. The remaining lysate could be stored on ice or freeze at -20 ºC.

7.3.4. Ni-NTA Resin

Ni-NTA resin (*Invitrogen*) was used to purify recombinant proteins expressed in *E. coli* from His-tagged vector pET-15b. Ni-NTA resin exhibits high affinity and selectivity for recombinant fusion proteins that have been tagged with six tandem histidine residues in tandem. Ni-NTA resin uses nitrolotriacetic acid (NTA), a tetradentate chelating ligand, in a highly cross-linked agarose matrix. NTA binds Ni^{+2} ions by four coordination sites.

7.3.4.1. Preparation of the Ni-NTA column

The Ni-NTA agarose was resuspended in its bottle by inverting and gently tapping the bottle repeatedly. Then, 1.5 mL of the resin was poured into a 10 mL purification column. The resin was settled completely by gravity (5-10 min) or gently pelleted it by low-speed centrifugation (1 min at 800 *g*). The supernatant was gently aspired. 6 mL sterile distilled water were added and the resin was resuspended by alternately inverting and gently tapping the column. The resin was settled using gravity

or centrifugation as described above, and the supernatant gently aspirated. For purification under native conditions, 6 mL of native binding buffer (table 37) were added. The resin was resuspended by alternately inverting and gently tapping the column. The resin was settled using gravity or centrifugation as described above, and gently aspirates the supernatant.

To store the column containing resin, 0.2% azide or 20% ETOH were added as a preservative and the column was capped or covered with parafilm. It was stored at room temperature.

7.3.4.2. Purification under native conditions

8 mL of lysate prepared under native conditions were added to a prepared purification column. For 60 min using gentle agitation to keep the resin suspended in the lysate solution. Settled the resin by gravity or low speed centrifugation (800 *g*), and carefully aspirated the supernatant. The supernatant was saved at 4 ºC for SDS-PAGE analysis. With 8 mL native wash buffer (table 38) washed the column. The resin was settled by gravity or low speed centrifugation (800 *g*), and carefully aspirated the supernatant. The supernatant was stored at 4 ºC until SDS-PAGE analysis. The last step was repeated three more times. The column was clamped in a vertical position and snapped off the cap on the lower end. The protein was eluted with 8-12 mL native elution buffer. 1 mL fractions were collected and analysed with SDS-PAGE. The eluted fractions were stored at 4 ºC. If -20 ºC storage was required, glycerol was added to the fractions.

8. PROTEOMIC APPROACH

This part of the project thesis was done in the laboratory of Prof. Robert J. Beynon at the University of Liverpool (UK) under the supervision of Dr. Guadalupe Gómez Baena.

8.1. Cell collection

When the absorbance at 674 nm reached ca. 0.05, 20 L culture of *Prochlorococcus* SS120 were splitted into two 10 L aliquots. One was used as control culture (no addition) and 100 µM azaserine was added to the other one. Samples were collected after 8 hours of azaserine addition as described in section 2.1.

8.2. Protein extracts

After thawing, the cell suspensions were broken as described in section 3.1. Protein concentration was measured by the Bradford method in a 96 well plate using extracts dilutions (section 4.6). The quality of extracts was checked by SDS-PAGE (section 6.1.1).

8.3. Trypsin digestion

8.3.1. In solution

Samples containing 100 µg of protein were incubated with *Rapigest* (*Waters Corporation*) at a final concentration of 0.05 % (w/v) for 10 min at 80 °C. Protein samples were then reduced with 3 mM dithiothreitol (DTT) for 10 min at 60 °C, followed by alkylation with 9 mM iodoacetamide for 30 min in the dark at room temperature. Finally, trypsin was added and incubated overnight at 37 °C. To stop the proteolytic reaction and to inactivate and precipitate, the detergent TFA (final concentration 0.5 % (v/v)) was added, followed by incubation for 45 min at 37 °C. To remove all insoluble material, samples were centrifuged at 13,000 *g* for 15 min at room temperature.

8.3.2. In gel

A small (1 mm^3) plug of a stained protein band was cut. The plug was washed alternately with 25 mM ammonium bicarbonate and 25 mM ammonium bicarbonate/Acetonitrile (2:1). The gel plug was incubated for 15 min at 37 ºC until it was destained. Sample was reduced by adding 25 µL of a 1.5 mg/mL solution of DTT (ca. 10 mM). Then it was incubated at 60 ºC, 60 min, and cooled to room temperature and quick spin to return liquid to the bottom of the tube was made. The liquid around the gel plug was aspirated using a pipette and discarded. The reduction step was followed by alkylation adding 25 µL of a 10 mg/mL solution of iodoacetamide (60 mM). The mixture was incubated at room temperature in the dark for 45 min. The plug was washed with 25 mM ammonium bicarbonate and then it was washed with acetonitrile to dehydrate the plug. At each cycle, the gel plug was incubated for 15 min at 37 ºC. Finally, 10 µL of trypsin (12.5 ng/µL in 25 mM AmBic) was added to the gel plug in an *eppendorf* tube for digestion. The mix was incubated for 12-16 h (overnight) at 37 ºC. The last step was the peptide recovery by centrifugation. Formic acid (10%

v/v) was added to attain a final concentration of 1% (v/v). The pooled digest was ready to MALDI-ToF analysis.

8.4. Mass Spectrometric Analysis

8.4.1. LC MS/MS: *Q Exactive*

All the samples were analyzed as tryptic peptides, resolved by high-resolution liquid chromatography (*U3000 Thermo Fisher*) prior to tandem mass spectrometry. The *Q Exactive* system (*Thermo Fisher*) was operated in data-dependent acquisition mode. Samples containing 500 ng or 1µg of protein were analysed and the 10 most intense multiply charged ions were isolated and sequentially fragmented. Precursors selected were dynamically excluded for 20 s. As peak list generating software we used *Proteome discoverer 1.4* (*ThermoFisher Scientific*) using default parameters. The peak lists obtained were searched against a database composed of reviewed entries of *Prochlorococcus* Uniprot database, using MASCOT as search engine (version 2.4.0, Matrix Science). Methionine oxidation as variable modification and one trypsin missed cleavage, a mass tolerance of 10 ppm for precursors and 0.01 Da for fragment ions were allowed. The false discovery rate (FDR) was calculated using the decoy database in MASCOT.

The peptide mixture (500 ng-1 µg) was trapped onto a *Symmetry* C18 precolumn (180 µm id, 20 mm long, 5 µm particles) (*Waters Corporation*) over 3 min, at a flow rate of 25 µL/min in 2% (v/v) acetonitrile /0.1% (v/v) formic acid. Bound peptides were resolved on a nanoAcquity UPLC C18 column (75 µm id, 150 mm long, 3 µm particles) (*Waters corporation*) at 300 nL/min over a 240 min linear gradient from 3 to 85% (v/v) acetonitrile in 0.1% v/v formic acid, controlled by *IntelliFlow* technology. 50 fmol of rabbit-phosphorilase B was added to the sample in order to use it as internal standard for absolute quantification.

Previous studies have shown that the *Q Exactive* produced a 10% increase in identification rate, peptides, and peptide spectrum matches with respect to other mass

spectrometers. The researchers point to a smaller maximum injection time for MS/MS, faster scan rate, and increased MS/MS spectra for the *Q Exactive* (Michalski et al., 2011, Sun et al., 2013). The *Q Exactive* also had higher resolution, which produced a low mass error for both precursor and product ions and positively limited the peptide matches during database interrogation.

8.4.2 MALDI-ToF MS: *Ultraflex* (*Bruker*)

The protein band of interest was digested as described above (8.3.2). 1 μL of the digestion mixture was spotted on the MALDI-TOF target. When it was dry, 1 μL of matrix (10 mg/mL of α-cyano-4-hidroxycinnamic dissolved in 60% of ACN-0.1 % TFA) was spotted, and left to dry. To calibrate the instrument we used a commercial standard with 5 different compounds of known mass charge ratio (m/z). The *Ultraflex* system was operated with the *FlexControl* software (*Bruker*). The spectrum obtained from each sample was analyzed with *FlexAnalysis* (*Bruker*).

8.5. Proteomic data analysis

LC-MS/MS data were processed for relative label-free quantification using *Progenesis LC-MS* (*Nonlinear Dynamics*), *Transomics* (*Waters*), *PEAKS7* (*PEAKS*) and for absolute quantification using *Progenesis Postprocessor* (QI *et al*., 2012). The latter software has been developed in Liverpool with the aim to get "Hi3" to do absolute quantification: the top3 module was developed to extract the highest three intensity peptides in each replicate, and the user can then calculate estimated absolute abundance values via knowledge of proteins that were spiked in known abundance. For label-free quantification and identification of proteins the steps followed in the analysis were: raw data import and quality control, retention time alignment, peptides quantification, identification and the report of interesting proteins with its *p* value and fold change.

9. METHODS FOR ANALYZING INTERACTIONS

During this project, the interaction of the nitrogen master regulator NtcA with the *glnA* promoter was analyzed in two different *Prochlorococcus* strains, MIT9313 and SS120, by using the *Surface Plasmon Resonance* technique (SPR) and EMSA.

9.1. *Surface Plasmon Resonance* technique, BIACORE X

This part of the project was performed in the laboratory of Prof. Andreas Burkovski under the supervision of Dr. Gerald Seidel, in the Lehrstuhl für Mikrobiologie at the Friederich-Alexander Universität in Erlangen, Germany.

All SPR measurements were carried out on a *BIACORE X* (figure 20) (*GE Healthcare*) instrument at 25 ºC. The SPR detection is a refractive index sensor. Measurements are dependent on surface concentration and temperature. SPR response is a measure of changes in the resonance angle (figure 21). As a rough approximation, a response of 1 RU is equivalent to a change in the surface concentration of about 1 pg/mm^2 (for proteins on sensor chip *CM5*).

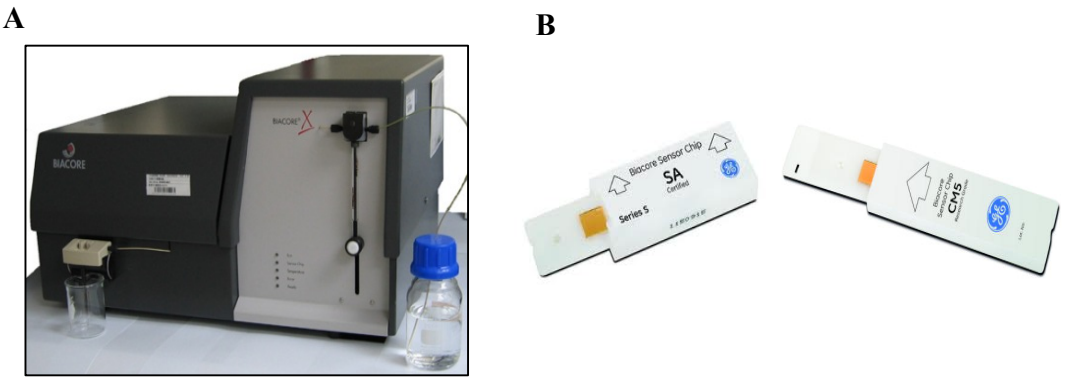

Figure 20: A. The model of *BIACORE*, *X*. B. Sensor Chips used in SPR technique *SA* (Streptavidin) and *CM5* during this study.

The response was measured in resonance units (RU) and was proportional to the molecular mass on the surface. For an interactant of a given mass, the response is proportional to the number of molecules at the surface.

The results were plotted in a sensorgram, that is a plot response against time, showing the progress of the interaction. The sensorgram is displayed on the computer screen during the course of an analysis.

In Biacore terminology, ligand refers to the immobilized component and the interactant present in the sample injected over the surface is referred to as the analyte.

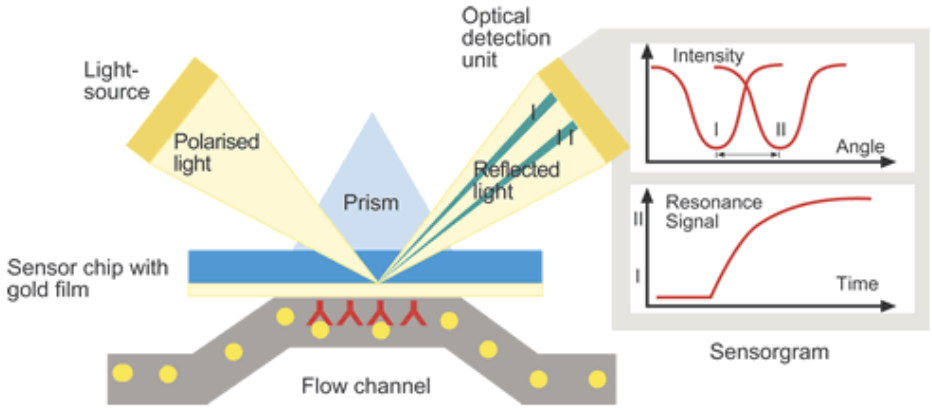

Figure 21: The diagram shows the basis of a SPR-based sensor

The general steps in BIACORE assay were:

1. **Surface preparation/ Immobilization**: the process by which the ligand is attached to the sensor chip surface.
2. **Sample injection**: the analyte is injected over the sensor chip surface and the interaction between the analyte and the immobilized ligand is monitored.
3. **Regeneration**: the process of removing bound analyte from the ligand on the surface.
4. **Evaluation**

9.1.1. DNA biotinylated

All 26 nt oligonucleotides were purchased from *MWG Eurofins/Ebersberg*. The forward strand was biotinylated at the 5´end. The specific oligonucleotides contained the binding site for NtcA from the promoter region of *glnA* and the reference oligonucleotides contained this binding site with mutations (table 40).

Table 40: Oligonucleotides used for Biacore assay

Oligonucleotides	Sequence 5´-3	Function
glmnF	TAGAAGGTACCTGTTGCTACAAAAAG	Forward *glnA* promoter MIT9313 biotinylated
glmnR	CTTTTTGTAGCAACAGGTACCTTCTA	Reverse *glnA* promoter MIT9313
rglmnF-4	TAGAAGAGAAAGGATCCGCAAAAAG	Forward reference *glnA* promoter MIT9313 biotinylated
rglmnR-4	CTTTTTTGCGGATCCTTTCTCTTCTA	Reverse reference *glnA* promoter MIT9313
glsnF	CCAATAGTCACAAAAAGTACTTATTG	Forward *glnA* promoter SS120 biotinylated
glsnR	CAATAAGTACTTTTTGTGACTATTGG	Reverse *glnA* promoter SS120
rglsnF	CCAATAAGCCCCACACGGCATTATTG	Forward reference *glnA* promoter SS120 biotinylated
rglsnR	CAATAATGCCGTGTGGGGCTTATTGG	Reverse referenc *glnA* promoter SS120

Red: Binding site conserved / Blue: Binding site conserved mutated.

Equal amounts of complementary strands (5 µM) were mixed in PCR tubes and hybridized in the heat block for 20 min at 80 ºC. Afterwards, the heat block was set at 60 ºC, then it was cooled down (ca. 20 min) and finally switched the heat block off and cooled down to room temperature.

For the visualization of the hybridization, a 20% polyacrylamide gel (table 41) was used. The samples were prepared by mixing 4 µL of DNA, 6 µL of *MilliQ* water and 3 µL of DNA loading dye. PAGE was run in TBE for 40 min at 120 V. The visualization of the gels was made with ethidium bromide and the molecular weight marker used was *Ultra low Range DNA*: 0.01- 0.3 kb (*peqGOLD*).

Table 41: Composition of 20% polyacrylamide gel

Components	Amount for 1 gel
40 % polyacrylamide (19:1)	7.5 mL
10X TBE	1.5 mL
Millipore	5.8 mL
10% APS	0.2 mL
TEMED	10 µL

9.1.2. Surface preparation

9.1.2.1. SPR with sensor *SA Chip*

Sensor *Chip SA (Biacore BA)* is designed to bind biotinylated molecules for interaction analysis in *BIACORE* instruments. Streptavidin-biotin coupling provides an alternative to other ligand coupling methods (covalent amine or thiol coupling), and is particularly valuable for applications in molecular biology where immobilization of nucleic acids through a 5´-biotin moiety is often the most practical approach. The surface of the *SA Chip* is streptavidin covalently immobilized on a carboxymethylated dextran matrix. Its binding specificity is biotin and its binding capacitiy is ≥ 1800 RU of a biotinylated oligonucleotide (30 bases long).

Surface preparation for use

The *SA Chip* was stored at 4 ºC. Before starting, it was equilibrated at room temperature for 30 min in order to prevent condensation of water vapour on the detector-side of the chip surface. The *BIACORE* instrument was prepared with new eluent buffer. The system was primed with HBS-EP buffer (available from *Biacore AB*). The Sensor *Chip SA* was inserted and docked as described in the instrument handbook.

For best performance, Sensor *Chip SA* was conditioned with three consecutive 1 min injections (flow of 20 µL/min) of 1 M NaCl in 50 mM NaOH before the assay was started. The sensorgram obtained is shown in figure 22.

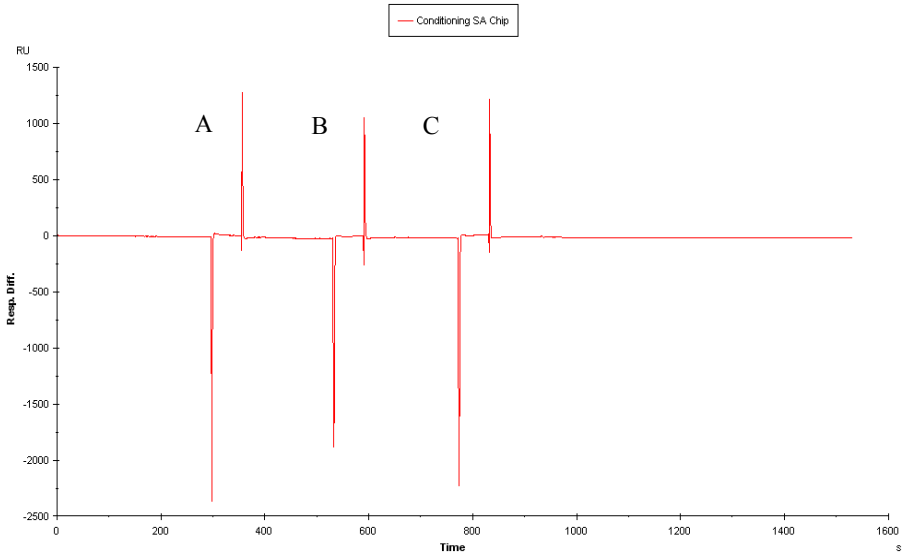

Figure 22: Sensorgram of the conditioning of *SA Chip*. A, B and C represents each injection of 1M NaCl in 50 mM NaOH.

The next step was coupling the DNA to the SA Chip. The 5 µM hybridized DNA sample was diluted to 5 nM with HBS-EP buffer. DNA was coupled until 100-150 RU were obtained. The specific binding site sample and the reference sample were prepared at the same time. The specific DNA was immobilized in flow cell 2 with a flow rate of 5 µL/min and 126 RU were coupled (figure 23, A) and the reference DNA was immobilized in flow cell 1 with a flow rate of 5 µL/min and 129 RU were coupled (figure 23, B).

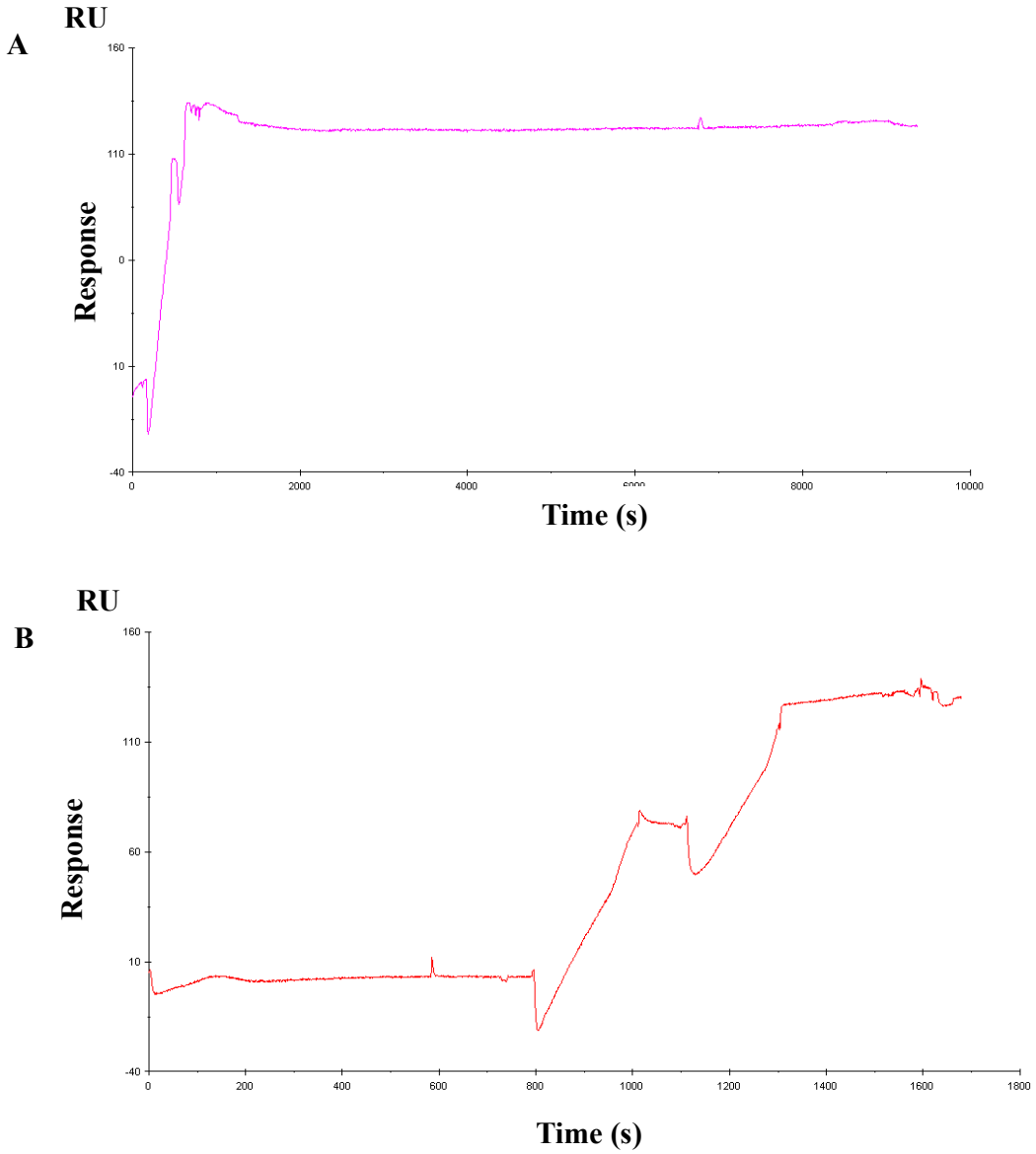

Figure 23: A. Sensorgram of coupling the reference DNA in flow cell 1. B. Sensorgram of coupling the specific DNA in flow cell 2.

9.1.2.2. SPR with Sensor *Chip CM5* with neutroavidin

Sensor Chip CM5 (*GE Healthcare*) is used for interaction analysis in *Biacore* systems. The surface has a carboximethylated dextran matrix covalently linked to a surface coating on a gold film. It is the most versatile chip currently available and it has excellent chemical stability.

Surface preparation for use

The *Sensor Chip* was equilibrated at room temperature for 15-30 min in order to prevent condensation of water vapour on the chip surface. The *BIACORE* instrument was prepared with HBS-EP running buffer. The *Sensor Chip* was docked in the instrument. The next step was the coupling of the Neutroavidin in both flow cells (1 and 2). First, the chip was activated injecting 50 µL of EDC (1-ethyl-3-(3-dimethylaminopropyl)-carbodiimide) and 50 µL of NHS (N-hydroxysuccionimide). Then, 5 µM Neutroavidin (1 mg/mL) and 10 mM Na-Acetate were injected and 35 µL of 1 M Ethanolamin (figure 24).

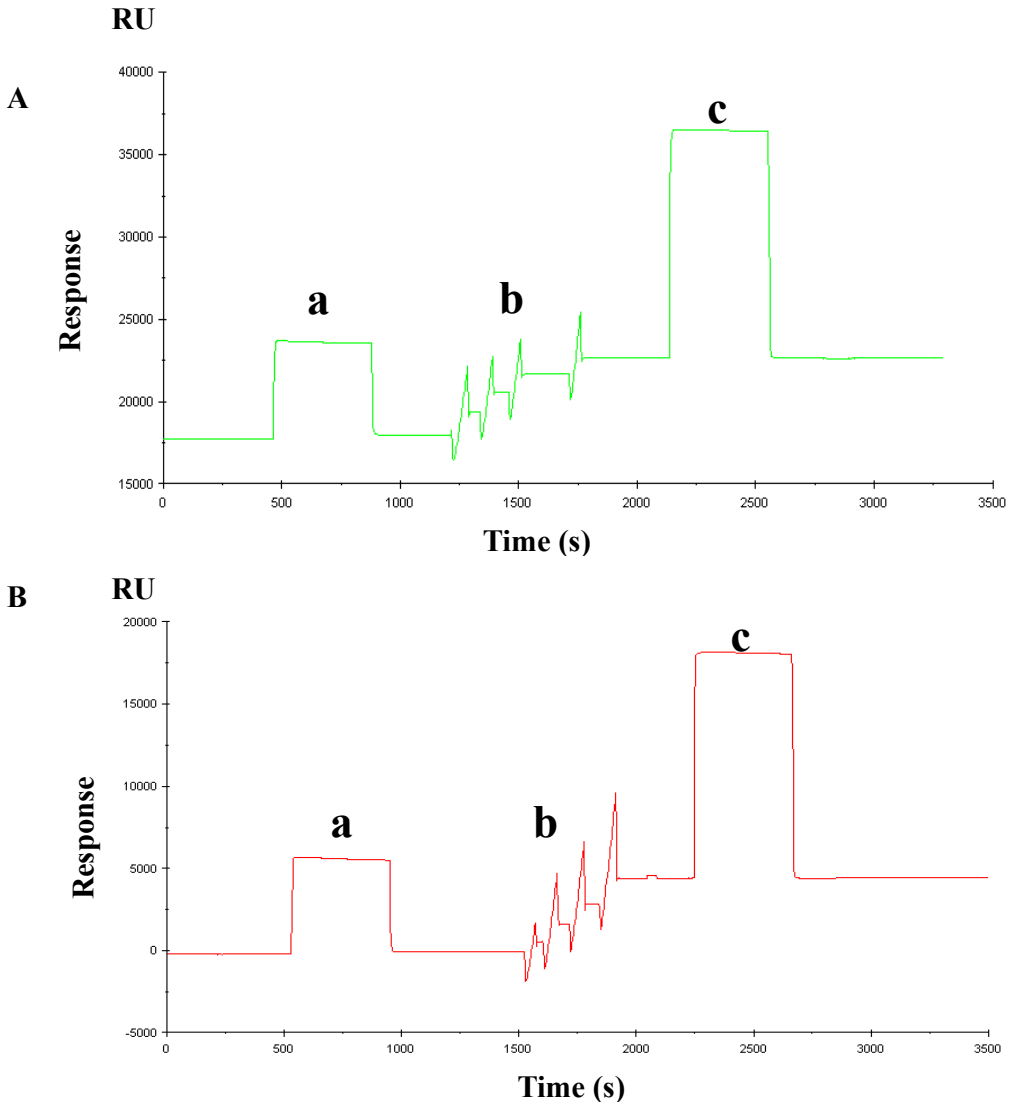

Figure 24: Sensorgram of Neutroavidin coupling on (A) FC1 and (B) FC2. Three different injections are highlighted: a. EDC+NHS, b. Neutroavidin, c. Ethanolamine.

9.1.3. Sample injection (for both Sensor Chips)

The samples containing NtcA from *Prochlorococcus* sp. SS120 and MIT9313 were diluted from the stock to 1 µM, 500 nM or 100 nM with HBS-EP buffer. To minimize sample dispersion at the beginning and the end of the injection, it is recommended to introduce a small volume of air with the sample (about 5 µL each) into the pipette tip before loading. This will separate the sample from running buffer and prevent mixing (figure 25). The protein was injected with a flow rate of 5 µL/min. The interaction was monitorized with the program *Biacore X Control Software*.

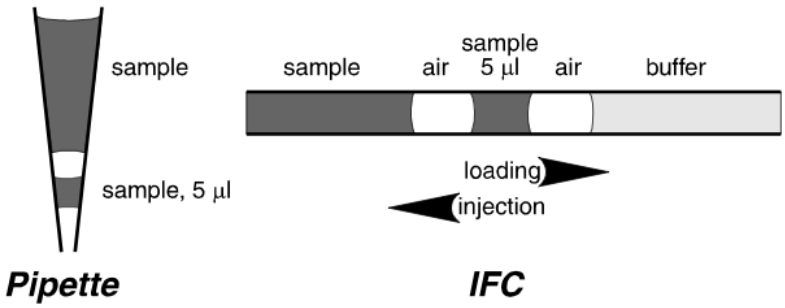

Figure 25: Air bubble technique for loading sample into the IFC. 5 µL of sample separated by two bubbles for maximum precision.

To analyze the effect of 2-OG on the binding between NtcA and the *glnA* promoter, 20 mL of 2-OG were prepared in HBS-EP buffer as the concentration required, adjusting the pH to 7.4 with 5% of NaOH. The system was equilibrated with new buffer prior protein injection.

9.1.4 Regeneration

To completely remove bound analyte from the surface, 0.2% of SDS was used in most of the cases. We have to point out that an efficient regeneration is crucial for high-quality data.

9.1.5. Evaluation of results

For the evaluation of the results the software *BIAevaluation* was used.

9.2. Electrophoretic mobility shift assay

Another way for analyzing interactions between DNA and protein was the Electrophoretic Mobility Shift Assay (EMSA). For this technique the DNA used was the same shown in table 40 without biotinylation. The binding reaction mixture contained: 1.5 µL of 10x binding buffer (table 42) supplemented with the different concentrations of 2-OG, 1.5 µL of 80% glycerol, 0.75 µL of 1 µg/µL BSA, DNA, 1 µM of protein and distilled water up to 15 µL. The reaction was incubated at room temperature for 30 min. 1.5 µL of DNA loading buffer was added to the mix and all of them were loaded into a 6% non-denaturing gel (table 43). The gel was run at room temperature with 200 V in 1X Tris-glycine buffer (diluted from 5x Tris-glycine buffer, table 44). The gel was stained with *SyberSafe* (*Invitrogen)* following the manufacturer instructions. The image was captured with a *ChemiDoc* system (*Bio-Rad)*.

Table 42: Binding Buffer

Composition	Final Concentration
Hepes-NaOH pH 8.0	120 mM
Tris-HCl pH 8.0	40 mM
KCl	0.6 M
EDTA	10 mM
DTT	10 mM
2-oxoglutarate	1, 5 and 10 mM

Table 43: 6% Non-denaturing gel

Composition	Amount for 1 gel
Stock 5x glycine buffer	3 mL
30% acrylamide:bis (30:0.38)	3 mL
50% glycerol	750 µL
H_2O	8.25 mL
10% APS	200 µL
TEMED	12.5 µL

Table 44: Stock 5x Tris-glycine

Composition	Amount for 1 L
250 mM Tris	30.27 g
1.9 M glycine	142.6 g
65 mM EDTA	24.2 g
H_2O	Up to 1 L

10. SOFTWARE

During this project thesis many different softwares for different purposes were used. This section shows a list of all of them and their function.

10.1. Software for genomics

Software/WebPage	Source/URL	Application
CYORF	http://cyano.genome.ad.jp/	Sequence information
Blast	http://blast.ncbi.nlm.nih.gov/Blast.cgi	Sequence comparison
Graphical Codon Usage Analyser	http://gcua.schoedl.de/	Check codon use for cloning
Seqman v7.0	*DNASTAR* (*Lasergene*)	Sequence analysis
Editseq v7.0	*DNASTAR* (*Lasergene*)	Sequence analysis
SeqBuilder v7.0	*DNASTAR* (*Lasergene*)	Plasmid construction
MegAlign v7.0	*DNASTAR* (*Lasergene*)	Alignment
Oligo v4.05	National Biosciences Inc. Plymouth	Oligo design
Primer3	University of Massachusetts Medical School http://biotools.umassmed.edu/bioapps/primer3_www.cgi	Oligo design
In Silico PCR Amplification	http://insilico.ehu.es/PCR/	In silico oligo test for PCR
Clone Manager 9 Professional Edition	*Sci-Ed Software*	Processing of DNA sequence data, primer design and administration of primer and vector database
iCycler IQ v3.0	*Bio-Rad*	Analysis of gene-expression data
ClustalW2 EMBL-EBI	http://www.ebi.ac.uk/Tools/msa/clustalw2/	Multiple sequence alignment

10.2. Software for proteomics

Software/WebPage	Source/URL	Application
Xcalibur	*Thermo Scientific*	Instrument control and visualization raw data
Proteome Discoverer 1.4	*Thermo Scientific*	Peak list generator, protein identification linked to Mascot and visualization of protein lists
MASCOT	http://www.matrixscience.com	Search engine for MS and MS/MS data
Progenesis LCMS	*Non Linear Support*	Label-free quantification
Transomics	*Waters*	Label-free quantification
DAVID	http://david.abcc.ncifcrf.gov/	Pathways analysis
Progenesis Postprocessor	University of Liverpool	Absolute quantification
PEAKS7	*PEAKS*	Peak list generator, de novo sequencing, visualization of raw data and label-free quantification
String 9.0	http://string-db.org/	Analysis of protein interaction networks
FlexAnalysis	*Bruker*	Analysis of spectra
BIAEVALUATION 4.0	*GE Healthcare*	Evaluation and processing of SPR data
Biacore X Software 2.2	*GE Healthcare*	Monitoring interactions in Biacore instruments
Quantity one	*Bio-Rad*	Image analysis/ Quantification of bands
Multigauge V3.0	*Fujifilm*	Image analysis

11. STATISTICAL ANALYSIS

Experiments were carried out at least with three independent biological samples. The results are shown with error bars corresponding to the standard deviation. Significance of data was assessed by using the Student's T test, and indicated in figures with asterisks: * means $p < 0.05$; ** means $p < 0.01$.

12. CHEMICALS

All chemicals were of reagent grade, obtained from *Merck, Sigma, Panreac, Bio-Rad, Amersham Biosciences/GE Healthcare, Promega, Novagen and Ambion.*

CHAPTER 1

Diversity of the C/N balance regulation in three strains of *Prochlorococcus marinus*

Introduction

Recent advances in the knowledge of nitrogen metabolism of the marine cyanobacterium *Prochlorococcus* show that it has fine regulatory systems to optimize nitrogen assimilation (Rocap *et al.*, 2003, García-Fernández & Diez, 2004, Lindell *et al.*, 2002). Some studies performed *in vivo* on *Prochlorococcus* showed that, in spite of possessing the genes involved in standard carbon/nitrogen regulation in cyanobacteria (namely *ntcA, glnB* and *pipX* encoding, respectively, NtcA, P_{II} and PipX), none of them seem to work as previously described. Furthermore, the regulation of enzymes such as glutamine synthetase (GS) (El Alaoui *et al.*, 2003, El Alaoui *et al.*, 2001, Gómez-Baena *et al.*, 2001) and isocitrate dehydrogenase (ICDH) (López-Lozano *et al.*, 2009) is clearly different from their counterparts in other cyanobacteria.

With that background, we have studied the role of 2-OG in the control of the C/N balance in *Prochlorococcus*, in order to check whether there exist differences with respect to other model cyanobacteria (Forchhammer & Tandeau de Marsac, 1994, Muro-Pastor *et al.*, 2005, Muro-Pastor & Florencio, 2003, Luque & Forchhammer, 2008, Flores & Herrero, 2005, Vazquez-Bermudez *et al.*, 2002). Besides, we are studying the possible existence of regulatory differences between different *Prochlorococcus* strains.

This study was performed through comparative analysis of three different strains: PCC 9511, representative member of ecotypes adapted to life near the ocean surface, is an axenic strain of MED4. The other two strains are MIT9313 and SS120, both belong to ecotypes adapted to live at depth, but they are very different in evolutive terms, the appearance of MIT9313 being much older in the *Prochlorococcus* phylogenetic tree (Biller *et al.*, 2014).

1. The role of 2-OG in the control of C/N balance in *Prochlorococcus marinus*

2-oxoglutarate is described as the molecule responsible for the control of the C/N balance in cyanobacteria (Muro-Pastor *et al.*, 2001, Herrero *et al.*, 2001, Vazquez-Bermudez *et al.*, 2002, Flores & Herrero, 2005, Flores *et al.*, 2005, Luque &

Forchhammer, 2008). However, no specific study has been carried out thus far addressing the role of 2-OG in the marine cyanobacterium *Prochlorococcus*.

For that purpose, a method to determine the intracellular concentration of this metabolite was optimized (Materials and Methods section 4.8). Firstly, a HPLC method was used, based on that described (Luque-Almagro, 2005), but the results obtained from preliminary analysis of 2-OG were unsuccessful, it was impossible to detect this molecule in control samples (data not shown). The second strategy was the adaptation of a spectrophotometric method (Senior, 1975), by testing different concentrations of NADPH and enzyme. Using different concentrations of 2-OG we detected the limit of quantification of the assay (10 μM). These experiments led to the utilization of the assay mixture composed of 100 mM of NH_4Cl, 0.2 mM of NADPH and 0.15 IU of glutamate dehydrogenase. Finally, we adjusted the volume of *Prochlorococcus* sample necessary to detect 2-OG.

The level of 2-OG was determined in different strains of *Prochlorococcus* under diverse conditions.

1.1 Effect of key nutrients absence on the level of 2-OG

Prochlorococcus has an extraordinary ecological success in marine oligotrophic ecosystems. These regions are poor in nutrient (mainly nitrogen, iron and phosphorus). Thus, the level of this metabolite was analysed under the absence of this key nutrients.

Ammonium is the preferred nitrogen source by cyanobacteria (Flores *et al.*, 2005, Muro-Pastor *et al.*, 2005), and the only one being assimilated by all *Prochlorococcus* strains thus far studied, although other nitrogen sources can be assimilated by specific strains. In order to analyse the impact of nitrogen stress on the level of intracellular 2-OG, we studied the effect of nitrogen starvation in two different strains, SS120 and PCC 9511 (figure 26).

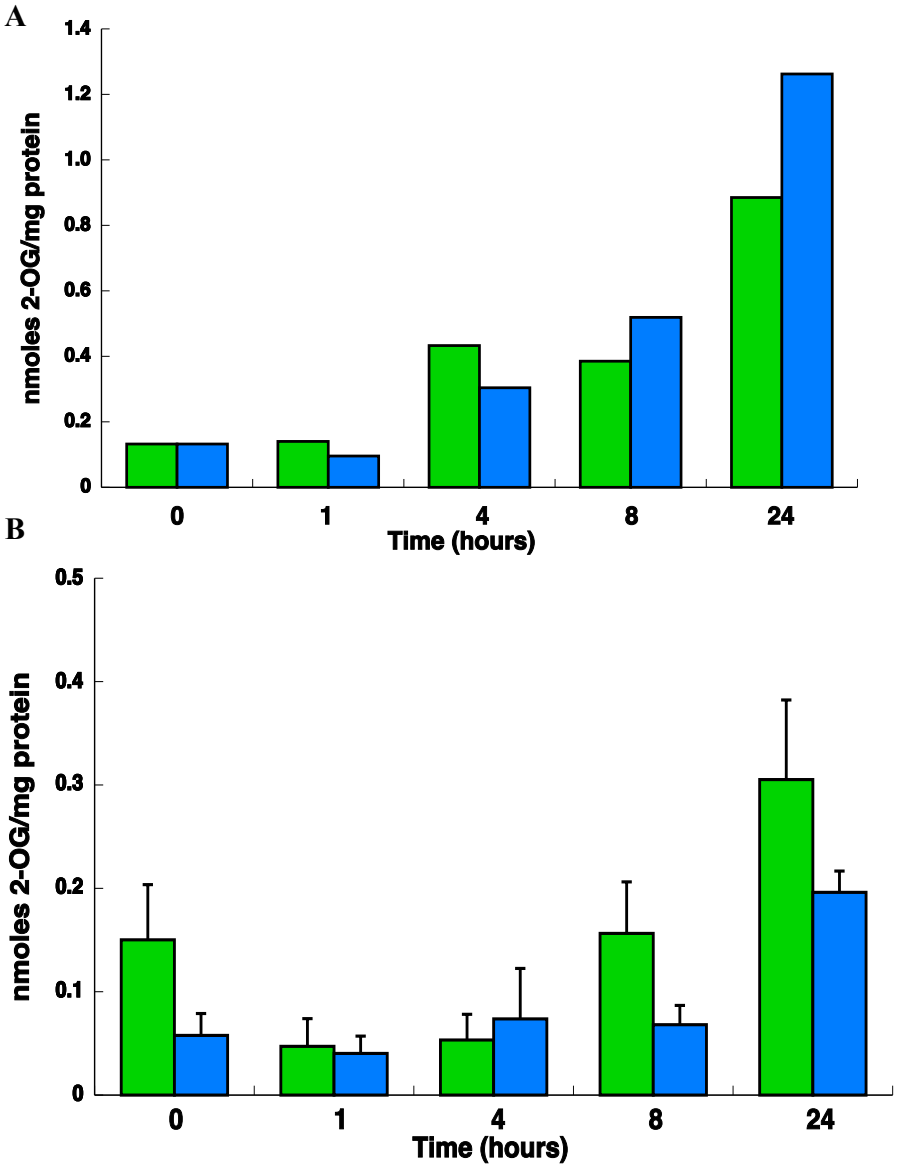

Figure 26: Effect of nitrogen starvation on the intracellular concentration of 2-OG. A. *Prochlorococcus marinus* SS120 and B. *Prochlorococcus marinus* PCC 9511. Crude extracts were obtained as described in Materials and Methods in section 3.2. The graph represents two independent biological replicates in the case of *Prochlorococcus* SS120 and four independent biological replicates for *Prochlorococcus* PCC 9511. Errors bars correspond to standard deviation. (**Nitrogen starvation** and **control** (culture grown with ammonium)).

The effect of nitrogen starvation on the intracellular level of 2-OG was more noticeable in *Prochlorococcus* SS120, the level of 2-OG increased with the time respect to the control, and it was very marked at 8 and 24 hours. Probably at this time there was no trace of nitrogen in the media. In the case of *Prochlorococcus* PCC

9511, there were no clear differences between nitrogen starvation and control, except at 8 hours (p = 0.0427), but at this time the concentration of 2-OG is lower under nitrogen starvation. That could mean that this situation does not provoke a perturbation on the level of this metabolite. Probably, the differential responses are due to the adaptation to their habitats, PCC 9511 lives in the surface of the water, where nitrogen concentration is lower that in deep waters, where SS120 thrives.

As it has been mentioned before, another two key nutrients in oligotrophic oceans are phosphorus and iron. *Prochlorococcus* SS120, the strain where we observed a clear effect after 24 hours of nitrogen starvation, was used in a long-term experiment in order to further analyse the effect of key nutrient starvation on the level of 2-OG. The results are shown in figure 27.

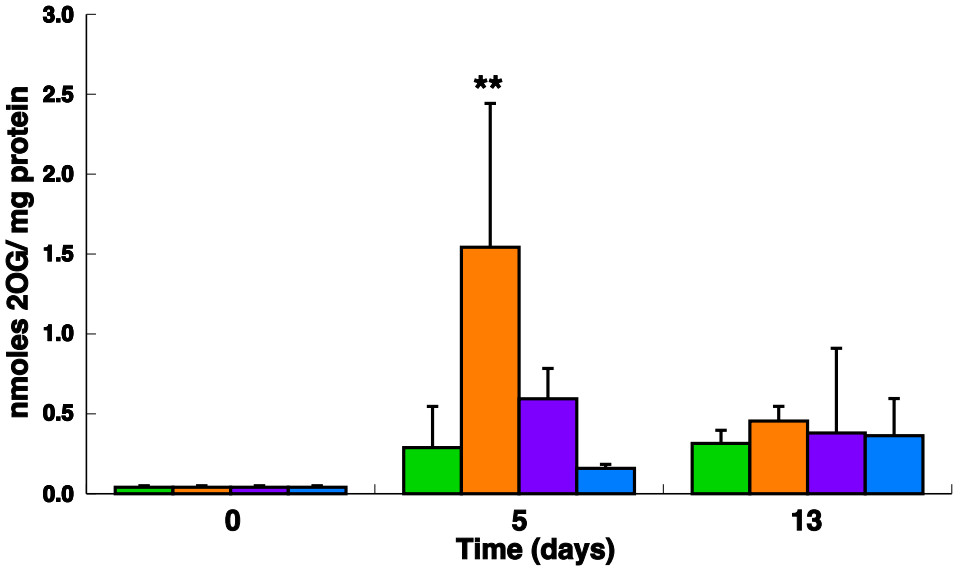

Figure 27: Effect of the key nutrient starvation on the level of intracellular 2-OG in *Prochlorococcus* SS120. The experiment was performed as described in Materials and Methods in section 2.1. It represents three independent biological samples. Errors bars correspond to standard deviation. **Control** (ammonium as nitrogen source), **iron starvation**, **phosphorus starvation** and **nitrogen starvation**.

After 5 days there was a sharp increase of this metabolite, the level was extremely high (ca. 1.5 nmoles/mg protein) upon iron starvation (p = 0.0005) and also high under phosphorus starvation. However, after 13 days of starvation, the level of 2-OG was similar in all conditions (including also the control samples), but higher than at 0 time.

1.2 Effect of nitrogen assimilation inhibitors on the level of 2-OG

The effect of 100 µM of MSX (L-methionine sulfoximine) and 100 µM of azaserine on the level of 2-OG on cultures of *Prochlorococcus marinus* was analyzed. They are inhibitors of the main pathway for nitrogen assimilation, GS-GOGAT (glutamine synthetase-glutamate synthase) in cyanobacteria, MSX blocks GS (Pace & McDermott, 1952) and azaserine blocks GOGAT (Pinkus, 1977) (figure 28).

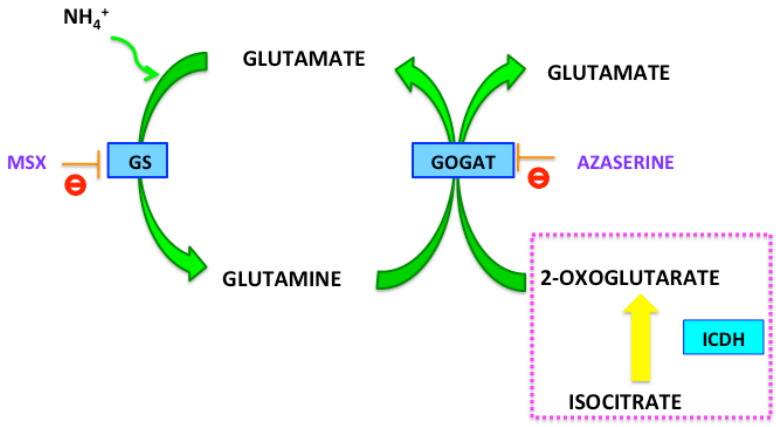

Figure 28: Specific inhibitors of GS-GOGAT pathway. MSX and azaserine block GS and GOGAT respectively.

MSX (figure 29, A) promoted an increase of the level of 2-OG after 3 hours of addition ($p = 0.1716$) and at 8 hours the level was still high ($p = 0.1299$). Besides, MSX provoked a decrease in the absorbance at 674 nm (figure 29, B), which highlighted the importance of the GS-GOGAT pathway for the growth of the cells.

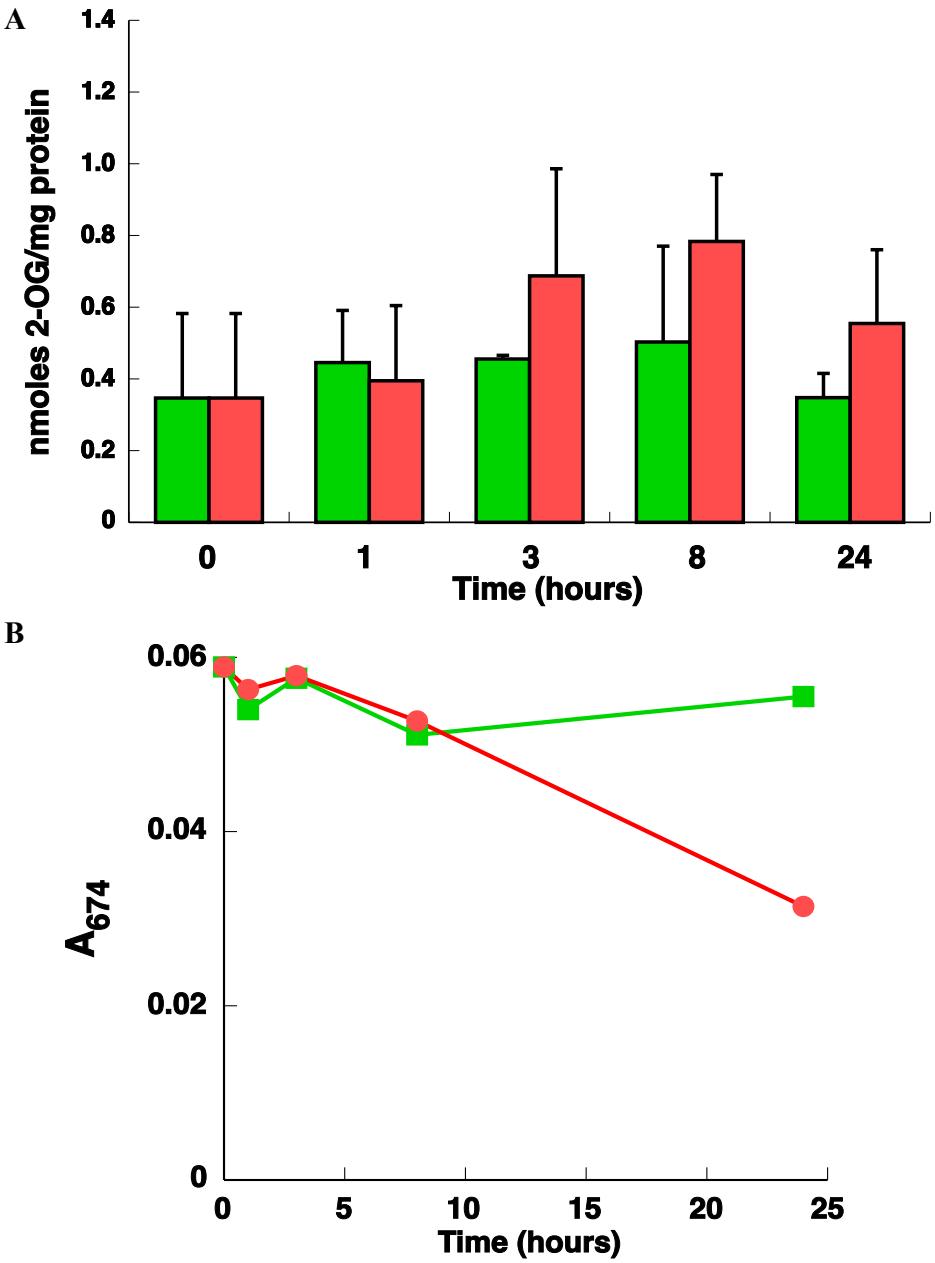

Figure 29: Effect of MSX. A. Level of 2-OG, B. Growth of *Prochlorococcus* SS120. 100 µM of **MSX** was added to the cultures and aliquots were taken at the indicated times. Graph A is the representation of four independent biological samples and graph B is the representation of data from one experiment, but the other three had identical behaviour. Errors bars correspond to standard deviation. **Control** condition means without inhibitor.

In order to study the effect of the azaserine, two different kinds of experiments were performed. Firstly, a time-course experiment up to 24 hours with two different strains, PCC 9511 and SS120 (figure 30). Secondly, in order to deep in the

differentiate control of *Prochlorococcus*, the experiment was performed with three different strains: MIT9313, PCC 9511 and SS120 and different concentrations of azaserine: 0, 1, 5, 20, 50 and 100 µM (figure 31).

The response to the addition of azaserine of SS120 was different from that of PCC 9511 (figure 30). *Prochlorococcus* SS120 exhibited a sharp increase of 2-OG, being maximum at 8 hours ($p = 0.0001$). However, in *Prochlorococcus* PCC 9511, the level of 2-OG increased significantly with time, being highest at 24 hours ($p = 0.001$).

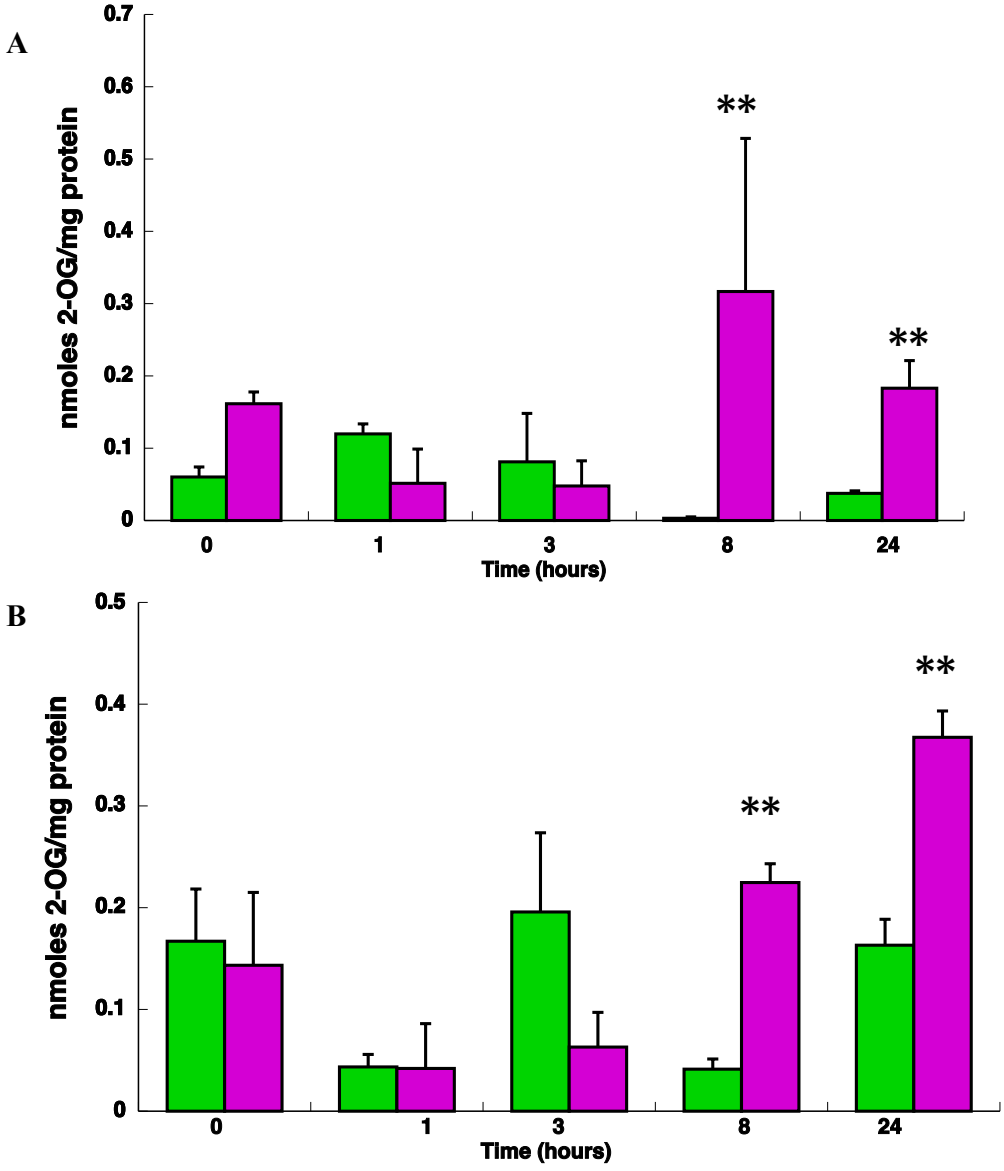

Figure 30: Effect of azaserine on the intracellular 2-OG level in A. *Prochlorococcus* SS120 and B. *Prochlorococcus* PCC 9511. 100 µM of **azaserine** was added to the cultures and aliquots were taken at the indicated times. **Control** condition means without inhibitor. The graph represents three independent biological replicates. Errors bars correspond to standard deviation.

In order to go into detail about the regulation of C/N metabolism in *Prochlorococcus* the effect of different concentration of azaserine on different strains was determined (figure 31). Although, there was not a clear pattern, in all the cases the intracellular level of 2-OG were higher when 100 µM of azaserine was added (PCC 9511 p = 0.0008 and SS120 p = 0.0503).

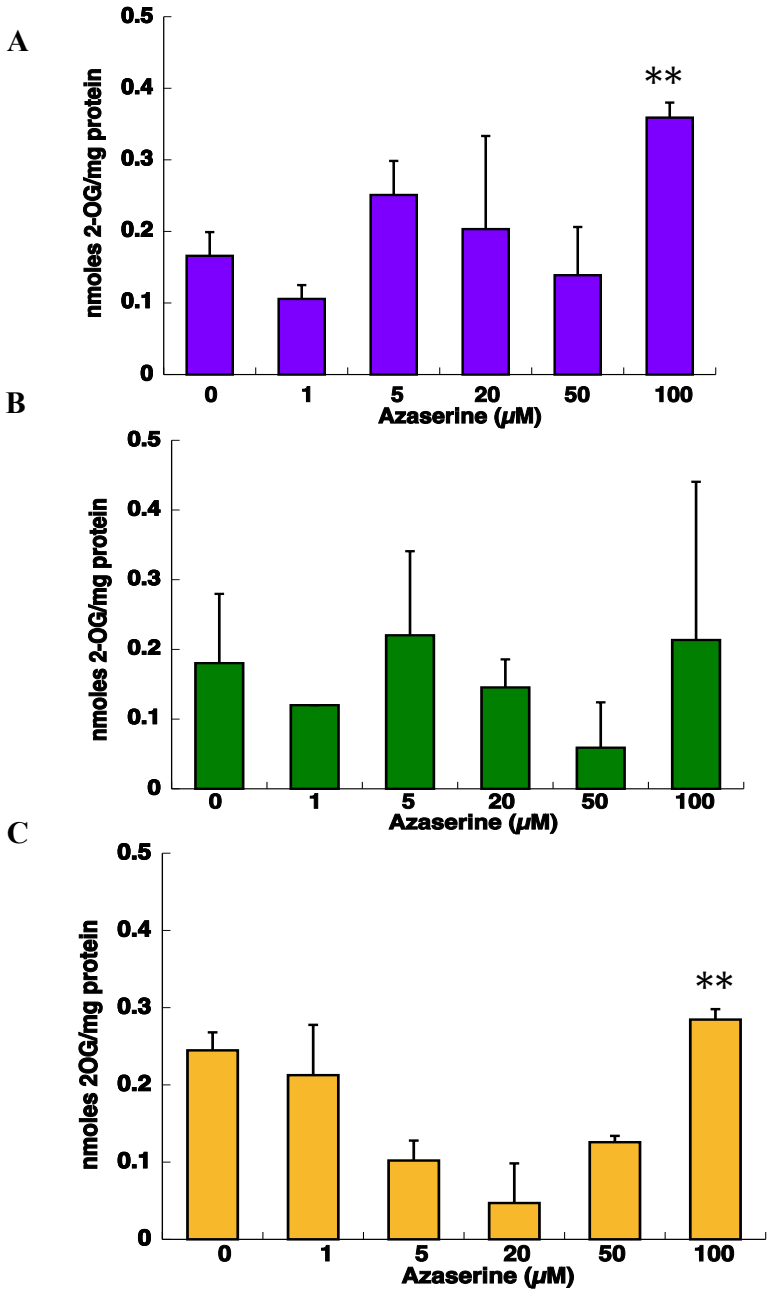

Figure 31: Effect of different concentration of azaserine in different strains from *Prochlorococcus.* Azaserine concentrations were added to the cultures of PCC 9511 (A), MIT9313 (B) and SS120 (C), and the cells were collected after 24 hours of treatment. The graph is the representation of three independent biological samples. Errors bars correspond to standard deviation.

Finally, from all the results obtained related with 2-OG we can conclude that the level of this metabolite in standard conditions is between 0.05 and 0.2 nmoles per mg of protein.

2. Effect of azaserine addition on the metabolism of *Prochlorococcus* SS120, MIT9313 and PCC 9511

Azaserine is an inhibitor of the main pathway of nitrogen assimilation. For that reason, when we add this compound to the cultures, its growth could be affected. To check this effect on the different strains, its growth was monotorized by measuring its absorbance at 674 nm during 24 hours (figure 32).

The graphs show that azaserine affects the growth of *Prochlorococcus* significantly after 24 hours. But at this time the sensibility to the inhibitor is different among strains. In the case of SS120 (figure 32, A), its growth decreased with the concentration of azaserine, but in MIT9313 was not affected the growth with 1 μM (figure 32, C). In PCC 9511 (figure 32, B) it was clearly affected with all the concentrations of the inhibitor after 24 h. Therefore, our results show that the more sensible strain to the effect of azaserine is PCC 9511.

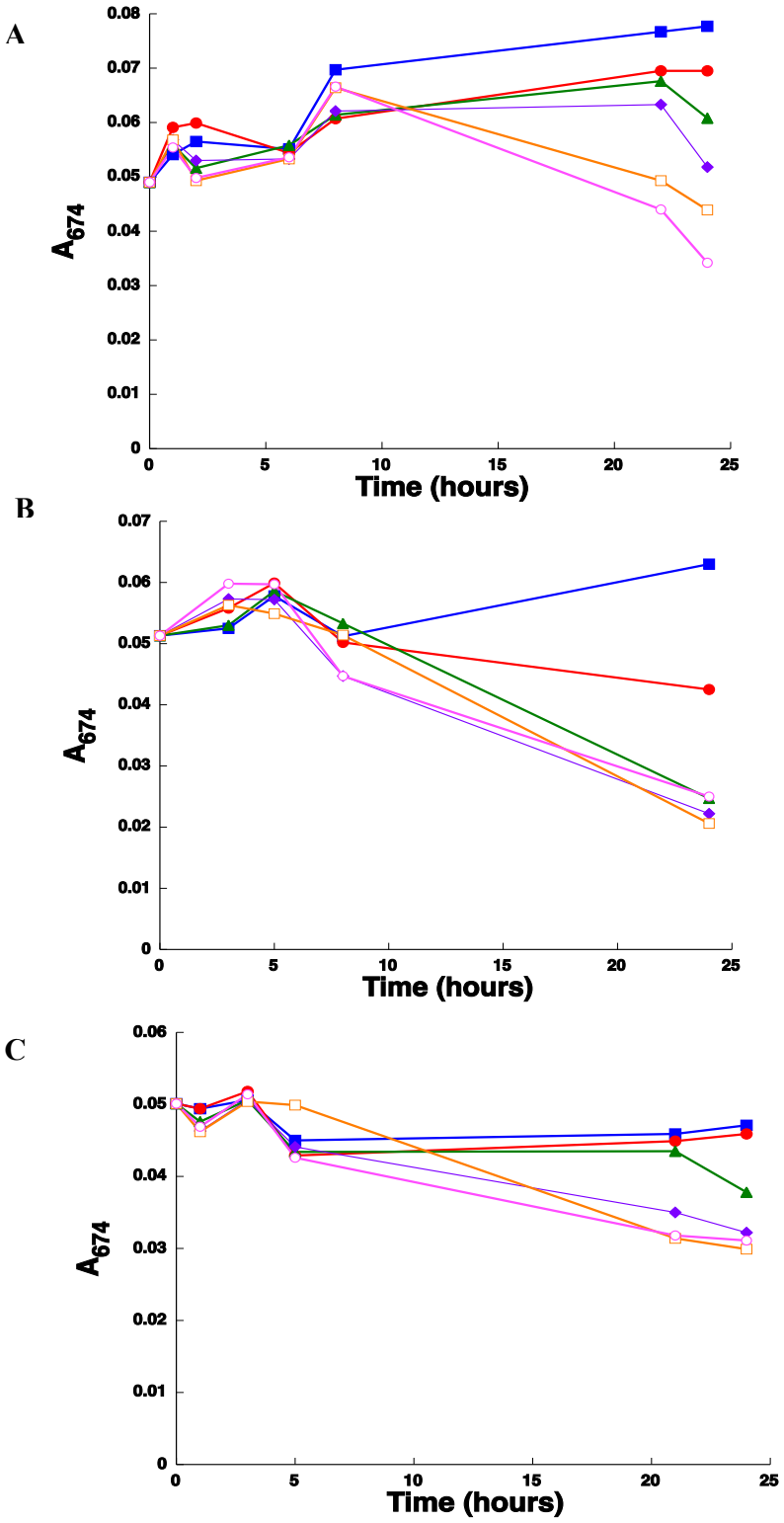

Figure 32: Effect of different concentration of azaserine on the growth of *Prochlorococcus*.

A. SS120, B. PCC 9511 and C. MIT9313. The azaserine was added and aliquots were taken at the indicated time and measured at 674 nm. Each chart is the representation of a single experiment, the other two replicates had the same behaviour. ■ 0; ● 1; ▲ 5; ◆ 20; □ 50 and ❍ 100 µM.

2.1 Changes on key enzymes

The central pathway of ammonium assimilation in cyanobacteria is composed by glutamine synthetase and glutamate synthase (GS-GOGAT). GS (EC 6.3.1.2) catalyzes the first step, that is, the ATP-dependent synthesis of glutamine from glutamate and ammonia. GOGAT (EC 1.4.7.1) catalyzes the transfer of the amido nitrogen of glutamine to 2-OG using ferredoxin as reductant.

The enzyme isocitrate dehydrogenase (ICDH; EC 1.1.1.42) catalyzes the oxidative decarboxylation of isocitrate to produce 2-OG. The incompleteness of the tricarboxylic acids cycle in marine cyanobacteria (Zhang & Bryant, 2011) confers a special importance to isocitrate dehydrogenase in the C/N balance, since 2-OG can only be metabolized through the GS-GOGAT pathway.

For that reason, we were focused on the effect of azaserine on the activity of both key enzymes of nitrogen metabolism. Besides, different strains (PCC 9511, MIT9313 and SS120) were used for comparative analysis.

As shown in figure 33, after 8 hours of 100 μM azaserine addition the activity of ICDH ($p = 0.0023$) and GS ($p = 0.0567$) increased in *Prochlorococcus* SS120.

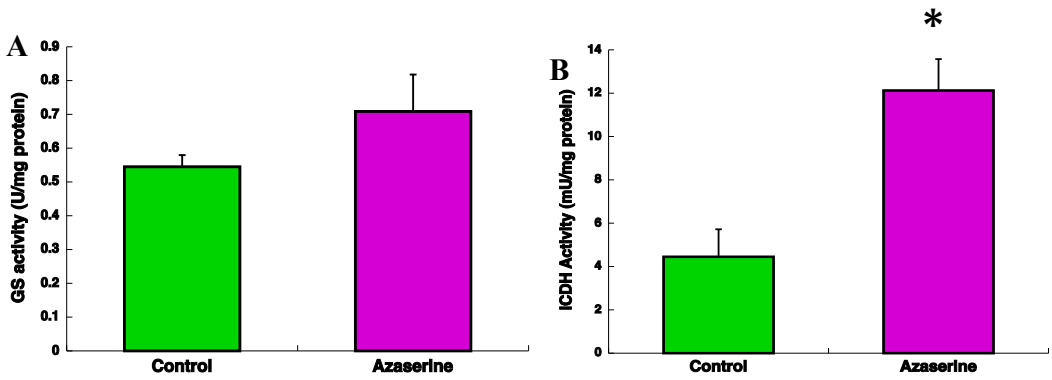

Figure 33: Effect of azaserine addition in *Prochlorococcus* SS120. A. GS Activity. B. ICDH activity. 100 μM of azaserine was added to the cultures and the cells were collected after 8 hours.

Control means without inhibitor. The graph represents the average from three independent biological replicates.

The concentration of both enzymes was determined (figure 34) under the same conditions. Surprisingly, both enzymes decreased its concentration after the treatment. This result was not expectable, because the activities in both cases were higher.

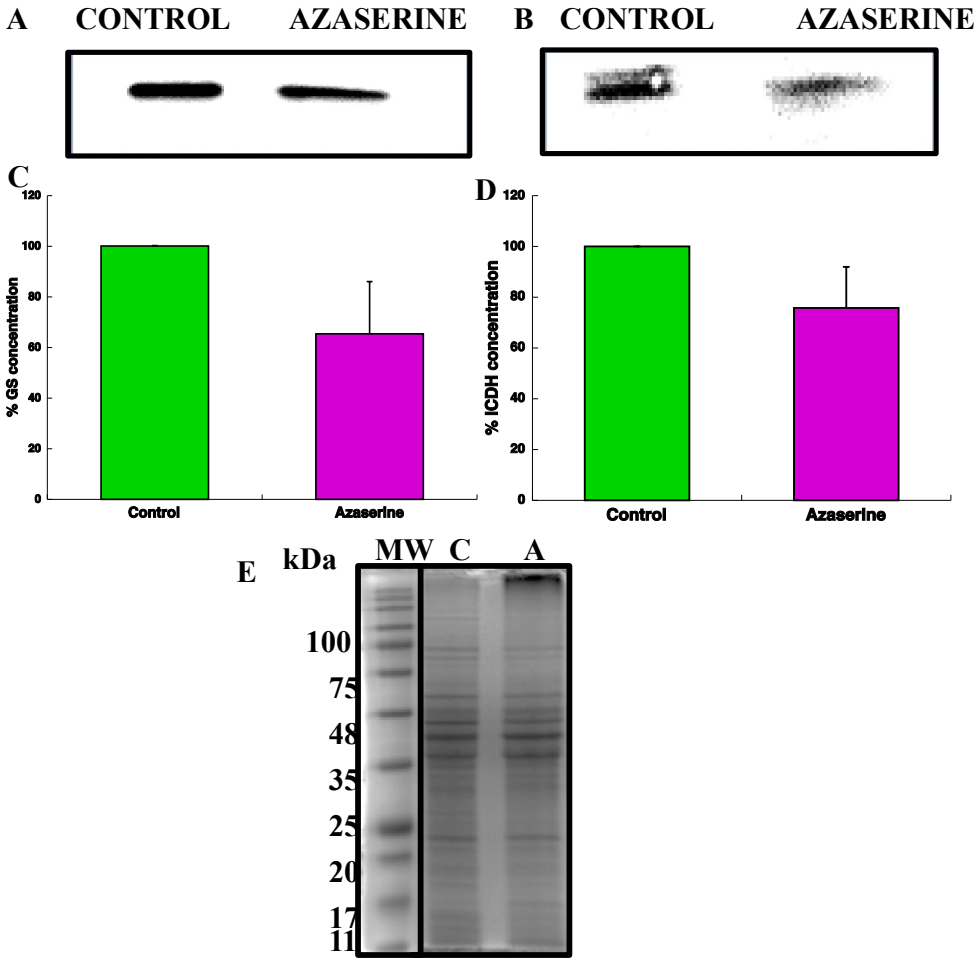

Figure 34: Effect of azaserine on the concentration of GS and ICDH from *Prochlorococcus* SS120. 100 µM of azaserine was added to the cultures and the cells were collected after 8 hours. A. Westerng blotting of GS, B. Western blotting of ICDH, C and D. Quantification of the intensities from the obtained bands. 100% correspond to the intensity for the control situation. E. SDS-PAGE (12%) coomassie stained to confirm that both lanes have equal amount of protein, 22.5 µg of protein loaded. MW = molecular weight; C = control and A = azaserine.

The evolution of ICDH activity in *Prochlorococcus* PCC 9511 after the addition of 100 µM azaserine is shown below (figure 35). The activity increased significantly after 24 hours ($p = 0.016$).

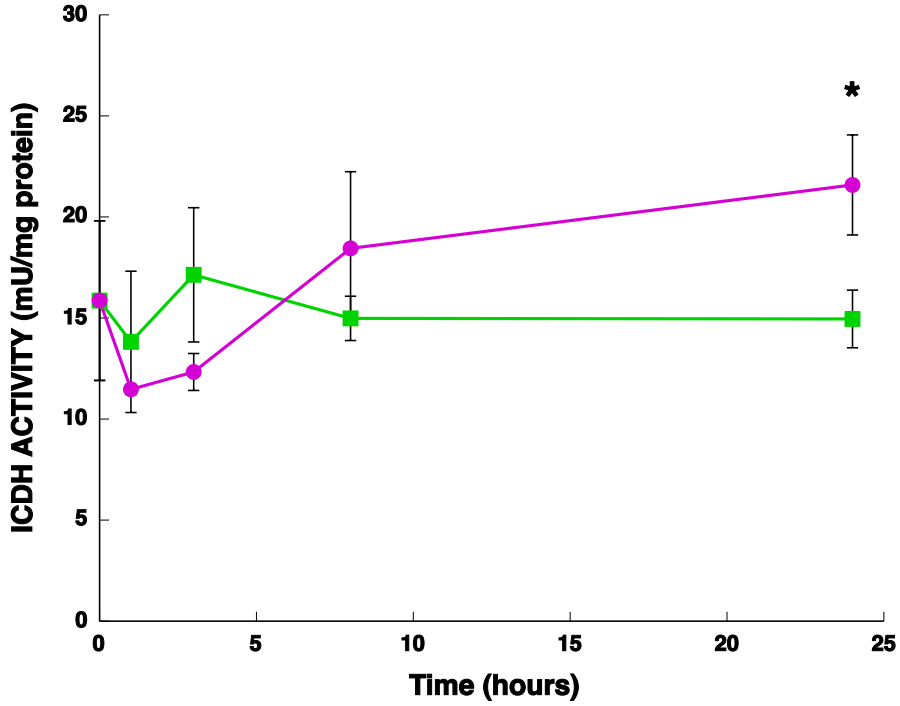

Figure 35: Effect of azaserine on the ICDH activity from *Prochloroccocus* PCC 9511. 100 µM of azaserine was added to the cultures and aliquots were taken at the indicated times. The graph represents the average from three independent biological replicates. Error bars correspond to standard deviation. ■ Control and ● azaserine.

The concentration of ICDH enzyme in time-course experiments up to 24 hours was determined (figure 36). In contrast to SS120, at 8 hours of addition the concentration of the enzyme was higher in azaserine condition.

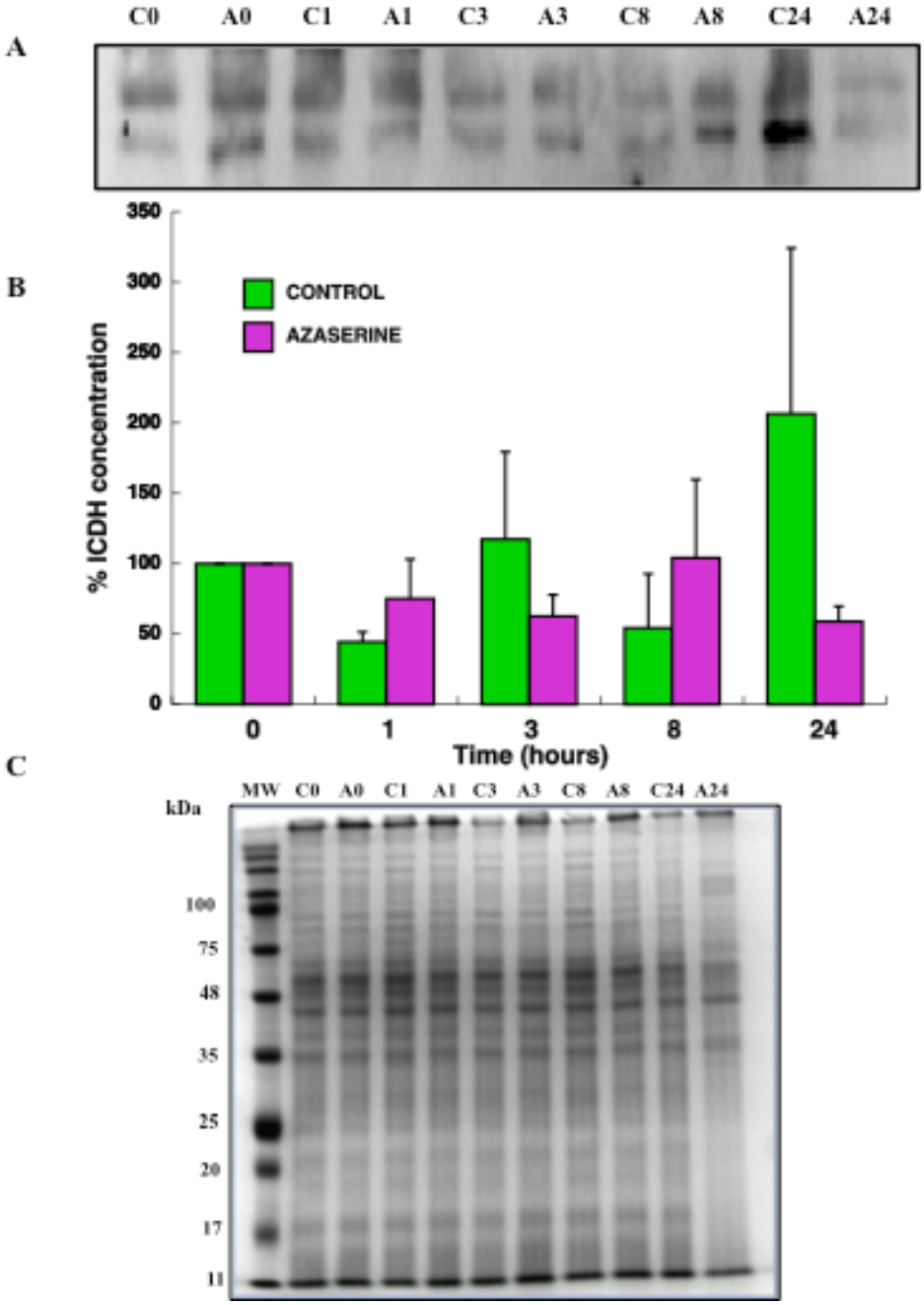

Figure 36: Effect of azaserine on the concentration of ICDH from *Prochlorococcus* PCC 9511. Azaserine at a final concentration of 100 µM was added to the cultures and aliquots were taken at the indicated times. A. Western blotting of ICDH. B. Quantification of the bands, assigning an arbitrary value of 100% to the time 0 of each series (control and azaserine). C. SDS-PAGE (12%) coomassie stained to control that the amount of protein is equal in all the lanes, 10 µg of proteins loaded. C. Lanes are marked with C (control) and A (azaserine), followed by sampling time (in hours).

To deep in the characterization of the enzyme ICDH, the axenic strain *Prochlorococcus* PCC 9511 was used. For that purpose, the concentration of ICDH was determined in different conditions that could affect it (figure 37). These

conditions were nutrient starvation (Fe, N and P), inhibitors of the main assimilation pathway (azaserine and MSX), inhibitors of the photosynthetic electron flow (DCMU and DBMIB) and darkness.

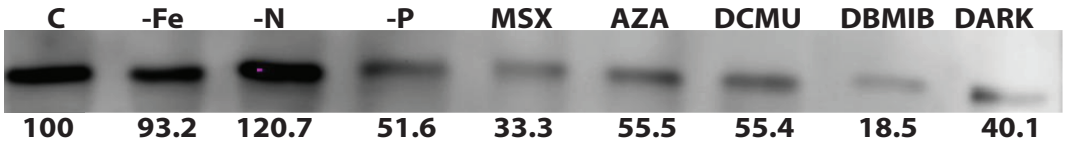

Figure 37: ICDH concentration of *Prochlorococcus* PCC 9511 from culture subjected to different conditions. Cells under iron starvation were collected after 8 hours of the treatment, and the rest of conditions were collected after 24 hours. C = control; -Fe = iron starvation; -N = nitrogen starvation; -P = phosphorus starvation; MSX= 100 µM L-metilsufoxide; AZA= 100 µM azaserine; DCMU= 0.3 µM; DBMIB= 0.06 µM; DARK= Darkness. Quantification of bands below the picture, 100% correspond to the intensity of control band.

Regard to nutrients starvation, the lack of iron, nitrogen and phosphorus produced different results (figure 37). As previously reported (El Alaoui *et al.*, 2003), the lack of iron provoked a marked decrease in the number of cells. For that reason, cells under iron starvation were collected after 8 hours instead of 24 hours as the other conditions. The iron starvation provoked a slight loss of the concentration of the enzyme and the phosphorus absence promoted a decrease of it. On the contrary, nitrogen starvation provoked a slight increase of ICDH.

Both inhibitors of the GS-GOGAT pathway promoted a decrease in the concentration of the enzyme, but it was more drastic with MSX (33.3% vs 55.5%) (figure 37).

DCMU and DBMIB are inhibitors of the photosynthetic electron flow, blocking the electron transfer before and after the plastoquinone pool, respectively (figure 38) (Rich *et al.*, 1991, Trebst, 1980).

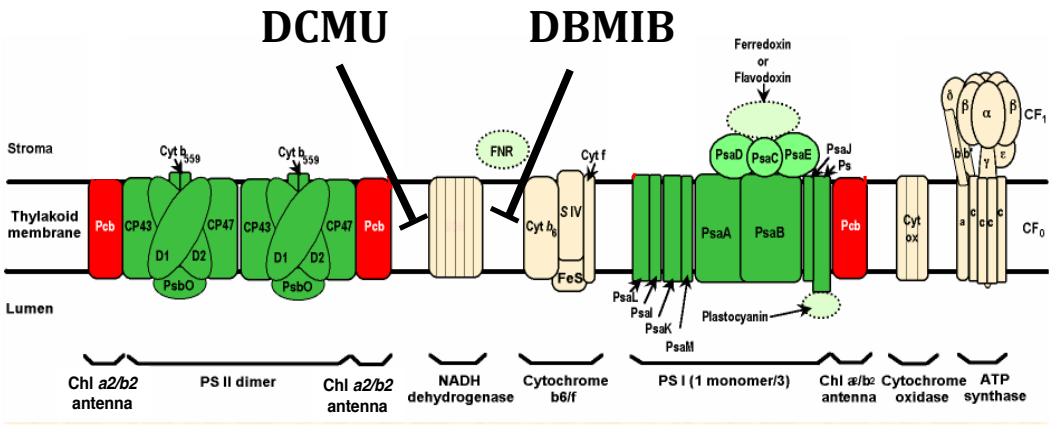

Figure 38. Effect of the inhibitors DCMU and DBMIB on the photosynthetic electron transport chain. Adapted and modified (Bibby *et al.*, 2003).

After 24 hours, DCMU and DBMIB promoted a decrease in the concentration of ICDH. Strikingly, DCMU promotes a less marked effect than DBMIB (55.4% vs 18.5 %) (figure 37).

The last studied condition was the absence of light, which is an important factor in the metabolic regulation of photosynthetic organisms. Darkness promoted a response similar to DCMU, the oxidation of the plastoquinone pool and the decrease in the NADPH intracellular levels, in both cases there were no great differences in the concentration of ICDH, 40.1% under darkness vs 55.4% under DCMU treatment.

During the first section of this chapter, our interest was focused on the metabolite 2-OG in order to prove that it is the molecule responsible for the control of the C/N balance in *Prochlorococcus*. ICDH is the enzyme that produces 2-OG, and we have described above that azaserine provokes an increase in both ICDH activity and concentration of 2-OG. Our interest was to test if 2-OG has a direct effect on the ICDH activity. For that, a standard ICDH reaction was carried out using different concentrations of 2-OG. It is important to point out, that these concentrations are much higher than the physiological for this metabolite (Muro-Pastor & Florencio, 1992). The results are summarized in table 45.

Table 45: Effect of 2-OG on the ICDH activity in *Prochlorococcus* PCC 9511

[2-OG] (mM)	ICDH Activity (mU/mg protein)	SD
0	8.68	1.52
1	7.76	1.65
3	7.6	1.81
6	6.18	1.51
10	4.91	1.92

As we can observe in the table 45, after the addition of 10 mM of 2-OG to the assay there was 44.5% less activity. With these results, we can conclude that the effect of 2-OG observed in figure 33 and 35 is not direct on the ICDH activity.

The possible variability between strains in relation with their regulatory mechanisms was assessed by studying the effect of different concentration of azaserine on these two key enzymes, GS and ICDH, using three different strains: PCC 9511, MIT9313 and SS120.

As it is shown in figure 39, the response of GS activity to the different concentrations of azaserine is quite different depending on the strain. In the case of SS120, the activity increased with the concentration of azaserine; however, this behaviour is not shared by the other strains, since they have a quite different pattern. In *Prochlorococcus* MIT9313, the activity did not change with the concentration of azaserine and in *Prochlorococcus* PCC 9511 the highest activity was found with 20 μM of azaserine.

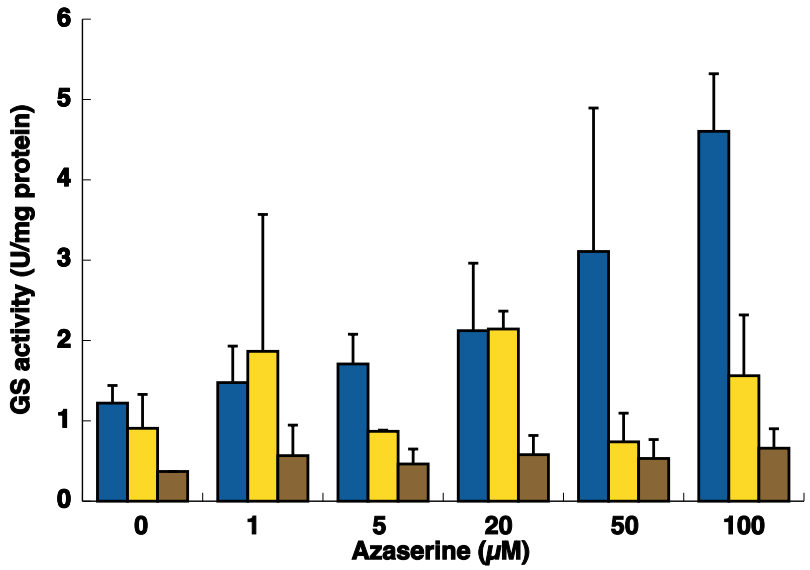

Figure 39: Effect of different concentration of azaserine on GS activity in different strains from *Prochlorococcus* (SS120, PCC 9511 and MIT9313). The cells were collected after 24 hours. The graph is a representation of three independent biological replicates of each strain. Error bars correspond to standard deviation.

The concentration of the GS was determined too (figure 40). The results show three different patterns. In PCC 9511 the concentration was increasing with the concentration of the inhibitor and in contrast, the GS from SS120 decreased. In MIT9313 the concentration of the enzyme decreased with 1µM and it was approximately the same with the rest of concentrations.

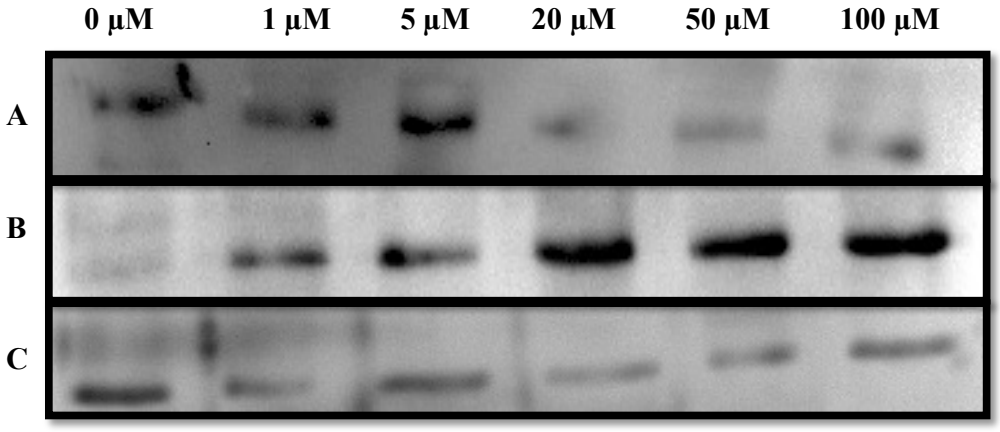

Figure 40: Effect of different concentration of azaserine on GS concentration. A. SS120, B. PCC 9511 and C. MIT9313. The different concentrations of azaserine were added to the cultures and cells were collected after 24 hours of treatment.

ICDH activity was measured under the same conditions than GS (figure 41). As we can notice, the pattern is similar in the case of *Prochloroccus* SS120 and PCC 9511, the activity being higher with low concentration of azaserine, these results are in good agreement with the western blotting shown in figure 42, where the concentration of the enzyme is higher with low concentrations of azaserine. In the case of MIT9313, the activity increased with azaserine concentration up to 20 µM, the same showed the concentration of the enzyme (figure 42, A) but the level of activity is not so high compared with SS120 and PCC 9511.

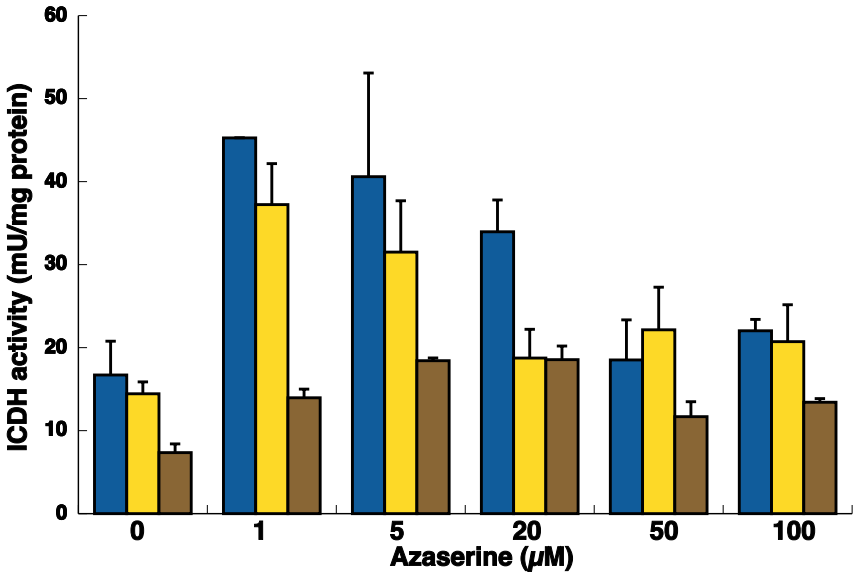

Figure 41: Effect of different concentration of azaserine on ICDH activity in different strains of *Prochlorococcus* (SS120, PCC 9511 and MIT9313). The cells were collected after 24 hours. The graph is a representation of three independent biological replicates of each strain. Error bars correspond to standard deviation.

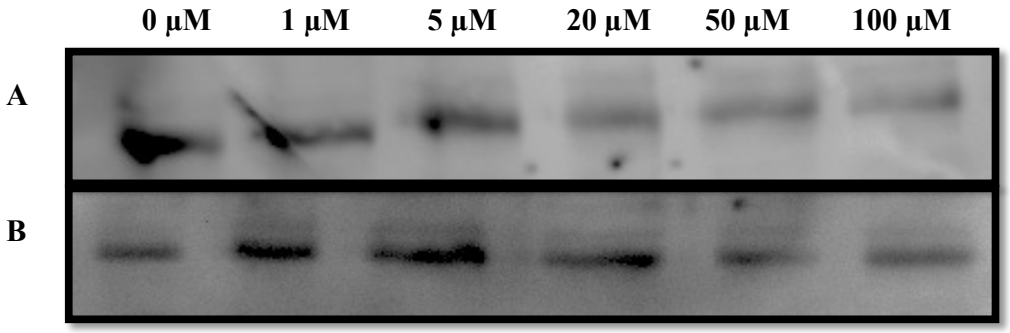

Figure 42: Effect of different concentration of azaserine on ICDH concentration. A. SS120, B. MIT9313. The different concentrations of azaserine were added to the cultures and cells were collected after 24 hours of treatment.

To find a motive of the different behaviour of GS and ICDH from these three strains of *Prochlorococcus* an alignment of their sequence was performed (figure 43 and 44, respectively). That reveal that they are quite conserved, suggesting that the differences are not due to a different structure or physic-chemicals properties of the enzymes, probably the differences could be explained for the natural selection, mainly on its regulatory mechanisms, with the selective pressure from the different habitats where they are predominant.

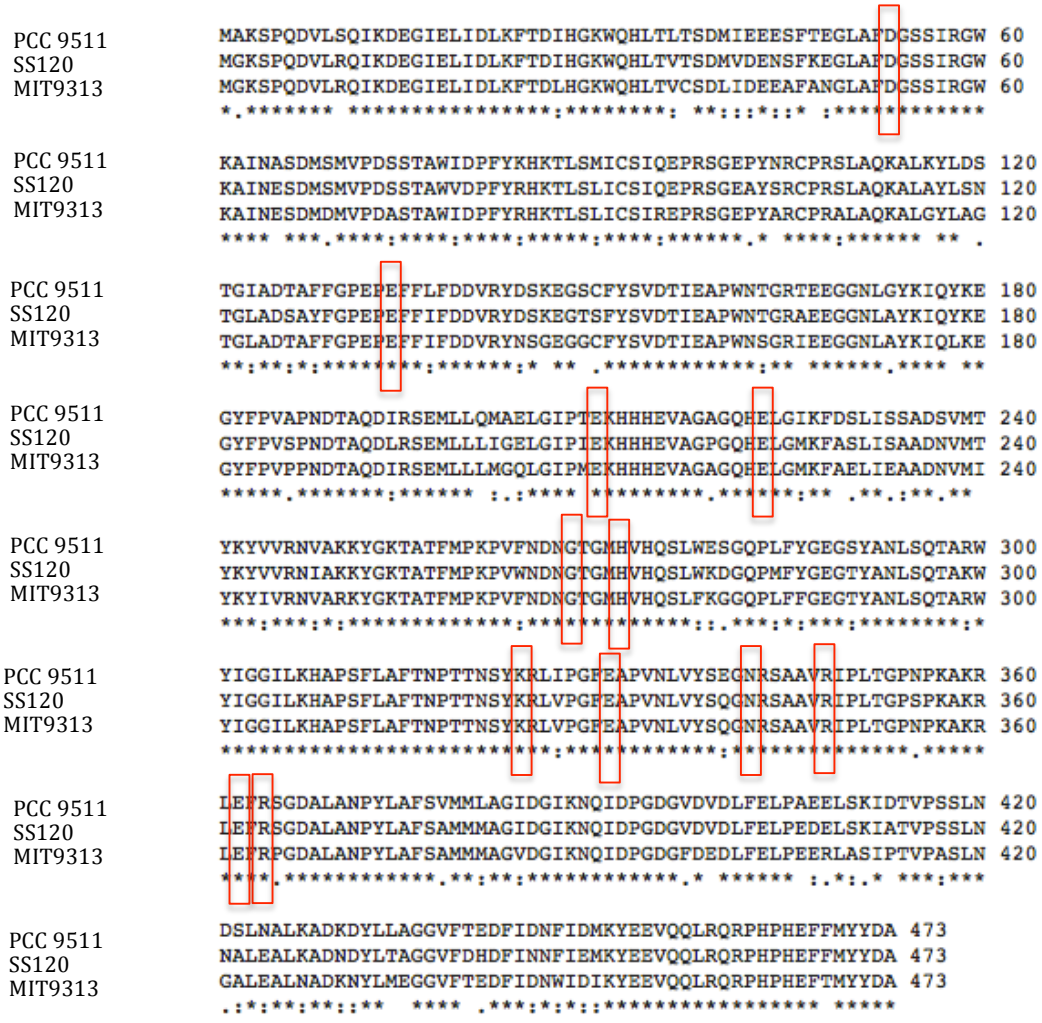

Figure 43: Multiple sequence alignment of GS from *Prochlorococcus* MIT9313, SS120 and PCC 9511. The sequences in FASTA format were taken from CYORF and ClustalW2 from *EMBL-EBI* was used to make the alignment. (*****) Indicates positions which have a single, fully conserved residue; (**:**) indicates conservation between groups of strongly similar properties and (**.**) indicates conservation between groups of weakly similar properties. Highlighted amino acids residues involved in the biosynthetic reaction.

```
MIT9313     MAQFEKLSPPSQGTAIRFVNGQPVIPNEPIIPFIRGDGTGVDIWPATQRVLDAAVTKAYQ 60
SS120       MVHYEKLSPPTTGEKIKFNNGLPIVPANPIIPYIRGDGTGVDIWPATQKVIDQAIEKAYG 60
PCC 9511    MPKFEKLNLPKEGELITFNQGKPNVPNNPIVPYIRGDGTGVDIWPATQLVLDEAIKKSYG 60
            * ::***. *. *  * * :* * :* :**:*:*************** *:* *: *:*

MIT9313     GVRRIEWFKVYAGDEACDLYGTYQYLPEDTLEAIRTYGVAIKGPLTTPIGGGIRSLNVAL 120
SS120       IDRKIEWFKIYAGDEACDLYGTYQYLPKDTIEAIREYGVAIKGPLTTPIGGGIRSLNVAL 120
PCC 9511    DERKINWFKVYAGDEACEIYGTYNYLPQDTIEAIRHFGVAIKGPLTTPIGGGIRSLNVAL 120
              *:*:***:*******::****:***:**:**** :**********************

MIT9313     RQIFDLYSCVRPCRYYKGTPSPHKRPQDLDVIVYRENTEDIYMGVEWEADDPVGKTLREH 180
SS120       RQKFDLYSCVRPCRYYQGTPSPHKHPENLDVIVYRENTEDIYIGIEWESNDPIGIKLIEH 180
PCC 9511    RQIFDLYSCVRPCKYYSGTPSPHKNPQNLDVIVYRENTEDIYMGIEWEADDHTCIDLINH 180
            ** **********:**.*******.*::***************:*:***::*     * :*

MIT9313     LNTVVIPANGKLGKRQIPEGSGIGIKPVSKHGSQRHIRKAIQHALRLKGDKRHVTLVHKG 240
SS120       LNNDVIPASPSLKNRIIPQGSGIGIKPVSKDGSQRHIRRAIQHALKLNGNKRHVTLVHKG 240
PCC 9511    LNNVVIPNSKNLKNRSIPDGSGIGIKPVSKLGSQRHIRKAIEHAKRLSGNKKHVTLVHKG 240
            **. *** . .* :* **:*********** *******:**:** :*.*:*:********

MIT9313     NIMKFTEGAFRDWGYELATSEFRDVCITERESWILGNLENDPQLSIQANARMIEPGYDSL 300
SS120       NIMKFTEGSFRDWGYELATNEFRNECITERESWILSNLEQNPRLSIENNAKLIDPGYESL 300
PCC 9511    NIMKYTEGAFRDWGYELAVNEFRADCITERESWILDNIHKNPEITIENNARKIEPGYDKL 300
            ****:***:*********..***  **********.*:.::*.::*: **: *:***:.*

MIT9313     TPERKASIDAEVHGVLDAIGTSHGNGQWKAMVLVDDRIADSIFQQIQTRPQEYSILATLN 360
SS120       TKEKKDIICNEVQLVINNIHKTHGNNKWKKMVLVDDRIADSIFQQIQTRPQEYSILATLN 360
PCC 9511    TSNKKAFICEEIKEVIASISNSHGNNKWEELIMVDDRIADSIFQQIQTRPQEYSILATLN 360
            * ::*  *  *:: *:  * .:***.:*: :::*****************************

MIT9313     LNGDYISDAAAAMVGGLGMAPGANIGENAAIFEATHGTAPKHAGLDRINPGSVILSGVMM 420
SS120       LNGDYISDAAAAIVGGLGMAPGANIGDRAAIFEATHGTAPKHAGLDRINPGSVILSGVMM 420
PCC 9511    LNGDYVSDAAAAIVGGLGMAPGANIGDNSAIFEATHGTAPKHAGLNKINPGSVILSGVMM 420
            *****:******:*************:.:****************::*************

MIT9313     LEFLGWQEAADLITKGLSAAIANQQVTYDLARLMDPPVDPVSCSGFSEAVISHF 474
SS120       LEYIGWQEAADLITKGLSQSIYDKQVTYDLARLMEPPQSPLSCSEFANAVIERF 474
PCC 9511    LEYFGWNEAAKLVTSGISKAIEEKKVTYDLARLMEPKVAPLSCSGFAEAIISNF 474
            **::**:***.*:*.*:* :* :::**********:*   *:*** *::*:*..*
```

Figure 44: Multiple sequence alignment of ICDH from *Prochlorococcus* MIT9313, SS120 and PCC 9511. The sequences in FASTA format were taken from CYORF and ClustalW2 from *EMBL-EBI* was used to make the alignment. (*****) Indicates positions which have a single, fully conserved residue; (**:**) indicates conservation between groups of strongly similar properties and (**.**) indicates conservation between groups of weakly similar properties.

2.2 Changes in the expression of genes related to nitrogen metabolism

The effect of different conditions, mainly azaserine addition, on the expression of genes related to nitrogen metabolism was further studied. The genes encoding key enzymes or regulatory proteins involved in nitrogen metabolism were selected: *glnA* (encoding GS), *icd* (encoding ICDH), *glsF* (encoding GOGAT) and *gdh* (encoding GDH); *ntcA* (encoding the transcriptional regulator NtcA), *glnB* (encoding the protein PII) and *pipX* (encoding PipX).

The *ntcA* expression pattern in three strains of *Prochlorococcus* was completely different (figure 45). While in SS120 the expression did not significantly change with the concentration of azaserine, in MIT9313 the expression of *ntcA* was increasing with the concentration of the inhibitor, being significantly higher at 50 and 100 µM ($p = 0.0047$ and $p = 0.0059$ respectively). In PCC 9511, *ntcA* expression peaked at 20 µM azaserine ($p = 0.0001$), with significant increases also at 5 and 50 µM ($p = 0.0279$ and $p = 0.0001$ respectively). It is worth noting that the increase in *ntcA* expression observed in this strain was much bigger than either in SS120 or MIT9313 (i.e., more than 4-fold than in MIT9313).

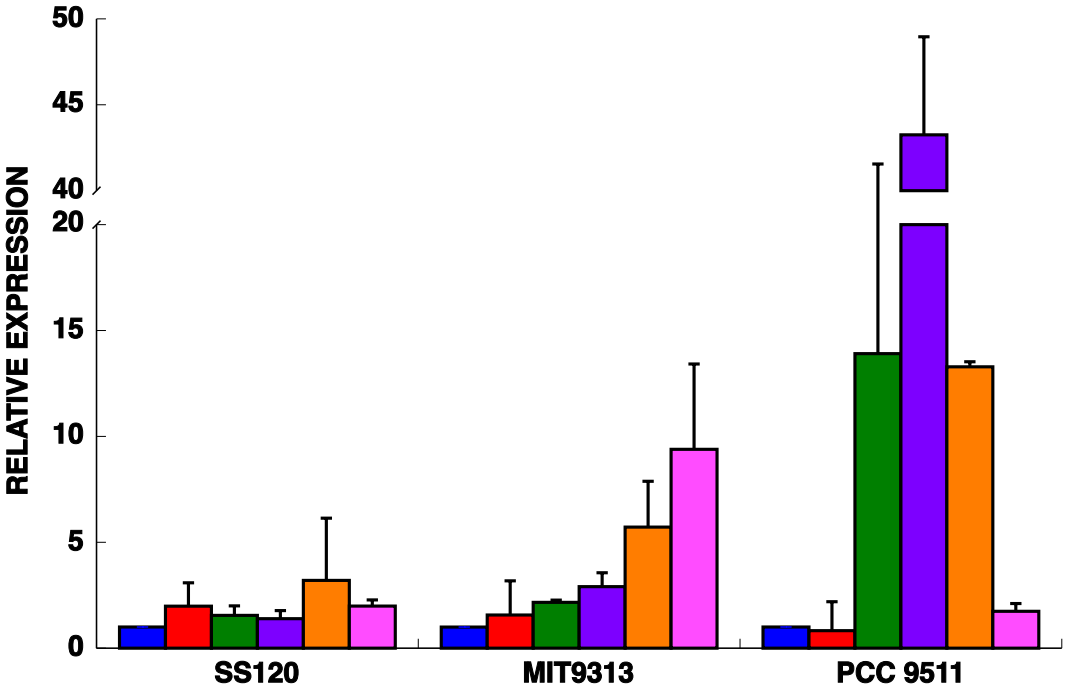

Figure 45: Effect of different concentration of azaserine on *ntcA* expression. Azaserine (0, 1, 5, 20, 50 and 100 µM) was added to cultures of different strains of *Prochlorococcus* (SS120, MIT9313 and PCC 9511). Samples were collected after 24 hours, and gene expression was measured by qRT-PCR. Data are the average of four independent biological replicates. Error bars correspond to standard deviation.

Another regulatory protein of interest is P_{II}, encoded by the gene *glnB*. The response of the expression of *glnB* in the three strains of *Prochlorococcus* is diverse (figure 46). In SS120 with the addition of 5 and 50 µM of azaserine the level of

expression decreased significantly (p = 0.0186). In the case of MIT9313 the expression increased slightly with 20 µM (p = 0.0001) and in PCC 9511 with 1 µM (p = 0.0001).

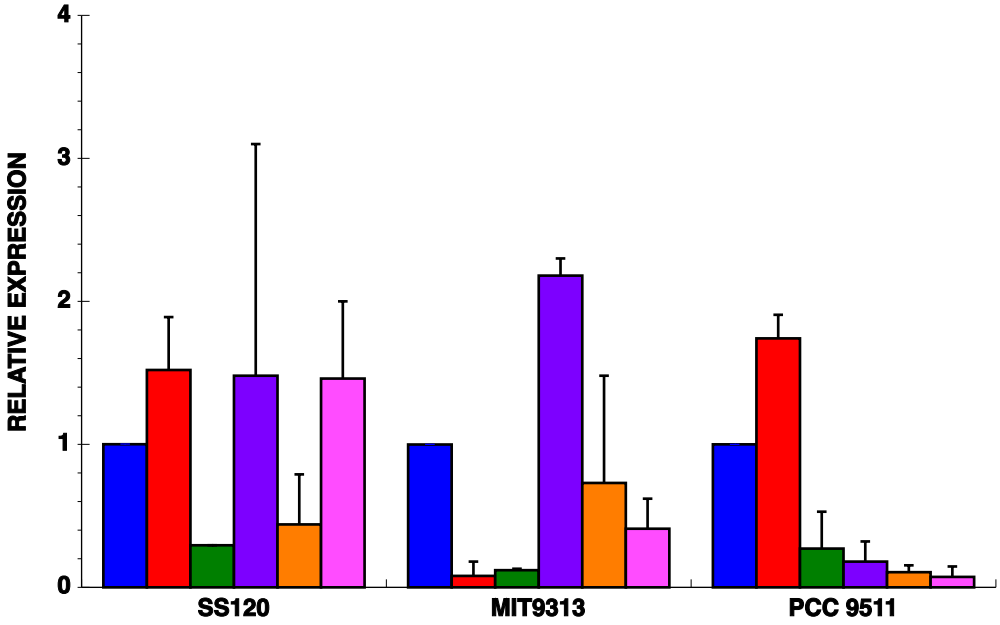

Figure 46: Effect of different concentration of azaserine on *glnB* expression. Azaserine (0, 1, 5, 20, 50 and 100 µM) was added to cultures of different strains of *Prochlorococcus* (SS120, MIT9313 and PCC 9511). Samples were collected after 24 hours, and gene expression was measured by qRT-PCR. Data are the average of four independent biological replicates. Error bars correspond to standard deviation.

Finally, the last regulatory protein described until now is PipX and it is encoded by the gene *pipX*. The figure 47 shows the results obtained in SS120 and MIT9313. After several attempts, the amplification of *pipX* from PCC 9511 was not possible to achieve. In *Prochlorococcus* MIT9313, the gene exhibited a marked increase of the expression with 1 µM of azaserine (p = 0.0001). Besides, the graph shows that in SS120 it increases significantly after the addition of the different concentration of azaserine.

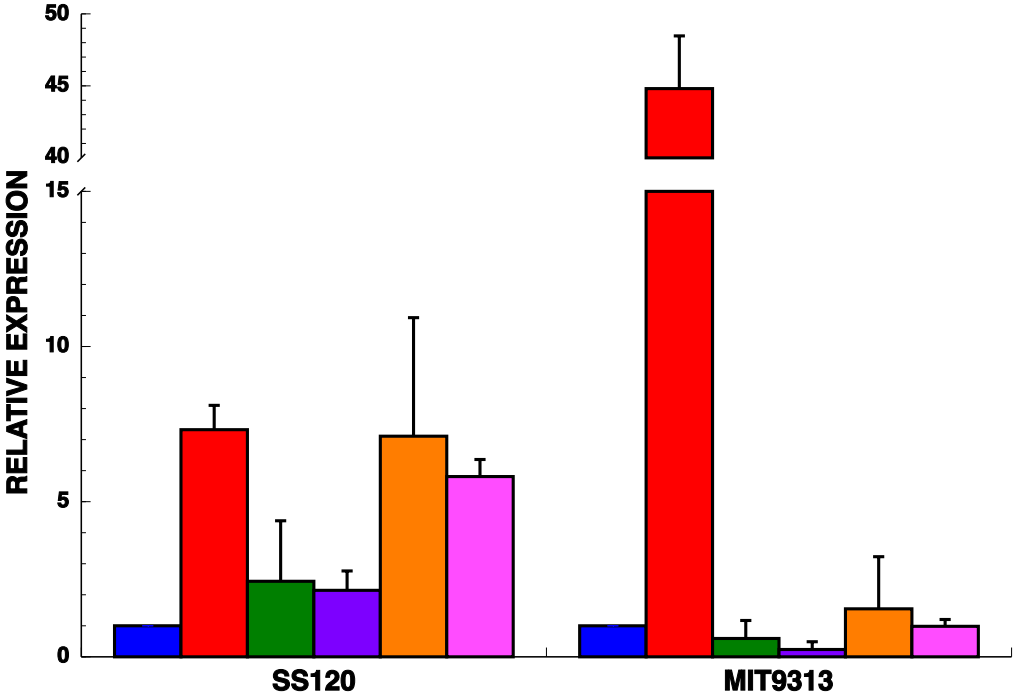

Figure 47: Effect of different azaserine concentration on *pipX* expression. Azaserine (0, 1, 5, 20, 50 and 100 µM) was added to cultures of different strains of *Prochlorococcus* (SS120 and MIT9313). Samples were collected after 24 hours, and gene expression was measured by qRT-PCR. Data are the average of four independent biological replicates. Error bars correspond to standard deviation.

The expression of three genes encoding key enzymes of nitrogen metabolism has been further studied under the same condition as regulatory proteins shown above. The *glsF* expression showed a steep rise with 1 µM in *Prochlorococcus* PCC 9511 ($p = 0.0001$). On the other hand, *Prochlorococcus* MIT9313 and SS120 did not show significant changes after the treatment with different concentrations of azaserine (figure 48).

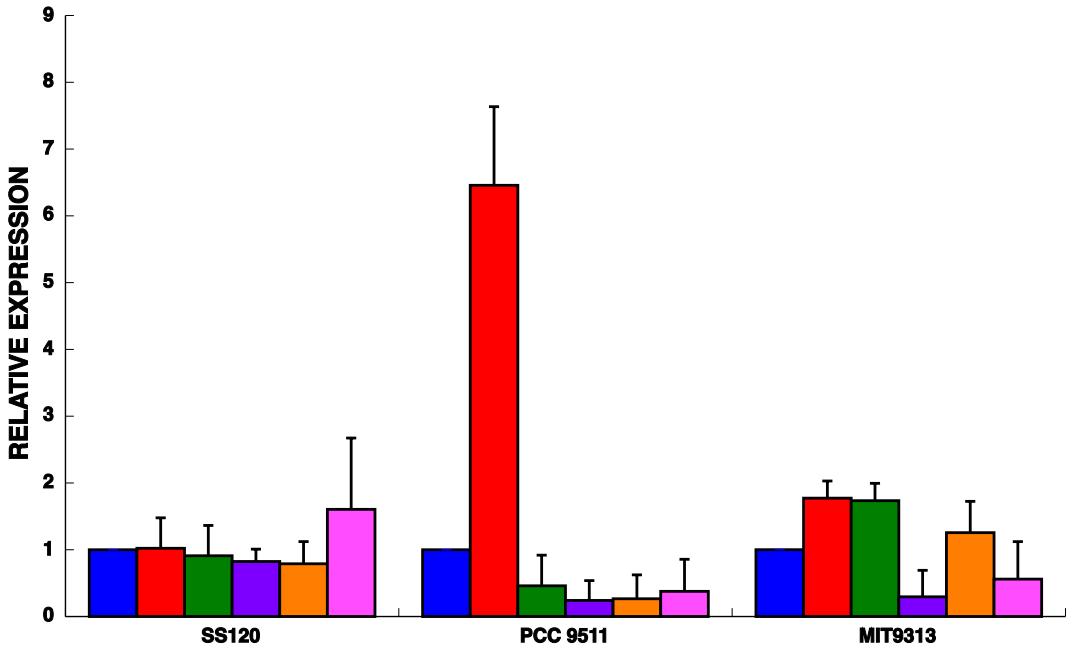

Figure 48: Effect of different azaserine concentration on *glsF* expression. Azaserine (0, 1, 5, 20, 50 and 100 µM) was added to cultures of different strains of *Prochlorococcus* (SS120, MIT9313 and PCC 9511). Samples were collected after 24 hours, and gene expression was measured by qRT-PCR. Data are the average of four independent biological replicates. Error bars correspond to standard deviation.

The expression of *glnA*, encoding GS, has been analyzed in PCC 9511 and SS120. Similar problems as described for *pipX* were found for *glnA* amplification in MIT9313. Figure 49 shows that *glnA* expression decreased in the strain SS120 after azaserine addition, showing an increase only at the concentration 100 µM. However, *in Prochlorococcus* PCC 9511, the increase of the concentration of azaserine promoted an increase in *glnA* expression. Surprisingly, after the addition of 5 µM and 100 µM the level of expression was similar and even higher than with the other concentrations used ($p = 0.0001$ both conditions).

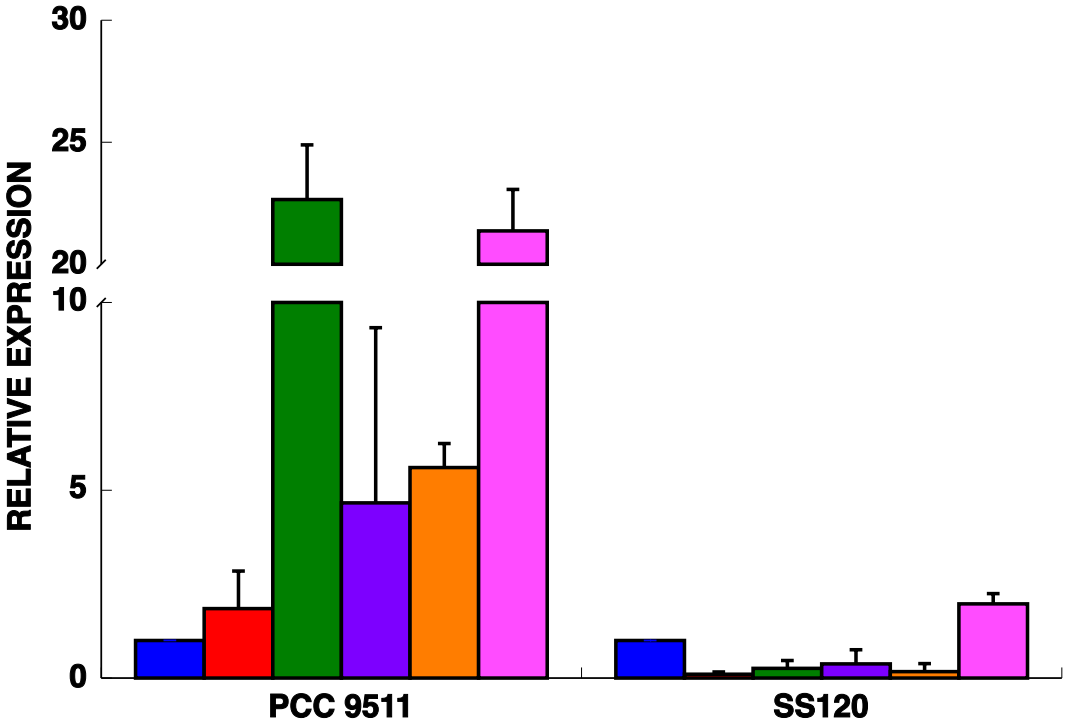

Figure 49: Effect of different azaserine concentration on *glnA* expression. Azaserine (0, 1, 5, 20, 50 and 100 µM) was added to cultures of different strains of *Prochlorococcus* (SS120 and PCC 9511). Samples were collected after 24 hours, and gene expression was measured by qRT-PCR. Data are the average of four independent biological replicates. Error bars correspond to standard deviation.

The ICDH is encoded by the *icd* gene. As we can see in figure 50 the pattern of the expression in three different strains of *Prochlorococcus* is clearly different. PCC 9511 showed an increase after the addition of different concentration of the inhibitor, but a great peak of expression was found with 5 µM of azaserine ($p = 0.0017$). In contrast, the expression in MIT9313 did not show any clear change (with the exception of 20 µM), and in SS120 a marked increase appeared with 100 µM of azaserine ($p = 0.0025$).

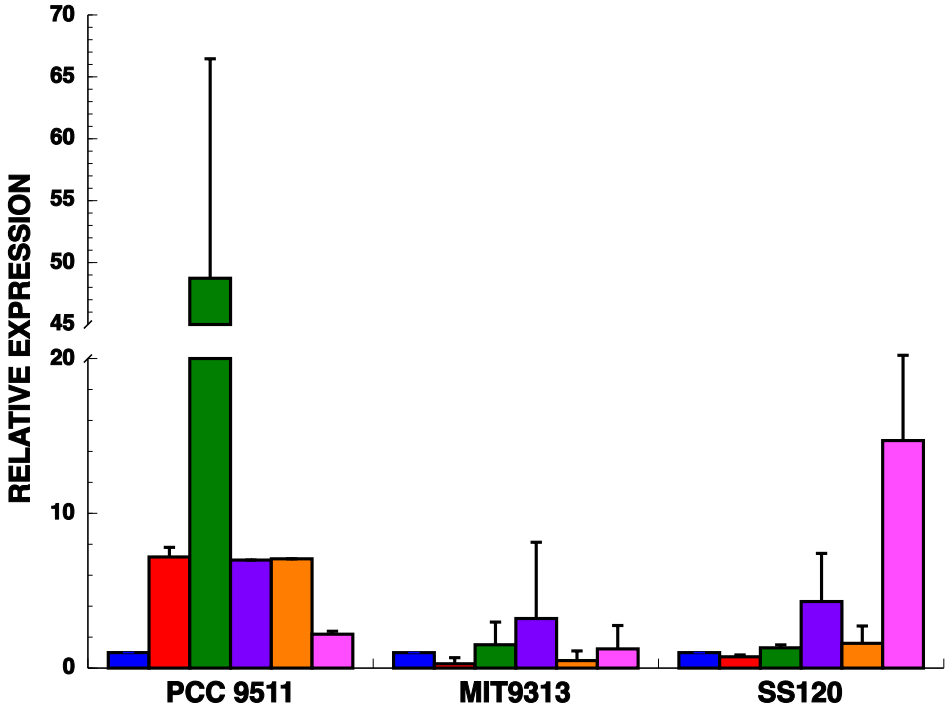

Figure 50: Effect of different azaserine concentration on *icd* expression. Azaserine (0, 1, 5, 20, 50 and 100 µM) was added to cultures of different strains of *Prochlorococcus* (SS120, MIT9313 and PCC 9511). Samples were collected after 24 hours, and gene expression was measured by qRT-PCR. Data are the average of four independent biological replicates. Error bars correspond to standard deviation.

Since the enzyme ICDH links the carbon and nitrogen metabolism pathways in cyanobacteria, we further studied the *icd* expression in the strains PCC 9511 and MIT9313, under different conditions (including azaserine addition), by performing time-course experiments. The expression of *icd* was determined at different times after 100 µM azaserine addition (figure 51). As the figure shows, the highest expression of the gene was after 24 hours.

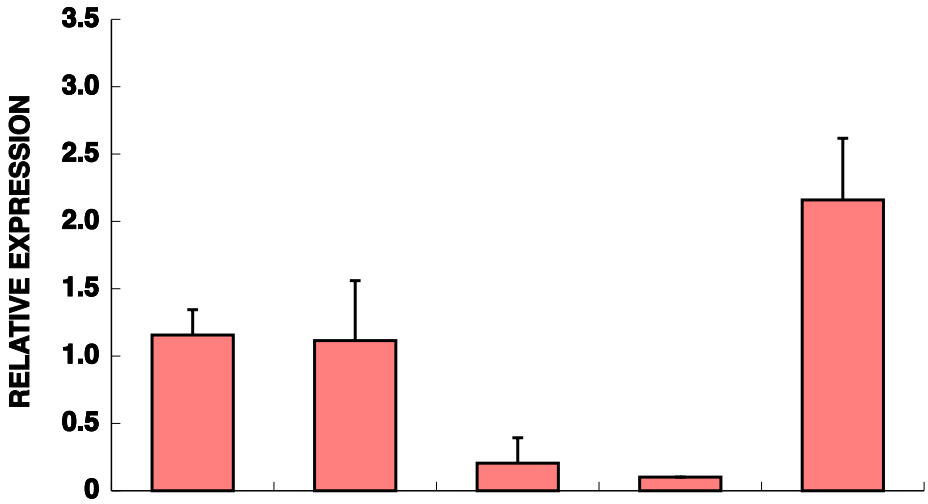

Figure 51: Time-course of the effect of azaserine on *icd* expression in *Prochlorococcus* PCC 9511. 100 µM azaserine was added at time = 0. Samples were taken at the time shown in the graph above and gene expression measured by qRT-PCR. Data are the average of three independent biological replicates. Error bars correspond to standard deviation.

Finally, other conditions were further studied in MIT9313. As we can observe in figure 52, the maximum induction of the gene *icd* occurred after 9 days of aging, 8 hours of 100 µM of MSX addition, 120 hours of nitrogen starvation and 24 hours of DBMIB addition.

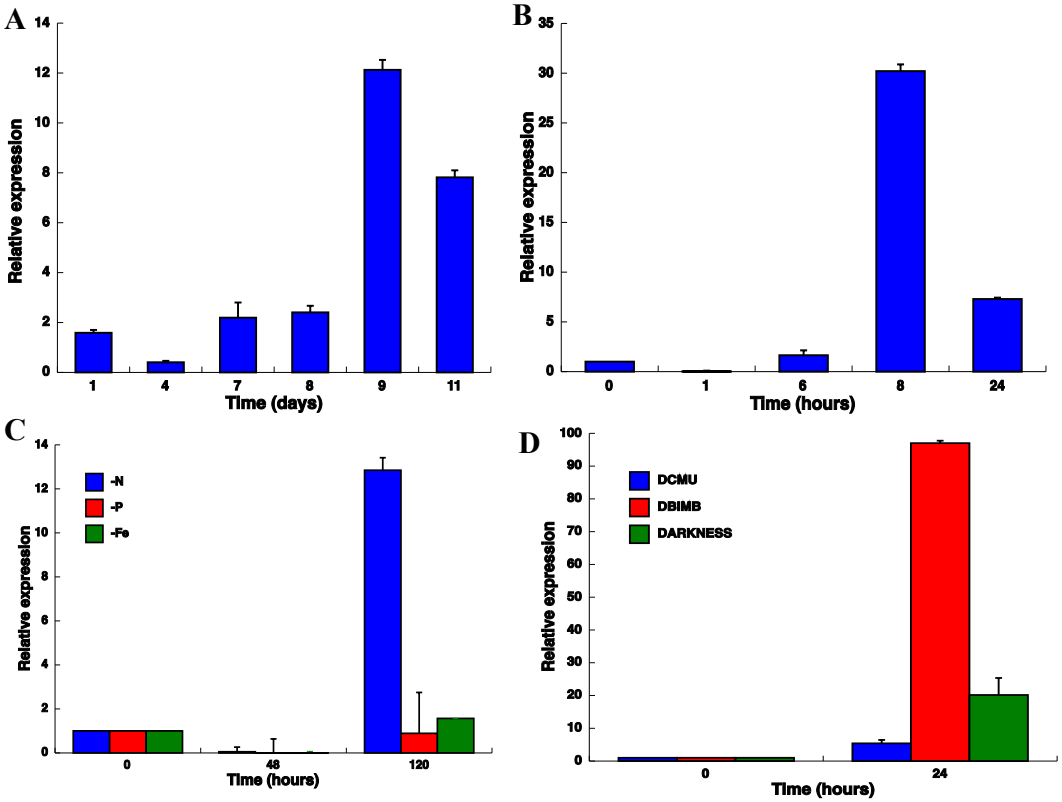

Figure 52: Effect of different treatments on *icd* expression in *Prochlorococcus* MIT9313. Samples from the culture subjected to the different treatment were taken at the indicated time and gene expression measured by qRT-PCR. **A. Effect of aging**, **B. Effect of MSX**, 100 µM of MSX was added to the culture, **C. Effect of nutrient starvation**, -N: nitrogen starvation, -P: phosphorus starvation and –Fe: iron starvation. **D. Effect of inhibitors of photosynthetic electron flow and darkness**. 0.3 µM of DCMU and 0.06 µM of DBMIB were added to the cultures. Data represent the average from three independent biological replicates. Error bars correspond to standard deviation.

The last gene studied was *gdh*, encoding glutamate dehydrogenase in MIT9313; this gene is not present in the other strains studied in this work. The conditions were the same as described above and the results are presented in the figure 53. The *gdh* expression increased slightly after addition of 5 and 20 µM azaserine.

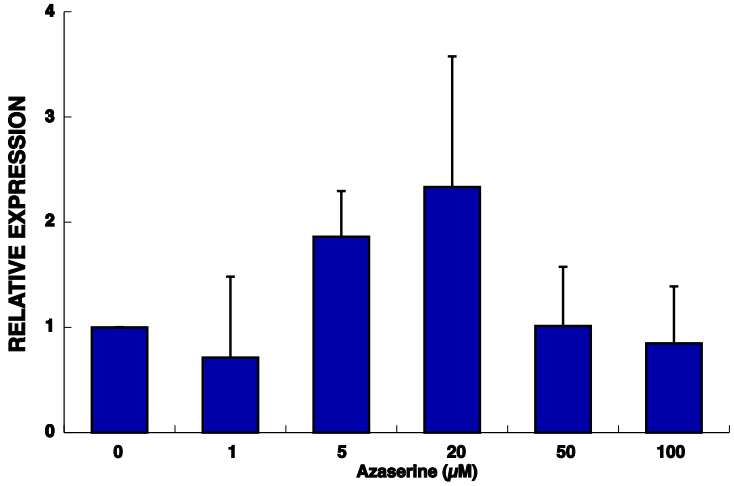

Figure 53: Effect of different azaserine concentration on *gdh* expression in *Prochlorococcus* MIT9313. Azaserine was added to cultures of *Prochlorococcus* MIT9313 that were collected after 24 hours, gene expression was measured by qRT-PCR. The graph is the average of four independent biological replicates. Error bars correspond to standard deviation.

2.3 Changes on the proteome of *Prochlorococcus* SS120

The effect of azaserine addition (100 μM) on the proteome of *Prochlorococcus* SS120 was analyzed through last generation mass spectrometer systems, such as *Q Exactive* (*Thermo Fisher*), a hybrid Quadrupole-Orbitrap mass spectrometer. The *Q Exactive* system allowed a 10% increase in identification rate for protein groups, peptides and peptide spectrum matches with respect to the *LTQ-Orbitrap Velos* system. The researchers point to a smaller maximum injection time for MS/MS, a faster scan rate, and increased MS/MS spectra for the *Q Exactive* system. It also had higher resolution, which produced a low mass error for both precursor and product ions and positively limited the peptide matches during database interrogation.

To evaluate changes on the *Prochlorococcus* SS120 proteome after the addition of azaserine, we followed the workflow shown in figure 54, performing experiments with three independent biological replicates.

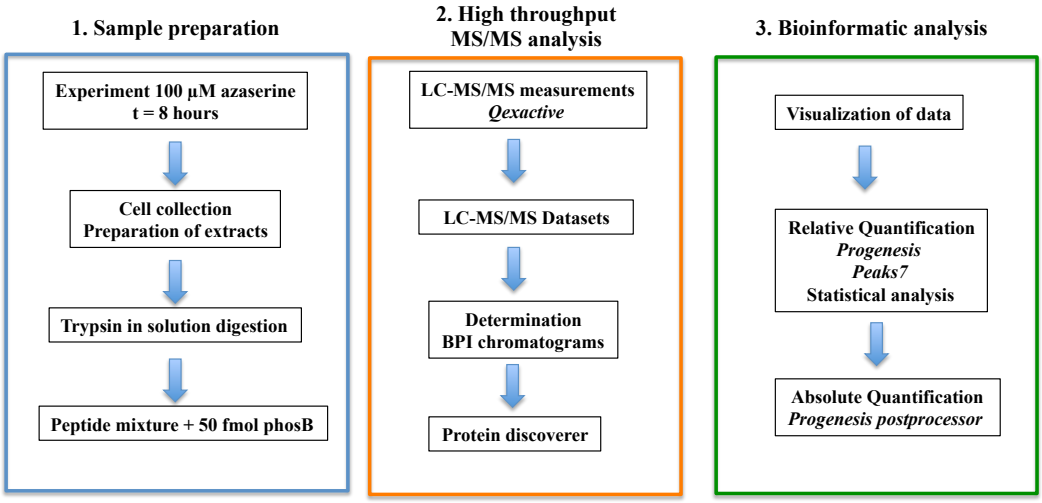

Figure 54: Experimental design. The flow chart describes the steps involved in the analysis of *Prochlorococcus* SS120 proteome.

Azaserine 100 µM was added to the cultures of *Prochlorococcus* SS120 and collected after 8 hours of treatment. The cells were broken with the French press. The first step was the quantification of the concentration of the protein in all the cultures (table 46) as explained in section 4.6 Materials and Methods.

Table 46: Protein concentration of each experiment

	CONTROL (mg/mL)	AZASERINE (mg/mL)
Experiment 1	5928.464	9754.769
Experiment 2	3265.981	5769.997
Experiment 3	4264.642	6170.934

Prior to loading samples in the mass spectrometer, the protein extracts before digestion, post-digestion and post-digestion with TFA (trifluoroacetic acid) were run in a 15% SDS-PAGE gel. As we can see in the figure 55, the quantification was accurate and there was no undigested protein. We can observe also that experiment 1 differs from 2 and 3. This will be discussed later.

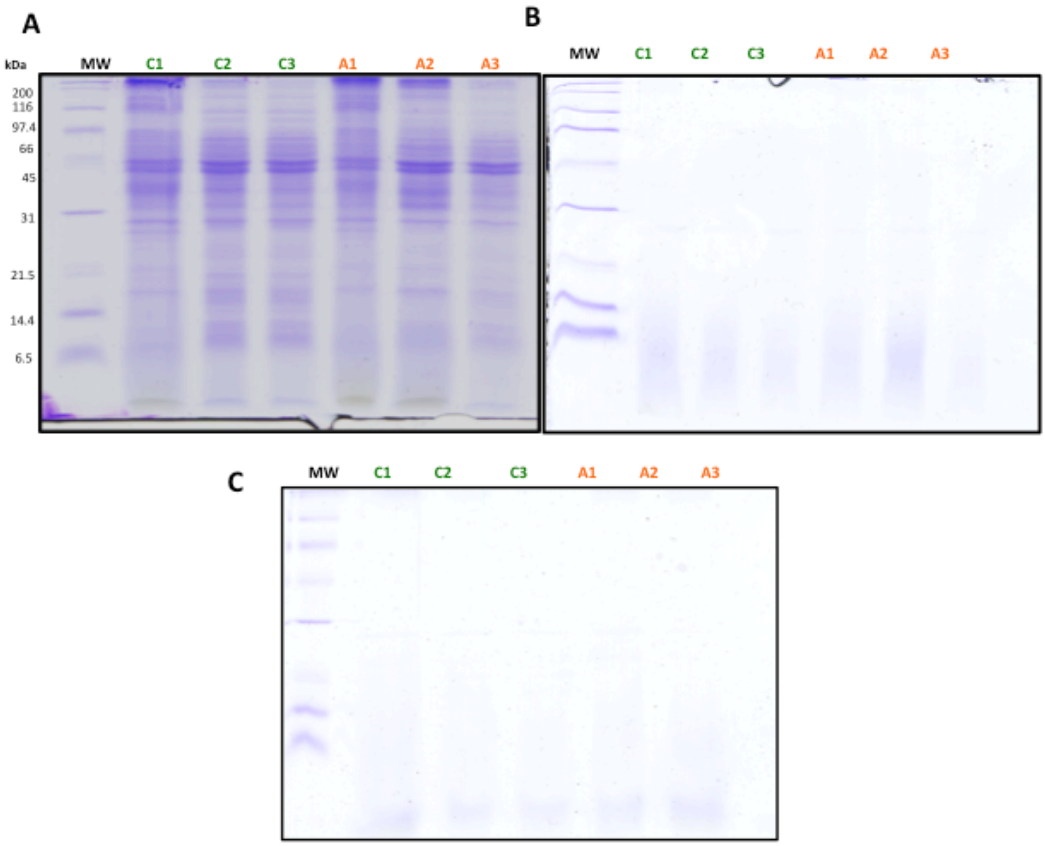

Figure 55: SDS-PAGE (15%) of protein extracts to check digestion steps. A. 25 µg of protein were loaded per lane. B. Post-digestion. C. Post-digestion + TFA. MW: Molecular weight; C1, C2 and C3: Control samples from experiment 1, 2 and 3; A1, A2 and A3: Azaserine-treated samples from experiment 1, 2 and 3.

In order to identify more proteins, an optimization of the method was performed, by using different amounts of protein loaded into the column and different gradient times (table 47).

Table 47: Optimization of the method for *Q Exactive*

Injection on Qexactive and gradient used	Hits	Hits > 2 peptides	Matches	Matches significant	Sequences	Sequences significant	Identification of the proteome
500 ng 2 hours gradient	525	412	5801	4865	3252	2783	28%
1 µg 2 hours gradient	570	453	7236	6179	3788	3252	30%
1 µg 4 hours gradient	**825**	694	11724	9648	6312	5386	**44%**

The table 47 shows that the third method was the best, obtaining 44% identifications of the predicted proteome. With this approximation, all the samples were run using a 4 hours gradient and 1 µg of protein loaded into the column.

To evaluate the chromatography during the running in the *Q Exactive* system, each chromatogram obtained through *Xcalibur software* (*Thermo Fisher*) was checked (figure 56).

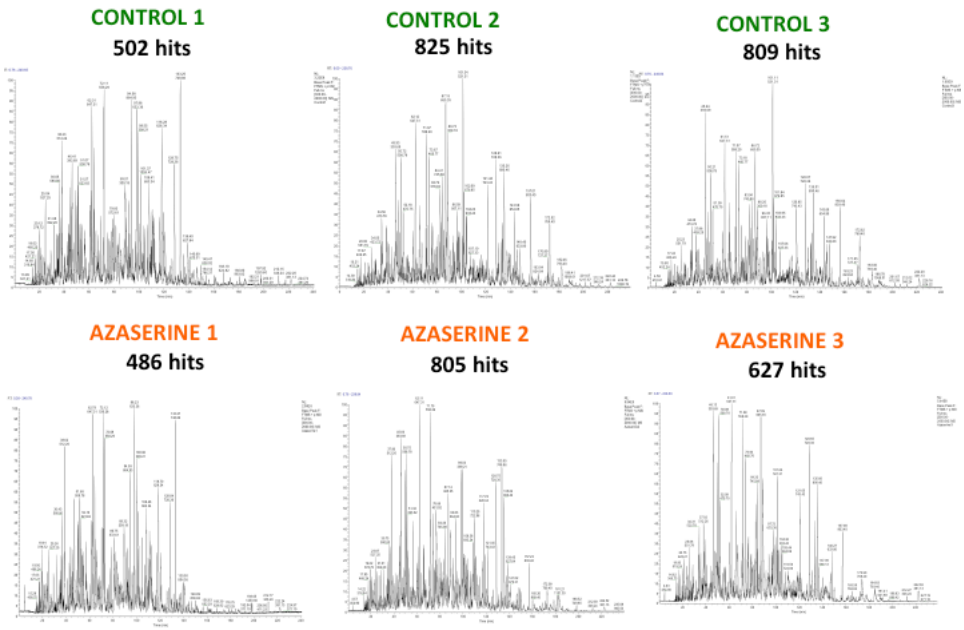

Figure 56: BPI (Base peak intensity) chromatograms. The number of hits obtained from each sample is indicated for each chromatogram.

As we can notice, all samples are complex mixtures and very similar between them. It is worth noting that in the first experiment we obtained fewer amounts of hits compared with the other two.

Using the software *Proteome Discoverer 1.4* from *Thermo Fisher* and a FDR (false discovery rate) of 1% with a database composed of entries of *Prochlorococcus* SS120 Uniprot, 915 proteins were identified, what represents nearly half (49%) of the predicted proteome of *Prochlorococcus* SS120 (1884 proteins). 818 proteins were identified with more than 2 peptides in the control samples, and 740 proteins in the azaserine-treated samples (table 48).

Table 48: Proteins identified in control vs azaserine samples

	# Proteins	> 2 peptides
CONTROL	886	818
AZASERINE	802	740

As shown in the Venn diagram (figure 57), 773 proteins common to both conditions were found, 113 were only identified in control samples and 29 were only identified in azaserine-treated samples.

Figure 57: Venn diagram. The figure shows the number of proteins identified in each condition and in common.

Using the DAVID software (http://david.abcc.ncifcrf.gov/), the functional annotation clustering was done by classifying the pathways where the identified proteins are involved. Figure 58, using the enrichment score, shows that we got representative members of all the main pathways in the cell.

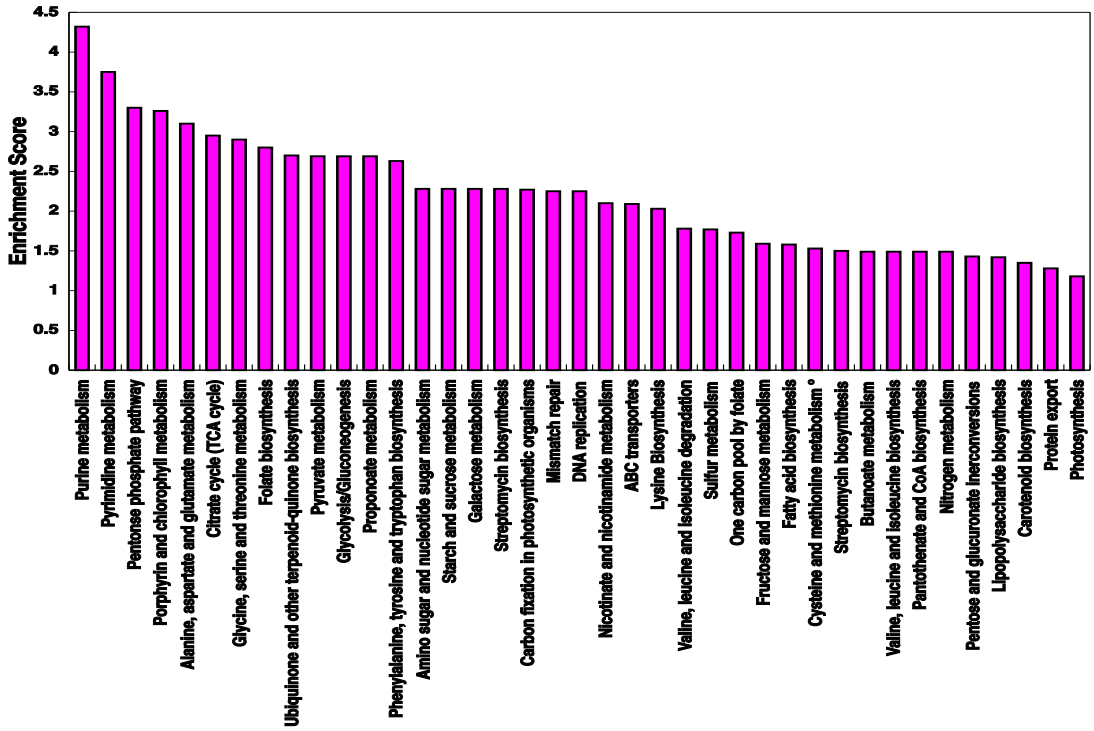

Figure 58: Enrichment score of all the pathways identified in DAVID. To represent the chart all the proteins identified was used.

Table 49 shows the list of proteins that are only identified in azaserine-treated samples.

Table 49: Proteins identified in azaserine condition

Accession number	Protein	Pathway/Molecular function
Q7V9U9	ATP:corrinoid adenosyltransferase	Porphyrin and chlorophyll metabolism
Q7VAY4	FAD dependent oxidoreductase	Oxidorreductase
Q7VCCO	DevC-like ABC transporter permease component	Putative ABC transport system
Q7VCG4	Alpha/Beta superfamily hydrolase	Hydrolase
Q7VDN4	Superfamily I DNA/RNA helicase	Nucleotide excision repair /Mismatch repair
Q7VDU6	Thioredoxin family protein	Cell redox homeostasis
Q7V9G4	Lipid A core O-antigen ligase related enzyme	Ligase
Q7V9T2	Lypid A disaccharide synthetase related enzyme	Lipid biosynthesis
Q7VAE8	High light inducible protein hli1	Proteins related with photosynthesis
Q7VBK4	1-acyl-sn-glycerol-3-phosphate acyltransferase	Glycerolipid metabolism

Q7VDB4	High light inducible protein hli9	Proteins related with photosynthesis
Q7VE96	Fe-S oxidoreductase	Oxidorreductase
Q7VB10	Adhesin-like protein	Unknown function
Q7VBZ1	D-alanyl-D-alanine carboxypeptidase	Peptidoglycan biosynthesis
Q7VC36	2-polyprenyl-6-methoxyphenol hydroxylase related enzyme	Ubiquinone and other terpenoid-quinone biosynthesis
Q7VDD3	ABC-type multidrug transport system permease component	ABC transporteres
Q7V9S2	D-lactate dehydrogenase, NADH independent	Pyruvate metabolism
Q7V9P4	Uncharacterized DedA family conserved membrane protein	Folate biosynthesis

The relative quantifications of the samples were done, 240 proteins changed significantly using *Progenesis LC-MS* (*Nonlinear support*) and *Transomics* (*Waters*), and with *Peaks7* only 83 proteins did it. The results are shown in figure 59.

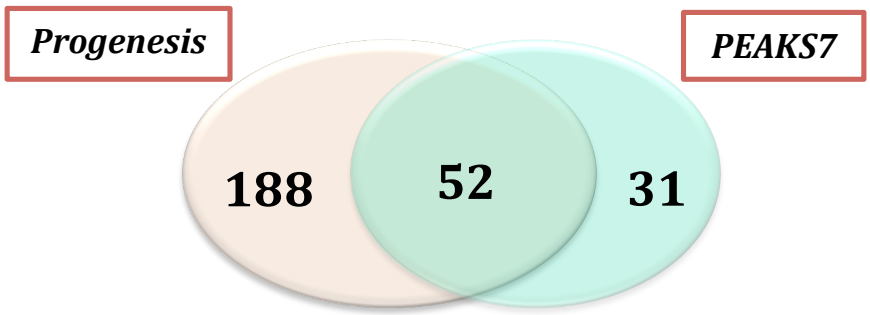

Figure 59: Venn diagram. The figure shows the number of proteins identified with each software and in common.

The Venn diagram (figure 59) shows that 52 proteins changed significantly common to both softwares. This supports the changes on those proteins, since these softwares use different algorithms. *Progenesis LC-MS* and *Transomics* allow peptide identification using the search engines and databases, on the other hand, the first step in *PEAKS7* for data analysis is the novo sequencing.

The figure 60 shows the correlation between abundances of proteins identified in the samples. The heatmap (figure 60, B) shows that control and azaserine samples from experiment one differs from the other experiments. That is confirmed by the

chart A. The good correlation is when the dispersion is adjusted to the straight, thus the correlation between samples from experiment 2 and 3 are quite good contrary that experiment one even it shows good correlation between them.

A

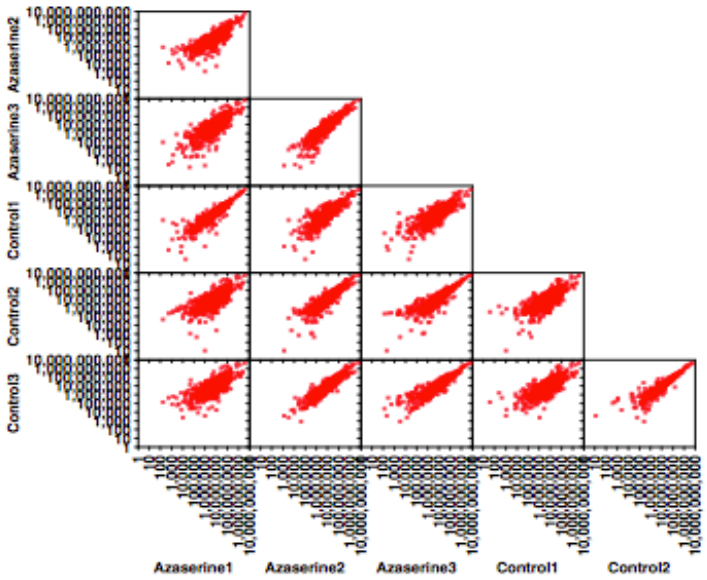

B

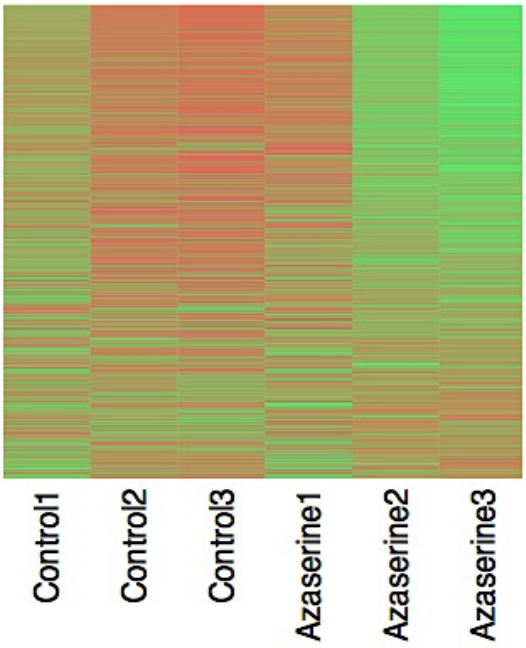

Figure 60: Correlation between abundances of proteins identified in the samples. A. Chart. B. Heatmap. Both diagram were done using R program.

The figure 61 shows the PCA (principal component analysis) obtained with the data from *Progenesis LC-MS*. The top panel from the figure shows that in the PCA, using all the proteins, the experiment 1 was grouped apart. However, if we used only the proteins that change significantly (figure 61, B), there was good separation between conditions.

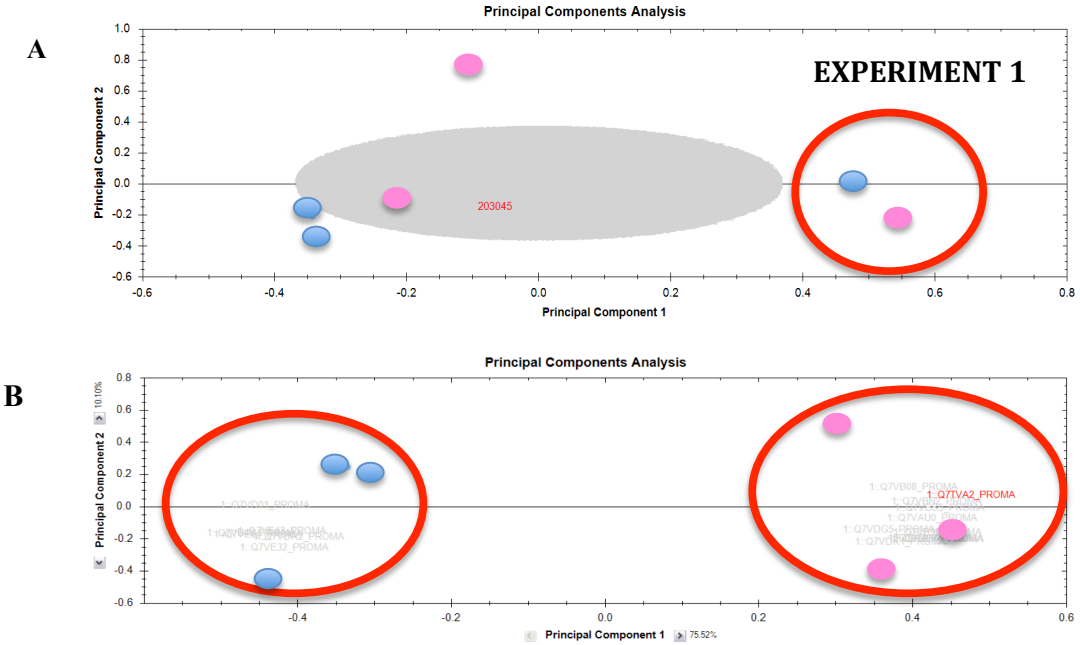

Figure 61: PCA from *Progenesis*. A. PCA with all the identifications. B. PCA with proteins changed significantly, $p < 0.05$. **Blue** corresponds to control and **Pink** corresponds to azaserine treatment.

Due to the above evidences (figure 55, 56, 60 and 61), we decided to work only with experiment 2 and 3. So, the proteins extracts of both experiments were run in the *Q exactive* twice and finally we got two biological replicates and two technical replicates.

The analysis showed that 240 proteins changed with a significant *p* value after 8 hours of azaserine treatment. From all these proteins, some are up-regulated shown in table S1 (*Supplementary data*) and other down-regulated and shown in table S2 (*Supplementary data*).

The samples were run into *Q Exactive* with 50 fmol/µL of phosB from Rabbit as standard. The software *Progenesis Postprocessor* was used to perform the absolute quantification. It is important to highlight that as far as we know, it is the first study

that showed half of the proteome of *Prochlorococcus* SS120. Besides, this study gives an absolute quantification of the identified proteins in the cell.

The results obtained with our proteins of interest are shown in table 50. Among the nitrogen metabolism-related proteins, the only proteins that changed significantly were P_{II} and PipX. Interestingly, there is good correlation between data obtained from *Progenesis LC-MS* (fold change) and *Progenesis Postprocessor* (fmol/µL).

Table 50: Summary of changes of proteins related with nitrogen metabolism

Proteins	Accession number	Fold change/condition	fmol/µL Control	fmol/µL Azaserine
NtcA	Q7VDU1	1.1 Azaserine	15.36	12.36
P_{II} (*)	Q7VA51	1.21 Control	236.59	134.9
PipX (*)	Q7VDI6	1.6 Control	6.35	3.16
GS	Q7VBQ4	1.12 Control	552.2	361.61
ICDH	Q7V9S5	1.34 Control	20.88	13.14
GOGAT	Q7VA01	1.25 Azaserine	38.47	39.57

(*) These proteins changed with a p value < 0.05

Among the proteins that are up-regulated there are some that are related with photosynthesis process (table S1, Supplementary data). To complete this study, the photosynthetic capacity was determined under the same conditions. As we can see, it was affected by the addition of azaserine ca. 25% (table 51).

Table 51: Photosynthetic efficiency of *Prochlorococcus* SS120

	Y (II) + SD	
Time /conditions	**Control**	**Azaserine**
8 hours	0.5 ± 0.02	0.377 ± 0.024

3. Study of the interaction NtcA-*glnA* promoter of *Prochlorococcus* SS120 and MIT9313

3.1 Purification of heterologous regulatory proteins from *Prochlorococcus* SS120 and MIT9313

The last approach was the study of the regulatory proteins involved in nitrogen metabolism, NtcA, P_{II} and PipX from *Prochlorococcus* SS120 and MIT9313. We wanted to include regulatory proteins from PCC 9511, but it was no possible due to the problems with the amplification of long fragments from this strain, although different strategies were used.

The first step was to clone the gene in an overexpression plasmid, pET-15b (*Novagen*) (figure 62) to express the protein with a hexahistidine tag attached at the N-terminal. Specific primers were designed to amplify *ntcA*, *glnB* and *pipX*. Restriction sites for BamHI and NdeI were introduced and they were cloned into pET15b using the *E. coli* BL21(DE3) strain. Then it was purificated by nickel affinity column.

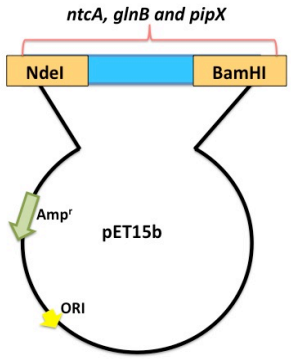

Figure 62: Plasmid used in the strategy to overexpress the proteins, pET15b.

The alignment of P_{II} proteins from the three strains of *Prochlorococcus* showed that this regulatory protein is highly conserved. P_{II} proteins are trimers of about 36 kDa, each trimer can bind up 2-OG and ATP/ADP allowing the sensing of the C/N and energy status of the cell (Ninfa & Jiang, 2005). In the different structures of P_{II} solved so far, one characteristic is the existence of three surface exposed loops per

monomer, B, C and T-loops (Forchhammer, 2008), they are highlighted in the amino acid sequence in figure 63. The serine residue is conserved in the three strains.

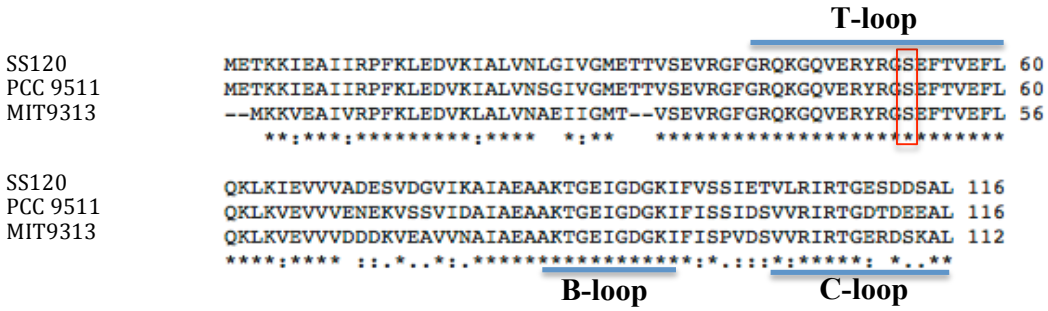

Figure 63: Alignment of P_{II} from *Prochlorococcus* SS120, PCC 9511 and MIT9313. The sequences in FASTA format were taken from CYORF and ClustalW2 from *EMBL-EBI* was used to make the alignment. (*****) Indicates positions which have a single, fully conserved residues; (**:**) indicates conservation between groups of strongly similar properties and (**.**) indicates conservation between groups of weakly similar properties. Serine residue and the loops are highlighted. (PCC = PCC 9511).

However, the alignment of PipX showed that they are not quite conserved among the strains from *Prochlorcoccus* (figure 64).

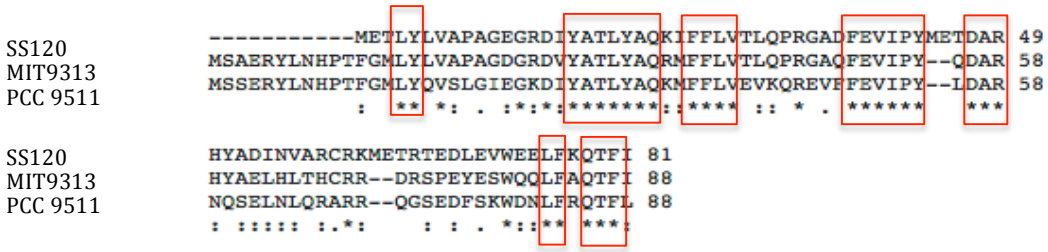

Figure 64: Alignment of PipX from *Prochlorococcus* SS120, PCC 9511 and MIT9313. The sequences in FASTA format were taken from CYORF and ClustalW2 from *EMBL-EBI* was used to make the alignment. (*****) Indicates positions which have a single, fully conserved residues; (**:**) indicates conservation between groups of strongly similar properties and (**.**) indicates conservation between groups of weakly similar properties. The regions conserved are highlighted. (PCC = PCC 9511).

The transcription factor NtcA was highly conserved in these three strains (figure 65). The motifs to bind to DNA (helix-turn-helix) are very conserved in all of them.

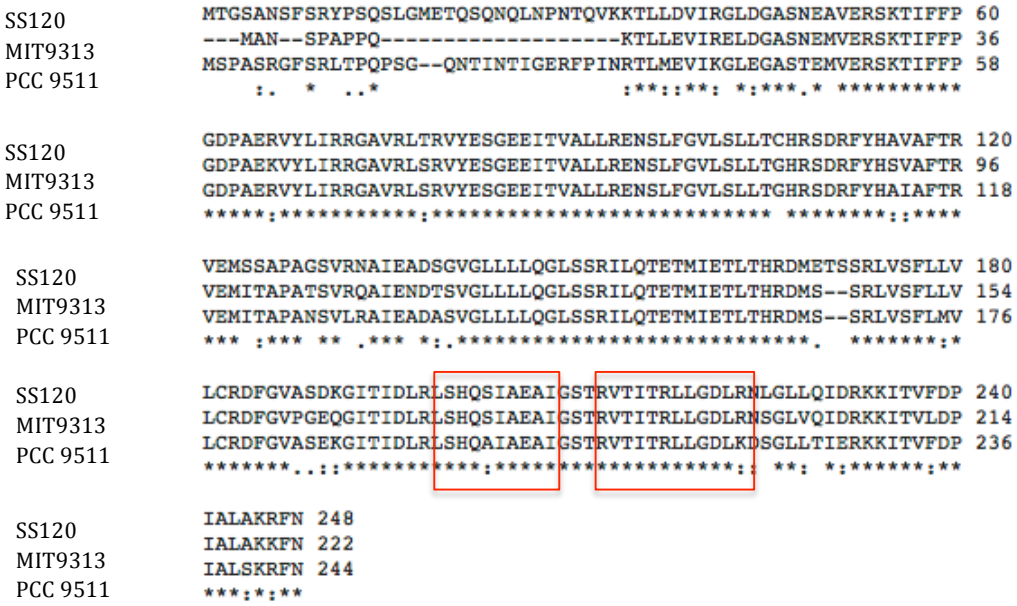

Figure 65: Alignment of NtcA from *Prochlorococcus* SS120, PCC 9511 and MIT9313. The sequences in FASTA format were taken from CYORF and ClustalW2 from *EMBL-EBI* was used to make the alignment. (*****) Indicates positions which have a single, fully conserved residues; (**:**) indicates conservation between groups of strongly similar properties and (**.**) indicates conservation between groups of weakly similar properties. Sequences of amino acids that bind to DNA are highlighted. (PCC = PCC 9511).

To obtain the recombinant proteins, 0.5 L of culture of *E. coli* BL21(DE3) were induced with 0.5 mM of IPTG for 4 h. Then, cells were collected and the pellet broken for the purification of the His-tag proteins through the nickel columns. The collected fractions were analysed in a SDS-PAGE 12% as shown in figure 66.

The theoretical molecular weight of P_{II} from *Prochlorococcus* MIT9313 and SS120 was 12 kDa and for PipX was 10 kDa. The predicted size of the proteins corresponded to the size obtained after the purification of those proteins. Similar results as shows the figure 66 were obtained with the other purifications.

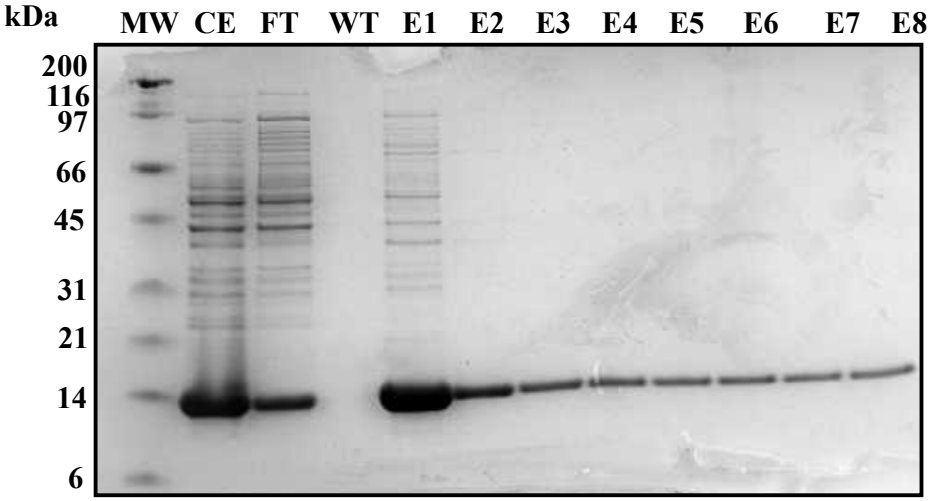

Figure 66: Purification of proteins P_{II} and PipX from *Prochlorococcus* SS120 and MIT9313. Crude extract obtained from *E. coli* BL21 (DE3) after induction of 0.5 mM IPTG for 4 hours. Purification of the protein His-tag through nickel column (section 7.3, Materials and Methods). The result of the purification was analysed by SDS-PAGE 12% and then Coomassie stained. M= Molecular weight; EC = crude extract; FT= flow-through; WT= wash through; E1-E8 elution fractions.

After the purification step, the samples were subjected to western-blotting using the antibody anti-His in order to prove that the purificated protein is our protein with the His-tag attached (figure 67). All the proteins analyzed were detected with the antibody anti-His in all the fractions loaded except in the fraction WT.

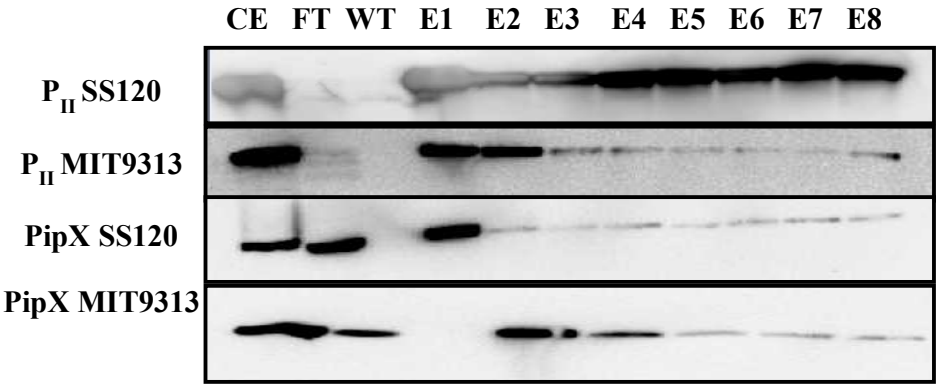

Figure 67: Western blots of overexpressed regulatory proteins from *Prochlorococcus* SS120 and MIT9313 strains. Samples were separated by 12% SDS-PAGE, electroblotted onto a membrane and incubated with monoclonal anti-poly-histidine for 1.5 hour. CE= crude extract; FT= flow-through; WT= wash through; from E1 to E8 elution fractions.

For a more extensive NtcA interaction, large amount of proteins and with high purity was required. Besides, we had the problem that a high proportion of the overexpressed NtcA proteins from both strains of *Prochlorococcus* were accumulated as inclusion bodies. Different strategies were used to enhance the solubility of the target protein. Firstly, the codon usage of NtcA from MIT9313 and SS120 in *E. coli* was checked by the program *Graphical codon usage analyser*. We obtained that there were four codons with low frequency, for MIT9313 these were: CTC, CGA, CTA and AGG and for SS120: AGG, CGA, CTC and CTA. Thus, the plasmid construction was introduced in the *Rosetta (DE3)* strain of *E. coli* that provided two codons (AGG and CTA). After the overexpression test, the results did not show any increment of the protein in the soluble fraction. The other strategy was the cold induction (16 ºC), but it did not work either.

Finally, we grew up to 6 L of culture of *E. coli* BL21(DE3) + pET-15b-NtcA to get enough amount of protein to purify through the *Äkta system* and set the adequate parameters to get the protein NtcA as pure as possible. Firstly, it was purificated by nickel column and then, after the SDS-PAGE analysis, the fractions that contained protein were loaded into exclusion molecular chromatography. The results obtained for the purification are shown in figure 68.

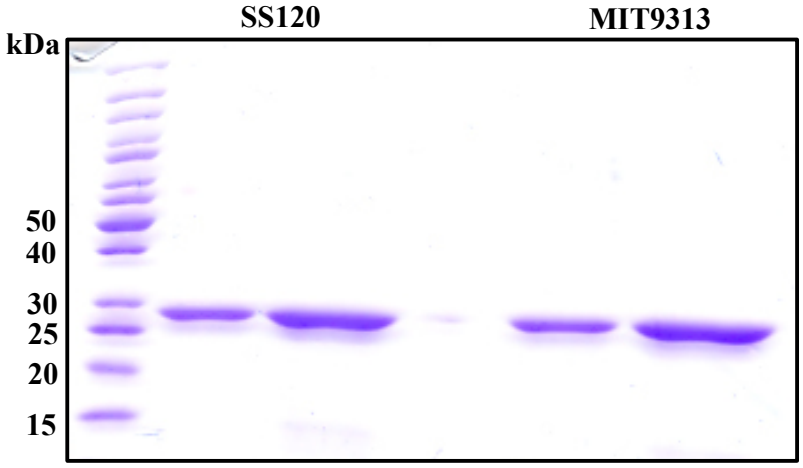

Figure 68: Heterologous NtcA(His)$_6$ purified from *Prochlorococcus* SS120 and MIT9313. 1 and 3 µg of the purified protein were loaded onto SDS-PAGE 12% and stained with coomassie.

After the purification of NtcA MIT9313 through the chromatography size exclusion molecular *Sephadex 75* an interesting pattern was found. The

chromatogram showed a typical interaction pattern between proteins as we can observe in figure 69. As we can observe in the gel two bands appeared with NtcA, one band is low molecular weight, ca. 10 kDa, and the other one is ca. 30 kDa. The samples were sent to the University of Liverpool to be analyzed by mass spectrometry. They were digested with trypsin and then run on the *Orbitrap Velos (Thermo Scientific)* and the results are summarized on the table S3 (*Supplementary data*). The possible proteins obtained that could interact with NtcA were ribosomal proteins.

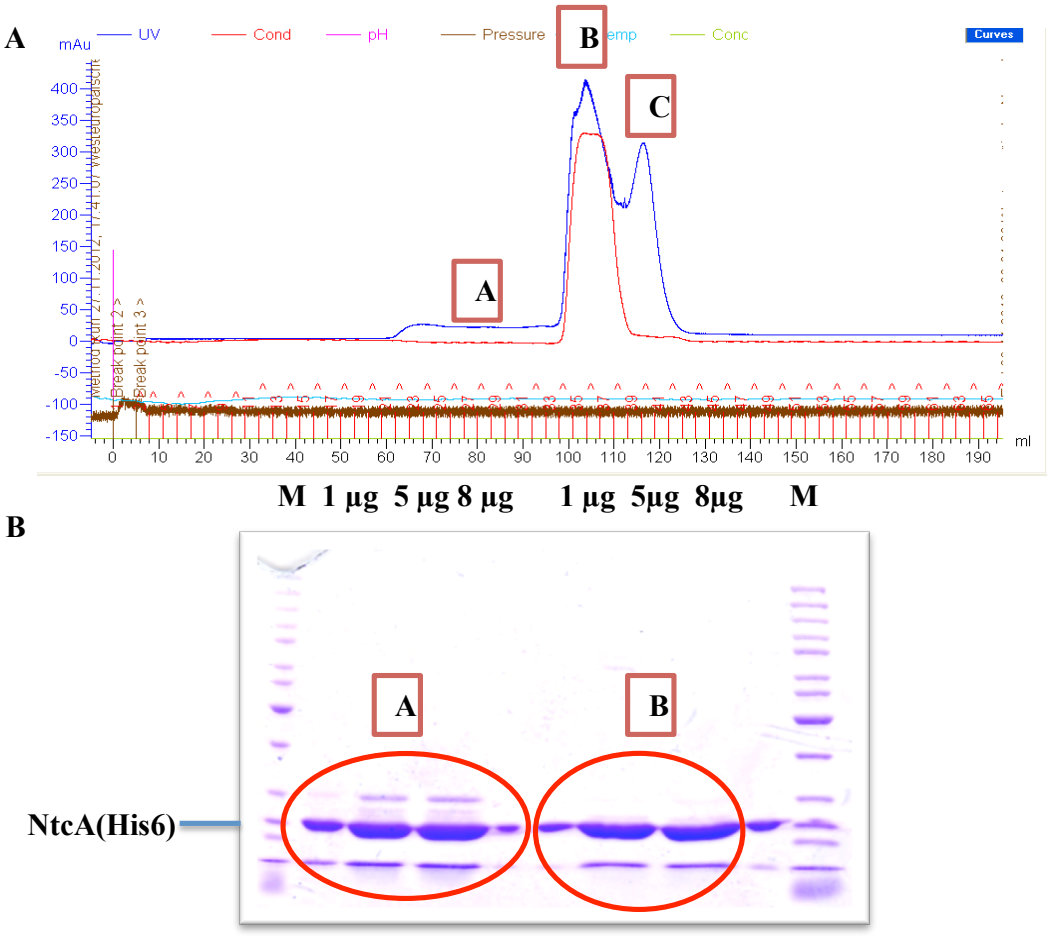

Figure 69: Size exclusion molecular chromatography of NtcA MIT9313. A. Chromatogram, different peaks are named with A, B and C. B. 10% SDS-PAGE. 1, 5 and 8 µg were loaded. The fractions from peak A had two bands and NtcA from MIT9313 and the fractions from peak B had one band and NtcA from MIT9313.

3.2 SPR study of the interaction between NtcA and the promoter for *glnA* in MIT9313 and SS120

The promoters of *glnA* from MIT9313 and SS120 were chemically generated and the mutated promoters were designed carefully in order to avoid another possible sequence for NtcA binding in other regions. The oligonucleotides used are summarized in table 40 in section 9.1.1 in Materials and Methods. The first step was the hybridazation of the oligonucleotides as show in figure 70.

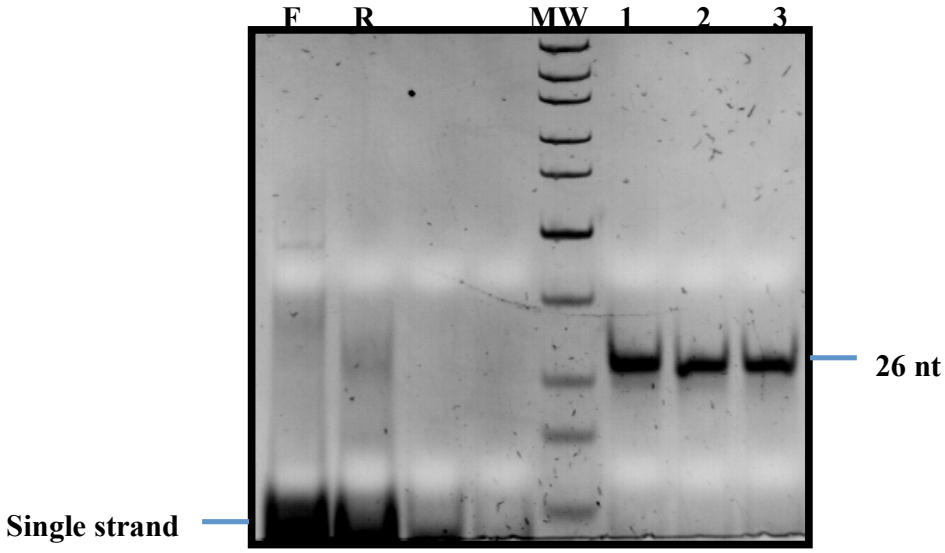

Figure 70: Hybridization of *glnA* promoter. The 26 nt long oligonucleotides were analysed on a 20% polyacrylamide gel. As control besides the *Peqlab ultra low range DNA standard* (0.01-0.3 kb) in the lane named MW, the single strand Forward (F) and Reverse (R) were loaded. The successfully hybridized samples are shown in lanes named 1, 2 and 3.

The interaction NtcA-*glnA* was analyzed with two effector molecules, glutamine and 2-OG. The results with different millimolar concentration of glutamine did not show any positive effect on the binding (data not shown). On the contrary, 2-OG had a positive effect on the binding although that effect is different between SS120 and MIT9313 (figure 71 and 72, respectively). The binding appeared in MIT9313 with 1 mM of 2-OG and that increased with the level of 2-OG, however this

interaction needed a higher level of 2-OG to bind in SS120. Once NtcA was bound, the binding increased with the level of 2-OG.

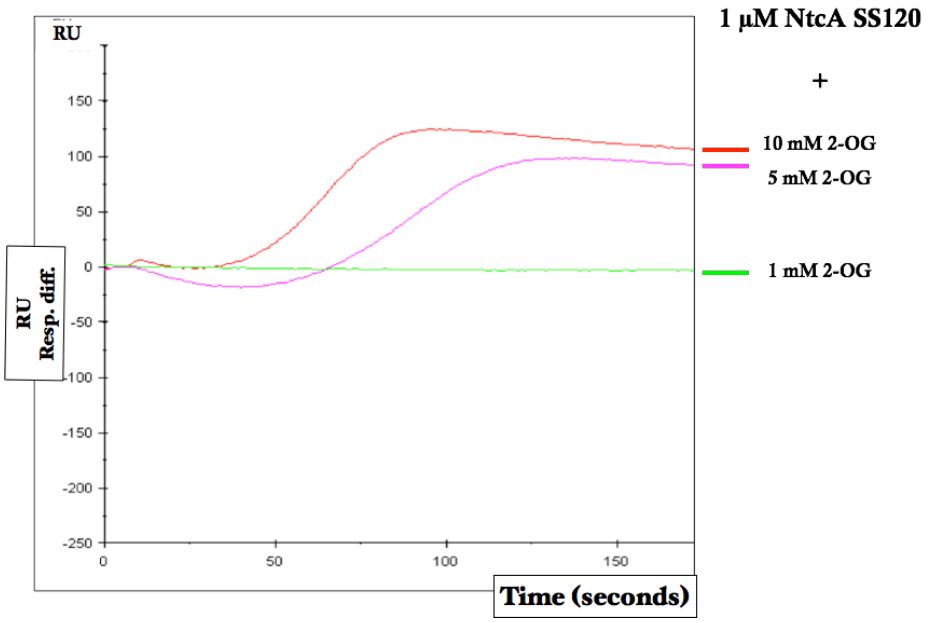

Figure 71: SPR analysis of the interaction between NtcA(His)$_6$ and the promoter for *glnA* in SS120. This sensorgram shows the interaction of 1 µM of NtcA(His)$_6$ with *glnA* promoter and a rising concentration of 2-OG. RU = response units. Resp. Diff. (RU) = signal difference from FC2 (*glnA*) and an unspecific oligonucleotides coupled to the reference cell FC1.

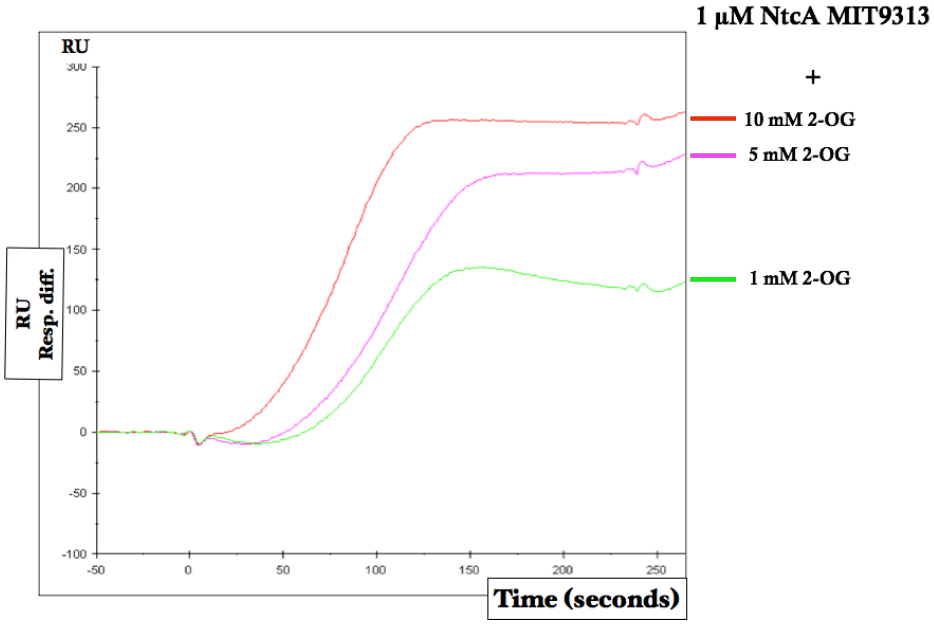

Figure 72: SPR analysis of the interaction between NtcA(His)$_6$ and the promoter for *glnA* in MIT9313. This sensorgram shows the interaction of 1 µM of NtcA(His)$_6$ with *glnA* promoter and a rising concentration of 2-OG. RU = response units. Resp. Diff. (RU) = signal difference from FC2 (*glnA*) and an unspecific oligonucleotides coupled to the reference cell FC1.

To confirm that 2-OG does not bind directly on the chip and could perturbate the measurement, an experiment run 2-OG without the protein was performed (figure 73). Clearly, 2-OG was not able to bind to DNA without the protein.

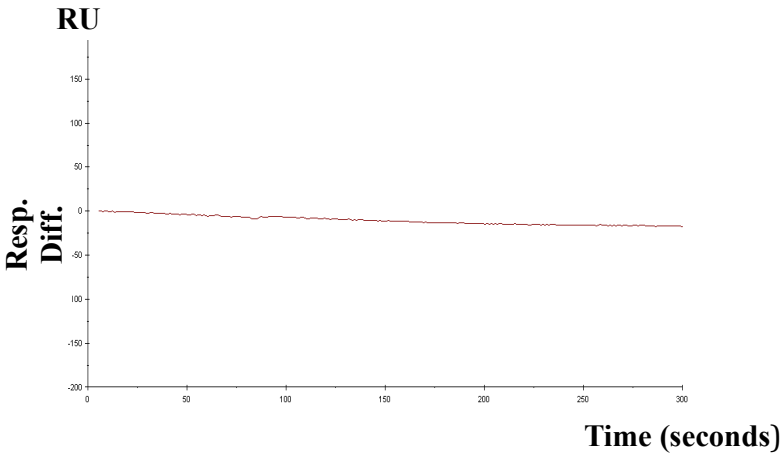

Figure 73: SPR measurement 2-OG with *glnA*. The sensorgram show the Response differential between FC2 (glnA promoter) and FC1 (unspecific oligonucleotide) with 2-OG.

3.3 EMSA study of the interaction between NtcA and the promoter for *glnA* in MIT9313 and SS120

To confirm the results of the interaction between NtcA and the promoter for *glnA* from *Biacore* another approach was carried out. We used electrophoretic mobility shift assay (EMSA) under the same conditions and with the same purified proteins using in the *Biacore* measurements (figure 74 and 75). In this case the DNA was ordered without biotinylation.

As it shown in figure 74 and 75, the results of the interaction were similar as these shown above. The binding of NtcA from MIT9313 is enhanced with 2-OG, being stronger when the concentration rises from 1 to 10 mM and in the case of NtcA from SS120 the binding needed a higher concentration of 2-OG. The panel named with B in both cases shows the interaction between NtcA from both strains and the promoter for *glnA* with the mutations to alter the canonical binding site. It shows that

there was no binding indicating that the $GTAN_{8/9}TAC$ is specific for NtcA *Prochlorococcus*.

Components	Lanes				
	1	2	3	4	5
***glnA*-promoter**	+	+	+	+	+
NtcA (1 µM)	-	+	+	+	+
2-OG	-	-	1 mM	5 mM	10 mM

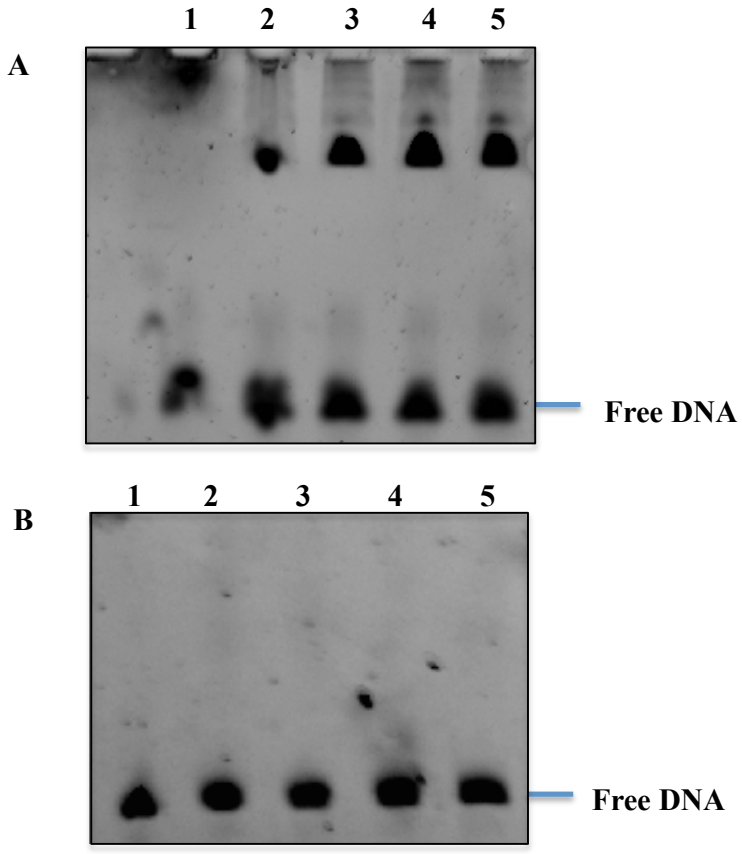

Figure 74: Specific binding of NtcA and the *glnA* promoter of *Prochlorococcus* MIT9313. A. The binding of NtcA at the indicated concentration to *glnA* promoter was examined by EMSA analysis in the presence of the indicated concentrations of 2-OG. B. The binding of NtcA at the indicated concentration to mutated *glnA* promoter.

Components	Lanes				
	1	**2**	**3**	**4**	**5**
***glnA*-promoter**	+	+	+	+	+
NtcA (1 µM)	-	+	+	+	+
2-OG	-	-	1 mM	5 mM	10 mM

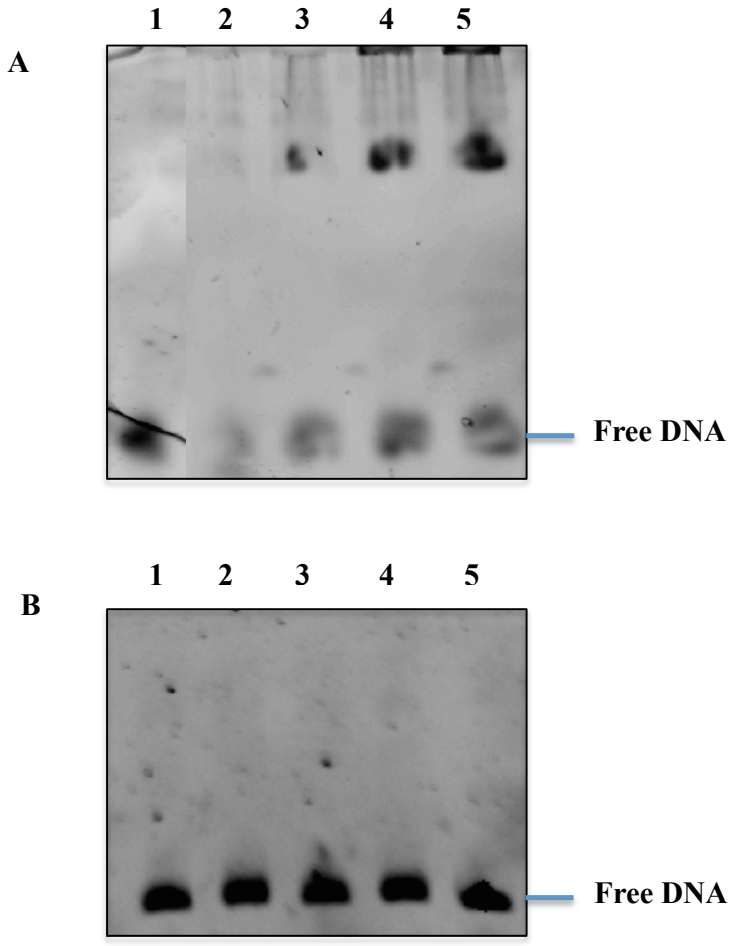

Figure 75: Specific binding of NtcA and the *glnA* promoter of *Prochlorococcus* SS120. A. The binding of NtcA at the indicated concentration to *glnA* promoter was examined by EMSA analysis in the presence of the indicated concentrations of 2-OG. B. The binding of NtcA at the indicated concentration to mutated *glnA* promoter.

It has been reported that the protein PipX binds to NtcA and 2-OG enhancing the transcription of genes related with nitrogen metabolism (Llácer *et al.*, 2010). To examine this possibility, we performed EMSA analysis in the presence of various

concentrations of 2-OG plus NtcA and PipX (figure 76). Interestingly, we found differences between both strains. In the case of MIT9313 the binding showed little change with the addition of the protein PipX, while in SS120 the binding was clearly enhanced with this addition (figure 76).

Components/Lanes	1	2	3	4
***glnA*-promoter**	+	+	+	+
NtcA (1 µM)	-	+	+	+
PipX (1 µM)	-	-	+	+
2-OG	-	5 mM	1 mM	5 mM

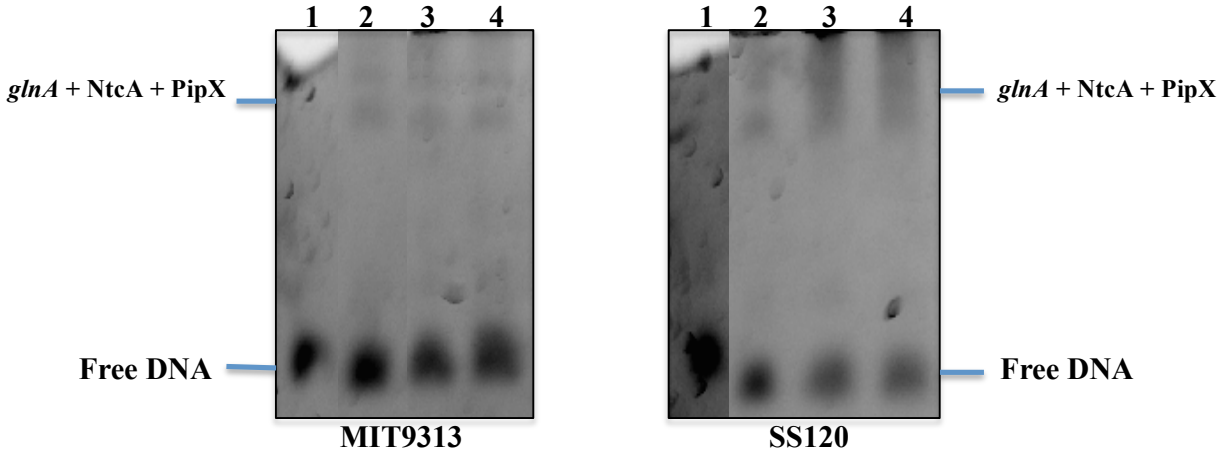

Figure 76: Interaction between NtcA and PipX and the promoter for *glnA* from *Prochlorococcus* MIT9313 and SS120. The binding of NtcA with PipX at the indicated concentration to *glnA* promoter was examined by EMSA analysis in the presence of the indicated concentrations of 2-OG**.**

Discussion

There were some evidences that the regulatory system of C/N metabolism in *Prochlorococcus* differs from the previously described for other cyanobacteria (Gómez-Baena *et al.*, 2014, Rangel *et al.*, 2009, López-Lozano *et al.*, 2009, El Alaoui *et al.*, 2003, Gómez-Baena *et al.*, 2001, El Alaoui *et al.*, 2001). In this study we further studied that fine regulatory systems doing a comparative study among three different strains, which belong to different ecotypes have different phylogenetic origins, in order to check the possible differences respect to other model

cyanobacteria and among them. The study was performed with different approaches, which will be discussed below.

1. The role of 2-OG in *Prochlorococcus marinus*

2-oxoglutarate is located at the junction between central carbon and nitrogen metabolisms, as an intermediate for both. In nitrogen metabolism, 2-OG acts as both a carbon skeletal carrier and an effector molecule.

In marine picocyanobacteria, which lack 2-OG dehydrogenase (Zhang & Bryant, 2011), the main metabolic role of 2-OG is the incorporation of nitrogen. This metabolic arrangement makes 2-OG an indicator of the C to N ratio of the cells (Flores & Herrero, 2005, Muro-Pastor *et al.*, 2001).

It has been suggested in different studies that the 2-OG is the molecule responsible for the C/N control in *Prochlorococcus* (López-Lozano et al., 2009), but there were no data that support it. There have been only sporadic reports of internal concentration of that metabolite in other cyanobacteria strains. Hence, we optimized a spectrophotometric method to determine the level of intracellular 2-OG. Then, this metabolite was measured under different conditions in different strains of *Prochlorococcus.*

Firstly, focused our attention on key nutrients (nitrogen, iron and phosphorus) in the oligotrophic regions where *Prochlorococcus* is abundant (Partensky *et al.*, 1999). Ammonium is the preferred source of nitrogen by cyanobacteria (Muro-Pastor *et al.*, 2005, Flores & Herrero, 2005), and the only one being assimilated by all *Prochlorococcus* strains thus far studied. The effect of nitrogen starvation on the level of intracellular 2-OG in two different strains SS120 and PCC 9511 in order to analyse the impact of nitrogen stress is shown in figure 26. Interestingly, the response was different in these strains. While in SS120 the level of 2-OG increased with the time, in PCC 9511 there were no significant changes compared to the control culture. Taking into account that they are strains that belong to different ecotypes, PCC 9511 is adapted to live at the surface layer of the water column where the level of nitrogen is

lower than deeper where SS120 thrives. Therefore, SS120 could be more sensible to differences on the level of nitrogen status than PCC 9511.

The highest level of 2-OG was reached in SS120 after 24 h of nitrogen deprivation, it was ca. 1.4 nmoles/mg protein, while the value reached in *Synechocystis* PCC 6803 was ca. 2 nmoles/mg protein (Muro-Pastor *et al.*, 2001) and in *Anabaena* sp. PCC 7120 was estimated at 2.51 nmoles/mg protein corresponding to an intracellular concentration of 0.1 mM (Laurent *et al.*, 2005). These values are 10, 7 and 2.5 fold higher respectively respect to the concentration found in the presence of ammonium. Hence, according to our calculations, the intracellular concentration of 2-OG was ca. 0.05-0.2 nmoles/mg protein under control conditions, in good agreement with the values described for *Synechocystis* sp. PCC 6803 but lower than for *Anabaena* sp. PCC 7120, ca. 1.15 nmol/mg protein (Muro-Pastor *et al.*, 2001, Mérida *et al.*, 1991, Laurent *et al.*, 2005).

In order to further study the effect of key nutrients in *Prochlorococcus* SS120, the effect of deprivation of phosphorus, iron and nitrogen were followed in long time experiments (figure 27). We were particularly interested in the case of nitrogen because the core of our work is the nitrogen metabolism. Lack of iron had a more striking effect than phosphorus, inducing a marked decrease in the number of cells (El Alaoui *et al.*, 2003), being harder the work with the obtained cultures. Anyway, the highest level of 2-OG was detected under 5 days of iron starvation; that response could be due to the essential role of iron since it is essential for cell growth, photosynthesis, respiration, nitrogen assimilation, and DNA synthesis replication because many iron-containing proteins catalyse key reactions involved in those processes (Boyer *et al.*, 1987, Leonhardt & Straus, 1992).

The effects of inhibitors of the main nitrogen assimilation pathway in cyanobacteria on the level of 2-OG were studied. After the addition of 100 μM of MSX (a specific inhibitor of GS) the level of that metabolite increased but not significantly, although the growth was lower indicated that the blocking of this key enzyme in nitrogen metabolism has an important effect on the survival of the cell. In contrast, the addition of 100 μM of azaserine (inhibitor of GOGAT) promoted an increment of the level of 2-OG in SS120 and PCC 9511 (figure 30) as we expected.

The response in these two strains is somehow different. In PCC 9511 azaserine induced a ca. 5.5 fold increase in the concentration of 2-OG after 8 h of the addition, moreover, after 24 h its concentration was still 2.3 fold higher compared to the controls. In SS120 azaserine promoted an increment 5 fold after 8 and 24 h of the treatment. All of the data are statistically significant. But, if we look the figure 30, while SS120 reached the maximum level of 2-OG after 8 hours of addition, PCC 9511 did after 24 h.

The last study consisted in determining the level of 2-OG with different concentration of azaserine (up to 100 μM) in three strains, SS120, PCC 9511 and MIT9313 (figure 31). Surprinsingly, the results were not as expected. We believed that the addition of azaserine should provoke an increase in the level of 2-OG. However, there was not a clear relation between the concentration of azaserine and the level of 2-OG. Possible causes may be because there are different pathways to be metabolized or cell death.

From that section of results we can conclude that our data strongly indicate that the nitrogen status of *Prochlorococcus marinus* is perceived through changes in the intracellular concentration of 2-OG, although that differs among strains.

2. Effect of azaserine on the metabolism of *Prochlorococcus marinus*

Blocking GOGAT in *Prochlorococcus* with azaserine should increase the intracellular concentration of 2-OG. We measured it and effectively after the addition of azaserine the level of 2-OG increased (discussed above). Then, we studied the effect of the increment of 2-OG on the growth, activities of key enzymes, the expression of genes related with the nitrogen metabolism and the proteome of *Prochlorococcus*.

The growth of *Prochlorocccus* was affected after 24 h of azaserine addition. These results were expected since the main pathway of nitrogen assimilation was blocked. Anyway, the pattern among the three strains was different but in all cases the growth was lower and PCC 9511 being the most affected.

In *Prochlorococcus* SS120 GS activity was higher after 8 h of azaserine addition as occurs in PCC 9511 (El Alaoui *et al.*, 2001). That is the standard response expected in most photosynthetic organisms (Mérida *et al.*, 1991), an increment of the enzymatic activity under conditions of nitrogen stress, this inhibitor created a comparable situation. On the contrary, the concentration of GS decreased after 8 h and it has been described in PCC 9511 it increased ca. 2.7 fold after 24 h (El Alaoui *et al.*, 2001).

The effect of azaserine addition provoked a significant increase of the ICDH activity in SS120 after 8 h (3 fold) and in PCC 9511 after 24 h (1.45 fold). Given such response we analyzed the effect of azaserine on ICDH concentration. A clear decrease on the concentration was shown in both strains. On the other side, *icd* expression in PCC 9511 decreased sharply until 8 h after azaserine additions but there was a strong increase at 24 h (figure 51). Besides, in the SS120 strain, azaserine induced similar changes in the expression of *icd*, an initial repression and a final increase ca. 9 fold after 24 h (López-Lozano *et al.*, 2009). Maybe the increment of the expression is a response to compensate the loss of ICDH enzyme induced by the inhibitor. The delay observed for *icd* induction in our results might be explained by the low amount of ribosomes in these slow growing cells, which is reflected in a lag between transcription and protein production that has been reported to be of 2-8 h in *Prochlorococcus* (Waldbauer *et al.*, 2012). The inhibitor MSX promoted a more drastic decrease of the concentration of ICDH than azaserine, but there is no information in the literature regarding the effect of that inhibitor on other cyanobacterial strains (figure 37).

The concentration of this key enzyme, ICDH, was altered under other conditions in PCC 9511 (figure 37). The concentration of the enzyme showed little change upon 24 h of nitrogen starvation. Moreover, in a global expression study on two *Prochlorococcus* strains (Tolonen *et al.*, 2006a), MED4 genetically identical to PCC 9511 showed a 2.46 fold increase in the expression of *icd* under nitrogen depletion. On the other hand, under phosphorus starvation the concentration of ICDH decreased nearly to the half. Under 8 h of iron starvation there was a slightly effect on the concentration suggesting a rapid loss of the activity. This could be a direct

consequence of the oxidative stress induced by iron starvation, as previously reported in other cyanobacteria (Latifi *et al.*, 2005).

Besides, darkness provoked a decrease in the concentration of the enzyme (ca. 60%), in good agreement with the results described for ICDH from *Synechocystis* sp. PCC 6803 (Muro-Pastor *et al.*, 1996). DCMU and DBMIB are inhibitors of the photosynthetic electron flow, blocking the electron transfer before and after the plastoquinone pool, respectively (figure 38) (Rich *et al.*, 1991, Trebst, 1980). DCMU and darkness provoke the oxidation of the plastoquinone pool derived from the decrease in the NADPH intracellular levels, so when 0.3 μM of DCMU was added to the *Prochlorococcus* PCC 9511 cultures the concentration of ICDH decreased to a value close to that found in darkness. It has been reported that the expression of the gene *icd* is up-regulated significantly after 8 hours of DBMIB and markedly down-regulated after 24 hours of addition in *Prochlorococcus* SS120 (López-Lozano *et al.*, 2009), so we expected a decrease of the concentration of the enzyme since the experiment were at 24 h time. Our results in good agreement showed that after addition 0.06 μM of DBMIB the enzyme had a sharply decreased (ca. 80%) on its concentration. On the other hand, a global expression study of redox response genes in *Synechocystis* sp. PCC 6803 showed no significant change for *icd* in presence of DCMU and DBMIB (Hihara et al., 2003).

To discard that the azaserine effect was induced by a direct effect of 2-OG on the ICDH activity, we added different known concentration of 2-OG to the reaction mixture and the activity was measured (table 45). We can observe that with concentrations much higher than physiological the 2-OG provoked a partial inactivation of the enzyme activity. Hence, we can conclude that the effect of 2-OG is not directly acting on the ICDH activity, we infer that azaserine provokes a transcriptional effect mediated by 2-OG.

The possible variability among strains of *Prochlorococcus* with regard to the regulatory mechanisms was assessed by studying the effect of different concentration of azaserine on activities and concentrations of key enzymes, GS and ICDH, and on the expression of genes encoding regulatory proteins and enzymes of nitrogen metabolism in three strains, PCC 9511, SS120 and MIT9313.

The GS activity showed different pattern between strains. In SS120 the activity increased with azaserine in contrast to the enzyme concentration, that decreased (figure 39 and 40 respectively). Moreover, the expression of the gene *glnA* was repressed under the same conditions (figure 49) and it has been reported similar results previously with 100 μM of azaserine (López-Lozano *et al.*, 2009). Our results suggest that the regulation of GS in SS120 occurs at the enzymatic level. In contrast, azaserine had no effect on the GS activity and concentration in MIT9313 (figure 39 and 40 respectively). It would be interesting to determine the expression of the gene in this strain in order to check if the azaserine affect GS at transcriptional level in MIT9313. We did several attempts but the amplifications were unsuccessful. PCC 9511 had a different pattern but somehow erratic. The GS activity increased with 1, 20 and 100 μM as it has been showed in the study carried out by El Alaoui and coworkers (El Alaoui *et al.*, 2001), but the maximum level was with 20 μM of azaserine. Besides, the enzyme concentration increased with the concentration of azaserine being the maximum with 100 μM, in good agreement with the increment found in the same strain after 24 h of azaserine addition (El Alaoui *et al.*, 2001). Although the expression increased too with the azaserine, the maximum level was with 5 and 100 μM. In conclusion from the results discussed above, the GS activity showed different pattern among strains.

The incompleteness of the TCA in marine picocyanobacteria confers a special importance to ICDH in the C/N balance, so it was interesting to determine the ICDH activity, concentration and expression under different concentration of azaserine. SS120 and PCC 9511 showed the same pattern, ICDH activity was high with low concentration of azaserine and decreased with the increment of the inhibitor. In the case of SS120 the activity was correlated with the concentration of the enzyme. Furthermore, the expression of *icd* differs between them. In SS120 the azaserine provoked an increment only with 100 μM of azaserine, however, in PCC 9511 all the concentrations promoted an increment of the expression, being the highest with 5 μM. MIT9313 showed a similar response in the activity, concentration and expression. In all the situations studied there was an increment with 1 μM being the maximum peak with 20 μM.

The expression of *icd* was further analyzed under other conditions in MIT9313 strain (figure 52). We studied its expression in *Prochlorococcus* MIT9313 cultures subjected to nutrients deprivation after 48 and 120 h. There was a 13 fold increment of *icd* expression under 120 h of nitrogen starvation in agreement with the results of Muro-Pastor and coworkers, who observed a 5 fold increase in the expression of *icd* in *Synechocystis* sp. PCC 6803 under nitrogen starvation (Muro-Pastor *et al.*, 1996). In contrast, the expression decreased in *Prochlorococcus* SS120 until 24 h (López-Lozano *et al.*, 2009). The phosphorus starvation promoted a decrease of the expression after 48 h in contrast to SS120, which expression was increased after that time (López-Lozano *et al.*, 2009). Another element whose concentration is limiting in many oligotrophic oceans is iron, the effect of its deprivation on the expression of *icd* was determined. It provoked downregulation after 48 h but there was a slight recovery after 120 h. These results are in good agreement with *icd* expression after 48 h previously reported in SS120 (López-Lozano *et al.*, 2009).

As we mentioned above, light is an important factor for photosynthetic organisms and DCMU, DBMIB are inhibitors of the photosynthetic electron flow, having DCMU a similar effect to darkness. After 24 h of darkness there was a slight increment in *icd* expression in MIT9313, in contrast to SS120 (López-Lozano *et al.*, 2009). DCMU promoted a similar effect in MIT9313 in good agreement with the results shown for SS120 (López-Lozano *et al.*, 2009). In the case of DBMIB, the response was completely different. Strikingly the *icd* expression in MIT9313 showed a marked increment after 24 h in agreement with the sharp increase observed in SS120 after 8 h (López-Lozano *et al.*, 2009).

MSX addition induced an upregulation after 8 h of addition, the response was faster in SS120 since upregulation that happened after 1 h of the addition of the inhibitor (López-Lozano *et al.*, 2009).

The *gdhA* gene was studied under different concentration of azaserine. Genome studies showed that *gdhA* appears in four *Prochlorococcus* strains (Kettler *et al.*, 2007): MIT9313, MIT9303 (low irradiance-adapted), MIT9215 and MIT9515 (high irradiance-adapted). In our study only MIT9313 has *gdhA* gene (figure 53). Its expression decreased with the highest azaserine concentration which correlates well

with the main physiological role of GDH in MIT9313, that is the utilization of glutamate to produce ammonium and 2-OG (Rangel *et al.*, 2009).

The figure 48 shows the effect of the different concentrations of azaserine on the glsF (GOGAT) in three strains of *Prochlorococcus*. In PCC 9511 the expression was upregultaed under 1 μM of azaserine and the others was unaffected. This is in agreement with the reported lack of regulation of GOGAT expression by the nitrogen sources (Herrero *et al.*, 2001, Flores & Herrero, 1994).

The expression of genes encoding the regulatory proteins NtcA, P_{II} and PipX were studied in the three strains of *Prochlorococcus*. In the case of NtcA three completely different patterns were found (figure 45). The expression of *ntcA* in SS120 was unaffected with azaserine in good agreement with the results previously shown (López-Lozano *et al.*, 2009). In contrast to MIT9313, where the expression increased with the concentration of the inhibitor. PCC 9511 was also upregulated but the maximum was obtained with 20 μM of azaserine. The expression of *ntcA* is repressed by ammonium in *Synechococcus* sp. Strains PCC 7942 (Luque *et al.*, 1994) and WH7803 (Lindell *et al.*, 1998) and expression studies, carried out with the closely related marine cyanobacteria *Synechococcus* WH8103 (Bird & Wyman, 2003) and WH7803 (Lindell & Post, 2001), have shown that nitrogen deprivation induced an upregulation in the levels of *ntcA* expression. Consequently, it seems that, *ntcA* from MIT9313 and PCC 9511 have a physiological response similar to that found in other cyanobacteria, unlike SS120.

The gene *glnB* encodes the P_{II} protein that is one of the most widespread signal transducers in the control of nitrogen metabolism (Arcondéguy *et al.*, 2001, Ninfa & Atkinson, 2000). In general, the P_{II} protein of the cyanobacterium is phosphorylated at residue S49 (Forchhammer & Tandeau de Marsac, 1994) but the P_{II} of *P. marinus* PCC 9511 was not phosphorylated under the different conditions tested, despite its highly conserved primary amino acid sequence, including the seryl residue at position 49 (Palinska *et al.*, 2002). That could means that P_{II} exerts the regulatory functions in *Prochlorococcus* without post-translational modification of the protein. The expression of *glnB* was different between the three strains used in this study. In PCC 9511 the gene was upregulated with 1 μM of azaserine and decreased the

expression with the increment of the inhibitor and in MIT9313 the maximum level was found with 20 μM of azaserine. Those results could be related with the results obtained in *Synechocystis* PCC 6803 where the expression of *glnB* was specifically activated under nitrogen deprivation (García-Domínguez & Florencio, 1997), since the situation with azaserine is similar to the absence of nitrogen due to blocking of the main nitrogen assimilatory pathway. SS120 showed no clear correlation between azaserine and the expression of *glnB*, it seems that the expression was unaffected and with 100 μM of azaserine the expression was similar that found by López-Lozano and coworkers (López-Lozano *et al.*, 2009).

PipX provides a functional link between the cyanobacterial global transcriptional regulator NtcA and the signal transduction protein P_{II} (Boumediene Laichoubi *et al.*, 2012, Espinosa *et al.*, 2006) and it has been recently described as a global regulator in cyanobacteria (Espinosa *et al.*, 2014). The expression of *pipX* in MIT9313 and SS120 was affected by azaserine but in a different way. While in SS120 the expression was induced with all the concentrations used, in MIT9313 it occurred only with 1 μM. Since PipX interacts with NtcA to enhance the transcription of genes related with nitrogen metabolism (Llácer *et al.*, 2010), we expected the upregulation of the gene under an increment of the level of 2-OG.

The biochemical and physiological techniques shown above have contributed to find differences on the regulatory C/N metabolism among strains. Proteomics has the potential to increase our overall understanding. Recent advancements in HTT (high throughput techniques) based on tandem mass spectrometry (MS) allowed to the scientists a greater insight concerning the integration, function and regulation of the proteome (Yen Ow & Wright, 2009). In our study we used the latest technology in mass spectrometer, *Q Exactive* from *Thermo Fisher*. To analyze the effect of azaserine on the proteome of *Prochlorococcus,* samples of SS120 were subjected to 100 μM of the inhibitor and were collected after 8 h. In figure 30 a sharp increase of the level of 2-OG was shown in SS120 after 8 h of azaserine addition, so we decided to use that strategy to study the effect of the increment of that metabolite on the proteome of *Prochlorococcus* SS120.

After the optimization of the amount of protein loaded onto the column in the mass spectrometer and the time to run the samples (table 47), 915 proteins were identified, which represents 49% of the predicted proteome of *Prochlorococcus* SS120 (Dufresne *et al.*, 2003), 113 proteins were identified only in control situation and 29 proteins only in azaserine. There are scarce proteomics studies in cyanobacteria (Yen Ow & Wright, 2009). Only one of them was in *Prochlorococcus marinus* MED4 (Pandhal *et al.*, 2007). Approximately 11% of the theoretical proteome was identified in that study. There was a study carried out in *Nostoc punctiforme* ATCC 29133 in which 1575 proteins (Anderson *et al.*, 2006) were identified from 7432 protein ORFs known in this organism (Meeks *et al.*, 2001), that represents 21% of the proteome. Another proteomic approximation in *Synechocystis* sp. PCC 6803 identified 53% of the predicted proteome (Wegener et al., 2010) a value close to ours. Thus, our study represents the highest coverage of the proteome of any strain of *Prochlorococcus* and one of the highest coverage in cyanobacteria to date.

The identified proteins were analyzed to determine the pathway in which there are involved using the tool DAVID (figure 58), we got representative members of all the main pathways in the cell. The samples were run with 50 fmol/µL of PhosB; this help us to perform absolute quantification using the *Progenesis postprocessor* tool (Qi *et al.*, 2012). With that work, 840 proteins were quantified in absolute terms in control situation and under azaserine treatment (S4, *Supplementary data*). To our knowledge, there are no similar data available to date. This is the first work that includes the precise quantification of approximately 50 % of the proteins of the *Prochlorococcus* proteome in different conditions.

In total, 240 proteins were considered as significantly up- (table S1, *Supplementary data*) or downregulated (table S2, *Supplementary data*). The differentially expressed proteins were selected based on the *p*-value assigned for the quantification ($p < 0.05$) and the detection with more than 1 peptide. The changes observed were due to the treatment as PCA shown in figure 61. These proteins are involved in different pathways, one interesting is the photosynthesis process. The situation that was promoted by the addition of azaserine was as follows: the level of 2-OG increased due to the blocking of the main nitrogen assimilation pathway. 2-OG binding to NtcA promoted the transcription of genes related with nitrogen

metabolism. There is a report that showed *in silico* putative binding sites for NtcA for many genes involved in various stages of photosynthesis (Su *et al.*, 2005). It is the case of the Ferredoxin-NADP oxidorreductase (Q7VBH1), *petH*, which was 1.7 fold higher under azaserine. Besides, it has been described that in *Synechocystis* PCC 6803 NtcA activates transcription of *petH* promoter (Omairi-Nasser *et al.*, 2014). Thus, the result suggests that *Prochlorococcus* photosynthesis and nitrogen assimilation could be tightly coordinated by NtcA.

The proteins of our interest, NtcA, P_{II}, PipX, GS, ICDH and GOGAT were identified in the proteomic anlasys. Our proteomics study show that the concentration of ICDH and GS decreased with azaserine treatment in good agreement with previous results described in figure 34.

NtcA appeared higher under azaserine condition as we expected. The other two regulatory proteins, P_{II} and PipX, were significantly down regulated. We expected that these proteins were higher after azaserine addition, it could be that the response to the treatment in that proteins will be delayed, once again. One possible explanation could be the lag that exists in *Prochlorococcus* between transcription and protein production (Waldbauer *et al.*, 2012).

3. Interaction between NtcA and *glnA* promoter from *Prochlorococcus* SS120 and MIT9313

All the data discussed until now show differences among these three strains of *Prochlorococcus* in relation with the sensibility to 2-OG. That was reflected in the different level of 2-OG under the same conditions, in different key activities and in the expression of genes related with nitrogen metabolism.

We also studied the regulatory proteins, NtcA, P_{II} and PipX. Although *Prochlorococcus* MIT9313 and SS120 have the three regulatory proteins, how they work and interact is not yet clear. They were overexpressed correctly in *E. coli* because the molecular sizes of proteins obtained were the same as the predicted size.

The alignment of P_{II} showed that proteins from MIT9313 and SS120 were highly conserved, including the seryl residue at position 49, the site for the phosphorylation of the protein in *Synechococcus* PCC7942 (Forchhammer & Tandeau de Marsac, 1994). P_{II} from *Prochlorococcus* PCC 9511 did not show any phosphorylation under different nitrogen sources (Palinska *et al.*, 2002) and also there is no *pphA* gene, encoding the phosphatase to dephosphorylate the P_{II}, in the *Prochlorococcus* genome (Rocap *et al.*, 2003). Future study would be carried out in order to analyze the possible interactions of P_{II} from *Prochlorococcus*.

NtcA interacted with the promoter GTA $N_{(8/9)}$ TAC (Tolonen *et al.*, 2006b) for *glnA* from *Prochlorococcus* MIT9313 and SS120. The results showed that the 2-OG is the molecule that promote the interaction between transcription factor and DNA in agreement with the results described in other cyanobacteria (Luque *et al.*, 1994, Tanigawa *et al.*, 2002, Vazquez-Bermudez *et al.*, 2002, Espinosa *et al.*, 2006). However, the results showed that the sensibility of NtcA to 2-OG on the binding differs between MIT9313 and SS120. SS210 needs a higher level of 2-OG to bind NtcA to the promoter. That agrees with the data showed for the *glnA* expression in SS120, the expression did not show a significant change under different concentrations of azaserine when the level of 2-OG increased.

Differential interaction from the complex NtcA-PipX with the promoter for *glnA* was found between SS120 and MIT9313. While in MIT9313 did not show a significant increment on the interaction with PipX, in SS120 the presence of PipX enhanced the binding to the promoter. That suggests the role of PipX on the transcription of the genes could differ in different strains of *Prochlorococcus*.

Finally, all the results obtained in that chapter confirm our main hypothesis. We believed that the regulatory mechanism differs in *Prochlorococcus* from the model freshwater cyanobacteria described to date and also these differences exist among strains. This would help us to understand how this cyanobacterium adapted to their different ecological niches.

CHAPTER 2

Physiological regulation of glutamine synthetase from *Synechococcus* WH7803

Introduction

Picocyanobacteria of the genera *Synechococcus* and *Prochlorococcus* dominate the photosynthetic biomass found in the surface waters of subtropical and tropical oceans, where they contribute substantially to global carbon fixation (Wyman & Bird, 2007, Chisholm *et al.*, 1988, Partensky *et al.*, 1999, Waterbury *et al.*, 1986).

Our team has been working on the nitrogen and carbon metabolism in *Prochlorococcus* since 1997, and has a wide experience on biochemical and molecular biology approaches to study enzymes related with the nitrogen metabolism. A collaboration with Prof. Wolfgang Hess´s team allowed us to work with *Synechococcus* WH7803. Consequently, comparative studies between these two marine cyanobacteria were performed, taking into account that they coexist in the oligotrophic regions of the oceans (Partensky *et al.*, 1999).

The first approach was to characterize the GS, an enzyme studied in detail by our team in *Prochlorococcus*. A mutant strain of *Synechococcus* WH7803 with an inactive sigma factor SigF was kindly provided by Prof. Wolfgang Hess, in order to study if its absence has an effect on this enzyme. For that, the GS activity and concentration were determined under different conditions, by using spectrophotometric assays and western blotting, respectively.

1. *In silico* study of glutamine synthetases from *Synechococcus* WH7803

Two different types of GS have been found in cyanobacteria, although most strains have only one (known as GS type I, GSI). Some cyanobacterial strains have in addition another GS (known as GS type III, GSIII) (Muro-Pastor *et al.*, 2005). Two close bands were detected in the western blots of GSI. The search in the databases available showed three different glutamine synthetases annotated. The information on the three possible GS from *Synechococcus* WH7803 is summarized in the table 52.

Table 52: Summary of the characteristics of the possible GS from *Synechococcus* WH7803

Enzyme	Gene name	Gene length (pb)	Protein length (aa)	Molecular Weight (kDa)	Theoretical isoelectric point	Position locus
GSI	*glnAI*	1,422	473	52.5	5.29	1,347
Putative GS	*glnAIII*	1,347	448	47.6	5.64	1,458
GSIII	*glnN*	2,172	723	79.4	5.93	2,387

As we can observe in the table 52, GS encoded by the genes *glnAI* and *glnAIII* have close molecular weight corresponding with the two bands found in the western blotting. The other putative GS encoded by *glnN* gene is clearly larger.

In order to check for a possible mistake in the annotation at the database, a protein alignment between them was performed (figure 77). They are clearly different.

Figure 77: Alignment between *glnAI* and *glnAIII*. Sequences were taken from the CYORF database and the alignment was performed by *Multialignment* program (*Lasergene*), using CLUSTAL V. The aminoacid sequences were named *glnAI* for GSI and *glnAIII* for the unknown GS. Black squares are the conserved aminoacids regard to the consensus sequence. Majority refers to the consensus sequence.

The search in the database using the gene *glnAIII* allowed us to find that in the genome of *Rhodopseudomonas palustris* there was a putative glutamine synthetase III encoded by this gene, the length of the gene was 1386 bp, and the predicted protein

had 461 aa. A multiple alignment was performed using *glnA*, *glnN* and *glnAIII* from different cyanobacteria. The figure 78 shows the percent identity between them. The identity between *glnAI* and *glnAIII* from *Synechococcus* WH7803 was really low (20.1%).

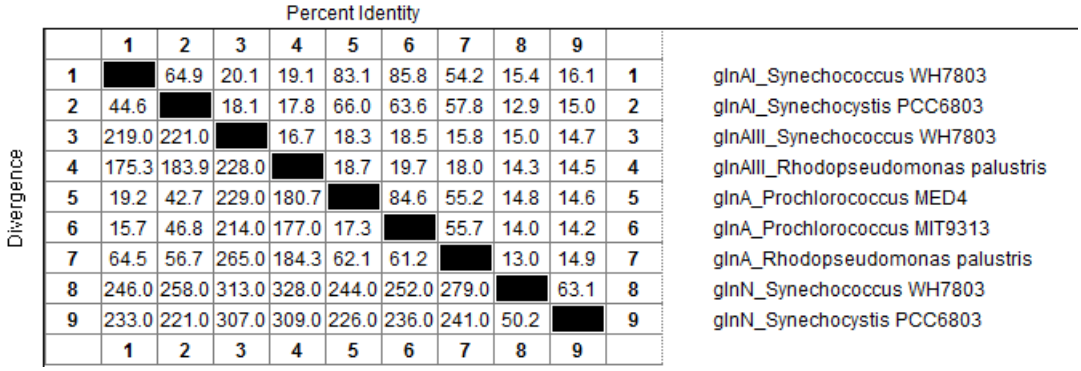

Figure 78: Percent identity in the amino acid sequence of different GSs from cyanobacteria. The sequences were taken from the database CYORF. The data were obtained from the *Multialignment* software (*Lasergene*) using CLUSTAL V. *glnAI* and *glnA* encoded the GSI; *glnN* encoded the GSIII and *glnAIII* encoded the unknown GS.

The phylogenetic tree (figure 79), obtained by the multiple alignments of sequences before mentioned, showed clearly three distinct clusters corresponding to *glnAI*, *glnN* and *glnAIII*.

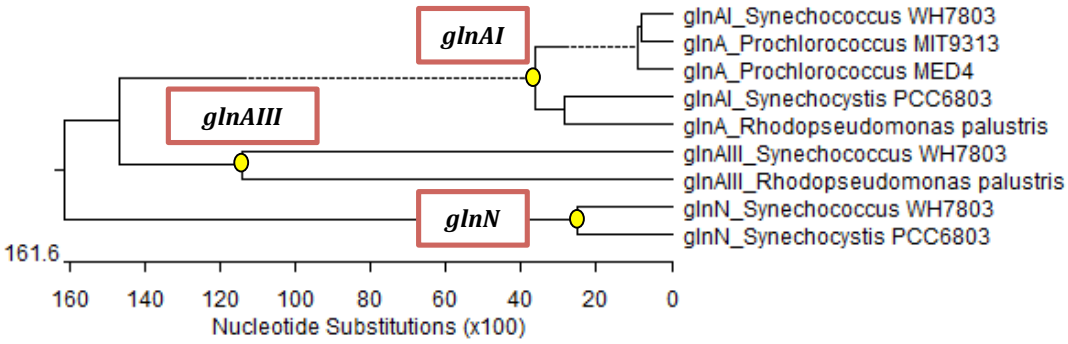

Figure 79: Phylogenetic relationships of GSs from different cyanobacteria. The sequences were taken from the database CYORF. The data were taken from the *Multialignment* software (*Lasergene*) using CLUSTAL V. The length of each branch corresponds to the nucleotide substitutions. *glnAI* and *glnA* encoded the GSI; *glnN* encoded the GSIII and *glnAIII* encoded the unknown GS. ● represents each specific node for each GS.

The interactions obtained from the software *String* 9.1 are shown in figure 80, a database of known and predicted protein interactions. The interactions include direct (physical) and indirect (functional) associations.

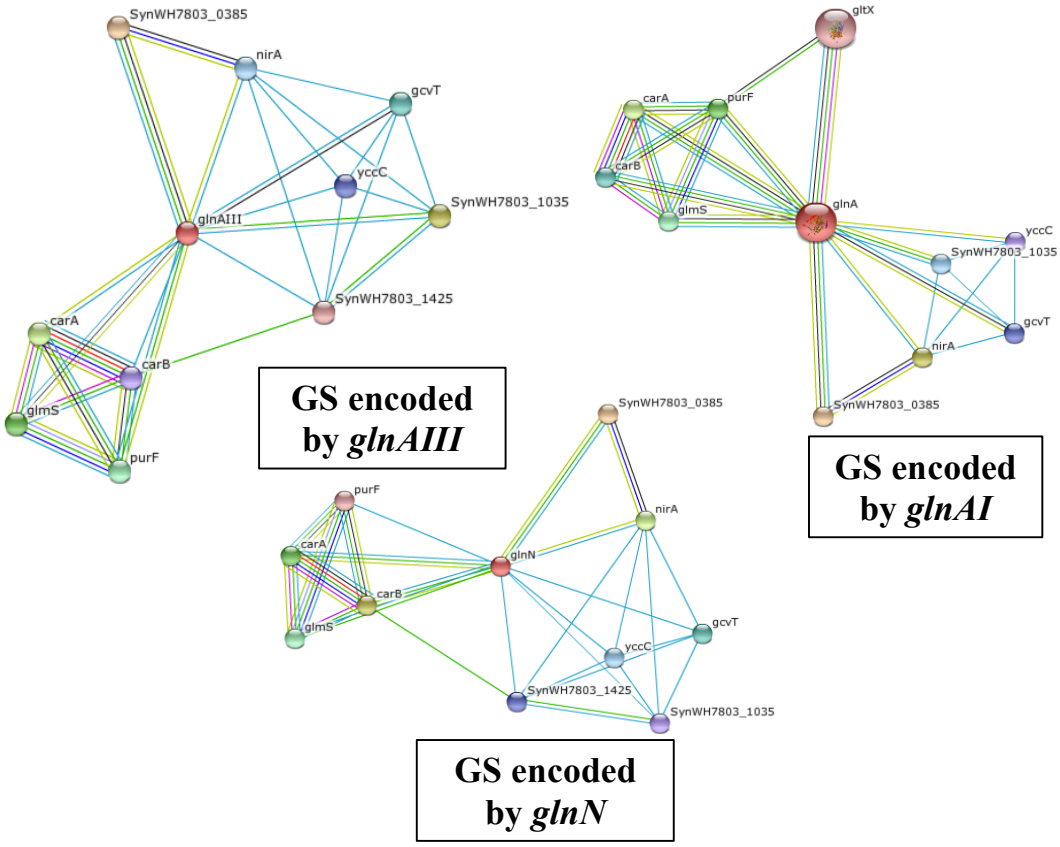

Figure 80: Interactions networks of *glnAIII, glnAI* and *glnN*. The different GS were used as central part for *String 9.1*. Different line colours represent the types of evidence associations. Line colour indicates the type of the supporting evidence; all underlying evidence can be inspected in dedicated viewers that are accessible from the network.

The shapes of the network seemed different, but the three GSs interacted with almost the same proteins, except that GS encoded by *glnAIII* and *glnN* interacted with SynWH7803_1425 (L-asparaginase II) and the protein from the gene *glnAI* interacted with the protein gltX (Glutamyl-tRNA synthetase).

Finally, Dr. Muro-Pastor from the IBVF (Seville) was carried out in order to confirm the third possible glutamine synthetase. The followed process was based in analyzing the functionality of this gene by its ability to complement an *Escherichia coli glnA* mutant, as described (Reyes & Florencio, 1994). The results showed that this third hypothetical GS had no GS activity (Dr. Muro-Pastor personal communication).

1. Optimization of the disruption method

Firstly, the cells were broken with a freezing/thawing method to determine GS activity as described for *Prochlorococcus* (El Alaoui *et al.*, 2001, Gómez-Baena *et al.*, 2001), but with this method the activity of the enzyme was not detected. Thus we tested another method using glass beads *B. Braun Melsungen AG* to disrupt the cells. The original protocol was: after thawing and centrifuging (Materials and Methods, section 3.3.2) the sample, the obtained pellet was resuspended in 250 µL of 50 mM Tris-HCl pH 7.5. Then, the suspension was mixed with 140.6 mg of *B. Braun Meslungen AG* (0.10-0.11 mm of diameter) glass beads and 5 cycles of 1minute vortex-1 minute ice were done. The mixture was centrifuged (as described in materials and methods) and the supernatant was used to determine the enzymatic activity. Different modifications of this original protocol were done (figure 81); samples named A were subjected to the method described above. In B samples the same method was used, but omitting the last centrifugation. In C samples, different times were used for each cycle vortex-ice: 90 seconds, 2 and 3 minutes.

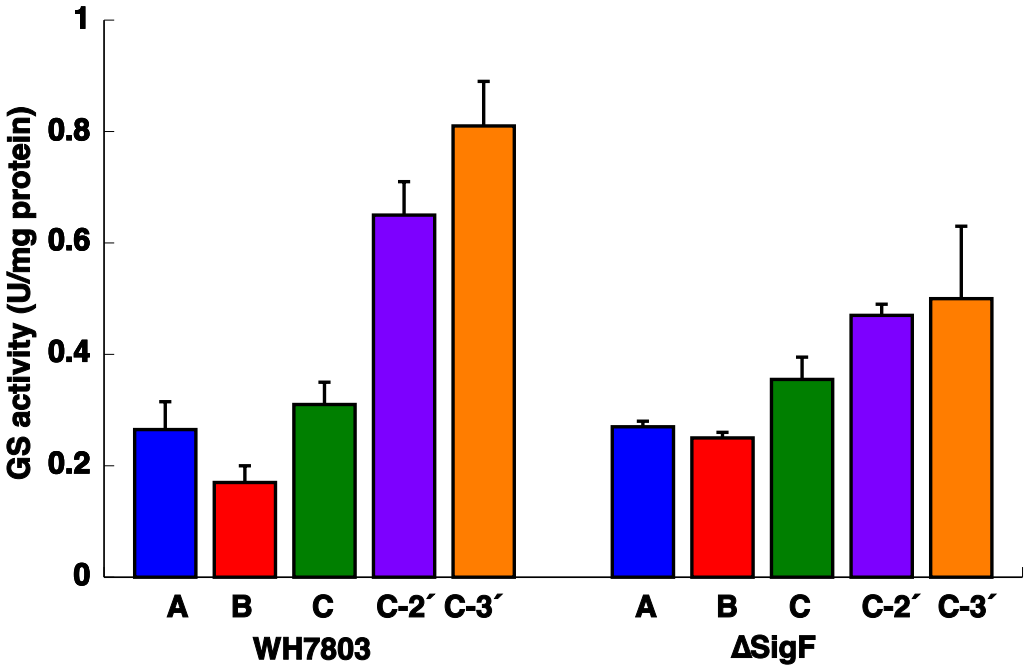

Figure 81: Effect of different disrupting methods on GS activity. Each bar corresponds to *Synechococcus* WH7803 or ΔSigF mutant subjected to the different disrupting methods described in the text. The chart represents the average of three independent biological replicates. Error bars correspond to standard deviation.

The modification of the protocol that showed the highest GS activity was the method designed with C-3´ (5 cycles of 3 minutes vortex and 3 minutes on ice). Therefore this was the method used for all the experiments.

Samples obtained through the freezing/thawing method were subjected to SDS-PAGE. After the gel was distained, no bands from the extract were detected. For that reason, in order to concentrate the samples the same modifications described above were introduced in the protocol to disrupt the cells. Besides, two different volumes of Tris-HCl to dissolve the pellet were added: 250 µL and 100 µL. The results of the electrophoresis are shown in figure 82.

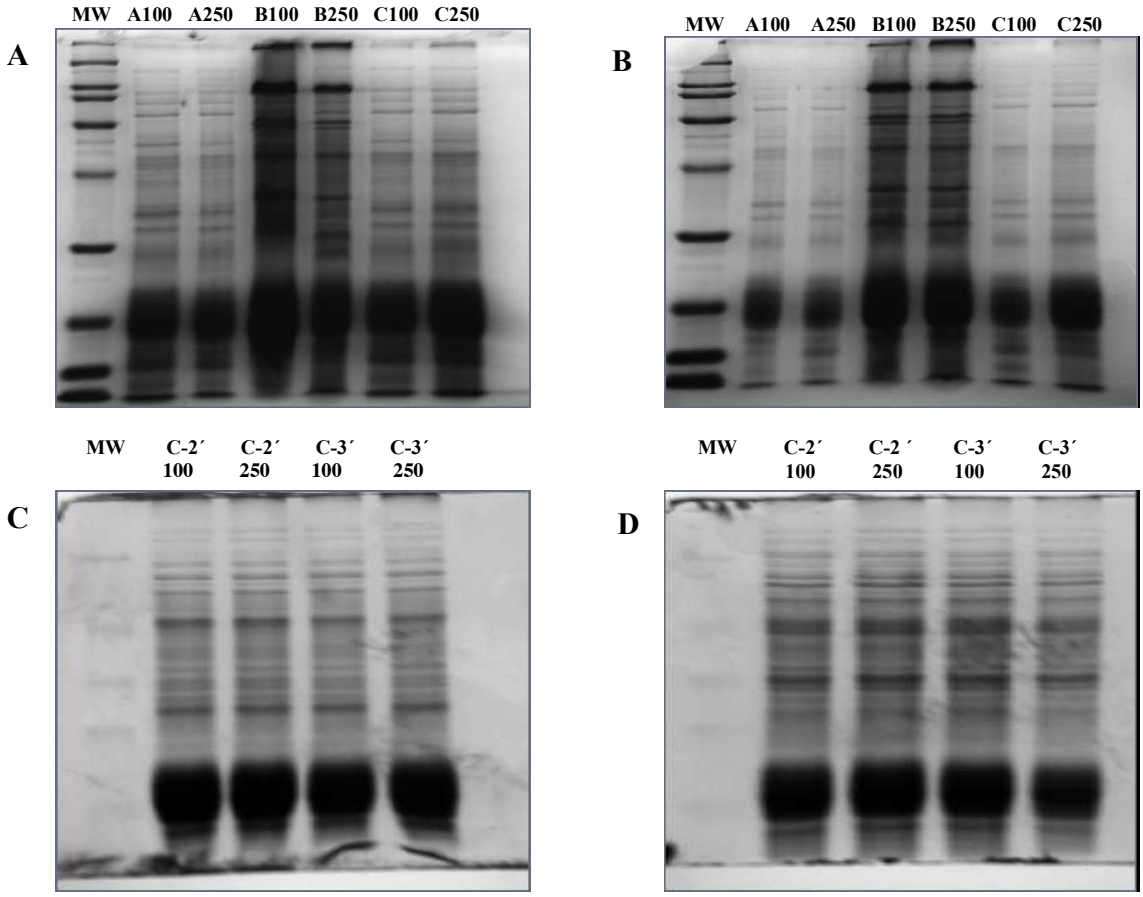

Figure 82: Protein extracts from *Synechococcus* WH7803 (A and C) **and ΔSigF**. (B and D) **obtained by different disruption methods**. The extracts were obtained as described in the text, 40 µg of proteins were loaded and subjected to SDS-PAGE. Gels were stained with Coomassie blue. MW corresponds to the molecular weight markers. The top labels show the disruption method, followed by the volume of Tris-HCl used to resuspend the pellet (100 µL or 250 µL).

From the obtained results, the method C-3´, with 100 µL of Tris-HCl to resuspend the pellet was chosen to perform western blotting with *Synechococcus* WH7803 and its mutant during these studies.

The results shown in figure 82 indicated that there is a differential protein pattern between the wild type and the mutant.

2. Characterization of glutamine synthetase

The GS is the pivotal enzyme of nitrogen metabolism, so it was the first interesting point to study. The effect of the absence of nitrogen source, different nitrogen sources or darkness was studied, and the results are described below.

2.1. Effect of nitrogen starvation

The figure 83 shows the effect of nitrogen starvation on GS activity from *Synechococcus* WH7803. The activity increased significantly after 24 hours of the absence of nitrogen ($p = 0.0166$), while the growth was higher under control conditions (figure 84).

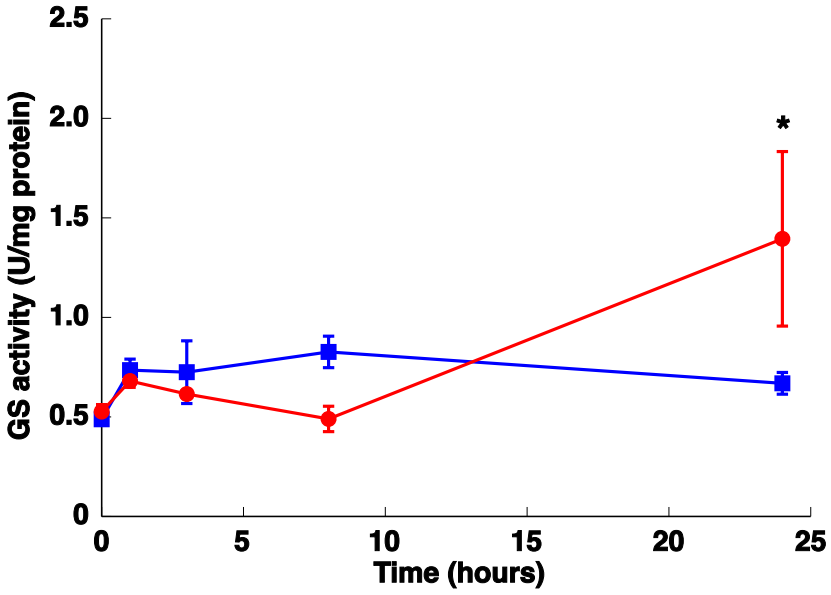

Figure 83: Effect of nitrogen starvation on GS activity of *Synechococcus* WH7803. Cultures were subjected to nitrogen starvation and aliquots were taken at the indicated times. The graph represents four independent biological replicates. Error bars correspond to standard deviation. Control (400 µM of ammonium) ■ and nitrogen starvation ●.

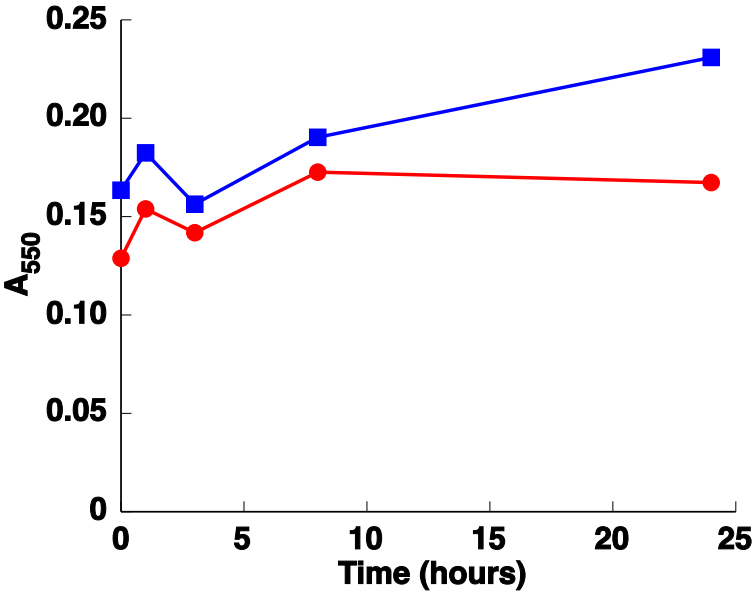

Figure 84: Effect of nitrogen starvation on the growth of *Synechococcus* WH7803. Cultures were subjected to nitrogen starvation and aliquots were taken at the indicated times. The graph represents one independent biological replicate and it is representative of three independent replictaes. Control (400 µM of ammonium) ■ and nitrogen starvation ●.

The western blotting from the same experiment showed that the highest concentration of the enzyme was reached after 24 hours of nitrogen starvation, in good agreement with the activity (figure 85).

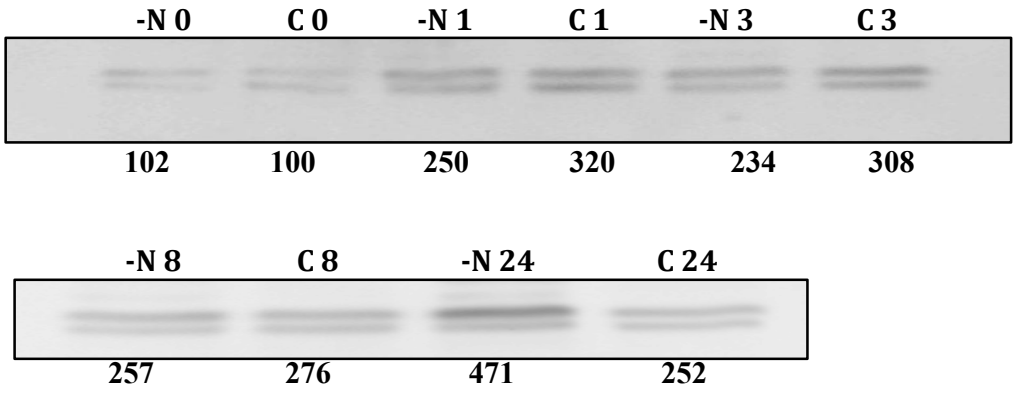

Figure 85: Effect of nitrogen starvation on GSI concentration of *Synechococcus* WH7803. Cultures were subjected to nitrogen starvation and aliquots were taken at indicated times. Western blotting was performed as described in Materials and Methods. Lanes are marked with C (control) and -N (nitrogen starvation), followed by sampling time (in hours). Quantification of bands below the picture, 100% corresponds to the intensity for the control sample at time 0.

2.2 Effect of different nitrogen sources

Synechococcus WH7803 is able to assimilate other nitrogen sources as nitrate and nitrite but no urea since it lacks urease (Collier *et al.*, 1999). In order to analyze the effect of nitrate and nitrite on the GS activity from *Synechococcus* WH7803, this was determined at different times (figure 86). After 24 hours the GS activity was similar with nitrate and nitrite although under nitrogen deprivation it was slightly higher. Nevertheless, after 120 hours the activity had a marked increase in the presence of nitrate, and under nitrogen starvation the activity was higher than after 24 hours. Finally, after 384 hours the GS activity was similar under nitrogen starvation and nitrate, probably due to at that time the nitrate could have been consumed originating a situation similar to nitrogen absence.

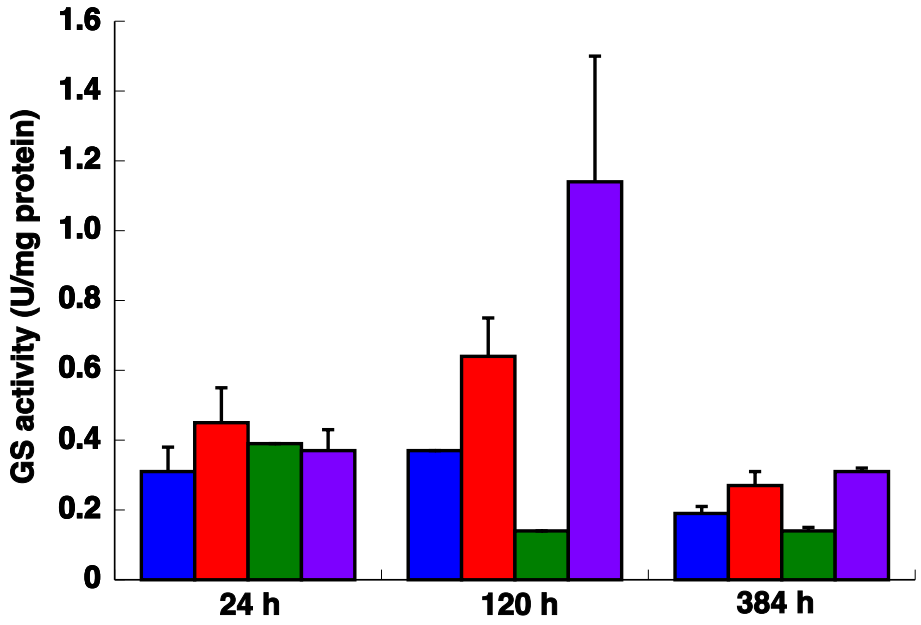

Figure 86: Effect of different nitrogen sources on GS activity from *Synechococcus* WH7803. The cultures were subjected to nitrogen starvation, 400 µM of ammonium (control), 800 µM of nitrate and 800 µM of nitrite. The cells were collected after 24, 120 and 384 hours of treatment. The chart represents the average from two independent biological replicates. Error bars correspond to standard deviation

2.3 Effect of darkness

The light is an important factor for photosynthetic organisms and the GSs of most photosynthetic organisms are regulated by light (Flores & Herrero, 1994).

Hence, the effect of subjecting cultures of *Synechococcus* WH7803 to darkness was investigated. The activity of GS had no change under darkness (figure 87, A) and the growth was slightly lower under darkness (figure 87, B).

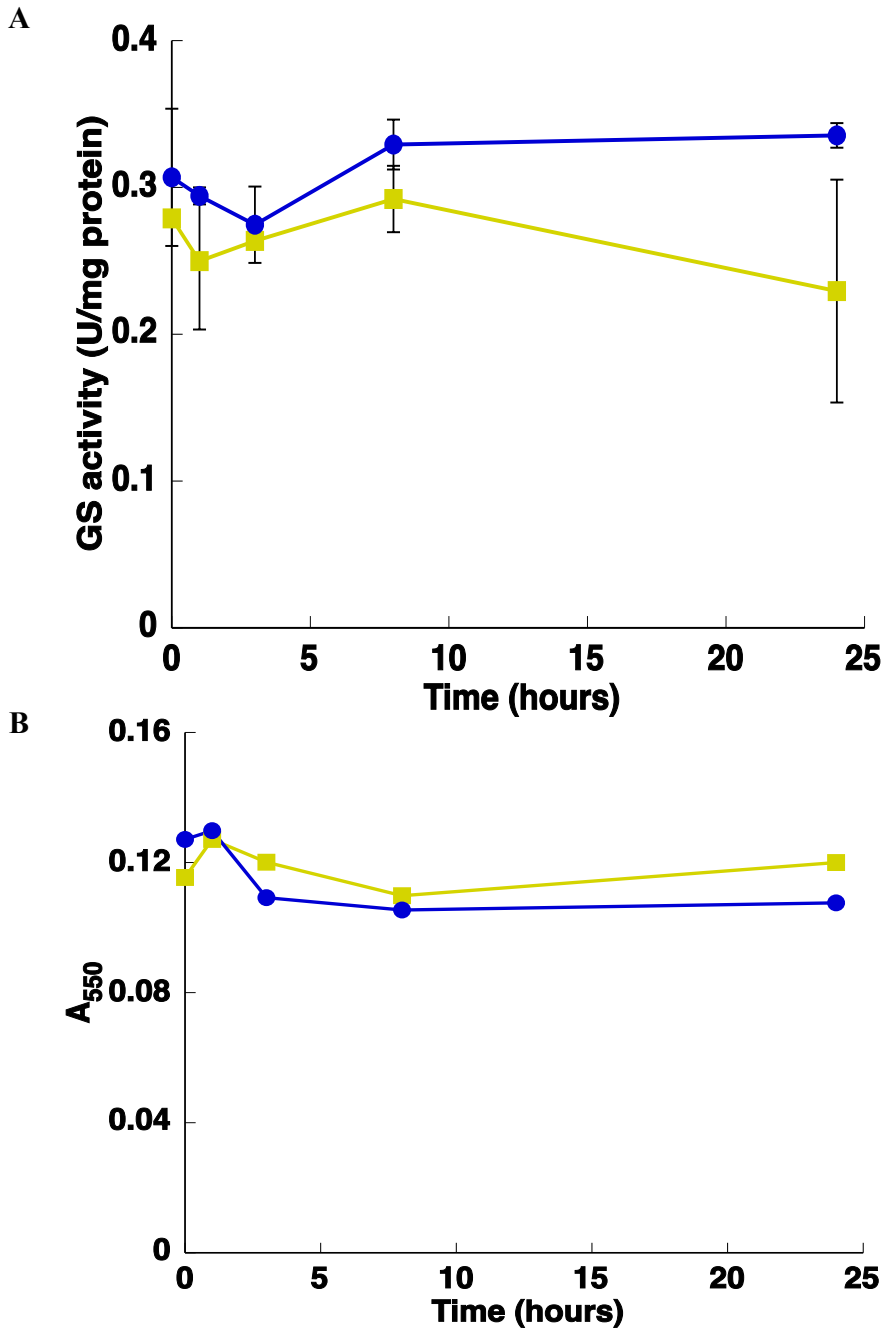

Figure 87: Effect of darkness on GS activity (A) and growth (B) from *Synechococcus* WH7803. Cultures were subjected to darkness ● and 40 µE of blue light (control) ■ and aliquots were taken at indicated times. The graph represents four independent biological replicates. Errors bars correspond to standard deviation.

There was no significant difference on the concentration of GSI between light and darkness condition at any of the times studied (figure 88).

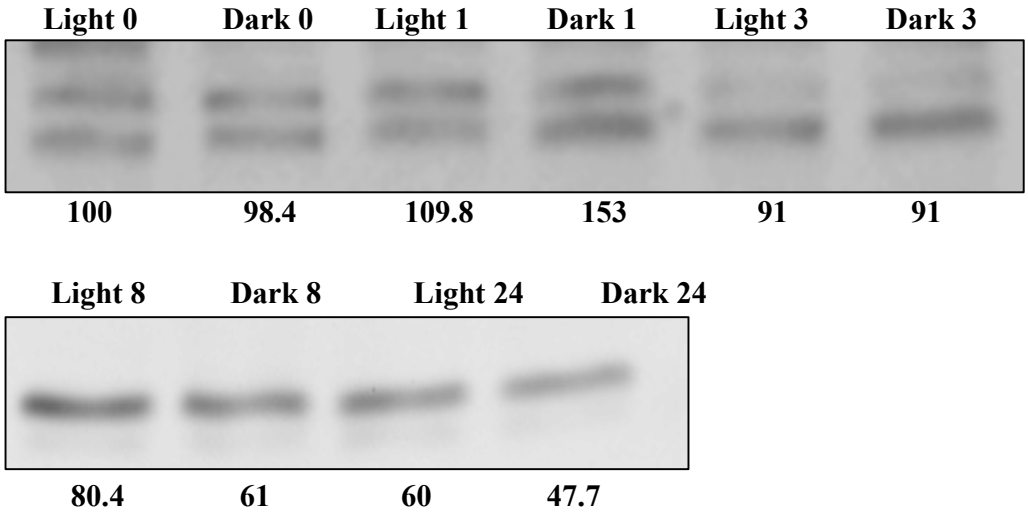

Figure 88: Effect of darkness on GSI concentration from *Synechococcus* WH7803. Cultures were subjected to darkness and aliquots were taken at indicated times. Western blotting was performed as described in Materials and Methods. Lanes are marked with the condition (light and darkness) followed by sampling time (in hours). Quantification of bands below the picture, 100% corresponds to the intensity for the control sample at time 0.

3. Characterization of glutamine synthetase on ΔSigF mutant

A SigF knockout mutant of *Synechococcus* WH7803 was used in this study. The mutant was constructed by a transposon mutagenesis approach in the group of Prof. Wolfgang Hess, University of Freiburg. We studied if there was any significant difference in the regulation of GS, linked to the absence of that gene.

3.1 Effect of nitrogen starvation

The GS activity was determined in the mutant during 24 hours of nitrogen starvation (figure 89). The response was the same as in the wild type, being higher under nitrogen starvation ($p = 0.0007$).

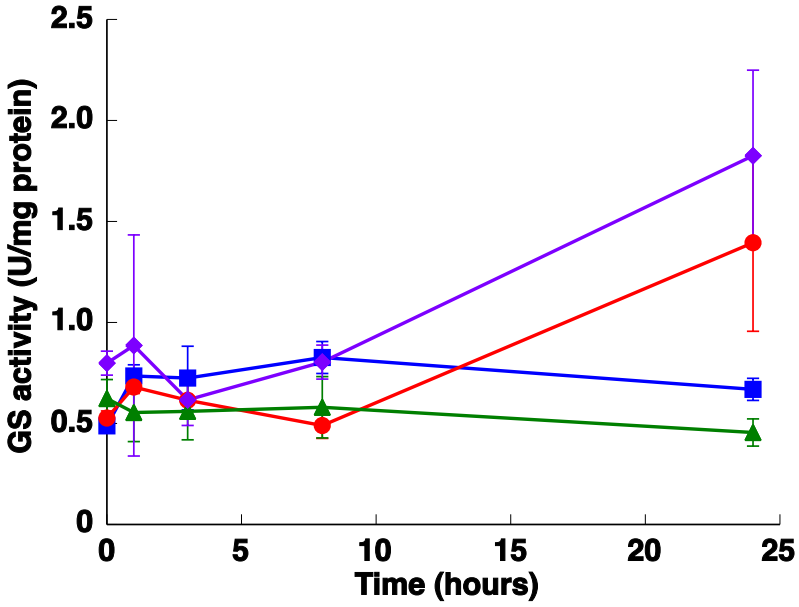

Figure 89: Effect of nitrogen starvation on GS activity from *Synechococcus* WH7803 and ΔSigF. The graph represents four independent biological replicates. Errors bars correspond to standard deviation. ■ *Synechococcus* WH7803 with ammonium as nitrogen source, ● *Synechococcus* WH7803 under nitrogen starvation, ▲ ΔSigF mutant with ammonium as nitrogen sources and ◆ ΔSigF mutant under nitrogen starvation.

The concentration of the GS was also studied under nitrogen starvation in the mutant (figure 90). The highest concentration was found after 3 and 8 hours of nitrogen absence.

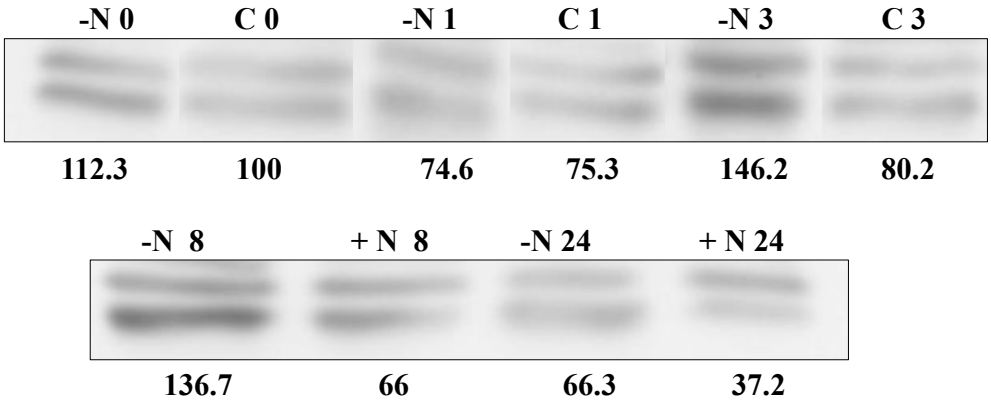

Figure 90: Effect of nitrogen starvation on GSI concentration from *Synechococcus* WH7803 ΔSigF. Cultures were subjected to nitrogen starvation and aliquots were taken at indicated times. Western blotting was performed as described in Materials and Methods. Lanes are marked with C (control) and -N (nitrogen starvation), followed by sampling time (in hours). Quantification of bands below the picture, 100% correspond to the intensity for the control sample at time 0.

3.2. Effect of darkness

Darkness did not provoke any clear effect neither on GS activity (figure 91) nor on its concentration (figure 92) in *Synechococcus* WH7803 ΔSigF. On the other hand, figure 91 shows similar trends in the wild type and the mutant.

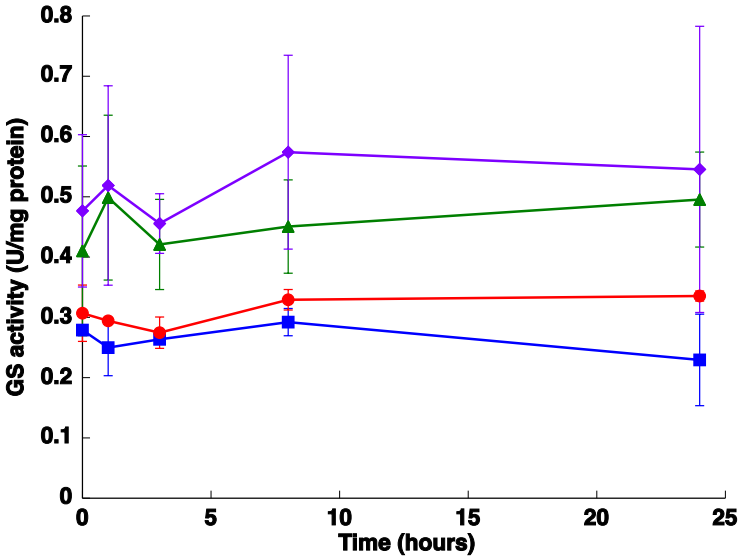

Figure 91: Effect of darkness on GS activity from *Synechococcus* WH7803 and ΔSigF. Cultures were subjected to darkness and aliquots were taken at the indicated times. The graph represents four independent biological replicates. Errors bars correspond to standard deviation. ■ *Synechococcus* WH7803 with 40 µE of blue light, ● *Synechococcus* WH7803 without light, ▲ ΔSigF mutant with 40 µE of blue light and ◆ ΔSigF mutant without light.

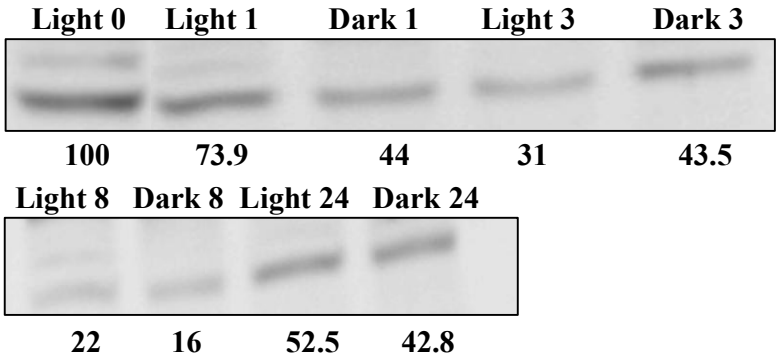

Figure 92: Effect of darkness on GSI concentration from *Syechococcus* ΔSigF. Cultures were subjected to darkness and aliquots were taken at the indicated times. Western blotting was performed as described in materials and methods. Lanes are marked with the conditions (light and darkness), followed by sampling time (in hours). Quantification of bands below the picture, 100% corresponds to the intensity for the control sample at time 0.

3.3 Effect of the absence of SigF factor on growth

Finally, in order to check if the lack of SigF had an effect on the growth of this cyanobacterium, the effects of nitrogen starvation and darkness were studied following the absorbance at 550 nm. The results are shown in figure 93. In the mutant and the wild type the growth was higher under ammonium than in the absence of nitrogen. In the case of darkness, the wild type and ΔSigF strains had the same behaviour, it was unaffected by the absence of light.

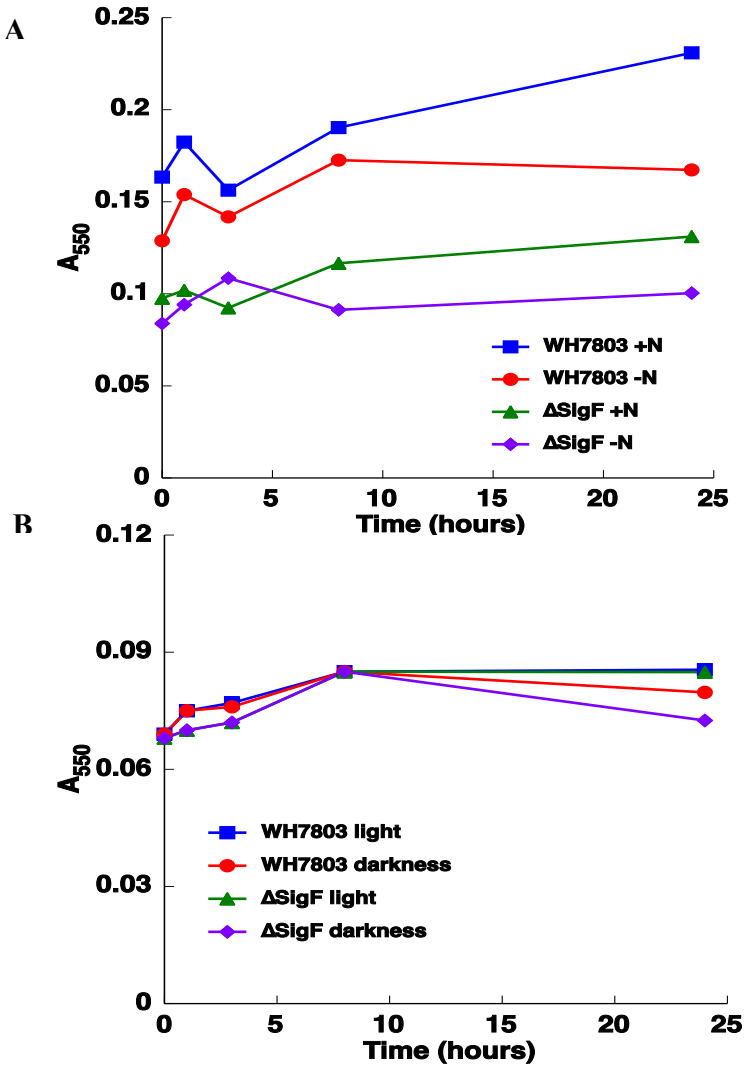

Figure 93: Effect of nitrogen starvation (A) and darkness (B) on the growth of *Synechococcus* WH7803 and ΔSigF mutant. Cultures were subjected to the different conditions and aliquots were taken at the indicated time. +N = 400 µM of ammonium and –N= nitrogen starvation.

Discussion

Synechococcus sp. WH7803 is a model cyanobacterium, representative of the *Synechococus* clades inhabiting mesotrophic areas of the ocean. Similar to the closely related *Prochlorococcus* it possesses a relatively streamlined genome (Dufresne *et al.*, 2008) and a small number of genes, but is genetically manipulable (Gierga *et al.*, 2012).

The use of different nitrogen sources by marine picocyanobacteria (*Synechococcus* and *Prochlorococcus*) is of particular interest because there are clear ecophysiological and genomic evidences for the critical role of their different nitrogen assimilatory capabilities in the ecology and evolution of these globally significant organisms (Moore *et al.*, 2002, López-Lozano *et al.*, 2002, Rocap *et al.*, 2003, García-Fernández *et al.*, 2004, García-Fernández & Diez, 2004, Tolonen *et al.*, 2006, Scanlan *et al.*, 2009, Partensky & Garczarek, 2010, Berube *et al.*, 2014).

As in other cyanobacteria, in *Synechococcus* the GS-GOGAT pathway plays a crucial role in nitrogen assimilation, since most forms of nitrogen are converted into ammonium before being further metabolized (Flores & Herrero, 1994).

Nitrate is the most abundant nitrogen species in ocean environments (Moore *et al.*, 2002). Surprisingly most *Prochlorococcus* strains tested to date are incapable of nitrate utilization (Moore *et al.*, 2002, López-Lozano *et al.*, 2002, Palinska *et al.*, 2000, Tolonen *et al.*, 2006, Berube *et al.*, 2014), whereas most *Synechococcus* strains grow well on this compound. In particular, the genes encoding the nitrate permease and nitrate and nitrite reductase are found in the genome of *Synechococcus* WH7803 (Scanlan *et al.*, 2009, Dufresne *et al.*, 2008). This marine cyanobacterium lacks the urease, so it is unable to growth with urea as a nitrogen source (Collier *et al.*, 1999).

The study of the possible existence of another GS on *Synechococcus* WH7803 was carried out. All picocyanobacteria analysed carry *glnA* (encoding type I glutamine synthetase). However, additional genes encoding glutamine synthetases were found in different *Synechococcus* strains, WH7805 (2), CC9311 (2), RS9917 (2) and WH5701 (4) (Scanlan *et al.*, 2009). Two GSs have been described in

Synechococcus WH7803, one of them is the GSI encoded by *glnA* and the other GSIII encoded by *glnN,* which is found in freshwater cyanobacteria as well. However, there are no studies about the role of GSIII in marine *Synechococcus*. As it is shown in section 1, another possible GS was found in the databases and its characteristics are summarized in table 52. In fact, this possible third GS encoded by *glnAIII* has a similar molecular weight to GSI from *Synechococcus* WH7803 (52.5 and 47.6 kDa respectively) and possibly it was detected using the antibody anti-GSI from *Synechocystis* PCC 6803 since two close bands appeared in our western blotting. Besides, 20% of identity in the alignment between *glnAI* and *glnAIII* was shown (figure 78) suggesting that it was not a mistake in the annotation in databases. The genome of a purple photosynthetic bacterium, *Rhodopseudomonas palustris,* has four glutamine synthetases, one of them is codified by the gene named *glnAIII* (Larimer et al., 2004). As far as we know, the role of this enzyme in this organism has not been studied.

The first approach was to check if the enzyme codified by the gene *glnAIII* from *Synechococcus* WH7803 had GS activity. As it has been explained in results, the protein encoded by *glnAIII* lacked such enzymatic activity (personal communication). A similar situation has been described in vertebrates, they also have a GSI named lengsin which is a major protein in eye lens. It belongs to the GSI family but has no enzyme activity (Grassi *et al.*, 2006).

Here, we have reported results on GS regulation obtained in cultures of *Synechococcus* WH7803, in order to understand its physiological behaviour and how it is affected by nutrient and light limitation in the field.

In order to detect GS activity in *Synechococcus* samples, we utilized the frozen/thawing method to disrupt the cells described for *Prochlorococcus* (El Alaoui *et al.*, 2001, Gómez-Baena *et al.*, 2001) however without success. The method of disruption of the cells was done using glass beads and introducing the adequate modifications. Although GS is a soluble protein, we could not detect it through the same method used in *Prochlorococcus*. That could be due to the cell wall of *Synechococcus* WH7803 being thicker than that of *Prochlorococcus*: it has been described that the cell wall of *Prochlorococcus* MIT9313 is approximately 4 nm

thick, which is considerably less than the approximately 16 nm observed for the peptidoglycan layer in the marine cyanobacterium *Synechococcus* WH8102 (Ting *et al.*, 2007).

In previous studies of GS, it has been observed that several conditions known to cause strong effects on its regulation in other cyanobacteria lacked such effect in *Prochlorococcus*, namely darkness and nitrogen starvation (El Alaoui *et al.*, 2001, El Alaoui *et al.*, 2003). Therefore, we decided to study the effect of the absence of nitrogen and light on GS activity and GSI concentration from *Synechococcus* WH7803 and to compare the results obtained with those described for *Prochlorococcus*. The effect of nitrogen starvation was studied and the concentration of GSI in cultures of *Synechococcus* WH7803 for 24 hours. The activity showed a significant increment after 24 hours (figure 83) in agreement with the increment on its concentration (figure 85). Similar results were described in *Synechococcus* WH7805, after 25 hours of absence of nitrogen the GS activity was higher than ammonium (Collier & Lovindeer, 2012). Besides, the results are in good agreement with the upregulation of the gene *glnA* in *Synechococcus* WH8103 after nitrogen deprivation (Bird & Wyman, 2003). These results suggest that GS from *Synechococcus* is upregulated by nitrogen starvation, this being the standard response in most photosynthetic organism including cyanobacteria (Mérida *et al.*, 1991).

There is an enormous variability in the *Prochlorococcus* group (Urbach & Chisholm, 1998, Rocap *et al.*, 1999, Rocap *et al.*, 2002, Partensky & Garczarek, 2010, Garczarek *et al.*, 2007), therefore it is complicated the comparison between one strain of *Synechococcus*, WH7803, and the whole group of its main competitor *Prochlrococcus.* Thus, the relation between them was made directly strain with strain. While *Prochlorococcus* PCC 9511 showed a slight decrease in GS activity under nitrogen deprivation (El Alaoui *et al.*, 2001), *Synechococcus* WH7803 (figure 83) and *Prochlorococcus* SS120 increased (El Alaoui *et al.*, 2003). On the other hand, the concentration of the GSI enzyme from *Synechococcus* (figure 85) increased ca. 2 fold compared with control after 24 hours of nitrogen starvation and there were minor changes in *Prochlorococcus* PCC 9511 and SS120 (table 2, (El Alaoui *et al.*, 2001)).

The GSs of most photosynthetic organisms, including cyanobacteria, are regulated by light (Flores & Herrero, 1994, Rowell *et al.*, 1979, Marqués *et al.*, 1992). Hence, the effect of darkness was investigated. The growth of *Synechococcus* WH7803 under darkness was slightly decreased and the GS activity remained almost unchanged even after 24 h of darkness (figure 87). This is an unusual response, as darkness promotes the down regulation of the GS in most other studied cyanobacteria (Flores & Herrero, 1994, Marqués *et al.*, 1992, Rowell *et al.*, 1979). This uncommon response was also described for *Prochlorococcus* PCC 9511 (El Alaoui *et al.*, 2001). The concentration of the enzyme in *Synechococcus* WH7803 did not show a marked change after darkness, although in *Prochlorococcus* SS120 a decrease of 20% of the GS concentration in crude extracts was found after 24 hour without light (El Alaoui *et al.*, 2001).

The small change induced by darkness in GS activity from *Synechococcus* *Prochlorococcus* represents another main difference in the regulation of this enzyme compared to its regulation in most photosynthetic organisms, the usual situation being that darkness promotes a marked decrease in GS activity (García-Fernández *et al.*, 1995, Marqués *et al.*, 1992, Rowell *et al.*, 1979, Taylor & Stewart, 1980, Tischner & Hüttermann, 1980). Thus, different strategies in *Prochlorococcus* and *Synechococcus* could be the explanation of that uncommon response. For instance, *Prochlorococcus* can grow at a depth of 200 m, receiving less than 0.1% of the surface irradiance. The extremely low irradiance reaching this habitat has induced low-light-adapted ecotypes to develop a variety of adaptation mechanisms, including a high chlorophyll b/chlorophyll a ratio, large amounts of very efficient antenna proteins, and the multiplication of the *pcb* genes encoding such antennae (Garczarek *et al.*, 2001, Garczarek *et al.*, 2000, Vanderstaay *et al.*, 1998, Garczarek *et al.*, 1998, Partensky *et al.*, 1993). In the case of marine *Synechococcus*, they developed an amazing variety of pigmentations allowing the capacity to cope with the wide range in light quality naturally occurring in subsurface waters over horizontal gradients (Six *et al.*, 2007, Waterbury *et al.*, 1986, Pittera *et al.*, 2014).

The phylogeny analysis of *glnA* from different marine and freshwater cyanobacteria (El Alaoui *et al.*, 2003) showed that marine *Synechococcus* and *Prochlorococcus* sequences are grouped together, separated from freshwater model

strains, in agreement with other studies based on 16 S RNA sequences. Combining these data with the results discussed above it can be suggested that the structure of glutamine synthetase in the marine picocyanobacterial clade has not been significantly modified during the evolution, in contrast with the possible modulation of its regulatory properties. These differences found respect to the key enzyme, GS, are probably due to the adaptation at different parts of the column water of the different strains of *Prochlorococus* and *Synechococcus*, possibly inducing changes in its regulation.

A main characteristic of *Prochlorococcus* is its success in very oligotrophic regions of the oceans, where it usually coexists with *Synechococcus*, so they adapt their regulatory mechanisms accordingly. One possible adaptation is the capacity to uptake different sources of nitrogen. That is an important factor being nitrogen a limiting element on these parts of the ocean. It has been described that most *Prochlorococcus* strains isolated to date are not able to uptake nitrate or utilize (López-Lozano *et al.*, 2002, Moore *et al.*, 2002), although it is very interesting to point out that the genome of the *Prochlorococcus* MIT9313 contains a gene with significant homology with cyanobacterial *nirA*, encoding the nitrite reductase, while the genes for nitrate uptake and reduction are missing (Moore *et al.*, 2002). Furthermore, it has been reported that MIT9313 is able to grow on nitrite and several *Prochlorococcus* strains have been recently shown grown on nitrate (Rocap *et al.*, 2001, Moore *et al.*, 2002, Berube *et al.*, 2014). This fact represents a key difference with most known marine *Synechococcus* strains and could be due to evolutionary pressures to remove genes non-essential for proliferation in oligotrophic environments, where usually *Prochlorococcus* outcompetes *Synechoccoccus*. In general, *Synechococcus* is more numerous in less oligotrophic waters and have a broader ecological range that extends where the nitrate is available (Partensky *et al.*, 1999). With that background, the GS activity was determined after different times growing on different micromolar nitrogen sources and without nitrogen (it is important to notice that the media used in *Synechococcus* cultures were artificial, so there were no nitrogen traces from the natural sea water, in contrast with the media used in *Prochlorococcus* cultures based on seawater). After 24 hours, the higher GS activity was found in the absence of nitrogen; however, the highest GS activity was found after 120 h growing with nitrate as nitrogen source contrasts to GS from

Prochlorococcus (El Alaoui *et al.*, 2003, El Alaoui *et al.*, 2001). Finally, after 384 h growing on different nitrogen sources, the GS activities were similar under nitrogen starvation or with nitrate (figure 86). After that period of time, it could be that the nitrate from the medium was completely consumed and the situation was similar to nitrogen deprivation.

Sigma factors are a family of proteins that associate with the prokaryotic DNA-dependent RNA polymerase in a reversible way to direct transcription initiation by recognizing specific promoter sequences (Inoue-Sakamoto *et al.*, 2007, Gruber & Bryant, 1998). It has been described that there are three different groups of sigma factors 70 in cyanobacteria but scarce data exists related with group 3. It seems that this group could be involved in different functions including heat shock, sporulation, extracytoplasmic function and flagellar on WH7803 (Inoue-Sakamoto *et al.*, 2007). *Synechococcus* WH7803 ΔSigF, a mutant constructed by transposon mutagenesis was used to analyze the effect of the absence of that factor on nitrogen metabolism. For that purpose, some conditions were studied, such as the effect of the absence of nitrogen and light on the enzyme GS. Nitrogen starvation (figure 89) and darkness (figure 91) promoted the same response in the mutant and wild type cultures. Surprisingly, the concentration of GSI was higher under 3 and 8 hours of nitrogen starvation in the mutant (figure 90), in contrast of the highest concentration of GSI found after 24 hours in wild type cultures.

Our results suggest that the SigF factor is not involved in the regulation of glutamine synthetase, thus indicating this factor does not seem to participate in the regulation of nitrogen metabolism in *Synechococcus* sp. WH7803.

The SigF factor had no effect on the growth of *Synechococcus* WH7803 at 24 ºC under our experimental conditions (figure 93). The results are in good agreement with the results shown by Kaori Inoue-Sakamoto and co-workers, who demonstrated that the growth rates at 22 ºC and 38 ºC were identical when comparing a SigF mutant and the wild type strain of *Synechococcus* sp. PCC 7002 (Inoue-Sakamoto *et al.*, 2007). However, they demonstrated that the absence of this factor promoted a slow growth at 15 ºC, suggesting that group 3 of sigma factors are

required for growth at low temperatures. It could be interesting to determine the growth of *Synechococcus* WH7803 and its mutant, ΔSigF, at low temperatures in order to test that hypothesis.

CHAPTER 3

Effect of low nitrogen availability on the nitrogen metabolism in *Synechococcus* WH7803

Introduction

The versatility of marine *Synechococcus* spp. has been related to its ability to grow over a wide range of light intensities and spectral quality (Kana & Glibert, 1987) and to utilize a wide variety of nitrogen sources. Different isolates of marine *Synechococcus* spp. have been reported to utilize ammonium, nitrate, nitrite, urea, and amino acids as the sole nitrogen source while employing systems for active uptake of these compounds (Glibert *et al.*, 1986, Lindell *et al.*, 1998, Collier *et al.*, 1999).

It has been described that in stratified Sargasso seawater nanomolar changes in nitrate concentrations occurred. This change was stoichiometrically consistent with the subsequent cellular production of a cyanobacterial (marine *Synechococcus* spp.) bloom (Glover *et al.*, 1988).

The question to answer could be how are *Synechoccocus* spp. able to successfully coexist with *Prochlorococcus* spp. even though they are apparently inferior in their capacity to take low concentrations of ammonium nitrogen? (Wyman & Bird, 2007) One possible explanation is that *Synechococcus* may be more efficient at the utilization of low concentration of alternative oxidized forms of nitrogen that generally are unavailable to *Prochloroccocus*.

With that background, the objective of this chapter was to analyze the effect of very low concentrations of different nitrogen sources on key enzymes and key genes related to nitrogen metabolism on *Synechococcus* WH7803. The results were interesting and showed the possible existence of a new detection system of the level of nitrogen. This new hypothesis needs to be further studied in the future.

1. Effect of nanomolar nitrogen concentration on the expression of genes related with nitrogen metabolism

In this study, the genes that have been studied were: *glnAI* (encoding GSI), *glnAIII* (encoding a possible GS), *glnN* (encoding GSIII), *narB* (encoding nitrate reductase), *nirA* (encoding nitrite reductase) and *nrtP* (encoding the transporter for NO_2^-/ NO_3^-). The scheme 94 shows the position in the nitrogen metabolism of each of the enzymes and transporters encoded by the genes studied.

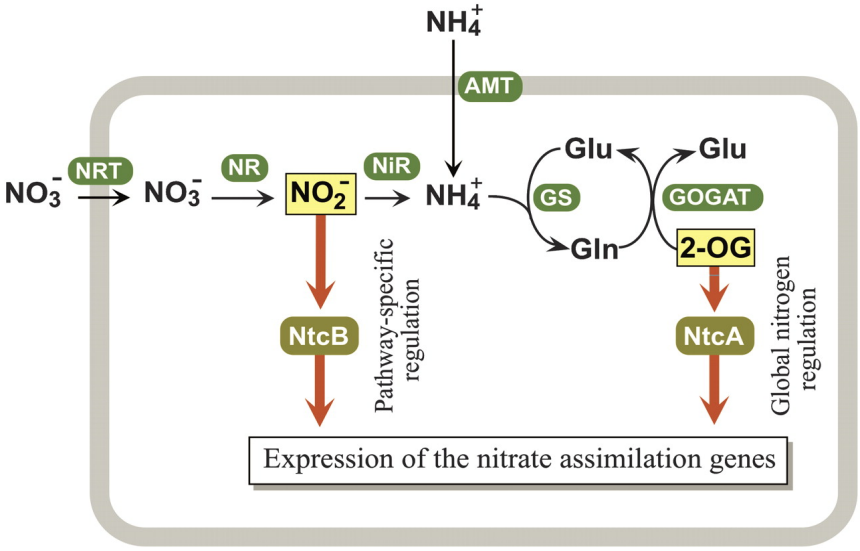

Figure 94: Scheme of the nitrogen assimilation pathway and regulation in cyanobacteria. AMT: ammonium transporter; NRT = transporter for nitrate; NR = nitrate reductase and NiR= nitrite reductase; GS = glutamine synthetase; GOGAT = glutamate synthase; 2-OG = 2-oxoglutarate; Glu = glutamate and Gln = glutamine. Taken from Ohashi Y *et al*. (Ohashi *et al.*, 2011).

The genes encoding nitrate reductase and nitrite reductase are clustered on the chromosome but they are organized in separate transcriptional units; *nrtP* is located upstream of *narB*. Interestingly, *glnAI* and *glnN* are located next to each other but orientated head to head. And finally, the gene *glnAIII* is close to the gene that encodes a nitrate/nitrite bispecific permease but the orientation is opposite (figure 95).

In the present work, the effect of low concentration of nitrate and nitrite on the expression of genes related with nitrate assimilation by qRT-PCR in *Synechococcus* WH7803 was studied.

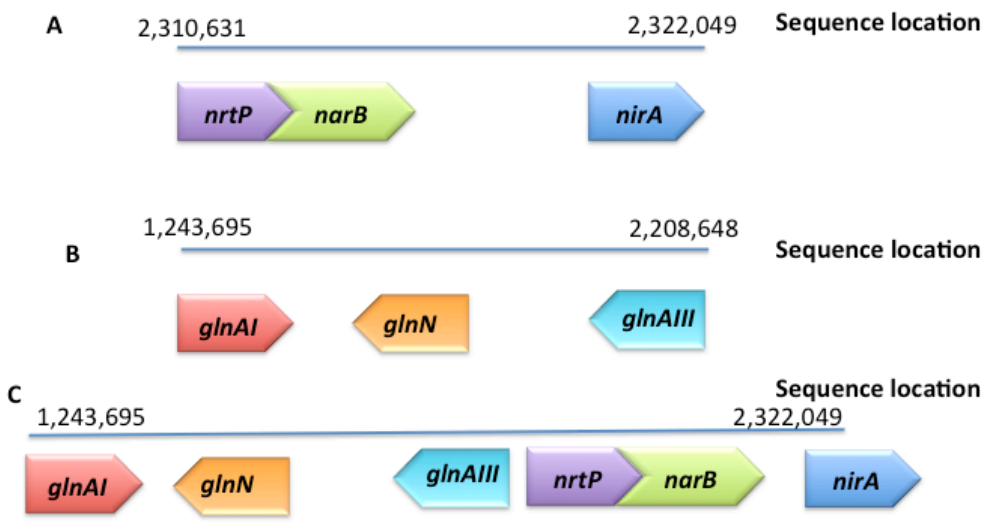

Figure 95: Organization of the nitrate and ammonium assimilation genes in the genome of *Synechococcus* WH7803. A. Organization for nitrate assimilation genes. B. Organization for GSs genes. C. Organization of all the genes studied. The information was obtained from NCBI gene webpage. Numbers on the top of each map denote the position on the genome. *glnAI* endcodes GSI; *glnN* encodes GSIII; *glnAIII* encodes putative GS; *nrtP* encodes transporter for NO_2/NO_3; *narB* encodes nitrate reductase and *nirA* encodes nitrite reductase.

The expression of *glnAI* was significantly higher than in the control with 800 nM of nitrate ($p = 0.0001$). Besides, the expression increased with the concentration within micromolar range, (figure 96). The expression of *glnAI* was higher with NO_3^- than under nitrogen starvation. Besides, the expression of *glnAI* when the cells were grown with 800 nM of NO_2^- is similar to that under nitrogen starvation (data not shown).

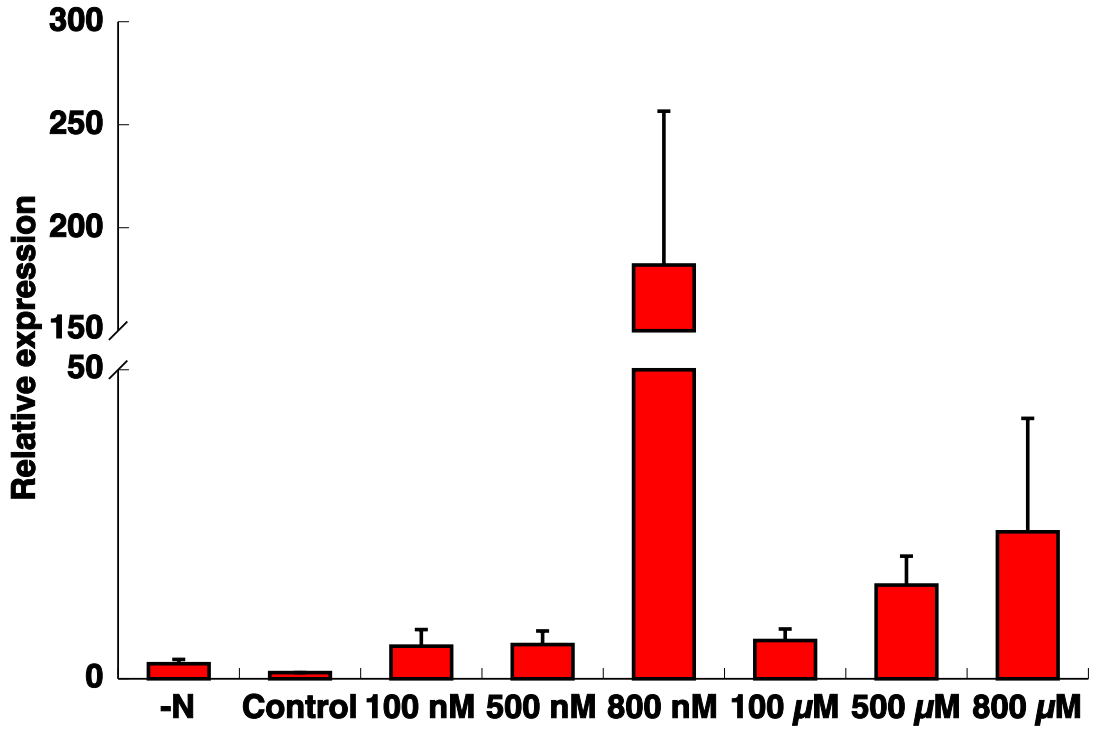

Figure 96: Effect of different concentration of nitrate on *glnAI* expression. Cells were grown with different concentration of nitrogen sources and they were collected after 24 hours. The graph represents the average of six independent biological replicates. Error bars correspond to standard deviation. –N: nitrogen starvation; control= 400 µM of ammonium and the rest of the samples contained nitrate at the concentration indicated in the figure.

The expression of the gene *glnAIII,* which encodes a putative GS, responded significantly to low concentration of nitrate as 800 nM ($p = 0.0014$) and to 100 µM ($p = 0.1042$), and with the rest of concentrations and nitrogen starvation the gene was repressed (figure 97).

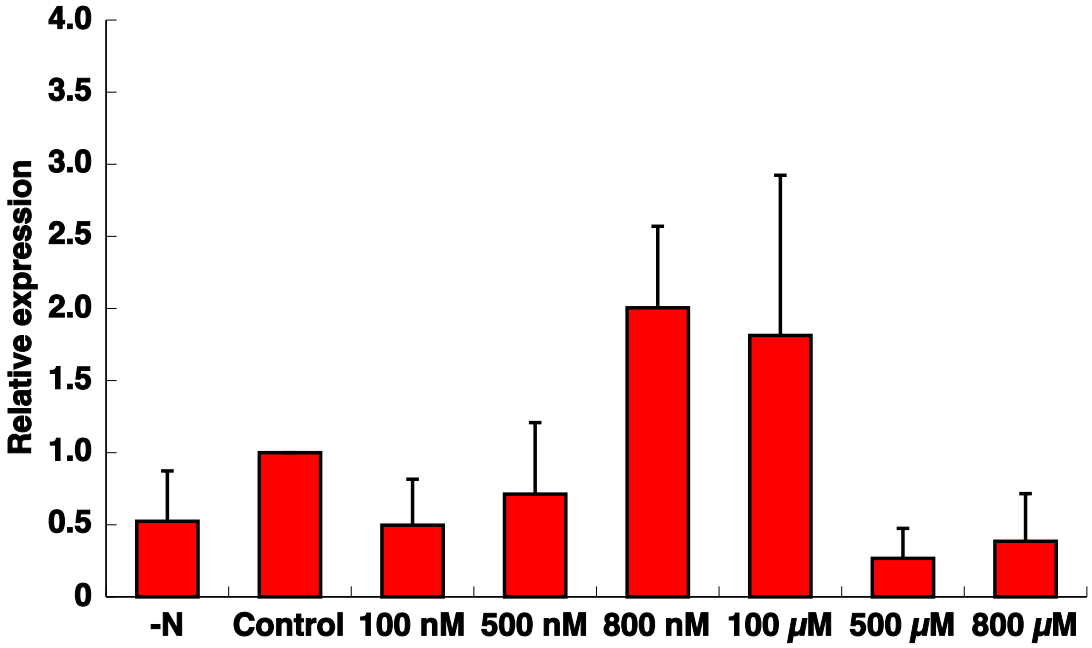

Figure 97: Effect of different concentration of nitrate on *glnAIII* expression. Cells were grown with different concentration of nitrogen sources and they were collected after 24 hours. The graph represents the average of six independent biological replicates. Error bars correspond to standard deviation. –N: nitrogen starvation; control= 400 µM of ammonium and the rest of the samples contained nitrate at the concentration indicated in the figure.

By contrast, when cell were grown in the presence of low concentration of nitrate and under nitrogen deprivation, the expression of *glnN* was not significativelly affected (figure 98).

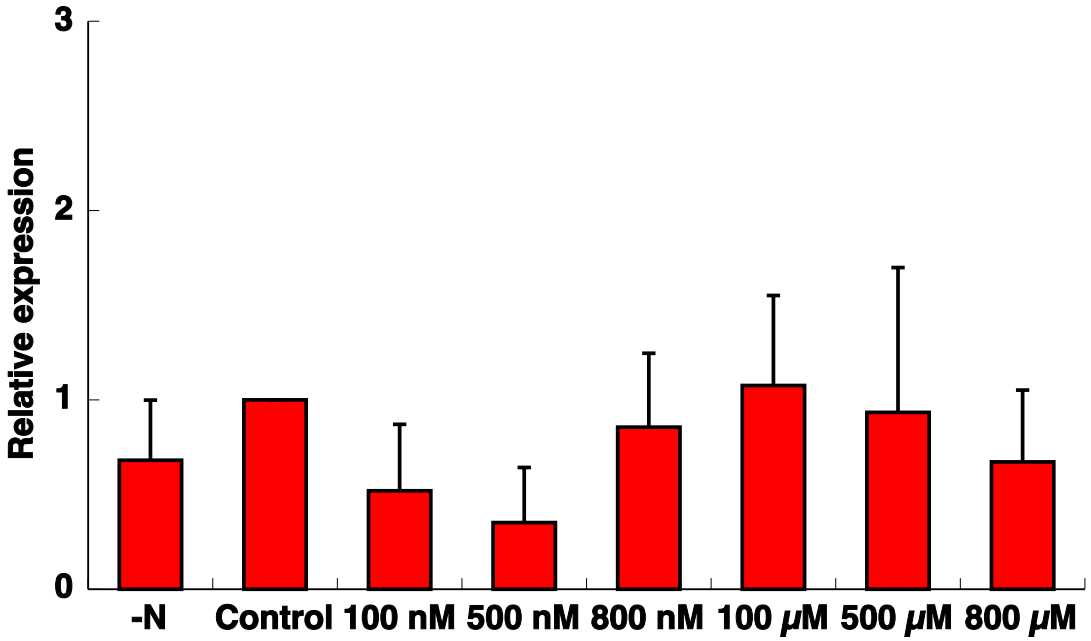

Figure 98: Effect of different concentration of nitrate on *glnN* expression. Cells were grown with different concentration of nitrogen sources and they were collected after 24 hours. The graph represents the average of six independent biological replicates. Error bars correspond to standard deviation –N: nitrogen starvation; control= 400 µM of ammonium and the rest of the samples contained nitrate at the concentration indicated in the figure.

On the contrary, the gene expression profile for *narB* showed that its expression increased with the concentration of nitrate. Under nitrogen deprivation the expression was higher than in the presence of ammonium (figure 99).

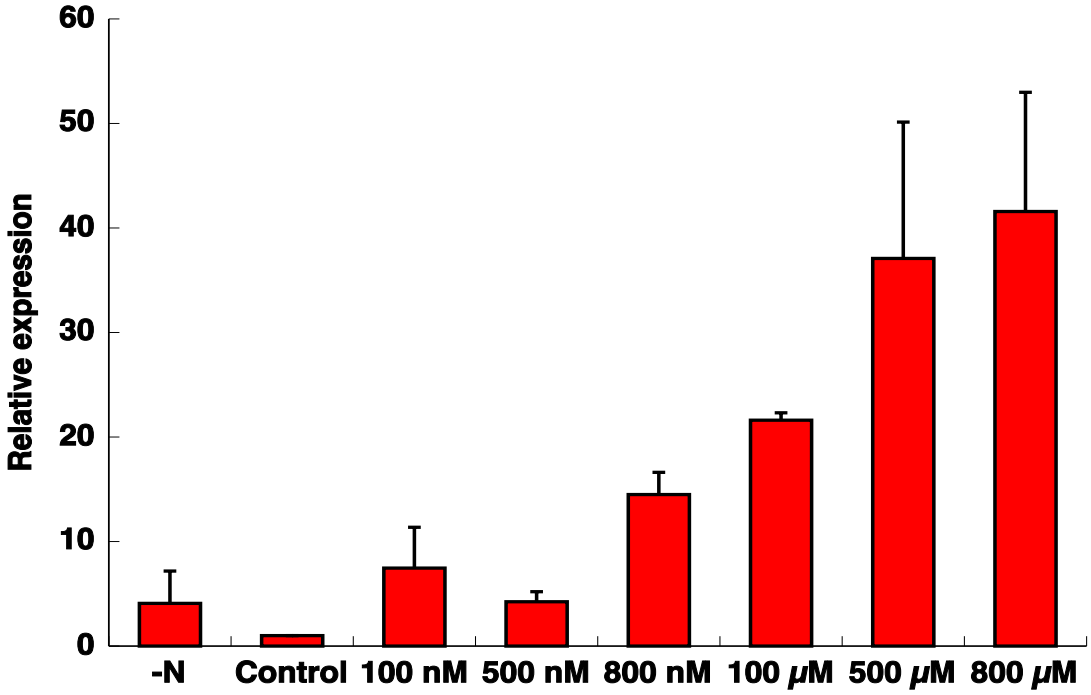

Figure 99: Effect of different concentration of nitrate on *narB* expression. Cells were grown with different concentration of nitrogen sources and they were collected after 24 hours. The graph represents the average of six independent biological replicates. Error bars correspond to standard deviation. –N: nitrogen starvation; control= 400 µM of ammonium and the rest of the samples contained nitrate at the concentration indicated in the figure.

Expression of *nirA* was higher when nitrate was added as a sole nitrogen source than under nitrogen starvation (figure 100). It increase with the concentration of nitrate.

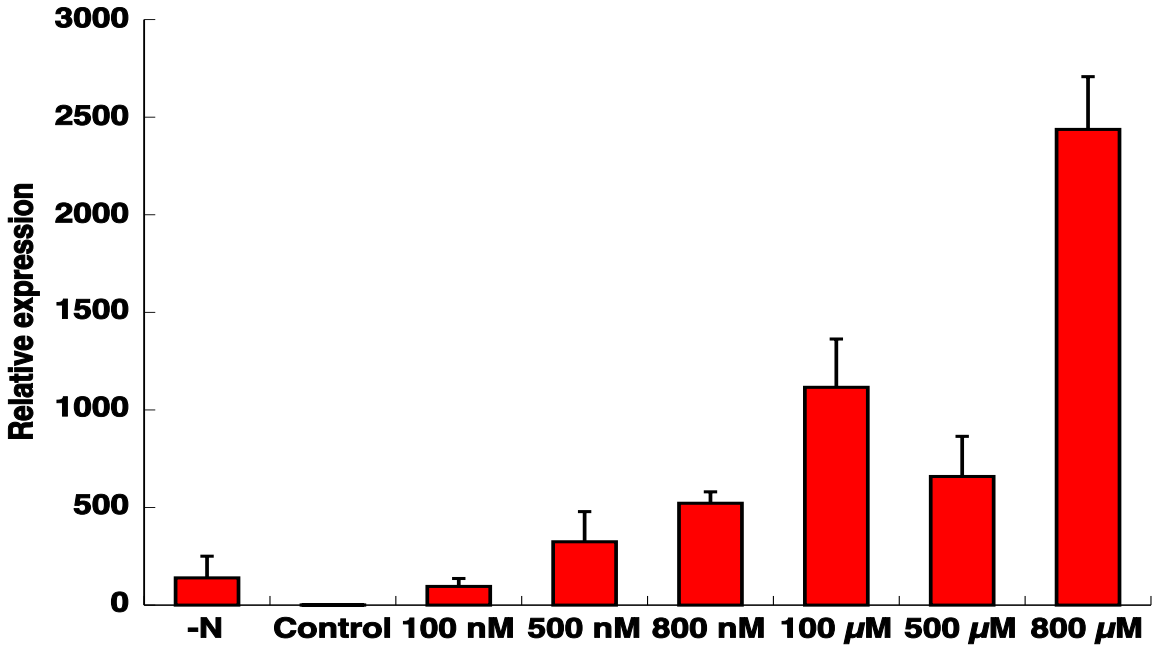

Figure 100: Effect of different concentration of nitrate on *nirA* expression. Cells were grown with different concentration of nitrogen sources and they were collected after 24 hours. The graph represents the average of six independent biological replicates. Error bars correspond to standard deviation. –N: nitrogen starvation; control= 400 µM of ammonium and the rest of the samples contained nitrate at the concentration indicated in the figure

Finally, the expression of *nrtP* was higher with different concentration of nitrate than under nitrogen starvation (figure 101). The maximum level of expression was reached with 800 µM of nitrate.

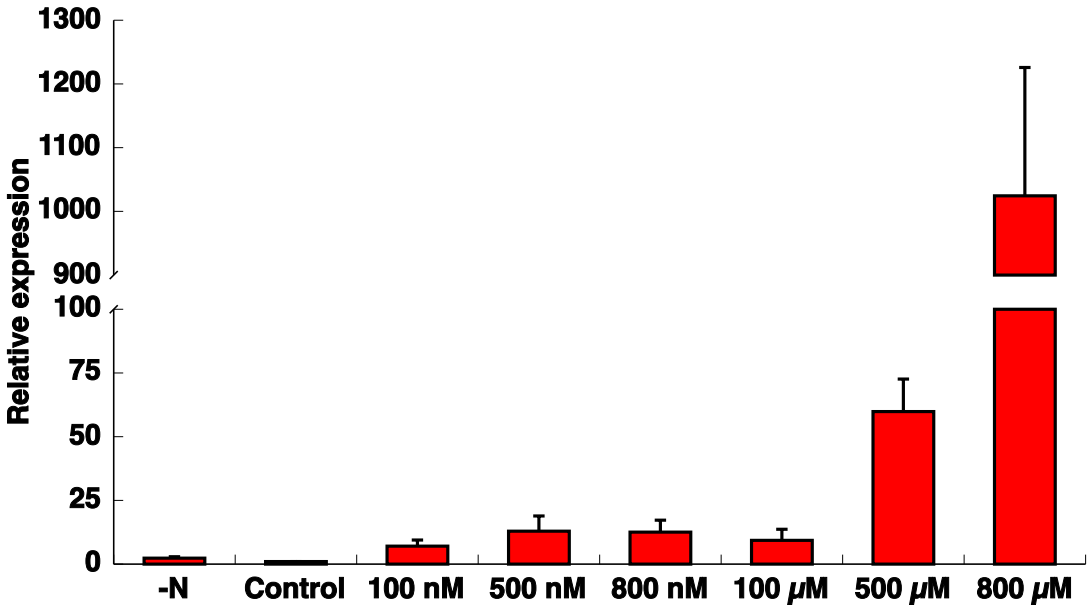

Figure 101: Effect of different concentration of nitrate on *nrtP* expression. Cells were grown with different concentration of nitrogen sources and they were collected after 24 hours. The graph represents the average of six independent biological replicates. Error bars correspond to standard deviation. –N: nitrogen starvation; control= 400 µM of ammonium and the rest of the samples contained nitrate at the concentration indicated in the figure.

2. Long time effect of micromolar nitrogen concentration on genes related with nitrogen metabolism

The genes were studied after growing for a long time with different nitrogen sources (figure 102 and 103). After 120 hours (figure 102), the expression of *nirA* was extremely high under 800 µM of nitrate. The expression of *glnAI* was much higher with nitrate than under nitrogen starvation.

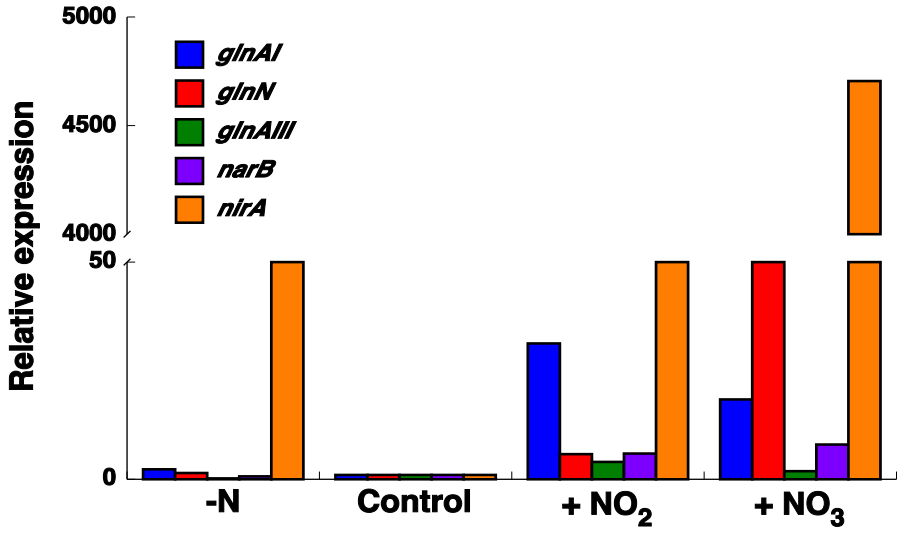

Figure 102: Long time effect of micromolar nitrogen sources on gene expression. Cells were grown with different concentration of nitrogen sources and they were collected after 120 hours. The graph represents the average of two independent biological replicates. –N= nitrogen starvation; control= 400 µM of ammonium; $+NO_2$ = 800 µM of nitrite and $+NO_3$ = 800 µM of nitrate.

After 384 hours under micromolar nitrogen sources, the highest expression was found in *narB* and *nirA* (figure 103). The maximum level of both genes was detected with 800 µM of nitrate.

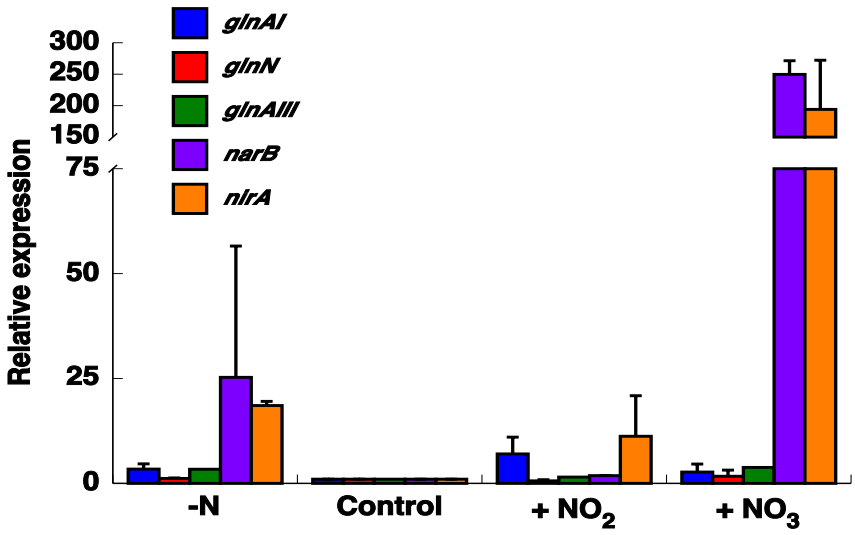

Figure 103: Long time effect of micromolar nitrogen sources on gene expression. Cells were grown with different concentration of nitrogen sources and they were collected after 384 hours. The graph is the average of two independent biological replicates. Error bars correspond to standard deviation. –N= nitrogen starvation; control= 400 µM of ammonium; $+NO_2$= 800 µM of nitrite and $+NO_3$= 800 µM of nitrate.

3. Long time effect of millimolar nitrogen concentration on genes related with nitrogen metabolism

We finally studied the long time effect of millimolar concentrations of nitrate on the expression of the genes studied in the sections above. The results show that the expression of *glnAI* decreased with the concentration of nitrate, although the expression of *glnN* was not significantly affected. Finally, the expression of *glnAIII* was induced when the cells were grown with millimolar concentration of nitrate as sole nitrogen source (figure 104).

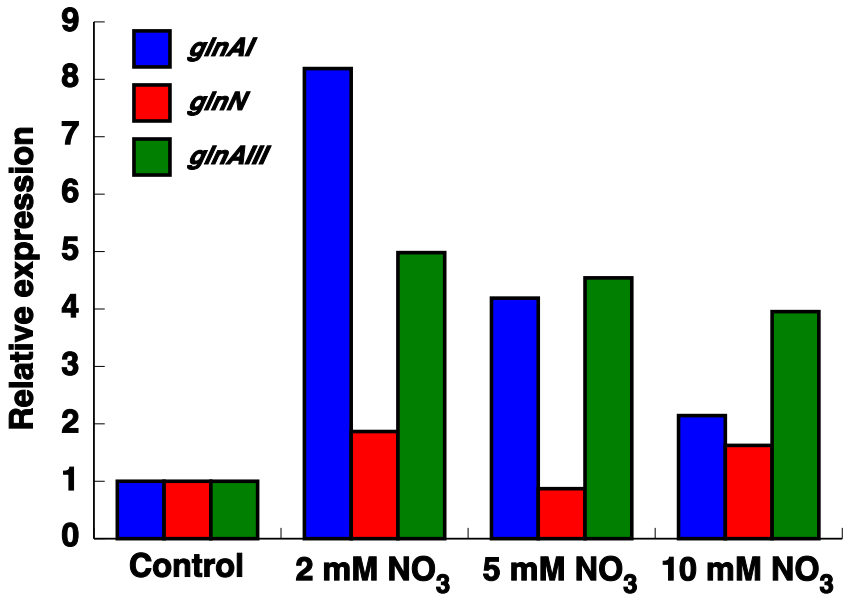

Figure 104: Long time effect of millimolar concentration of nitrate on gene expression. Cells were grown with different concentration of nitrogen sources and they were collected after 384 hours. The graph represents one independent biological replicates. Control= 400 µM of ammonium and the rest of samples had the concentration of NO_3^- indicated in the figure.

The expression of *narB* and *nirA* increased with the concentration of nitrate, being much higher in the case of *nirA* (figure 105).

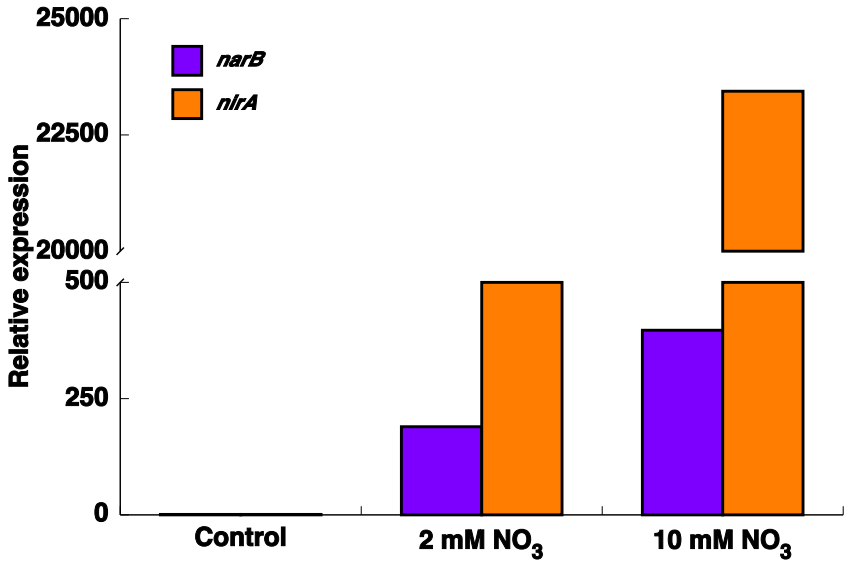

Figure 105: Long time effect of millimolar concentration of nitrate on gene expression. Cells were grown with different concentration of nitrogen sources and they were collected after 384 hours. The graph represents one independent biological replicates. Control= 400 µM of ammonium and the rest of samples had the concentration of NO_3^- indicated in the figure.

4. Effect of nitrogen availability on enzymes involved in nitrogen metabolism

The GS transferase activity was measured within a wide range of nitrogen sources concentrations (figure 106). As we can observe in the graph, the activity increased significantly under nitrogen starvation ($p = 0.0232$) and after the addition of 800 nM of NO_2 ($p = 0.0616$).

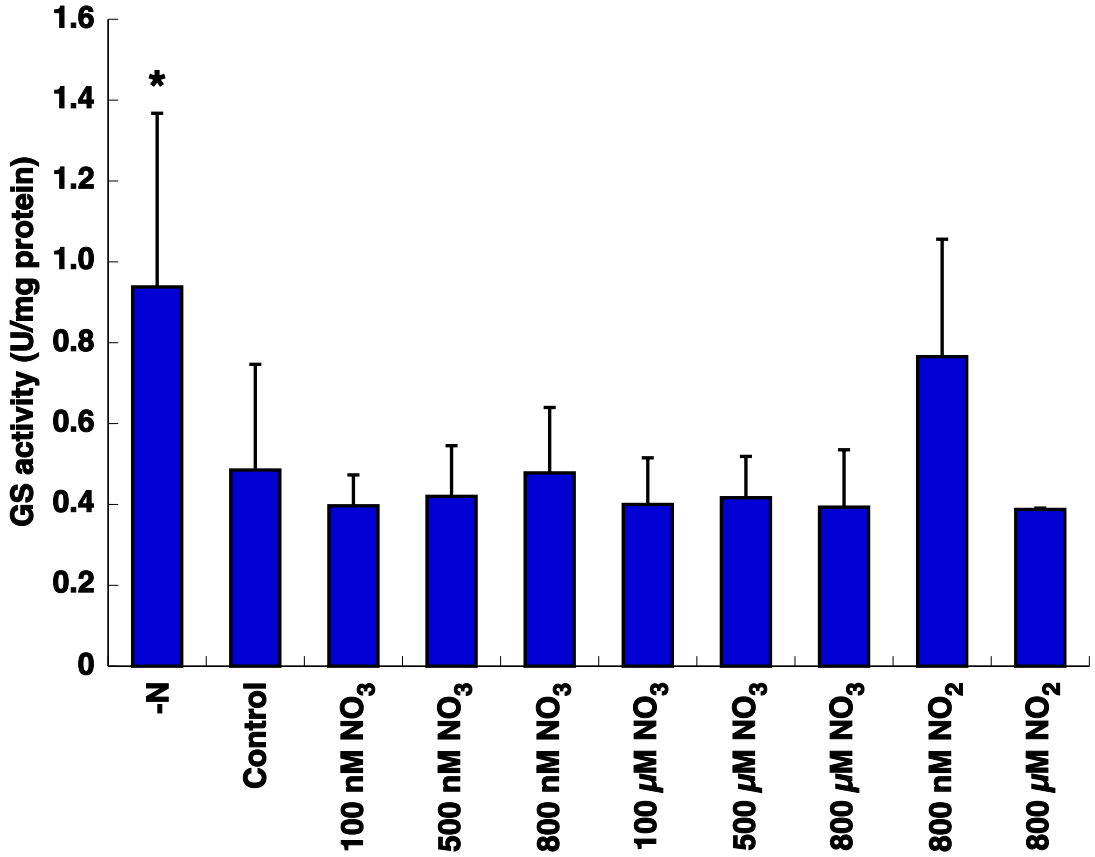

Figure 106: Effect of different nitrogen sources on GS activity from *Synechococcus* WH7803. Nitrogen sources at the indicated concentrations were added to the cultures and the cells were collected after 24 hours. The graph represents the average of eight independent biological replicates. Error bars correspond to standard deviation. –N = nitrogen starvation; control = 400 µM of ammonium and the rest of the samples contained nitrate or nitrite at the concentration indicated in the figure.

Besides, the concentration of GSI and GSIII was determined under those conditions (except under NO_2 as nitrogen source) (figure 107). GSI and GSIII were higher under nitrogen starvation than with ammonium. On the other side, GSI was higher under micromolar concentrations of nitrate in contrast to GSIII that was higher under nanomolar concentrations.

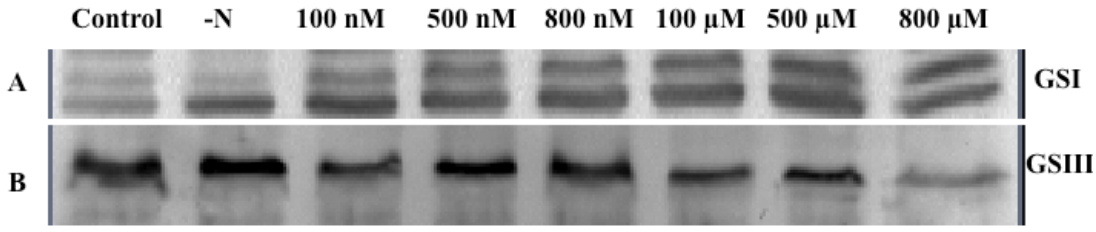

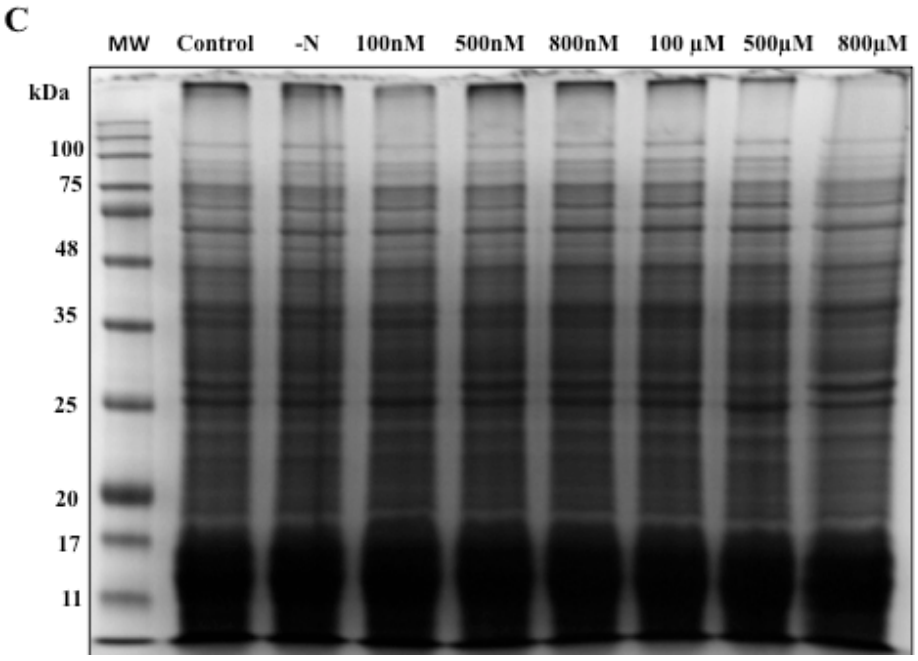

Figure 107: Effect of different concentration of nitrate on the concentration of GSI (A) and GSIII (B). The different concentrations of nitrate indicated in the figure were added to the cultures and the cells were collected after 24 hours of treatment. A. Western blotting of GSI. B. Western blotting of GSIII. C. SDS-PAGE (12%) Coomassie stained to check that the amount of protein was equal in all the lanes, 45 µg of proteins loaded. –N = nitrogen starvation; Control = 400 µM of ammonium as nitrogen source. The rest of the samples contained nitrate at the concentration indicated in the figure.

The GS activity was determined in the presence of nitrate, nitrite and ammonium at different times (figure 108). As we can observe, the GS activity was significantly higher after 24 hours of nitrogen starvation ($p = 0.016$), similar result was shown in figure 106. When nitrate, nitrite and ammonium were added the GS activity remained without variation.

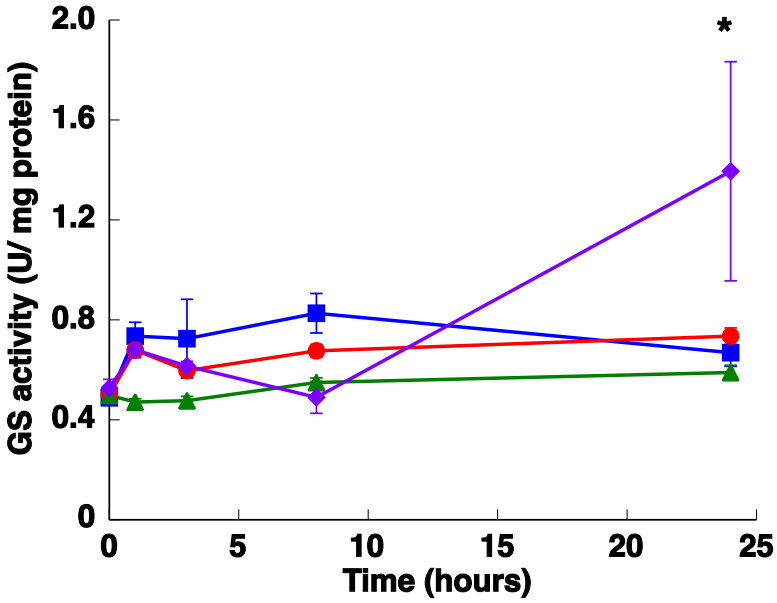

Figure 108: Effect of nanomolar concentration of nitrate and nitrite on GS activity from *Synechococcus* WH7803. The cultures were subjected to the conditions ◆ nitrogen starvation, ■ 400 µM of ammonium and 800 nM of nitrate ● and nitrite ▲. The cells were collected at the indicated time. The chart represents the average of three independent biological replicates.

The concentration of GSI is clearly higher after 24 hours of nitrogen starvation than in presence of nitrate (figure 109) in good agreement with the activity shown in figure 108.

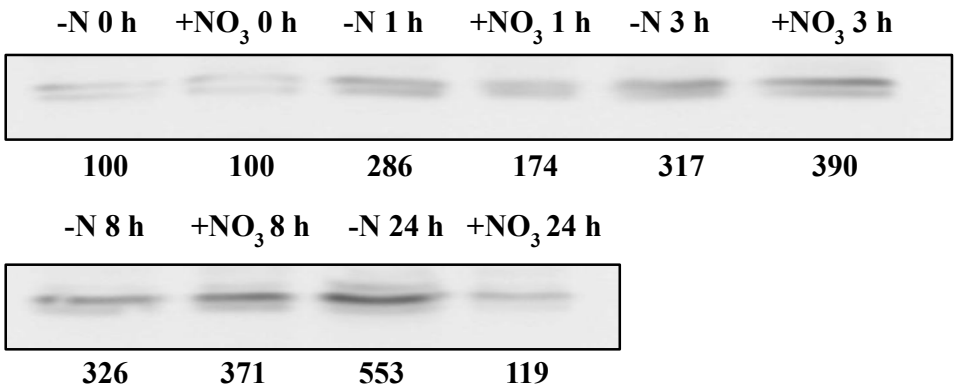

Figure 109: Effect of nitrogen starvation or 800 nM of nitrate on GSI from *Synechococcus* WH7803. The cells were subjected to nitrogen starvation (-N) and 800 nM of NO_3 (+NO_3) and they were collected at the indicated times. Western blotting of GSI. Lanes are marked with the conditions followed by sampling time (in hours). Quantification of bands below the picture, 100% correspond to the intensity at time 0 h.

Nitrate reductase (EC 1.7.7.2) plays a crucial role in the nitrogen metabolism, it is the first enzyme responsible for the assimilation of nitrate. Its activity was determined under different nitrogen sources (figure 110, 111). The cells were routinely grown on ammonium as nitrogen source. The activity was significantly high ($p = 0.0009$) after 8 hours of nitrogen starvation and also high ($p = 0.0127$) after 24 hours in 800 nM of nitrate.

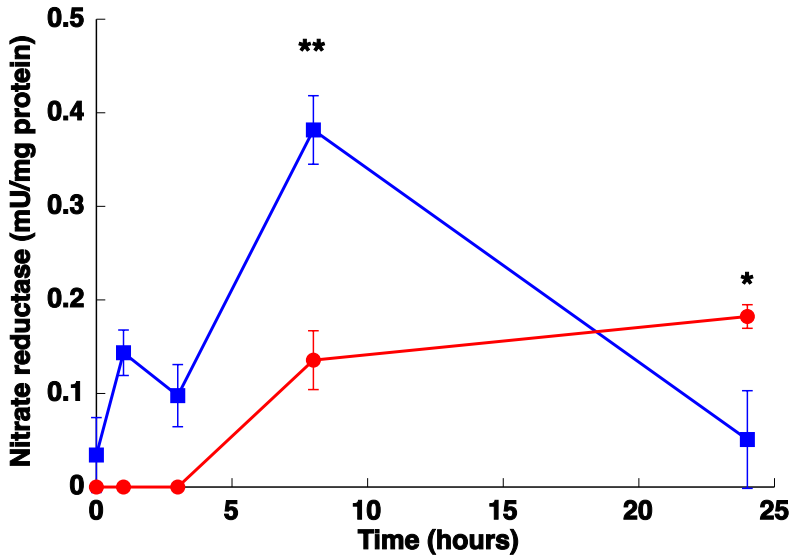

Figure 110: Effect of nitrate and nitrogen starvation on nitrate reductase activity from *Synechococcus* WH7803. The cultures were kept under nitrogen starvation (■) and 800 nM of nitrate (●) and the cells were collected at the indicated times. The chart represents the average of three independent biological samples. Error bars correspond to standard deviation.

The effect of different nitrogen sources on nitrate reductase activity was studied (figure 111). After 24 hours, the maximum activity was found with nitrate. It is important to highlight that when ammonium is present there was nitrate reductase activity.

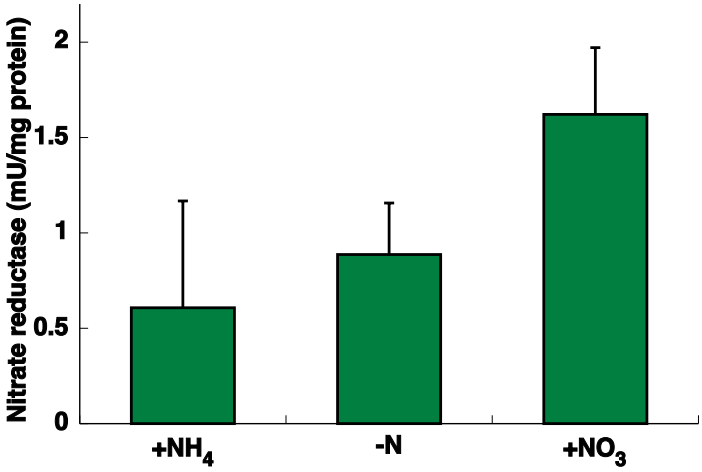

Figure 111: Effect of different nitrogen sources on nitrate reductase activity from *Synechococcus* WH7803. The cultures were grown under either 400 µM ammonium, nitrogen starvation or 800 nM nitrate and the cells were collected after 24 hours. The chart represents the average of four independent biological samples. Error bars correspond to standard deviation.

The nitrate reductase activity was studied with cultures grown with micromolar concentration of nitrate or nitrite (data no shown). After 24 and 120 hours the activity was higher with nitrate besides, the level of activity reached was higher than the activity found under nanomolar concentrations. These are preliminary results that need more biological replicates for confirmation.

It has been described that removal of nitrogen from the growth medium of cyanobacteria generally causes "chlorosis" (Allen & Smith, 1969, Allen & Hutchison, 1980, Wood & Haselkorn, 1980, Kana *et al.*, 1992, Sauer *et al.*, 2001). Hence the effect of nitrogen starvation and nanomolar concentrations of nitrate and nitrite on the content of phycoerythrin (PE) was determined (figure 112).

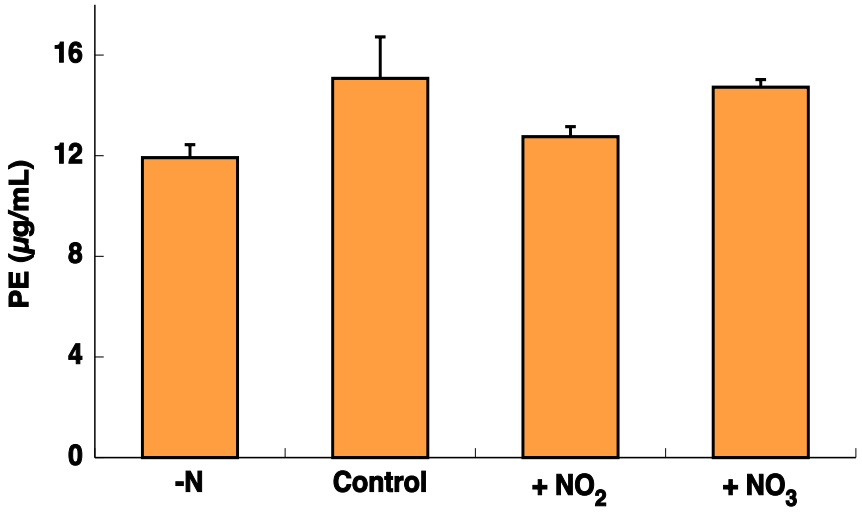

Figure 112: Effect of different nitrogen sources on the PE content in *Synechococcus* WH7803. The cells were grown under the different conditions and they were collected after 24 hours of treatment. The graph represents the average of three independent biological samples. Error bars correspond to standard deviation. –N: nitrogen starvation; control = 400 µM of ammonium; $+NO_2$ = 800 nM of nitrite and $+NO_3$ = 800 nM of nitrate.

The results showed that after 24 hours of nitrogen starvation there was a significant reduction close to 21% ($p = 0.0336$) in the content of PE and when the cells were grown with nitrite the reduction was around 15% ($p = 0.0759$).

5. Effect of nanomolar nitrogen concentration on GSI and GSIII from *Synechococcus* WH7803 ΔSigF

There were no significant differences in GS activity between the wild type and the mutant under different nitrogen sources (figure 113).

Some differences were found in GSI concentration (figure 114), between wild type and the mutant when the cultures were grown with ammonium, nitrate or under nitrogen starvation. The concentration of GSI was higher in wild type. Nonetheless, when cells were grown with 800 nM of nitrite, the concentration of GSI was higher in the mutant.

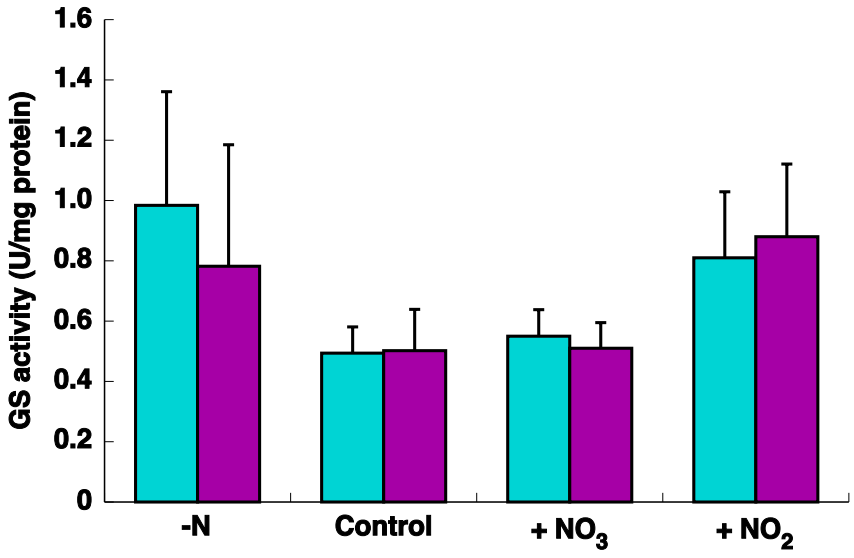

Figure 113: Effect of different nitrogen sources on GS from *Synechococcus* WH7803 (■) and ΔSigF (■). Cultures were subjected to the different conditions and cells collected 24 hours after the treatment. The graph represents the average of four independent biological replicates. Error bars correspond to standard deviation. –N = nitrogen starvation; Control = 400 µM of ammonium and 800 nM of nitrate ($+NO_3$) and nitrite ($+NO_2$).

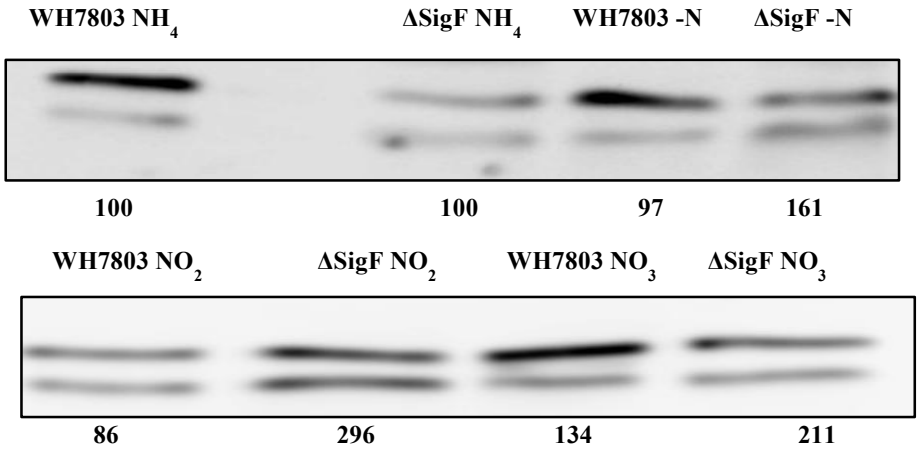

Figure 114: Effect of nitrogen sources on the concentration of GSI from *Synechococcus* WH7803 and ΔSigF. Cultures were subjected to the different conditions cells collected 24 hours after the treatment. NH_4 = 400 µM of ammonium; -N = nitrogen starvation; NO_2 = 800 nM of nitrite and NO_3 = 800 nM of nitrate. Quantification of bands below the picture, 100% correspond to the intensity of the cells grown with ammonium.

The GS activity in the ΔSigF mutant grown under different nitrogen sources responded as in the wild type (figure 115). In both cases, the highest GS activity was found after 24 hours of nitrogen starvation.

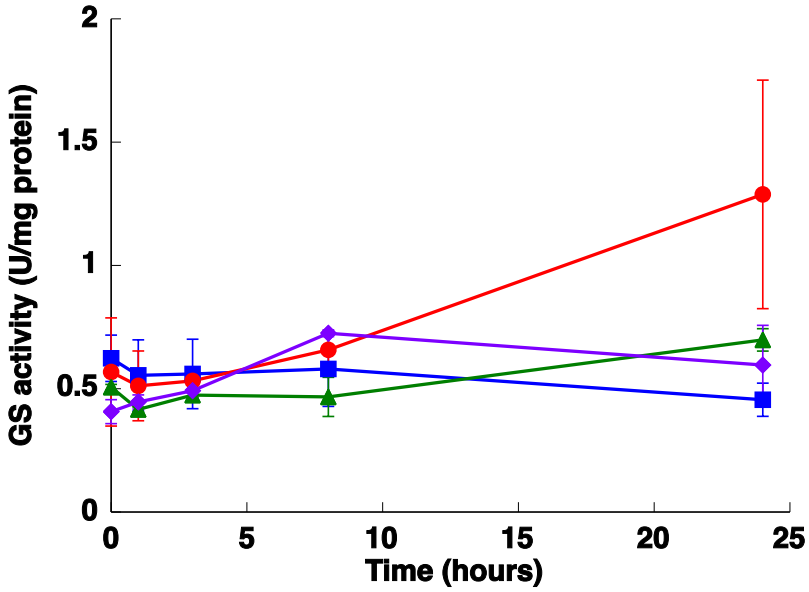

Figure 115: Effect of different concentration of nitrogen sources on GS activity from *Synechococcus* WH7803 ΔSigF. The cells were routinely grown on ammonium. The cultures were subjected to the conditions shown in the graph, ● nitrogen starvation, ■ 400 µM of ammonium and 800 nM of nitrate ◆ and nitrite ▲. The cells were collected at the indicated time. The chart represents the average of three independent biological replicates. Error bars correspond to standard deviation.

The concentration of GSI did not show significant differences under 800 nM of nitrate vs nitrogen starvation (figure 116).

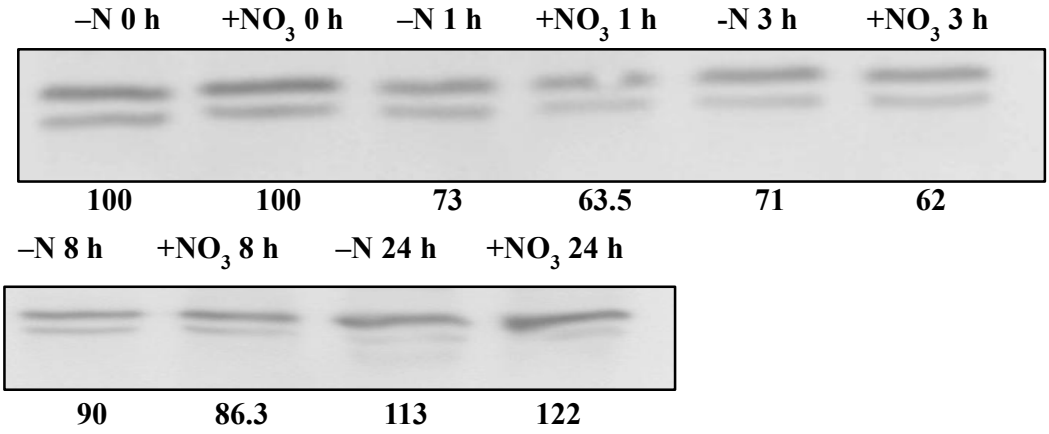

Figure 116: Effect of nitrogen starvation or nitrate on GSI from *Synechococcus* WH7803 ΔSigF. The cells were subjected to –N (nitrogen starvation) and +NO_3 (800 nM NO_3) and collected at the indicated times. Lanes are marked with the conditions followed by sampling time (in hours). Quantification of bands below the picture, 100 % correspond to the intensity at time 0 h.

Furthermore, GSIII concentration was determined under the same conditions as GSI (figure 117), and surprisingly GSIII was not detected in the mutant. This fact could be motivated by the absence of the factor SigF. Moreover, GSIII appeared under all the conditions in the wild type (figure 117).

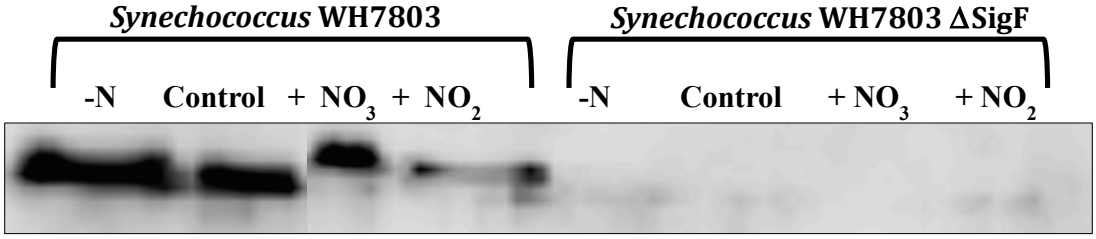

Figure 117: Effect of different nitrogen sources on the concentration of GSIII from *Synechococcus* WH7803 and ΔSigF. Cultures were subjected to the different conditions and cells collected 24 hours after the treatment. Control, 400 µM ammonium; -N, nitrogen starvation; $+NO_2$, 800 nM nitrite; $+NO_3$, 800 nM nitrate.

Discussion

Nitrogen metabolism in the marine cyanobacterium *Synechococcus* has been investigated to a far less extent than in freshwater cyanobacteria, and while there are similarities to some strains, there are also some intriguing differences (Wyman & Bird, 2007, Bird & Wyman, 2003, Lindell & Post, 2001, Lindell *et al.*, 1998). In this chapter, we focused on finding an explanation for the capacity to co-occur with *Prochlorococcus* in spite of the apparently lower capacity of marine *Synechococcus* to take ammonium as nitrogen source and even though they have a higher cell nitrogen quota (Wyman & Bird, 2007). For that reason, we paid special attention to other oxidized forms of nitrogen, for instance nitrate and nitrite, that most *Prochlorococcus* strains isolated to date are not able to assimilate. These two important marine picocyanobacteria cohabit at the upper surface layer of the water column where the concentrations of the oxidized forms of nitrogen are low (table 1, introduction). The study was performed with a range from nanomolar to micromolar concentration of nitrate and nitrite, in order to characterize the physiological and ecological response of *Synechococcus* WH7803.

In order to analyse if the expression of the gene *glnAIII* (putative GS) is related with the nitrogen status of the cell, the effect of different concentration and nitrogen sources on its expression was studied (figure 97, 102, 103 and 104). As we can observe

in the results, the expression was upregulated with millimolar concentration of nitrate. The pattern with low concentration of nitrate was somehow erratic and it was difficult to obtain a clear conclusion.

From the results obtained it is complicated to answer the question of why these three GS family genes survive against evolutive pressure. There are several hypotheses that will be interesting to contrast in the future. One of them is that this possible GS gained a function different from glutamine synthesis as in the case of lengsin, which is responsible for the lens homeostasis and transparency (Grassi *et al.*, 2006). Other possibility is that it has distinct physiological functions as GS, for instance, in *Synechocystis* PCC 6803 the enzyme GSIII, but not GSI, was involved in nitrogen starvation (Reyes & Florencio, 1994) and finally the last explanation could be the possibility of having different subcellular localization. The two last hypotheses have no sense if the putative GS has no GS activity.

The glutamine synthetase GSIII was not further studied in *Synechococcus* WH7803 (Scanlan *et al.*, 2009). Our findings show that the protein GSIII appeared under all the studied conditions (figure 107); under nitrogen starvation, with ammonium or different concentrations of nitrate and nitrite. Moreover, the expression of the gene *glnN* was also studied when the cells were grown with different nitrogen sources and the expression was not influenced. On the contrary, the level of *glnN* mRNA was found strongly increased in nitrogen free medium in *Synechocystis* PCC6803 (Reyes & Florencio, 1994). Thus, the result suggests that the role of GSIII in marine *Synechococcus* is different.

The possible influence of the absence of the sigma factor (SigF) on the concentration of the protein GSIII was also studied (figure 117). As we can observe, the GSIII was not detected in cells of the mutant grown on different nitrogen sources. This suggests that SigF could be involved on the transcriptional control of the GSIII mRNA.

The most common arrangement of the nitrate assimilation genes is the operon *nirA-nrtABCD-narB* (termed the *nirA* operon) and its variants found in many fresh-water cyanobacteria. A variation of the *nirA* operon, including *nrtP* in place of *nrtABCD* as the NRT-encoding gene, is found in some marine cyanobacteria. In most marine cyanobacteria strains, *nirA* forms a putative *nirA-focA* operon including *Prochlorococcus* strains with the capacity to take nitrite (Ohashi *et al.*, 2011). When the

organization of the nitrate and ammonium assimilation genes in *Synechococcus* WH7803 was studied, a different arrangement was found. The position for *nirA* has been described invariably at the beginning of the operon, in our case it is at the end. In that case, the first gene of the operon was *nrtP* (figure 95). The transcription units for *glnN* and *glnAIII* were head to head configuration, implying coordinated expression between them.

The effect of nitrogen source and availability on the expression of the nitrate/nitrite assimilation machinery of marine *Synechococcus* spp. has not been investigated in as much detail as in freshwater cyanobacteria (Bird & Wyman, 2003, Wyman & Bird, 2007, Lindell & Post, 2001, Lindell *et al.*, 1998).

The two transcription factors involved in the regulation of nitrate assimilation, NtcA and NtcB, act not only as transcription activators but also as the sensors of 2-OG and nitrite, respectively (Aichi & Omata, 1997, Aichi *et al.*, 2001, Tanigawa *et al.*, 2002, Vazquez-Bermudez *et al.*, 2002). In accordance with its importance as the global nitrogen regulator, NtcA is found in all the cyanobacterial strains characterized to date, whereas NtcB is absent in the α-cyanobacteria, for instance in *Synechococcus* WH7803. The studied genes have a NtcA-dependent transcription, in spite of a canonical binding site differing from other *Synechococcus*, as WH8103 (Bird & Wyman, 2003).

It has been described that the nitrate assimilatory genes are regulated in detail in freshwater cyanobacteria. In the regulation participates the 2-OG, the major intracellular signal. When nitrogen is limiting growth, accumulation of 2-OG activates the transcription factor NtcA to induce transcription of the nitrate assimilation genes (Ohashi *et al.*, 2011, Herrero *et al.*, 2001, Flores & Herrero, 1994, Luque *et al.*, 1994).

The common response is that the gene *glnA* is up regulated when the cells were grown under nitrogen deprivation (Muro-Pastor *et al.*, 2005, Herrero *et al.*, 2001). Our results showed that the expression of *glnAI* is up regulated under nitrogen starvation but it is higher when the cells were grown in the presence of low concentration of nitrate, being extremely high under 800 nM of nitrate. In conclusion, our results suggest that NtcA may enhance the transcription under low concentrations of nitrogen oxidized forms. This implies the occurrence of an unknown mechanism to monitor very low concentrations of nitrate to trigger the expression of *glnAI* and other related genes.

The capacity to utilize both nitrate and nitrite is absolutely dependent upon activation by NtcA in this oceanic strain WH7803, since neither nitrogen source can support growth of an *ntcA* mutant, whereas growth on ammonium is unaffected (Post, 2005). Our results are consistent with this model: under nitrogen deprivation the transcription of *narB* and *nirA* has to increase, as shown in figure 99 and 100. The transcription of *narB* increased with the concentration of nitrate. A similar response was obtained with *nirA*.

The gene *nrtP* encodes a nitrate/nitrite permease in *Synechococcus* WH7803 (Sakamoto *et al.*, 1999). Its presence in marine cyanobacteria, rather than the ABC transporter usually found in freshwater cyanobacteria (Omata *et al.*, 1993), suggests that important differences in nutrient transporters may occur in marine and freshwater cyanobacteria (Sakamoto *et al.*, 1999). A similar situation has been observed with the glucose transporter identified in *Prochlorococcus* with features clearly different with respect to that identified in freshwater strains (Muñoz-Marín *et al.*, 2013). NtcA probably controls the transcription of the gene *nrtP* (Inoue-Sakamoto et al., 2007). In *Synechococcus* PCC 7002 there were *nrtP* transcripts detected in cells grown on nitrate but not on urea or ammonia (Sakamoto *et al.*, 1999). In our case, the transcription of the permease increased with the concentration of nitrate.

The results from this study indicated that the regulation of the nitrogen assimilation pathway occurs at transcriptional level. Our main interest was to study the effect of a range from nanomolar to micromolar concentration of nitrogen sources; therefore, the GS activity was further studied under such conditions (figure 106, 108). The activity of this enzyme did not show significant changes when the cells were grown with ammonium as nitrogen source or in 100 nM to 800 μM of nitrate or nitrite, although after 24 h of nitrogen starvation the GS activity increased significantly and in good agreement with the concentration of the enzymes GSI and GSIII.

The effect of nitrate as nitrogen source in the concentration of both GSI and III, were analysed with a broad range of nitrate concentration (figure 107). Different patterns can be observed from the results. It seems that the concentration of GSI was higher under micromolar concentration of nitrate, in contrast, the concentration of GSIII was higher under nanomolar of nitrate. Both of them were higher under nitrogen

starvation as occurs in the freshwater model cyanobacterium, *Synechocystis* PCC6803 (Reyes & Florencio, 1994).

In order to further study whether the absence of sigma factor F has some effect on the assimilation of nanomolar concentrations of oxidized forms of nitrogen, the GS activity and the concentration of GSI were determined in the ΔSigF cells. There was no difference between wild type and mutant cells suggesting that the absence of this sigma factor is not involved in the regulation of the glutamine synthetase when the cells were grown with nanomolar concentration of nitrate and nitrite.

The ferredoxin-nitrate reductase catalyzes the reduction of nitrate to nitrite, which is the first step in the assimilatory reduction of nitrate (Losada & Guerrero, 1979, Manzano *et al.*, 1976). This key enzyme in the nitrogen metabolism of *Synechococcus* WH7803 was further studied. Our results showed that there was nitrate reductase activity even when the cells were grown under nitrogen deprivation indicating that nitrate was not required as an obligate inducer. Although, when the cells grew with nitrate the activity was higher compared with nitrogen starvation after 24 hours, as it has been shown for *Anacystis nidulans* or *Nostoc* sp. strain 6719 (Herrero *et al.*, 1981). Ammonium represses the nitrate reductase in freshwater cyanobacteria (Losada & Guerrero, 1979, Syrett & Leftley, 1976, Herrero *et al.*, 1981). The ammonium does not exert its effect directly, but it has to be incorporated in carbonated skeletons through the GS-GOGAT pathway (Herrero *et al.*, 1981). In *Synechocystis* PCC 6803 it has been described that ammonium repressed *nirA* and *narB* expression (Alfonso *et al.*, 2001). Our findings showed a different response in *Synechococcus* WH7803, since activity of nitrate reductase was found even when the cells were growing on ammonium, in agreement with the results of Zehr and co-workers (Zehr *et al.*, 1989), where they strongly suggest that phytoplankton contain a constitutive nitrate reductase activity under ammonium that can be used to rapidly reduce nitrate and allow its utilization when is available.

The process known as chlorosis occurs when nitrogen is removed from the growth media of cyanobacteria and causes a drastic reduction in phycobiliproteins (Allen & Smith, 1969). This phenomenon is rapid with typically 80 to 95% of the phycobiliproteins degraded during the first 24 h of starvation, due to a proteinase that is activated in that stage (Allen & Hutchison, 1980, Wood & Haselkorn, 1980). Our

results showed that after 24 h of nitrogen starvation the reduction of the phycoerythrin content was about 21%, in good agreement with the results from Kana and coworkers that showed minor loss of PE, 25 %, after three days of nitrogen starvation in *Synechococcus* WH7803 (oligotrophic regions) compared with WH8018 (coastal) which had lost 85% of the pigments (Kana *et al.*, 1992), the most common response. That unusual response from *Synechococcus* WH7803 may reflect an adaptation to oligotrophic surface waters. Our results showed an unexpected loss of phycoerythrin about 15% when cells were grown under 800 nM of nitrite, a value close to the situation of nitrogen deprivation. Nonetheless, when *Synechococcus* WH7803 grew on low nitrate concentration (figure 112), we found a PE content similar to the control (ammonium), suggesting that the cells were not nitrogen stressed.

The results obtained with nanomolar concentrations of nitrite seem to be similar to nitrogen starvation. All determined parameters (GS activity, *glnAI* expression and PE content) were almost the same under either nitrogen deprivation or NO_2^- samples. Thus, the results suggest that the uptake of nanomolar nitrite is not as efficient as that of nitrate.

Primary production in the oceans is supported by two major forms of nitrogen: ammonium which is reduced and is provided by the recent decomposition of organic matter in the water column, and nitrate which is oxidized and diffuses into the euphotic zone from deep water. It is generally believed that ammonium is a major source of nitrogen for phytoplankton in oligotrophic oceans. However, some studies suggested that nitrate might be also important (Zehr *et al.*, 1989, Glover *et al.*, 1988). This importance is reflected by mixing events at the ocean water that promote changes in the concentration of nitrate. These mechanisms require that phytoplankton, which may have been growing primarily on ammonium, become rapidly capable of transporting, reducing and incorporating nitrate (Zehr *et al.*, 1989).

In conclusion, the results shown in this chapter suggest that the ability of *Synechococcus* WH7803 to coexist with *Prochlorococcus* at the surface layer of the column water could be partly due to the capacity to detect and uptake very low concentration of nitrate. This is in good agreement with the results of the *Synechococcus* bloom in the Sargasso Sea when nitrate is available at nanomolar concentrations (Glover *et al.*, 1988). To our knowledge similar results have not been

shown yet, and this study require other approaches in order to confirm the hypothesis and give a detailed scheme of the adaptation of marine *Synechococcus*. The uptake of very low concentrations of nutrients in the oceans might be more important than initially believed, as shown recently by the discovery of nanomolar concentrations of glucose in the Atlantic Ocean, by a glucose transporter with a Ks constant in the nanomolar range (Muñoz-Marín *et al.*, 2013). Thus, our interest to further study the transport of nitrate in *Synechococcus* WH7803.

The results obtained can be summarized in a model that includes changes at transcriptional, enzymatic and translation level that occur in cultures from *Synechococcus* WH7803 grown under three different conditions, nitrogen starvation, with nanomolar and micromolar of nitrate (figure 118).

In conclusion, the results reported in this chapter show that there is a differential regulation of the nitrate reductase respect to the freshwater cyanobacteria. The system that allow to *Synechococcus* detect the nanomolar concentration of nitrate is yet unknown. In future work we will deep into the mechanism. That could have a great physiological sense in the environment where *Synechococcus* thrives. The environment is scarce in nutrients, the contrary situation of the habitat where other freshwater cyanobacteria lives.

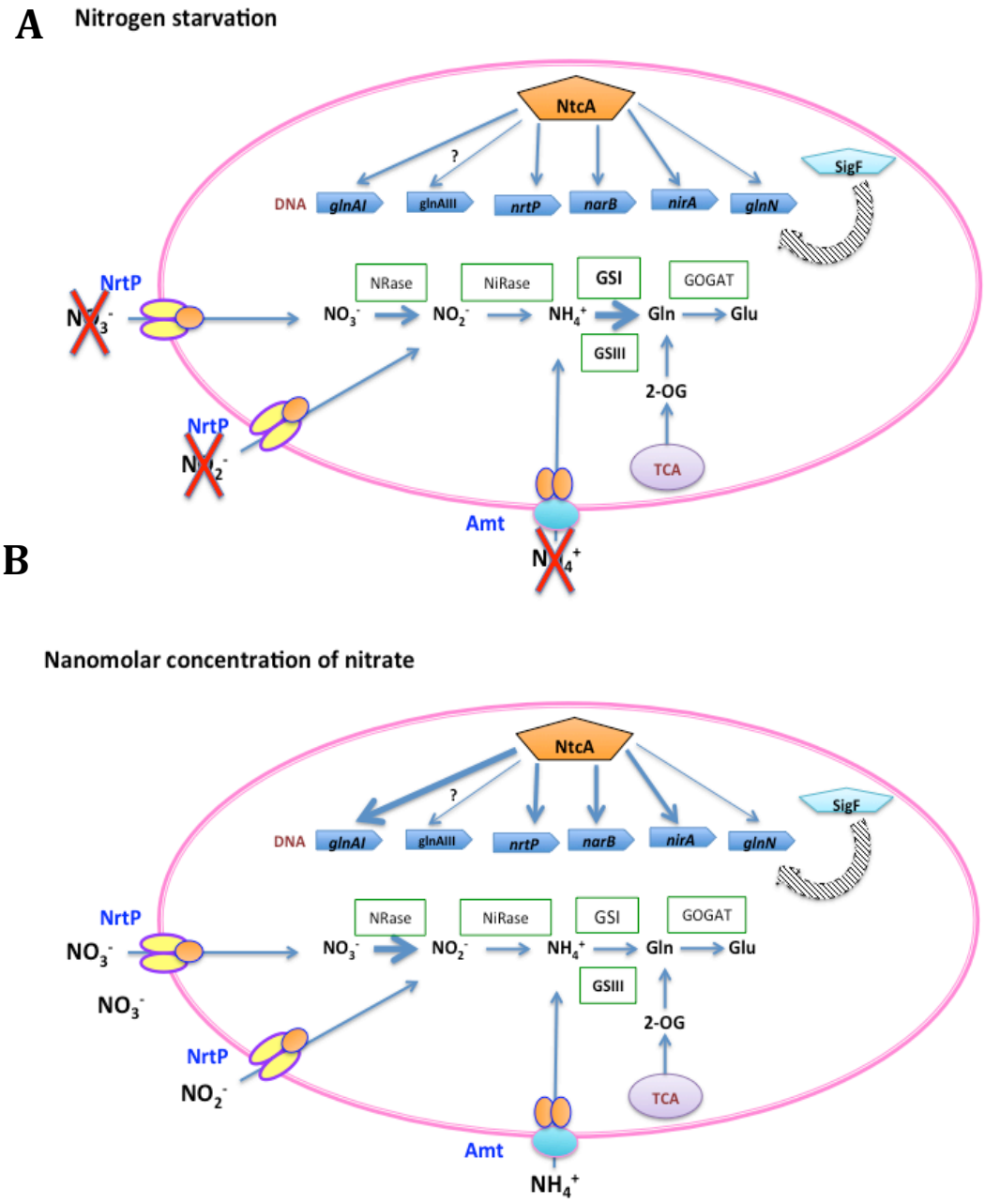
A
Nitrogen starvation
NtcA
?
SigF
DNA
glnAI
glnAIII
nrtP
narB
nirA
glnN
NrtP
NRase
NiRase
GSI
GOGAT
Gln
Glu
GSIII
2-OG
TCA
Amt
B
Nanomolar concentration of nitrate

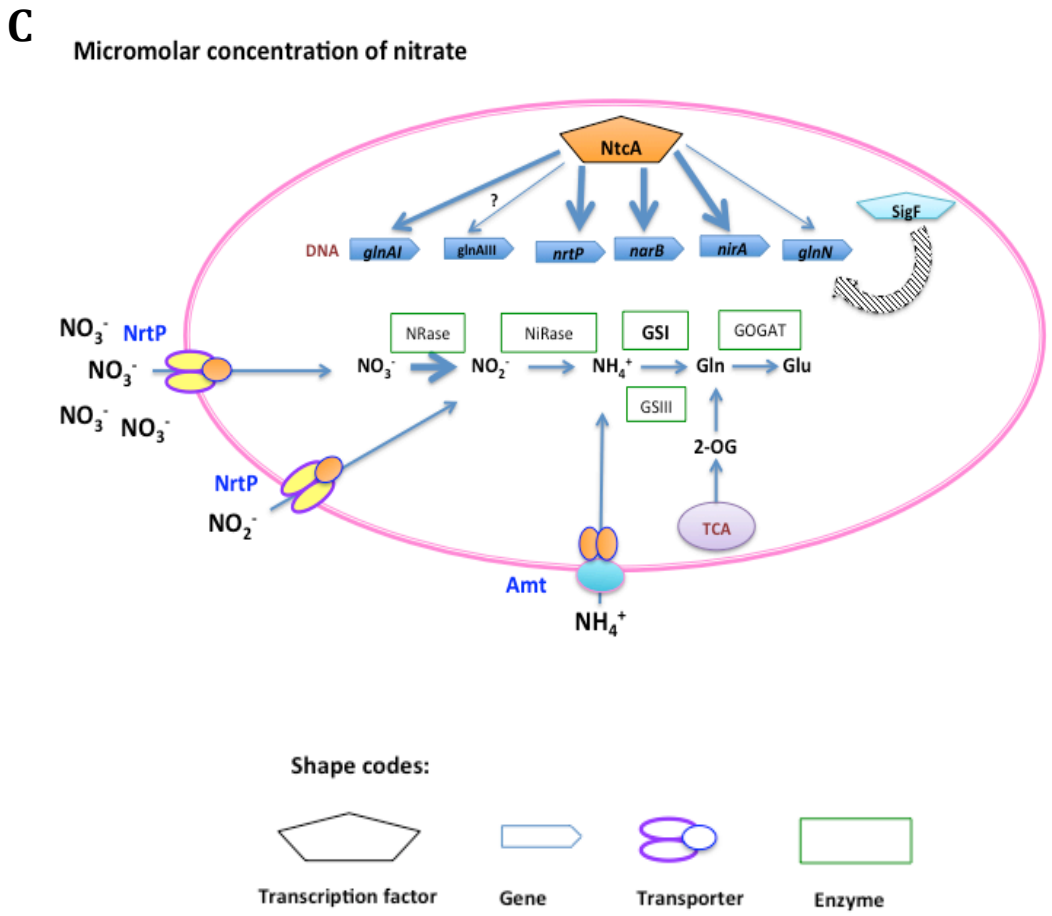

Figure 117: Model of nitrogen metabolism regulation in *Synechococcus* WH7803 under nitrogen starvation, growing with nanomolar or micromolar of nitrate.

CONCLUSIONS

1. 2-oxoglutarate is the molecule responsible to sense the C/N metabolism in *Prochlorococcus.*

2. The results show a clear difference in 2-OG sensing between strains from *Prochlorococcus;* this probably reflects the adaptations to their habitats, and their nitrogen availability.

3. Azaserine provokes a clear change in the proteome of *Prochlorococcus* SS120 probably due to the sharp increase of intracellular 2-OG concentration. Besides, the results suggest that NtcA could coordinate photosynthesis and nitrogen assimilation pathway in *Prochlorococcus.*

4. There is a transcriptional regulation of the genes related with the assimilation of nitrate when it is in low concentration in *Synechococcus* WH7803. This suggests the existence of some mechanism to detect the nanomolar concentration of nitrate.

5. The GS from *Synechococcus* WH7803 responds to nitrogen starvation but not to darkness, behaviour different with respect to GS from *Prochlorococcus*.

1. El 2-oxoglutarato es la molécula responsable del control del balance C/N en *Prochlorococcus.*

2. Los resultados muestran una clara diferencia en la sensibilidad al 2-oxoglutarato entre estirpes de *Prochlorococcus*; esto probablemente sea el reflejo de las adaptaciones a los hábitats y a la disponibilidad de nitrógeno.

3. La azaserina provoca un clara cambio en el proteoma de *Prochlorococcus* SS120 probablemente debido al incremento en la concentración intracelular del 2-oxoglutarato. Además, los resultados sugieren que NtcA puede coordinar fotosíntesis y asimilación de nitrógeno en *Prochlorococcus*.

4. Existe una regulación a nivel transcripcional de genes relacionados con la asimilación de nitrato cuando éste está en concentraciones bajas en *Synechococcus* WH7803. Esto sugiere la existencia de algún mecanismo que detecte concentraciones nanomolares de nitrato.

5. La GS de *Synechococcus* WH7803 responde a ausencia de nitrógeno pero no a la oscuridad, diferente comportamiento de esta enzima respecto *Prochlorococcus*.

BIBLIOGRAPHY

Aichi, M. & T. Omata, (1997) Involvement of NtcB, a LysR family transcription factor, in nitrite activation of the nitrate assimilation operon in the cyanobacterium *Synechococcus* sp. strain PCC 7942. *J. Bacteriol.* **179**: 4671-4675.

Aichi, M., N. Takatani & T. Omata, (2001) Role of NtcB in activation of nitrate assimilation genes in the cyanobacterium *Synechocystis* sp. strain PCC 6803. *J. Bacteriol.* **183**: 5840-5847.

Alfonso, M., I. Perewoska & D. Kirilovsky, (2001) Redox control of *ntcA* gene expression in *Synechocystis* sp. PCC 6803. Nitrogen availability and electron transport regulate the levels of the NtcA protein. *Plant Physiol.* **125**: 969-981.

Allen, M. & F. Hutchison, (1980) Nitrogen limitation and recovery in the cyanobacterium Aphanacapsa 6308. *Arch. Microbiol.* **128**: 1-7.

Allen, M. & A. Smith, (1969) Nitrogen chlorosis in Blue-green Algae. *Arch. Microbiol.* **69**: 114-120.

Anderson, D., E. Campbell & J. Meeks, (2006) A soluble 3D LC/MS/MS proteome of the filamentous cyanobacterium Nostoc punctiforme. *J. Proteome Res.* **5**: 3096-3104.

Arcondéguy, T., R. Jack & M. Merrick, (2001) P_{II} signal transduction proteins, pivotal players in microbial nitrogen control. *Microbiol. Mol. Biol. Rev.* **65**: 80-105.

Arrigo, K., (2005) Marine microorganisms and global nutrient cycles. *Nature* **437**: 349-355.

Badger, M., D. Hanson & G. Price, (2002) Evolution and diversity of CO2-concentrating mechanisms in cyanobacteria. *Funct. Plant Biol.* **29**: 161-173.

Berube, P., S. Biller, A. Kent, J. Berta-Thompson, S. Roggensack, K. Roache-Johnson, M. Ackerman, L. Moore, J. Meisel, D. Sher, L. Thompson, L. Campbel, A. Martiny & S. Chisholm, (2014) Physiology and evolution of nitrate acquistion in *Prochlrococcus ISME J* **in press**.

Bibby, T., I. Mary, J. Nield, F. Partensky & J. Barber, (2003) Low-light-adapted *Prochlorococcus* species possess spedific antennae for each photosystem. *Nature* **424**: 1051-1054.

Biller, S., P. Berube, J. Berta-Thompson, L. Kelly, S. Roggensack, L. Awad, K. Roache-Johnson, H. Ding, S. Giovannoni, G. Rocap, L. Moore & S. Chisholm, (2014a) Genomes of diverse isolates of the marine cyanobacterium Prochlorococcus. *Sci. Data*.

Biller, S., P. Berube, D. Lindell & S. Chisholm, (2014b) *Prochlorococcus*: the structure and function of collective diversity. *Nat. Rev. Microbiol.* **Accepted**.

Bird, C. & M. Wyman, (2003) Nitrate/Nitrite Assimilation System of the Marine Picoplanktonic Cyanobacterium *Synechococcus* sp. Strain WH 8103: Effect of Nitrogen Source and Availability on Gene Expression. *Appl. Environ. Microbiol.* **69**: 7009-7018.

Bjorkman, K.M., A.L. Thomson-Bulldis & D.M. Karl, (2000) Phosphorus dynamics in the North Pacific subtropical gyre. *Aquat. Microb. Ecol.* **22**: 185-198.

Boumediene Laichoubi, K., J. Espinosa, M. Castells & A. Contreras, (2012) Mutational analysis of the cyanobacterial nitrogen regulator pipx. *PloS one* **7**: 1-11.

Boyer, G., A. Gillam & C. Trick, (1987) Iron chelation and uptake. In: The Cyanobacteria. P. Fay & C. Van Baalen (eds). Elsevier Biomedical, pp. 415-436.

Bradford, M., (1976) A rapid and sensitive method for the quantitation of microgram quantities of protein utilizing the principle of protein-dye binding. *Anal. Biochem.* **72**: 248-254.

Bryant, D.A., (1995) *Advance in Photosynthesis: The molecular biology of cyanobacteria*. Department of Plant Biology, University of Illinois, Urbana, Illinois, U..S.A.

Burillo, S., I. Luque, I. Fuentes & A. Contreras, (2004) Interactions between the nitrogen signal transduction protein P_{II} and N-acetyl glutamate kinase in organisms that perform oxygenic photosynthesis. *J. Bacteriol.* **186**: 3346-3354.

Candau, P., C. Manzano & M. Losada, (1976) Bioconversion of light energy into chemical energy through reduction with water of nitrate to ammonia. *Nature* **262**: 715-717.

Capone, D., (2000) The marine microbial nitrogen cycle. In: Microbial ecology of the oceans. D. Kirchman (ed). New York: Wiley-Liss, Inc., pp. 455-493.

Capone, D., (2001) Marine nitrogen fixation: what's the fuss? *Curr. Opin. Microbiol.* **4**: 341-348.

Capone, D.G., (2008) The marine nitrogen cycle. *Microbe* **3**: 186-192.

Chávez, S. & P. Candau, (1991) An NAD-specific glutamate dehydrogenase from cyanobacteria. Identification and properties. *FEBS Lett.* **285**: 35-38.

Chávez, S., J. Reyes, F. Chauvat, F. Florencio & P. Candau, (1995) The NADP-glutamate dehydrogenase of the cyanobacterium *Synechocystis* 6803 cloning, transcriptional analysis and disruption of the *gdhA* gene. *Plant Mol. Biol.* **28**: 173-188.

Chisholm, S., R. Olson, E. Zettler, R. Goericke, J. Waterbury & N. Welschmeyer, (1988) A novel free living prochlorophyte abundant in the oceanic euphotic zone. *Nature* **334**: 340-343.

Coleman, M. & S. Chisholm, (2007) Code and context: *Prochlorococcus* as a model for cross-scale biology. *Trends Microbiol.* **15**: 398-407.

Collier, J., B. Brahamsha & B. Palenik, (1999) The marine cyanobacterium *Synechococcus* sp. WH7805 requires urease (urea amidohydrolase, EC-3.5.1.5) to utilize urea as a nitrogen source - Molecular genetic and biochemical analysis of the enzyme. *Microbiology (Reading)* **145**: 447-459.

Collier, J. & R. Lovindeer, (2012) Differences in growth and physiology of marine Synechococcus (cyanobacteria) on nitrate versus ammonium are not determined solely by nitrogen source redox state. *J. Phycol.* **48**: 106-116.

Conrad, C., J. Choi, C. Malakowsky, J. Talent, R. Dai, P. Marshall & R. Gracy, (2001) Identification of protein carbonyls after two-dimensional electrophoresis. *Proteomics* **1(7)**: 829-834.

Costello, M., A. Cheung & N. Hauwere, (2010) Surface area and the seabed area, volume, depth, slope, and topographic variation for the world´s seas, oceans and countries. *Environ. Sci. Technol.* **44**: 8821-8828.

Crespo, J., M. Garcia-Dominguez & F. Florencio, (1998) Nitrogen control of the *glnN* gene that codes for GS Type-III, the only glutamine synthetase in the cyanobacterium *Pseudanabaena* sp. PCC 6903. *Mol. Microbiol.* **30**: 1101-1112.

Dore, J.E. & D.M. Karl, (1996) Nitrite distributions and dynamics at Station ALOHA. *Deep-Sea Research II* **43**: 385-402.

Dufresne, A., L. Garczarek & F. Partensky, (2005) Accelerated evolution associated to genome reduction in a free-living prokaryote. *Genome Biol* **6**: R14.

Dufresne, A., M. Ostrowski, D. Scanlan, L. Garczarek, S. Mazard, B. Palenik, I. Paulsen, N. Tandeau de Marsac, P. Wincker, C. Dossat, S. Ferriera, J. Johnson, A. Post, W. Hess & F. Partensky, (2008) Unraveling the genomic mosaic of a ubiquitous genus of marine cyanobacteria. *Genome Biol* **9**: R90.

Dufresne, A., M. Salanoubat, F. Partensky, F. Artiguenave, I. Axmann, V. Barbe, S. Duprat, M. Galperin, E. Koonin, F. Le Gall, K. Makarova, M. Ostrowski, S. Oztas, C. Robert, I. Rogozin, D. Scanlan, N. Tandeau de Marsac, J. Weissenbach, P. Wincker, Y. Wolf & W. Hess, (2003) Genome sequence of the cyanobacterium *Prochlorococcus marinus* SS120, a nearly minimal oxyphototrophic genome. *Proc. Natl. Acad. Sci. USA* **100**: 10020-10025.

El Alaoui, S., J. Diez, L. Humanes, F. Toribio, F. Partensky & J. García-Fernández, (2001) *In vivo* regulation of glutamine synthetase activity in the marine chlorophyll *b*-containing cyanobacterium *Prochlorococcus* sp. strain PCC 9511 (Oxyphotobacteria). *Appl. Environ. Microbiol.* **67**: 2202-2207.

El Alaoui, S., J. Díez, A. López-Ruiz, G. Gómez-Baena, F. Partensky & J. García-Fernández, (1999) Asimilación de nitrógeno en el procariota fotosintético marino *Prochlorococcus*. In: Avances en el Metabolismo del Nitrógeno: Bioquímica, Fisiología y Biología Molecular. F. Cánovas & F. Florencio (eds). Servicio de Publicaciones. Universidad de Málaga, pp.

El Alaoui, S., J. Diez, F. Toribio, G. Gómez-Baena, A. Dufresne & J. García-Fernández, (2003) Glutamine synthetase from the marine cyanobacteria *Prochlorococcus* spp.: characterization, phylogeny and response to nutrient limitation. *Environ. Microbiol.* **5**: 412-423.

Espinosa, J., M. Castells, K. Laichoubi & A. Contreras, (2009) Mutations at PipX suppress lethality of PII-deficient mutants of Synechococcus elongatus PCC7942. *J. Bacteriol.* **191**: 4863-4869.

Espinosa, J., K. Forchhammer, S. Burillo & A. Contreras, (2006) Interaction network in cyanobacterial nitrogen regulation: PipX, a protein that interacts in a 2-oxoglutarate dependent manner with P_{II} and NtcA. *Mol. Microbiol.* **61**: 457-469.

Espinosa, J., K. Forchhammer & A. Contreras, (2007) Role of the *Synechococcus* PCC 7942 nitrogen regulator protein PipX in NtcA-controlled processes. *Microbiology (Reading)* **153**: 711-718.

Espinosa, J., F. Rodríguez-Mateos, P. Salinas, V. Lanza, R. Dixon, F. de la Cruz & A. Contreras, (2014) PipX, the coactivar of NtcA, is a global regulator in cyanobacteria. *Proceedings of the National Academy of Sciences of the United States of America*: 1-8.

Falkowski, P., R. Barber & V. Smetacek, (1998) Biogeochemical controls and feedbacks on ocean primary production. *Science* **281**: 200-206.

Falkowski, P. & M. Oliver, (2007) Mix and match: how climate selects phytoplankton. *Nature Reviews Microbiology* **5**: 813-819.

Falkowski, P. & R.J. Scholes, (2000) The global carbon cycles: a test of our knowledge of earth as a system. *Science* **290**.

Flombaum, P., J.L. Gallegos, R.A. Gordillo, J. Rincón, L.L. Zabala, N. Jiao, D.M. Karl, W.K.W. Li, M.W. Lomas, D. Veneziano, C.S. Vera, J.A. Vrugt & A.C. Martiny, (2013) Present and future global distributions of the marine cyanobacteria *Prochlorococcus* and *Synechococcus*. *Proceedings of the National Academy of Sciences of the United States of America* **110**: 9824-9829.

Florencio, F., S. Marques & P. Candau, (1987) Identification and characterization of a glutamate dehydrogenase in the unicellular cyanobacterium *Synechocystis* PCC 6803. *FEBS Lett.* **223**: 37-41.

Florencio, F. & J. Reyes, (2002) Regulation of ammonium assimilation in cyanobacteria. In: Photosynthetic Nitrogen Assimilation and Associated Carbon Metabolism. C. Foyer & G. Noctor (eds). Dordretch: Kluwer Academic Publishers, pp. 93-113.

Flores, E., J. Frías, L. Rubio & A. Herrero, (2005) Photosynthetic nitrate assimilation in cyanobacteria. *Photosynthesis Res.* **83**: 117-133.

Flores, E. & A. Herrero, (1994) Assimilatory nitrogen metabolism and its regulation. In: The molecular biology of cyanobacteria. D. Bryant (ed). Dordrecht: Kluwer Academic Publishers, pp. 487-517.

Flores, E. & A. Herrero, (2005) Nitrogen assimilarion and nitrogen control in cyanobacteria. *Biochem. Soc. Trans.* **33**: 164-167.

Forchhammer, K., (1999) The PII protein in *Synechococcus* PCC 7942 senses and signals 2-oxoglutarate under ATP-replete conditions In: The Phototrophyc Prokaryotes. G. Peschek, W. Löffelhardt & G. Schmetterer (eds). New York: Kluwer Academic pp. 549-553.

Forchhammer, K., (2004) Global carbon/nitrogen control by P_{II} signal transduction in cyanobaceria: from signals to targets. *FEMS Microbiol. Rev.* **28**: 319-333.

Forchhammer, K., (2008) P_{II} signal transducers: novel functional and structural insights. *Trends Microbiol.* **16**: 65-72.

Forchhammer, K. & A. Hedler, (1997) Phosphoprotein PII from cyanobacteria. Analysis of functional conservation with the PII signal-transduction protein from Escherichia coli. *Eur. J. Biochem.* **244**: 869-875.

Forchhammer, K. & N. Tandeau de Marsac, (1994) The P_{II} protein in the cyanobacterium *Synechococcus* sp. strain PCC 7942 is modified by serine phosphorylation and signals the cellular N-status. *J. Bacteriol.* **176**: 84-91.

Forde, B., (2000) Nitrate transporters in plants: structure, function and regulation. *Biochim. Biophys. Acta* **1465**: 219-235.

Fuller, N., D. Marie, F. Partensky, D. Vaulot, A. Post & D. Scanlan, (2003) Clade-specific 16S rDNA oligonucleotides reveal the predominance of a single marine *Synechococcus* clade throughout a stratified water column in the Red Sea. *Appl. Environ. Microbiol.* **69**: 2430-2443.

García-Domínguez, M. & F. Florencio, (1997) Nitrogen availability and electron transport control the expression of *glnb* gene (encoding P_{II} protein) in the cyanobacterium *Synechocystis* sp. PCC 6803. *Plant Mol. Biol.* **35**: 723-734.

García-Domínguez, M., J. Reyes & F. Florencio, (1997) Purification and characterization of a new type of glutamine synthetase from cyanobacteria. *Eur. J. Biochem.* **244**: 258-264.

García-Domínguez, M., J. Reyes & F. Florencio, (1999) Glutamine synthetase inactivation by protein-protein interaction. *Proceedings of the National Academy of Sciences of the United States of America* **96**: 7161-7166.

García-Domínguez, M., J. Reyes & F. Florencio, (2000) NtcA represses transcription of *gifA* and *gifB*, genes that encode inhibitors of glutamine synthetase type I from *Synechocystis* sp. PCC 6803. *Mol. Microbiol.* **35**: 1192-1201.

García-Fernández, J. & J. Diez, (2004) Adaptive mechanisms of the nitrogen and carbon assimilatory pathways in the marine cyanobacteria *Prochlorococcus*. *Res. Microbiol.* **155**: 795-802.

García-Fernández, J., A. López-Ruíz, J. Alhama, J. Roldán & J. Díez, (1995) Effect of glutamine on glutamine-synthetase regulation in the green alga *Monoraphidium braunii*. *Planta (Berlin)* **195**: 434-439.

García-Fernández, J., N. Tandeau de Marsac & J. Diez, (2004) Streamlined regulation and gene loss as adaptive mechanisms in *Prochlorococcus* for optimized nitrogen utilization in oligotrophic environments. *Microbiol. Mol. Biol. Rev.* **68**: 630-638.

García-Pichel, F., J. Belnap, S. Neuer & F. Schanz, (2003) Estimates of cyanobacterial biomass and its distribution. *Algol. Stud* **109**: 213-228.

Garczarek, L., A. Dufresne, N. Blot, A. Cockshutt, A. Peyrat, D. Campbell, L. Joubin & C. Six, (2008) Function and evolution of the *psbA* gene family in marine *Synechococcus*: *Synechococcus* sp. WH7803 as a case study. *ISME Journal*: 1-17.

Garczarek, L., A. Dufresne, S. Rousvoal, N. West, S. Mazard, D. Marie, H. Claustre, P. Raimbault, A. Post, D. Scanlan & F. Partensky, (2007) High vertical and low horizontal diversity of *Prochlorococcus* ecotypes in the Mediterranean Sea in summer. *FEMS Microbiol. Ecol.* **60**: 189-206.

Garczarek, L., W. Hess, J. Holtzendorff, G. van der Staay & F. Partensky, (2000) Multiplication of antenna genes as a major adaptation to low light in a marine prokaryote. *Proceedings of the National Academy of Sciences of the United States of America* **97**: 4098-4101.

Garczarek, L., F. Partensky, H. Irlbacher, J. Holtzendorff, M. Babin, I. Mary, J. Thomas & W. Hess, (2001) Differential expression of antenna and core genes in *Prochlorococcus* PCC 9511 (Oxyphotobacteria) grown under a modulated light-dark cycle. *Environ. Microbiol.* **3**: 168-175.

Garczarek, L., G. Vanderstaay, J. Thomas & F. Partensky, (1998) Isolation and characterization of photosystem-I from 2 strains of the marine oxychlorobacterium *Prochlorococcus*. *Photosynthesis Res.* **56**: 131-141.

Gierga, G., B. Voss & W.R. Hess, (2012) Non-coding RNAs in marine Synechococcus and their regulation under environmentally relevant stress conditions. *ISME Journal*.

Giovannoni, S. & M. Rappé, (2000) Evolution, diversity, and molecular ecology of marine prokaryotes. In: Microbial Eccology of the Oceans. D.L. Kirchman (ed). Wiley-Liss, pp.

Glibert, P., T. Kana, R. Olson, D. Kirchman & R. Alberte, (1986) Clonal comparisons of growth and photosynthetic responses to nitrogen availability in marine *Synechococcus* spp. *J. Exp. Mar. Biol. Ecol.* **101**: 199-208.

Glibert, P. & T. Ray, (1990) Different patterns of growth and nitrogen uptake in two clones of marine *Synechococcus* spp. *Marine Biology (Berlin)* **107**: 273-280.

Glover, H.E., B.B. Prézelin, L. Campbell, M. Wyman & C. Garside, (1988) A nitrate dependent *Synechococcus* bloom in surface Sargasso Sea water. *Nature* **331**: 161-163.

Goericke, R., (2011) The structure of marine phytoplankton communities: patterns, rules and mechanisms. *Phytoplankton community structure* **52**: 182-197.

Goericke, R. & D. Repeta, (1992) The pigments of *Prochlorococcus marinus* - The presence of divinyl chlorophyll-A and chlorophyll-B in a marine prokaryote. *Limnol. Oceanogr.* **37**: 425-433.

Gómez-Baena, G., J. Diez, J. García-Fernández, S. El Alaoui & L. Humanes, (2001) Regulation of glutamine synthetase by metal-catalyzed oxidative modification in the marine oxyphotobacterium *Prochlorococcus*. *Biochim. Biophys. Acta* **1568**: 237-244.

Gómez-Baena, G., M. Domínguez-Martín, R. Donaldson, J. García-Fernández & J. Diez, (2014) Nutrient starvation makes glutamine synthetase more sensitive to oxidative modification in *Prochlorococcus marinus* PCC 9511. *Life*

Gómez-Baena, G., J. García-Fernández, A. Lopez-Lozano, F. Toribio & J. Diez, (2006) Glutamine synthetase degradation is controlled by oxidative proteolysis in the marine cyanobacterium *Prochlorococcus marinus* strain PCC 9511. *Biochim. Biophys. Acta* **1760**: 930-940.

Grantham, H., E. Game, A. Lombard, A. Hobday, A. Richardson, L. Beckley, R. Pressey, J. Huggett, J. Coetzee, C. Van der Linge, S. Petersen, D. Merkle & H. Possingham, (2011) Accommodating dynamic oceanographic processes and pelagic biodiversity in marine conservation planning. *PloS one* **6**: 1-16.

Grassi, F., N. Moretto, C. Rivetti, S. Cellai, M. Betti, A. Marquez, G. Maraini & S. Ottonello, (2006) Structural and functional properties of lengsin, a pseudo-glutamine synthetase in the transparent human lens. *Biochem. Biophys. Res. Commun.* **350**: 424-429.

Gruber, T. & D. Bryant, (1998) Characterization of the alternative sigma factors SigD and SigE in *Synechococcus* sp. strain PCC 7002. SigE is implicated in transcription of post-exponential phase specific genes. *Arch. Microbiol.* **169**: 211-219.

Hayden, B., M. Bonete, P. Brown, A. Moir & P. Engel, (2002) Glutamate dehydrogenase of *Halobacterium salinarum*: evidence that the gene sequence currently assigned to the NADP+-dependent enzyme is in fact that of the NAD+-dependent glutamate dehydrogenase. *FEMS Microbiol. Lett.* **211**: 37-41.

Herrero, A., E. Flores & M. Guerrero, (1981) Regulation of nitrate reductase levels in the cyanobacteria *Anacystis nidulans*, *Anabaena*-sp strain 7119 and *Nostoc*-sp 6719. *J. Bacteriol.* **145**: 175-180.

Herrero, A., A. Muro-Pastor & E. Flores, (2001) Nitrogen control in cyanobacteria. *J. Bacteriol.* **183**: 411-425.

Herrero, A., A. Muro-Pastor, A. Valladares & E. Flores, (2004) Cellular differentiation and the NtcA transcription factor in filamentous cyanobacteria. *FEMS Microbiol. Rev.* **28**: 469-487.

Hess, W., F. Partensky, G. Van der Staay, J. García-Fernández, T. Börner & D. Vaulot, (1996) Coexistence of phycoerythrin and a chlorophyll *a/b* antenna in a marine prokaryote. *Proc. Natl. Acad. Sci. USA* **93**: 11126-11130.

Heywood, J.L., M.V. Zubkov, G.A. Tarran, B.M. Fuchs & P.M. Holligan, (2006) Prokaryoplankton standing stocks in oligotrophic gyre and equatorial provinces of the Atlantic Ocean: evaluation of interanual variability. *Deep Sea Res. (II Top. Stud. Oceanogr.)* **53**: 1530-1547.

Hihara, Y., K. Sonoike, M. Kanehisa & M. Ikeuchi, (2003) DNA microarray analysis of redox-responsive genes in the genome of the cyanobacterium *Synechocystis* sp. strain PCC 6803. *J. Bacteriol.* **185**: 1719-1725.

Hoffman, L., (1999) Marine cyanobacteria in tropical regions: diversity and ecology. *Eur. J. Phycol.* **34**: 371-379.

Holtzendorff, J., F. Partensky, S. Jacquet, F. Bruyant, D. Marie, L. Garczarek, I. Mary, D. Vaulot & W. Hess, (2001) Diel expression of cell cycle-related genes in synchronized cultures of *Prochlorococcus* sp. strain PCC 9511. *J. Bacteriol.* **183**: 915-920.

Hu, B., L. Shen, X. Xu & P. Zheng, (2011) Anaerobic ammonium oxidation (anammox) in different natural ecosystems. *Biochem. Soc. Trans.* **39**: 1811-1816.

Imamura, S. & M. Asayama, (2009) Sigma factors for cyanobacterial transcription. *Gene Regul Syst Bio* **3**: 65-87.

Imamura, S., S. Yoshihara, S. Nakano, N. Shiozaki, A. Yamada, K. Tanaka, H. Takahashi, M. Asayama & M. Shirai, (2003) Purification, characterization, and gene expression of all sigma factors of RNA polymerase in a cyanobacterium. *J. Mol. Biol.* **325**: 857-872.

Inoue, H., H. Nojima & H. Okayama, (1990) High efficiency transformation of *Escherichia coli* with plasmids. *Gene* **96**: 23-28.

Inoue-Sakamoto, K., T. Gruber, S. Christensen, H. Arima, T. Sakamoto & D.A. Bryant, (2007) Group 3 sigma factors in the marine cyanobacterium Synechococcus sp. strain PCC 7002 are required for growth at low temperature *J. Gen. Appl. Microbiol.* **53**: 89-104.

Ishihama, A., (1993) Protein-protein communication within the transcription apparatus. *J. Bacteriol.* **175**: 2483-2489.

Jiang, P. & A. Ninfa, (1999) Regulation of autophosphorylation of Escherichia coli nitrogen regulator II by the PII signal transduction protein *J. Bacteriol.* **181**: 1906-1911.

Johnson, Z., E. Zinser, A. Coe, N. McNulty, E. Woodward & S. Chisholm, (2006) Niche partitioning among *Prochlorococcus* ecotypes along ocean-scale environmental gradients. *Science* **311**: 1737-1740.

Kana, T., N. Feiwel & L. Flynn, (1992) Nitrogen starvation in marine *Synechococcus* strains: clonal differences in phycobiliprotein breakdown and energy coupling. *Mar. Ecol. Prog. Ser.* **88**: 75-82.

Kana, T. & P. Glibert, (1987) Effect of irradiances up to 2000 μE m-2 s-1 on marine *Synechococcus* WH7803. 1. Growth, pigmentation and cell composition. 2. Photosynthetic responses and mechanisms. *Deep-Sea Res.* **34**: 479-495.

Karl, D. & M. Church, (2014) Microbial oceanography and the Hawaii ocean time-series programme. *Nat. Rev. Microbiol.* **12**: 1-15.

Kettler, G., A. Martiny, K. Huang, J. Zucker, M. Coleman, S. Rodrigue, F. Chen, A. Lapidus, S. Ferriera, J. Johnson, C. Steglich, G. Church, P. Richardson & S. Chisholm, (2007) Patterns and implications of gene gain and loss in the evolution of *Prochlorococcus*. *PLoS Genet.* **3**: 2515-2528.

Kim, Y., M. Yoshizawa, S. Takenaka, S. Murakami & K. Aoki, (2002) Ammonia assimilation in *Klebsiella pneumoniae* F-5-2 that can utilize ammonium and nitrate ions simultaneously: purification and characterization of glutamate dehydrogenase and glutamine synthetase. *J. Biosci. Bioeng.* **93**: 584-588.

Kirchman, D., (2008) *Microbial ecology of the oceans,* p. 542. John Wiley & Sons, New Yersey.

Klausmeier, C., E. Litchman, T. Daufresne & S. Levin, (2004) Optimal nitrogen-to-phosphorus stoichiometry of phytoplankton. *Nature* **429**: 171-174.

Korner, H., H.J. Sofia & W.G. Zumft, (2003) Phylogeny of the bacterial superfamily of Crp-Fnr transcription regulators: exploiting the metabolic spectrum by controlling alternative gene programs. *FEMS Microbiol. Rev.* **27**: 559-592.

Krumhardt, K.M., K. Callnan, K. Roache-Johnson, T. Swett, D. Robinson, E.N. Reistetter, J.K. Saunders, G. Rocap & L.R. Moore, (2013) Effects of phosphorus starvation versus limitation on the marine cyanobacterium Prochlorococcus MED4 I: uptake physiology. *Environ. Microbiol.* **15**: 2114-2128.

Kudela, R. & R. Dugdale, (2000) Nutrient regulation of phytoplanktoon productivity in Monterey Bay, California. *Deep Sea Res. (II Top. Stud. Oceanogr.)* **47**: 1023-1053.

Kuypers, M., G. Lavik, D. Woebken, M. Schmid, B. Fuchs, R. Amann, B. Jorgensen & M. Jetten, (2005) Massive nitrogen loss from the Benguela upwelling system through anaerobic ammonium oxidation. *Proccedings of the National Academy of Sciences USA* **102**: 6478-6483.

Kuypers, M., A. Sliekers, G. Lavik, M. Schmid, B. Jørgensen, J. Kuenen, J. SDamsté, M. Strous & M. Jetten, (2003) Anaerobic ammonium oxidation by anammox bacteria in the Black Sea. *Nature* **422**: 608-611.

La Roche, J., J. Murray, M. Orellana & J. Newton, (1995) Flavodoxin expression as an indicator of iron limitation in marine diatoms *J. Phycol.* **31**: 520-530.

La Roche, J., G. van der Staay, F. Partensky, A. Ducret, R. Aebersold, R. Li, S. Golden, R. Hiller, P. Wrench, A. Larkum & B. Green, (1996) Independent evolution of the prochlorophyte and green plant chlorophyll *a/b* light-harvesting proteins. *Proccedings of the National Academy of Sciences USA* **93**: 15244-15248.

Lamp, P. & M. Kuypers, (2011) Microbial nitrogen cycling processes in oxygen minimum zones. *Ann. Rev. Mar. Sci.* **3**: 317-345.

Larimer, F., P. Chain, L. Hauser, J. Lamerdin, S. Malfatti, L. Do, M. Land, D. Pelletier, J. Beatty, A. Lang, F. Tabita, J. Gibson, T. Hanson, C. Bobst, J. Torres y Torres, C. Peres, F. Harrison, J. Gibson & C. Harwood, (2004) Complete genome sequence of the metabolically versatile photosynthetic bacterium Rhodopseudomonas palustris. *Nat. Biotechnol.* **22**: 55-61.

Latifi, A., R. Jeanjean, S. Lemeille, M. Havaux & C. Zhang, (2005) Iron starvation leads to oxidative stress in *Anabaena* sp. strain PCC 7120. *J. Bacteriol.* **187**: 6596-6598.

Laurent, S., H. Chen, S. Bedu, F. Ziarelli, L. Peng & C. Zhang, (2005) Nonmetabolizable analogue of 2-oxoglutarate elicits heterocyst differentiation under repressive conditions in *Anabaena* sp. PCC 7120. *Proc. Natl. Acad. Sci. USA*.

Leonhardt, K. & N. Straus, (1992) An iron stress operon involved in photosynthetic electron transport in the marine cyanobacterium *Synechococcus* sp. PCC 7002. *Journal of General Microbiology* **138**: 1613-1621.

Li, W., (1994) Primary production of prochlorophytes, cyanobacteria, and eukaryotic ultraphytoplankton - Measurements from flow cytometric sorting. *Limnol. Oceanogr.* **39**: 169-175.

Li, W., P. Dickie, B. Irwin & A. Wood, (1992) Biomass of bacteria, cyanobacteria, prochlorophytes and photosynthetic eukaryotes in the Sargasso Sea. *Deep-Sea Research Part I Oceanographic Research Papers* **39**: 501-519.

Lichtle, C., J. Thomas, A. Spilar & F. Partensky, (1995) Immunological and ultrastructural characterization of the photosynthetic complexes of the prochlorophyte *Prochlorococcus* (Oxychlorobacteria). *J. Phycol.* **31**: 934-941.

Lindell, D., D. Erdner, D. Marie, O. Prasil, M. Koblizek, F. Le Gall, R. Rippka, F. Partensky, D. Scanlan & A. Post, (2002) Nitrogen stress response of *Prochlorococcus* strain PCC 9511 (Oxyphotobacteria) involves contrasting regulation of *ntcA* and *amt1*. *J. Phycol.* **38**: 1113-1124.

Lindell, D., E. Padan & A. Post, (1998) Regulation of *ntcA* expression and nitrite uptake in the marine *Synechococcus* sp. strain WH 7803. *J. Bacteriol.* **180**: 1878-1886.

Lindell, D. & A. Post, (2001) Ecological aspects of *ntcA* gene expression and its use as an indicator of the nitrogen status of marine *Synechococcus* spp. *Appl. Environ. Microbiol.* **67**: 3340-3349.

Llácer, J., J. Espinosa, M. Castells, A. Contreras, K. Forchhammer & V. Rubio, (2010) Structural basis for the regulation of NtcA-dependent transcription by proteins PipX and PII. *Proc. Natl. Acad. Sci. USA* **107**: 15397-15402.

Lomas, M. & F. Lipschultz, (2006) Forming the primary nitrite maximum: Nitrifiers or phytoplankton? *Limnol. Oceanogr.* **51**: 2453-2467.

Lonetto, M., M. Gribskov & C.A. Gross, (1992) The sigma 70 family: sequence conservation and evolutionary relationships. *J. Bacteriol.* **174**: 3843-3849.

Longhurst, A.R. & W. Harrison, (1989) The biological pump-profiles of plankton production and consumption in the upper ocean. *Prog. Oceanogr.* **22**: 47-123.

López-Lozano, A., (2007) Caracterización y regulación fisiológica de la isocitrato deshidrogenasa de *Prochlorococcus* sp. In: Departamento de Bioquímica y Biología Molecular. Córdoba: Universidad de Córdoba, pp. 154.

López-Lozano, A., J. Diez, S. El Alaoui, C. Moreno-Vivián & J. García-Fernández, (2002) Nitrate is reduced by heterotrophic bacteria but not transferred to *Prochlorococcus* in non axenic cultures. *FEMS Microbiol. Ecol.* **41**: 151-160.

López-Lozano, A., G. Gómez-Baena, M. Muñoz-Marín, O. Rangel, J. Diez & J. García-Fernández, (2009) Expression of genes involved in nitrogen assimilation and the C/N balance sensing in *Prochlorococcus* sp. strain SS120. *Gene Expression* **14**: 279-289.

Losada, M. & M. Guerrero, (1979) The photosynthetic reduction of nitrate and its regulation. Photosynthesis in Relation to Model System. In. J. Barber (ed). Elsevier, pp. 366-403.

Luque, I., E. Flores & A. Herrero, (1994) Molecular mechanism for the operation of nitrogen control in cyanobacteria. *EMBO (European Molecular Biology Organization) Journal* **13**: 2862-2869.

Luque, I. & K. Forchhammer, (2008) Nitrogen assimilation and C/N balance sensing. In: The Cyanobacteria. Molecular Biology, Genomics and Evolution. A. Herrero & E. Flores (eds). Norfolk, UK: Caister Academic Press, pp.

Luque-Almagro, V., (2005) Metabolismo del cianuro y del cianato en Pseudomonas pseudoalcaligenes CECT5344. Aplicaciones biotecnológicas. In: Departamento de Bioquímica y Biología Molecular. Universidad de Córdoba, pp.

Mackinney, G., (1941) Absorption of light by chlorophyll solutions. *J. Biol. Chem.* **140**: 315-322.

Manzano, C., P. Candau, C. Gómez-Moreno, A. Relimpio & M. Losada, (1976) Ferredoxin dependent photosynthetic reduction of nitrate and nitrite by particles of *Anacystis nidulans*. *Mol. Cell. Biochem.* **10**: 161-169.

Marañón, E., M. Behrenfeld, N. González, B. Mouriño & M. Zubkov, (2003) High variability of primary production in oligotrophic waters of the Atlantic Ocean: uncoupling from phytoplankton biomass and size structure. *Mar. Ecol. Prog. Ser.* **257**: 1-11.

Marinov, I., S. Doney & I. Lima, (2010) Response of ocean phytoplankton community structure to climate change over the 21st century: partitioning the effects of nutrients, temperature and light. *Biogeosciences* **7**: 3941-3959.

Marqués, S., A. Mérida, P. Candau & F. Florencio, (1992) Light-mediated regulation of glutamine synthetase activity in the unicellular cyanobacterium *Synechococcus* sp. PCC 6301. *Planta (Berlin)* **187**: 247-253.

Martin, G., W. Haehnel & P. Böger, (1997) Oxidative inactivation of glutamine synthetase from the cyanobacterium *Anabaena variabilis*. *J. Bacteriol.* **179**: 730-734.

Martin, J., (1992) Iron as a limiting factor in oceanic productivity In: Primary productivity and Biogeochemcial Cycles in the Sea. P. Falkowski & A. Woodhead (eds). New York: Plenum, pp. 123-137.

Martinez, J. & F. Azam, (1993) Aminopeptidase activity in marine chroococcoid cyanobacteria. *Appl. Environ. Microbiol.* **59**: 3701-3707.

Martiny, A., S. Kathuria & P. Berube, (2009) Widespread metabolic potential for nitrite and nitrate assimilation among *Prochlorococcus* ecotypes. *Microbiology (Reading)* **106**: 10787-10792.

Meeks, J., J. Elhai, T. Thiel, M. Potts, F. Larimer, J. Lamerdin, P. Perdki & R. Atlas, (2001) An overview of the genome of *Nostoc punctiforme*, a multicellular, symbiotic cyanobacterium. *Photosynthesis Res.* **70**: 85-106.

Mérida, A., P. Candau & F. Florencio, (1991) Regulation of glutamine synthetase activity in the unicellular cyanobacterium *Synechocystis* sp. strain PCC 6803 by the nitrogen source: effect of ammonium. *J. Bacteriol.* **173**: 4095-4100.

Michalski, A., E. Damoc, J. Haushild, O. Lange, A. Wieghaus, A. Makarov, N. Nagara, J. Cox, M. Mann & S. Horning, (2011) Mass spectrometry-based proteomics using Q Exactive, a High- performance Benchtop Quadrupole Orbitrap Mass Spectrometer. *Mol. Cell. Proteomics*: 1-11.

Mikami, B. & S. Ida, (1984) Purification and properties of ferredoxin-nitrate reductase from the cyanobacterium *Plectonema boryanum*. *Biochimica et Biophysica Acta* **791**: 294-304.

Montesinos, M., A. Muro-Pastor, A. Herrero & E. Flores, (1998) Ammonium/methylammonium permeases of a cyanobacterium - Identification and analysis of three nitrogen-regulated amt genes in *Synechocystis* sp. PCC 6803. *J. Biol. Chem.* **273**: 31463-31470.

Moore, L., (1997) Physiological ecology of *Prochlorococcus*: a comparison of isolates from diverse oceanographic regimes. In: Massachussets Institute of Technology. Cambridge, pp.

Moore, L. & S. Chisholm, (1999) Photophysiology of the marine cyanobacterium *Prochlorococcus* - Ecotypic differences among cultured isolates. *Limnol. Oceanogr.* **44**: 628-638.

Moore, L., A. Coe, E. Zinser, M. Saito, M. Sullivan, D. Lindell, K. Frois-Moniz, J. Waterbury & S. Chisholm, (2007) Culturing the marine cyanobacterium *Prochlorococcus*. *Limnol. Oceanogr.* **5**: 353-362.

Moore, L., R. Goericke & S. Chisholm, (1995) Comparative physiology of *Synechococcus* and *Prochlorococcus* - Influence of light and temperature on growth, pigments, fluorescence and absorptive properties. *Mar. Ecol. Prog. Ser.* **116**: 259-275.

Moore, L., A. Post, G. Rocap & S. Chisholm, (2002) Utilization of different nitrogen sources by the marine cyanobacteria *Prochlorococcus* and *Synechococcus*. *Limnol. Oceanogr.* **47**: 989-996.

Moore, L., G. Rocap & S. Chisholm, (1998) Physiology and molecular phylogeny of coexisting *Prochlorococcus* ecotypes. *Nature* **393**: 464-467.

Morel, A., Y. Ahn, F. Partensky, D. Vaulot & H. Claustre, (1993) *Prochlorococcus* and *Synechococcus* - A comparative study of their optical properties in relation to their size and pigmentation. *J. Mar. Res.* **51**: 617-649.

Mulholland, M. & D. Capone, (2000) The nitrogen physiology of the marine N2-fixing cyanobacteria *Trichodesmium* spp. *Trends Plant Sci.* **5**: 148-153.

Muñoz-Marín, M.C., I. Luque, M.V. Zubkov, P.G. Hill, J. Diez & J.M. García-Fernández, (2013) *Prochlorococcus* can use the Pro1404 transporter to take up glucose at nanomolar concentrations in the Atlantic Ocean. *Proc. Natl. Acad. Sci. USA* **110**: 8597-8602.

Muro-Pastor, M. & F. Florencio, (1992) Purification and properties of NADP-isocitrate dehydrogenase from the unicellular cyanobacterium *Synechocystis* sp. PCC 6803. *Eur. J. Biochem.* **203**: 99-105.

Muro-Pastor, M. & F. Florencio, (1994) NADP(+)-isocitrate dehydrogenase from the cyanobacterium *Anabaena* sp. strain PCC 7120: Purification and characterization of the enzyme and cloning, sequencing, and disruption of the *icd* gene. *J. Bacteriol.* **176**: 2718-2726.

Muro-Pastor, M. & F. Florencio, (2003) Regulation of ammonium assimilation in cyanobacteria. *Plant Physiology and Biochemistry (Paris)* **41**: 595-603.

Muro-Pastor, M., J. Reyes & F. Florencio, (1996) The $NADP^+$-isocitrate dehydrogenase gene (*icd*) is nitrogen regulated in cyanobacteria. *J. Bacteriol.* **178**: 4070-4076.

Muro-Pastor, M., J. Reyes & F. Florencio, (2001) Cyanobacteria perceive nitrogen status by sensing intracellular 2-oxoglutarate levels. *J. Biol. Chem.* **276**: 38320-38328.

Muro-Pastor, M., J. Reyes & F. Florencio, (2005) Ammonium assimilation in cyanobacteria. *Photosynthesis Res.* **83**: 135-150.

Ninfa, A. & M. Atkinson, (2000) PII signal trasduction proteins. *Trends Microbiol.* **8**: 172-179.

Ninfa, A. & P. Jiang, (2005) PII signal transduction proteins: sensors of alpha-ketoglutarate that regulate nitrogen metabolism. *Curr. Opin. Microbiol.* **8**: 168-173.

Ohashi, Y., W. Shi, N. Takatani, M. Aichi, S. Maeda, S. Watanabe, H. Yoshikawa & T. Omata, (2011) Regulation of nitrate assimilation in cyanobacteria. *J. Exp. Bot.*: 1-14.

Olson, R., E. Zettler, M. Altabet, J. Dusenberry & S. Chisholm, (1990) Spatial and temporal distributions of prochlorophyte picoplankton in the North Atlantic Ocean. *Deep-Sea Research Part I Oceanographic Research Papers* **37**: 1033-1051.

Omairi-Nasser, A., C. Galmozzi, A. Latifi, M. Muro-Pastor & G. Ajlani, (2014) NtcA is responsible for accumulation of the small isoform of ferredoxin:NADP oxidoreductase. *Microbiology* **160**: 789-794.

Omata, T., X. Andriesse & A. Hirano, (1993) Identification and characterization of a gene cluster involved in nitrate transport in the cyanobacterium *Synechococcus* sp. PCC 7942. *Mol. Gen. Genet.* **236**: 193-202.

Ong, L. & A. Glazer, (1991) Phycoerythrins of marine unicellular cyanobacteria. I. Bilin types and locations and energy transfer pathways in *Synechococcus* spp. *phycoerythrins*. *J. Biol. Chem.* **266**: 9515-9527.

Pace, J. & E. McDermott, (1952) Methionine sulphoximine and some enzyme systems involving glutamine. *Nature* **169**: 415-416.

Paerl, H., (1991) Ecophysiological and trophic implications of light-stimulated amino acid utilization in marine picoplankton. *Appl. Environ. Microbiol.* **57**: 473-479.

Palinska, K., T. Jahns, R. Rippka & N. Tandeau de Marsac, (2000) *Prochlorococcus marinus* strain PCC 9511, a picoplanktonic cyanobacterium, synthesizes the smallest urease. *Microbiology (Reading)* **146**: 3099-3107.

Palinska, K.A., W. Laloui, S. Bedu, S. Loiseaux-De Goer, A. Castets, R. Rippka & N. Tandeau De Marsac, (2002) The signal transducer P_{II} and bicarbonate acquisition in *Prochlorococcus marinus* PCC 9511, a marine cyanobacterium naturally deficient in nitrate and nitrite assimilation. *Microbiology (Reading)* **148**: 2405-2412.

Pandhal, J., P. Wright & C. Biggs, (2007) A quantitative proteomic analysis of light adaptation in a globally significant marine cyanobacterium *Prochlorococcus marinus* MED4. *Journal of Proteome Research* **6**: 996-1005.

Paneque, A., F.F. Del Campo, J.M. Ramirez & M. Losada, (1965) Flavin nucleotide nitrate reductase from spinach. *Biochim. Biophys. Acta* **109**: 79-85.

Parpais, J., D. Marie, F. Partensky, P. Morin & D. Vaulot, (1996) Effect of phosphorus starvation on the cel cycle of the photosynthetic prokaryote *Prochlorococcus* spp. *Mar. Ecol. Prog. Ser.* **132**: 265-274.

Partensky, F., J. Blanchot & D. Vaulot, (1999a) Differential distribution and ecology of *Prochlorococcus* and *Synechococcus* in oceanic waters: a review. In: Marine cyanobacteria. L. Charpy & A. Larkum (eds). Monaco: Bulletin de l'Institut Océanographique, Numéro spécial, pp. 457-476.

Partensky, F. & L. Garczarek, (2003) The photosynthetic apparatus of *chlorophyll b*- and *d*-containing oxyphotobacteria. In: Photosynthesis in Algae. A. Larkum, S. Douglas & J. Raven (eds). Dordrecht: Kluwer Academic Publishers, pp. 29-62.

Partensky, F. & L. Garczarek, (2010) P*rochlorococcus*: Advantages and Limits of Minimalism. *Ann. Rev. Mar. Sci.*

Partensky, F., W. Hess & D. Vaulot, (1999b) *Prochlorococcus*, a marine photosynthetic prokaryote of global significance. *Microbiol. Mol. Biol. Rev.* **63**: 106-127.

Partensky, F., N. Hoepffner, W. Li, O. Ulloa & D. Vaulot, (1993) Photoacclimation of *Prochlorococcus* sp (Prochlorophyta) strains isolated from the North Atlantic and the Mediterranean sea. *Plant Physiology (Rockville)* **101**: 285-296.

Pearce, J., C. Leach & N. Carr, (1969) The incomplete tricarboxylic acid cycle in the blue-green alga *Anabaena variabilis*. *Journal of General Microbiology* **55**: 371-378.

Pelroy, R., R. Rippka & R. Stanier, (1972) Metabolism of glucose by unicellular blue-green algae. *Arch. Microbiol.* **87**: 303-322.

Pfaffl, M., (2001) A new mathematical model for relative quantification in real-time RT-PCR. *Nucleic Acids Res.* **29**: e45.

Pinkus, L., (1977) Glutamine binding sites. *Methods Enzymol.* **46**: 414-427.

Pittera, J., F. Humily, M. Thorel, D. Grulois, L. Garczarek & C. Six, (2014) Connecting thermal physiology and latitudinal niche parttioning in marine *Synechococcus*. *ISME J* **8**: 1221-1236.

Post, A., (2005) Nutrient limitation of marine cyanobacteria. In: Harmful cyanobacteria. J. Huisman, H. Matthijs & Visser (eds). Kluwer Academic Publisher, pp.

Qi, D., P. Brownridge, D. Xia, F. Mackay, F. Gonzalez-Galarza, J. Kenyani, V. Harman, R. Beynon & A. Jones, (2012) A software Toolkit and interface for performing stable isotope labeling and Top3 quantification using Progenesis LC-MS *OMICS: J. Integrative Biol.* **16**: 489-495.

Rangel, O., G. Gómez-Baena, A. López-Lozano, J. Diez & J. García-Fernández, (2009) Physiological role and regulation of glutamate dehydrogenase in *Prochlorococcus* MIT9313. *Environ. Microbiol. Reports* **1**: 56-64.

Redfield, A., (1934) On the proportions of organic derivations in sea water and their relation to the composition of plankton. In.: Daniel, RJ, pp. 177-192.

Reyes, J. & F. Florencio, (1994) A new type of glutamine synthetase in cyanobacteria: the protein encoded by the *glnN* gene support nitrogen assimilation in *Synechocystis* sp. strain PCC 6803. *J. Bacteriol.* **176**: 1260-1267.

Rich, P., S. Madgwick & D. Moss, (1991) The interactions of duroquinol, DBMIB and NQNO with the chloroplast cytochrome b_6f complex. *Biochimica et Biophysica Acta* **108**: 1188-1195.

Rippka, R., (1972) Photoheterotrophy and chemoheterotrophy among unicellular blue-green algae. *Arch. Microbiol.* **87**: 93-98.

Rippka, R., T. Coursin, W. Hess, C. Lichtlé, D. Scanlan, K. Palinska, I. Iteman, F. Partensky, J. Houmard & M. Herdman, (2000) *Prochlorococcus marinus* Chisholm et al. 1992 subsp. pastoris subsp. nov. strain PCC 9511, the first axenic chlorophyll a_2/b_2-containing cyanobacterium (Oxyphotobacteria). *Int. J. Syst. Evol. Microbiol.* **50**: 1833-1847.

Rippka, R., J. Deruelles, J. Waterbury, M. Herdman & R. Stanier, (1979) Generic assignments, strain histories and properties of pure cultures of cyanobacteria. *Journal of General Microbiology* **111**: 1-61.

Rocap, G., D. Distel, J. Waterbury & S. Chisholm, (2002) Resolution of *Prochlorococcus* and *Synechococcus* ecotypes by using 16S-23S ribosomal DNA internal transcribed spacer sequences. *Appl. Environ. Microbiol.* **68**: 1180-1191.

Rocap, G., F. Larimer, J. Lamerdin, S. Malfatti, P. Chain, N. Ahlgren, A. Arellano, M. Coleman, L. Hauser, W. Hess, Z. Johnson, M. Land, D. Lindell, A. Post, W. Regala, M. Shah, S. Shaw, C. Steglich, M. Sullivan, C. Ting, A. Tolonen, E. Webb, E. Zinser & S. Chisholm, (2003) Genome divergence in two *Prochlorococcus* ecotypes reflects oceanic niche differentiation. *Nature* **424**: 1042-1047.

Rocap, G., F. Larimer, J. Lamerdin, S. Stilwagon & S. Chisholm, (2001) From base pairs to niche differentiation: ecological insights from two complete genomes of *Prochlorococcus*. In: ASLO Aquatic Sciences Meeting 2001. J. Ackerman & S. Twombly (eds). Alburquerque, New Mexico, pp. 36.

Rocap, G., L. Moore & S. Chisholm, (1999) Molecular phylogeny of *Prochlorococcus* ecotypes. *Bulletin de l'Institut Oceanographique (Monaco)* **Numéro special 19**.

Rowell, P., M. Sampaio, J. Ladha & W. Stewart, (1979) Alteration of cyanobacterial glutamine synthetase activity *in vivo* in response to light and NH_4^+. *Arch. Microbiol.* **120**: 195-200.

Rubio, L.M., E. Flores & A. Herrero, (2002) Purification, cofactor analysis, and site-directed mutagenesis of *Synechococcus* ferredoxin-nitrate reductase. *Photosynthesis Res.* **72**: 13-26.

Ryther, J. & W. Dunstan, (1971) Nitrogen, phosphorus, and eutrophication in the coastal marine environment. *Science* **171**: 1008-1013.

Saito, M., M. McIlvin, D. Moran, T. Goepfert, G. DiTullio, A. Post & C. Lamborg, (2014) Multiple nutrient stresses at interesecting Pacific ocean biomes detected by protein biomarkers. *Science* **345**: 1173.

Sakamoto, T., K. Inouesakamoto & D. Bryant, (1999) A novel nitrate/nitrite permease in the marine cyanobacterium *Synechococcus* sp strain PCC-7002. *J. Bacteriol.* **181**: 7363-7372.

Sallala, A. & N. Nimera, (1990) The presence of glutamate dehydrogenase in *Chlorogloepsis fritschii*. *FEMS Microbiol. Lett.* **67**: 215-220.

Sampaio, M., P. Rowell & W. Stewart, (1979) Purification and some properties of glutamine synthetase from the nitrogen-fixing cyanobacteria *Anabaena cylindrica* and a *Nostoc* sp. *Journal of General Microbiology* **111**: 181-191.

Sauer, J., U. Schreiber, R. Schmid, U. Völker & K. Forchhammer, (2001) Nitrogen starvation-induced chlorosis in *Synechococcus* PCC 7942. Low-level photosynthesis as a mechanism of long-termal survival. *Plant Physiol.* **126**: 233-243.

Scanlan, D., (2001) Cyanobacteria: ecology, niche adaptation and genomics. *Microbiol. Today* **28**: 128-130.

Scanlan, D., (2003) Physiological diversity and niche adaptation in marine *Synechococcus*. *Adv. Microb. Physiol.* **47**: 1-64.

Scanlan, D., M. Ostrowski, S. Mazard, A. Dufresne, L. Garczarek, W. Hess, A. Post, M. Hagemann, I. Paulsen & F. Partensky, (2009) Ecological Genomics of Marine Picocyanobacteria. *Microbiol. Mol. Biol. Rev.* **73**: 249-299.

Scanlan, D. & N. West, (2002) Molecular ecology of the marine cyanobacterial genera *Prochlorococcus* and *Synechococcus*. *FEMS Microbiol. Ecol.* **40**: 1-12.

Schwarz, R. & K. Forchhammer, (2005) Acclimation of unicellular cyanobacteria to macronutrient deficiency: emergence of a complex network of cellular responses. *Microbiology (Reading)* **151**: 2503-2514.

Senior, P., (1975) Regulation of nitrogen metabolism in *Escherichia coli* and *Klebsiella aerogenes*: Studies with the continuous-culture technique. *J. Bacteriol.* **123**: 407-418.

Shapiro, L. & E. Haugen, (1988) Seasonal distribution and temperature tolerance of *Synechococcus* in Boothbay Harbor, Maine. *Estuar. Coast. Shelf Sci.* **26**: 517-525.

Sharp, J., (1983) The distribuions of inorganic nitrogen and dissolved and particulate organic nitrogen in the sea. In: Nitrogen in the marine environment. E. Carpenter & D. Capone (eds). New York: Academic Press, pp. 1-35.

Shukla, A., A. Biswas, N. Blot, F. Partensky, J.A. Karty, L.A. Hammad, L. Garczarek, A. Gutu, W.M. Schluchter & D.M. Kehoe, (2012) Phycoerythrin-specific bilin lyase-isomerase controls blue-green chromatic acclimation in marine Synechococcus. *Proceedings of the National Academy of Sciences of the United States of America* **109**: 20136-20141.

Sieracki, M., E. Haugen & T. Cucci, (1995) Overestimation of heterotrophic bacteria in the Sargasso sea - Direct evidence by flow and imaging cytometry. *Deep-Sea Research Part I Oceanographic Research Papers* **42**: 1399+.

Six, C., J. Thomas, L. Garczarek, M. Ostrowski, A. Dufresne, N. Blot, D. Scanlan & F. Partensky, (2007) Diverstiy and evolution of phycobilisomes in marine *Synechococcus* spp.: a comparative genomics study. *Genome Biol* **8**: 1-22.

Smith, A.J., J. London & R.Y. Stanier, (1967) Biochemical basis of obligate autotrophy in blue-green algae and thiobacilli. *J. Bacteriol.* **94**: 972-983.

Sohm, J.A., E.A. Webb & D.G. Capone, (2011) Emerging patterns of marine nitrogen fixation. *Nature Reviews Microbiology* **9**: 499-508.

Stanier, R., (1977) The position of cyanobacteria in the world of phototrophs. *Carlsberg Research Communications* **42**: 77-98.

Stanier, R. & G. Cohen-Bazire, (1977) Phototrophic prokaryotes: The cyanobacteria. *Annu. Rev. Microbiol.* **31**: 225-274.

Steglich, C., N. Frankenberg-Dinkel, S. Penno & W. Hess, (2005) A green light-absorbing phycoerythrin is present in the high-light-adapted marine cyanobacterium *Prochlorococcus* sp. MED4. *Environ. Microbiol.* **7**: 1611-1618.

Steglich, C., C. Mullineaux, K. Teuchner, W. Hess & H. Lokstein, (2003) Phosophysical properties of *Prochlorococcus marinus* SS120 divinyl chlorophylls and phycoerythrin *in vitro* and *in vivo*. *FEBS Lett.* **553**: 79-84.

Stewart, R., (2008) Introduction to physical oceanography.

Su, Z., V. Olman, F. Mao & Y. Xu, (2005) Comparative genomics analysis of NtcA regulons in cyanobacteria: regulation of nitrogen assimilation and its coupling to photosynthesis. *Nucleic Acids Res.* **33**: 5156-5171.

Sun, L., G.P. Zhu & N. Dovichi, (2013) Comparison of the LTQ-Orbitrap Velos and the Q-Exactive for proteomic analysis of 1-1000 ng RAW 264.7 cell lysate digests. *Rapid Commun. Mass Spectrom.* **27**: 157-162.

Syrett, P. & J. Leftley, (1976) Nitrate aand urea assimilation by algae. In: Perspectives in experimental biology. N. Sunderland (ed). Oxford and New York, pp.

Tanigawa, R., M. Shirokane, S. Maeda Si, T. Omata, K. Tanaka & H. Takahashi, (2002) Transcriptional activation of NtcA-dependent promoters of *Synechococcus sp.* PCC 7942 by 2-oxoglutarate *in vitro*. *Proc. Natl. Acad. Sci. USA* **99**: 4251-4255.

Tarran, G., M. Zubkov, M. Sleigh, P. Burkill & M. Yallop, (2001) Microbial community structure and standing stocks in the NE Atlantic in June and July of 1996. *Deep-Sea Research II* **48**: 963-985.

Taylor, A. & G. Stewart, (1980) The effect of ammonia and light-dark transitions on the level of glutamine synthetase activity in *Osmunda regalis*. *Plant Science Letters* **20**: 125-131.

Temple, S., C. Vance & J. Gantt, (1998) Glutamate synthase and nitrogen assimilation *Trends Plant Sci.* **3**: 51-56.

Ting, C., C. Hsieh, S. Sundararaman, C. Mannella & M. Marko, (2007) Cryo-electron tomography reveals the comparative three-dimensional architecture of *Prochlorococcus*, a globally important marine cyanobacterium. *J. Bacteriol.* **189**: 4485-4493.

Ting, C., G. Rocap, J. King & S. Chisholm, (2002) Cyanobacterial photosynthesis in the oceans: the origins and significance of divergent light-harvesting strategies. *Trends Microbiol.* **10**: 134-142.

Tischner, R. & A. Hüttermann, (1980) Regulation of glutamine synthetase by light and during nitrogen deficiency in synchronous *Chlorella sorokiniana*. *Plant Physiology (Rockville)* **66**: 805-808.

Tolonen, A., J. Aach, D. Lindell, Z. Johnson, T. Rector, R. Steen, G. Church & S. Chisholm, (2006a) Global gene expression of *Prochlorococcus* ecotypes in response to changes in nitrogen availability. *Mol. Syst. Biol.* **2**: 53.

Tolonen, A., G.B. Liszt & W. Hess, (2006b) Genetic Manipulation of *Prochlorococcus* Strain MIT9313: Green Fluorescent Protein Expression from an RSF1010 Plasmid and Tn5 Transposition. *Appl. Environ. Microbiol.* **72**: 7607-7613.

Trebst, A., (1980) Inhibitors in the electron flow. *Methods Enzymol.* **69**: 675-715.

Urbach, E. & S. Chisholm, (1998) Genetic diversity in *Prochlorococcus* populations flow cytometrically sorted from the Sargasso Sea and Gulf Stream. *Limnol. Oceanogr.* **43**: 1615-1630.

Urbach, E., D. Scanlan, D. Distel, J. Waterbury & S. Chisholm, (1998) Rapid diversification of marine picophytoplankton with dissimilar light- harvesting structures inferred from sequences of *Prochlorococcus* and *Synechococcus* (Cyanobacteria). *J. Mol. Evol.* **46**: 188-201.

Vanderstaay, G., S. Moonvanderstaay, L. Garczarek & F. Partensky, (1998) Characterization of the photosystem I subunits Psai and Psal from 2 strains of the marine oxyphototrophic prokaryote *Prochlorococcus*. *Photosynthesis Res.* **57**: 183-191.

Vázquez-Bermúdez, M., E. Flores & A. Herrero, (2002a) Analysis of binding sites for the nitrogen-control transcription factor NtcA in the promoters of *Synechococcus* nitrogen-regulated genes. *Biochimica et Biophysica Acta* **1578**: 95-98.

Vázquez-Bermúdez, M., J. Paz-Yepes, A. Herrero & E. Flores, (2002b) The NtcA-activated *amt1* gene encodes a permease required for uptake of low concentrations of ammonium in the cyanobacterium *Synechococcus* sp. PCC 7942. *Microbiology (Reading)* **148**: 643-647.

Vazquez-Bermudez, M.F., A. Herrero & E. Flores, (2002) 2-oxoglutarate increases the binding affinity of the NtcA (nitrogen control) transcription factor for the *Synechococcus glnA* promoter. *FEBS Lett.* **512**: 71-74.

Waldbauer, J.R., S. Rodrigue, M.L. Coleman & S.W. Chisholm, (2012) Transcriptome and proteome dynamics of a light-dark synchronized bacterial cell cycle. *PloS one* **7**: e43432.

Waterbury, J. & R. Rippka, (1989) Subsection I. Order Chroococcales Wettstein 1924, emend. Rippka *et al*., 1979. In: Bergey's Manual of Systematic Bacteriology. J. Staley, M. Bryant, N. Pfenning & J. Holt (eds). Baltimore: Williams & Wilkins, pp. 1728-1746.

Waterbury, J., S. Watson, R. Guillard & L. Brand, (1979) Widespread occurrence of a unicellular, marine planktonic, cyanobacterium. *Nature* **277**: 293-294.

Waterbury, J., S. Watson, F. Valois & D. Franks, (1986) Biological and ecological characterization of the marine unicellular cyanobacterium *Synechococcus*. In: Photosynthetic picoplankton. T. Platt & W. Li (eds). Canadian Journal of Fisheries and Aquatic Sciences, pp. 71-120.

Watson, G. & F. Tabita, (1996) Regulation, unique gene organization, and unusual primary structure of carbon fixation genes from a marine phycoerythrin-containing cyanobacterium. *Plant Mol. Biol.* **32**: 1103-1115.

Webb, E., I. Ehrenreich, S. Brown, F. Valois & J. Waterbury, (2009) Phenotypic and genotypic characterization of multiple strains of the diazotrophic cyanobacterium, *Crocosphaera watsonii*, isolated from the open ocean. *Environ. Microbiol.* **11**: 338-348.

Wegener, K., A. Singh, J. Jacobs, T. Elvitigala, E. Welsh, N. Keren, M. Gritsenko, B. Ghoshi, D. Campll, R. Smith & H. Pakrasi, (2010) Global proteomics reveal an atypical strategy for Carbon/Nitrogen assimilation by cyanobacterium under diverse environmental perturbations. *Molecular & Cellular Proteomics*: 2678-2689.

Wei, T., T. Ramasubramanian, F. Pu & J. Golden, (1993) *Anabaena* sp. strain PCC 7120 *bifA* gene encoding a sequence-specific DNA- binding protein cloned by *in vivo* transcriptional interference selection. *J. Bacteriol.* **175**: 4025-4035.

West, N. & D. Scanlan, (1999) Niche partioning of *Prochlorococcus* populations in a stratified water column in the Eastern North Atlantic ocean. *Appl. Environ. Microbiol.* **65**: 2585-2591.

Wood, A., J. Aurikko & D. Kelly, (2004) A challenge for 21st centry molecular biology and biochemistry: what are the causes of obligate autotrophy and methanotrophy? *FEMS Microbiol. Rev.* **28**: 335.

Wood, N. & R. Haselkorn, (1980) Control of phycobiliprotein proteolysis and heterocyst differentiation in Anabaena. *J. Bacteriol.* **141**: 1375-1385.

Wyman, M., (1992) An in vivo method for the estimation of phycoerythrin concentrations in marine cyanobacteria. *Limnol. Oceanogr.* **37**: 1300-1306.

Wyman, M. & C. Bird, (2007) Lack of control of nitrite assimilation by ammonium in an oceanic picocyanobacterium, *Synechococcus sp.* strain WH 8103. *Appl. Environ. Microbiol.* **73**: 3028-3033.

Xiong, W., D. Brune & W. Vermaas, (2014) The g-aminobutyric acid shunt contributes to closing the tricarboxylic acid cycle in Synechocystis sp. PCC 6803. In: 9th European Workshop on the Molecular Biology of Cyanobacteria. Texel, The Netherlands, pp. 59.

Xu, Y., P. Carr, P. Clancy, M. Garcia-Dominguez, K. Forchhammer, F. Florencio, S. Vasudevan, N. Tandeau De Marsac & D. Ollis, (2003) The structures of the PII proteins from the cyanobacteria *Synechococcus sp.* PCC 7942 and *Synechocystis sp*. PCC 6803. *Acta Crystallographica Section D Biological Crystallography* **59**: 2183-2190.

Yen Ow, S. & P. Wright, (2009) Current trends in high throughput proteomics in cyanobacteria. *FEBS Lett.* **583**: 1744-1752.

Zehr, J., D. Capone & P. Falkowski, (1989) Rapid incorporation of $^{13}NO_3$ by NH_4-limited phytoplankton. *Mar. Ecol. Prog. Ser.* **51**: 237-241.

Zehr, J. & B. Ward, (2002) Nitrogen cycling in the ocean: new perspectives on processes and paradigms. *Appl. Environ. Microbiol.* **68**: 1015-1024.

Zehr, J., J. Waterbury, P. Turner, P. Montoya, E. Omoregle, G. Steward, A. Hansen & D. Karl, (2001) Unicellular cyanobacteria fix N_2 in the subtropical North Pacific Ocean. *Nature* **412**: 635-638.

Zehr, J.P. & R.M. Kudela, (2011) Nitrogen cycle of the open ocean: from genes to ecosystems. *Ann Rev Mar Sci* **3**: 197-225.

Zhang, S. & D.A. Bryant, (2011) The tricarboxylic acid cycle in cyanobacteria. *Science* **334**: 1551-1553.

Zubkov, M. & G. Tarran, (2005) Amino acid uptake of *Prochlorococcus* spp. in surface waters across the South Atlantic Subtropical Front. *Aquat. Microb. Ecol.* **40**: 241-249.

Zubkov, M.V., I. Mary, E. Woodward, P.E. Warwick, B.M. Fuchs, D.J. Scanlan & P.H. Burkill, (2007) Microbial control of phosphate in the nutriet-depleted North Atlantic subtropical gyre. *Environ. Microbiol.* **9**: 2079-2089.

SUPPLEMENTARY DATA

Supplementary Table S1: Proteins up-regulated in presence of azaserine listed by functional pathways (*Progenesis*). *Pvalue* < 0.05. Peptides used for quantification > 2**.**

Accession Number	Protein	Max Fold Change	Pvalue	Peptides used for quantification	Progenesis postprocessor (fmol/µl)	
Oxidative phosphorylation					**Control**	**Azaserine**
Q7VE32	NAD(P)H-quinone oxidorreductase chain 6	4.5	0.0162	4	1.71 ± 0.53	4.57 ± 1.8
Q7VE42	NAD(P)H-quinone oxidorreductase chain 5	2.33	0.0479	3	0.87 ± 0.28	1.7 ± 1.22
Pyruvate metabolism					**Control**	**Azaserine**
Q7VDY1	Lactoyglutathione lyase family enzyme	1.8	0.0019	4	6.83 ± 1.37	8.65 ± 3.28
Q7VCH4	Pyruvate dehydrogenase E1 component	1.3	0.0084	11		
Ubiquinone and other terpenoid-quinone biosynthesis					**Control**	**Azaserine**
Q7VDL8	1,4-dihydroxy-2-naphthoyl CoA hydrolase	1.9	0.0034	2	0.57 ± 0.249	0.84 ± 0.175
Photosynthesis					**Control**	**Azaserine**
Q7VBH1	Ferredoxin-NADP oxidorreductase, petH	1.7	0.019	31	134.2 ± 13.4	202 ± 72.63
Q7VBJ5	Photosystem II Protein P, psbB	2.6	0.042	4	7.12 ± 1.96	22.9 ± 2.57
Q7VCR3	Possible NADH-Ubiquinone/plastoquinone oxidorreductase	2.64	0.01	7	4.8 ± 1.087	9.9 ± 4.358
Lipopolysaccharide biosynthesis					**Control**	**Azaserine**
Q7VAP2	Lipid-A-disaccharide synthase	1.5	0.041	4	3.86 ± 1.64	4.44 ± 1.25

Accession Number	Protein	Max Fold Change	Pvalue	Peptides used for quantification	Progenesis postprocessor (fmol/µl)	
Porphyrin and chlorophyll metabolism					**Control**	**Azaserine**
Q7VDP9	Protoporphyrin IX-Mg-Chelatase subunit	1.237	0.045	8		
Glycerolip metabolism					**Control**	**Azaserine**
QYVBK4	1-acyl-sn-3-glycerol 3-phosphate acyltransferase	1.32	0.033	4	5.31 ± 2.58	5.51 ± 0.99
Fructose and mannose metabolism					**Control**	**Azaserine**
Q7VEE9	NAD-dependent epimerase/dehydratase	1.385	0.021	6	1.45 ± 0.42	2.23 ± 0.748
Folate biosynthesis					**Control**	**Azaserine**
Q7VE06	Anthranilate/para-aminobenzoate synthase	2.63	0.00064	4	9.04 ± 5.58	11.77 ± 3.84
RNA degradation/ DNA repair					**Control**	**Azaserine**
Q7VBJ8	Superfamily II DNA/RNA helicase (DeaD)	1.81	0.00268	5	2.53 ± 1.3	3.28 ± 1.52
Q7VDQ9	Predicted DNA repair enzyme contains HhH domain and nuclease of RecB family	1.98	0.0477	3	3.68 ± 0.66	5.25 ± 1.38
Purine metabolism					**Control**	**Azaserine**
Q7VDQ1	NUDIX/MutT family pyrophosphohydrolase	1.89	0.0018	7	13.26 ± 2.57	18.79 ± 1.55
ABC transporters/ Transporters					**Control**	**Azaserine**
Q7VDD4	ABC type multidrug transport system ATPase	1.556	0.0018	3	132.4 ± 45	157.5 ± 43.8
Q7V9N7	Mg/Co/Ni transporter MgtE	1.39	0.0072	10		
Q7VEA8	ATPase component of ABC transporters	2.5	0.0112	5	30.2 ± 7.6	70.85 ± 32.94
Q7VCK3	Porin homolog	1.42	0.0465	4	667.26 ± 41.21	738.29 ± 128
Q7VEB6	Di/Tricarboxylate	1.5	0.05	4	13 ± 6	14.22 ± 4.55
Q7VD21	ABC type multidrug transport system ATPase	2.93	0.00189	8	24.28 ± 10	62.67 ± 30.23

Accession Number	Protein	Max Fold Change	Pvalue	Peptides used for quantification	Progenesis postprocessor (fmol/ µL)	
Amino acid biosynthesis					**Control**	**Azaserine**
Q7VC45	Carbamoyl-phosphate synthase large chain	3.77	$5.05 \cdot 10^{-5}$	6	9.67 ± 1.41	14 ± 3.04
Q7VE04	Histidinol-phosphate	2.07	0.011	4		
Thiamine metabolism					**Control**	**Azaserine**
Q7VEG2	Glycine/D-aminoacid oxidase family enzyme	2.127	0.047	5	7.03 ± 4.97	10.79 ± 1.4

Supplementary Table S2: Proteins down-regulated in presence of azaserine listed by functional pathways (*Progenesis*). *Pvalue* < 0.05. Peptides used for quantification >2.

Accession Number	Protein	Max Fold Change	Pvalue	Peptides used for quantification	Progenesis postprocessor (fmol/µL)	
Phenylalanine, tyrosine and tryptophan biosynthesis					**Control**	**Azaserine**
Q7VBP4	3´- phosphoshikimate 1-carboxyvinyltransferase	1.6	0.00368	17	65.86 ± 13.8	34.82 ± 16.6
Q7VD45	N-(5´-phosphorybosil)anthranilate isomerase	1.54	0.01	5	5.15 ± 2.39	4.02 ± 0.55
Q7V9U2	Anthranilate/para-aminobenzoate synthase	1.89	0.016	13	14.36 ± 2.51	5.91 ± 3.32
Q7VA09	Prephenate dehydratase	1.7	0.00091	4	4.74 ± 2.52	3.8 ± 0.75
Q7VB04	Chorismate mutase	2.2	0.015	4	18.8 ± 4.91	7.94 ± 1.2
Alanine, aspartate and glutamate metabolism					**Control**	**Azaserine**
Q7VA67	Alanine dehydrogenase	2.17	0.0056	8	6.8 ± 2.67	2.92 ± 0.46
Purine metabolism					**Control**	**Azaserine**
Q7VA48	Adenylosuccinate lyase	1.74	0.00813	16	27.6 ± 6.87	15.58 ± 5.1
Q7VD34	Xanthosine triphosphate pyrophosphatase	1.61	0.015	6	8.93 ± 4.2	4.11 ± 1.9
Q7VBF7	IMP dehydrogenase/GMP reductase	1.5	0.042	16	78 ± 7.3	32.89 ± 14.3
Q7VDW2	Sulfate adenylyltransferase	1.93	0.0064	17	45.5 ± 22.03	21.9 ± 4.51
Q7VC89	Phosphoribosylformylglycinamidine synthase (FGAM)	2.05	0.021	2	7.13 ± 1.9	2.32 ± 0.74
Valine, leucine and isoleucine biosynthesis					**Control**	**Azaserine**
Q7VD57	Acetolactate synthase	2.33	0.0109	19	42 ± 12.34	8.74 ± 5.7
Q7VBY4	Branched-chan aminoacid aminotransferase	3.3	0.00012	14	43.1 ± 6.83	10.5 ± 1.42

Accession Number	Protein	Max Fold Change	Pvalue	Peptides used for quantification	Progenesis postprocessor (fmol/µL)	
Cysteine and methionine metabolism					**Control**	**Azaserine**
Q7VDH3	Cysteine synthase	1.82	0.023	25	210.9 ± 31.9	102.38 ± 11.18
Q7VE70	Cysteine synthase	3.44	0.001	22	90 ± 7.2	16.14 ± 7.14
Q7VBY3	5-Methyltetrahydrofolate homocysteine	2	0.047	17	4.97 ± 1.2	2.64 ± 2.18
Q7VDH1	Cystathione beta-lyase	1.61	0.0269	17	17 ± 3.71	6.9 ± 0.42
Pyrimidine metabolism					**Control**	**Azaserine**
Q7VD69	Dihydroorotase	1.94	0.0061	14	43.4 ± 5.09	15.68 ± 1.18
Q7VB53	Thioredoxin reductase	1.66	0.04	14	95.2 ± 23.8	44.65 ± 9.174
Q7VDX6	Thioredoxin reductase	2.25	0.00036	5	36.16 ± 9	18.75 ± 2.03
Starch and sucrose metabolism					**Control**	**Azaserine**
Q7VCA0	Glucose-1-phosphate adenyltransferase	1.542	0.0198	23	87.9 ± 17	50.65 ± 1.5
Q7V9R8	Phosphorylase	1.75	0.01	17	23.75 ± 1.7	9.4 ± 1.63
Q7V9K6	Glycosyltransferase	2.55	0.02	10	13.4 ± 5.3	4.57 ± 3.5
Nicotinate and nicotinamide metabolism					**Control**	**Azaserine**
Q7VA68	NAD synthase	2.874	0.04	3	1.75 ± 0.9	0.97 ± 0.53

Accession Number	Protein	Max Fold Change	Pvalue	Peptides used for quantification	Progenesis postprocessor (fmol/µL)	
Pentose phosphate pathway					**Control**	**Azaserine**
Q7VBH0	Glucose-6-phosphate-1-dehydrogenase	1.94	0.038	16	10.1 ± 1.8	3.62 ± 2.8
Q7VD78	Sugar kinase	3.57	0.025	5	5.73 ± 1.2	3.72 ± 1.4
Q7V9Q9	Transketolase	1.75	0.0053	29	128.5 ± 47.8	50.6 ± 12.4
Q7VB20	Transketolase	1.257	0.048	6	9.44 ± 1.62	6.93 ± 0.75
Q7VB19	1-deoxy-xylulose 5-phosphate synthase	1.7	0.0166	10	16.8 ± 2.15	6.6 ± 0.3
Glutathione metabolism					**Control**	**Azaserine**
Q7VB77	Glutathione peroxidase	1.915	0.0072	11	96.6 ± 4.1	29.3 ± 10.7
Q7VE83	Glutathione S-transferase zeta class	1.725	0.03	11	40.7 ± 8.35	17.3 ± 8.8
Glycolysis/Gluconeogenesis					**Control**	**Azaserine**
Q7VBQ1	Acetyl-coenzyme A synthetase	1.68	0.0069	17	33.97 ± 4.93	11.48 ± 2.62
Q7VDH5	Dihydrolipoamide S-acetyltransferase	1.83	0.0036	26	115.5 ± 21.7	60.3 ± 5.54
Lysine biosynthesis					**Control**	**Azaserine**
Q7VBI7	Diaminopimelate decarboxylase	1.4	0.0185	14	14.3 ± 4.3	8.24 ± 1.98
Fructose and mannose metabolism					**Control**	**Azaserine**
Q7VEF0	GDP-D-mannose dehydratase	3.78	0.0421	5	4.8 ± 1.66	1.06 ± 0.878

Accession Number	Protein	Max Fold Change	Pvalue	Peptides used for quantification	Progenesis postprocessor (fmol/µL)	
Fatty acid biosynthesis					**Control**	**Azaserine**
Q7VE54	Malonyl CoA-acyl carrier protein	1.74	0.011	11	70.78 ± 1.98	27.35 ± 7
Q7VEI6	Biotin carboxyl carrier protein	2.4	0.011	6	151.5 ± 44.87	46.67 ± 3.6
Q7VDC8	Short-chain dehydrogenase/reductase family	1.69	0.009	7	16.37 ± 7.8	9.75 ± 2.61
Q7VD68	Phospholycerate mutase	1.69	0.0315	9	10.49 ± 1.3	5.02 ± 1.3
Folate biosynthesis					**Control**	**Azaserine**
Q7VC40	Dihydropteroate synthase and related enzyme	2.594	0.0435	2	1.49 ± 0.31	0.64 ± 0.23
Q7VDQ0	7,8-dihydro-6-hydroxymethylpterin-pyrophosphokinase	1.995	0.00063	7	22.85 ± 1.65	20.33 ± 9.37
Q7VE86	6-pyruvoyl-tetrahydropterin synthase	1.83	0.00577	11	69.32 ± 9.2	27.11 ± 3.35
Q7VE38	Methylenentetrahydrofolate reductase	1.6	0.0209	4	2.48 ± 0.19	1.027 ± 0.87
Oxidative phosphorylation					**Control**	**Azaserine**
Q7VEB7	NADH dehydrogenase	4.36	0.0163	7	12.25 ± 8.3	2.5 ± 0.84
Q7VD73	Inorganic pyrophosphatase	1.8	0.0416	8	29.95 ± 5	13.4 ± 2.19
Photosynthesis					**Control**	**Azaserine**
G3XCS9	Phycoerithrin clas III alpha chain CpeA	1.51	0.044	12	277.7 ± 39.47	147.59 ±10
Glyoxylate and dicarboxylate metabolism					**Control**	**Azaserine**
Q7VAS7	FAD/FMN-containing dehydrogenase	1.684	0.0024	9	10.41 ± 3.95	3.57 ± 2.37

Accession Number	Protein	Max Fold Change	Pvalue	Peptides used for quantification	Progenesis postprocessor (fmol/µL)	
Aminoacyl-tRNA biosynthesis					**Control**	**Azaserine**
Q7VCB0	Glycine tRNA ligase beta subunit	1.7	0.02	12	21.81 ± 1.12	10.65 ± 1.25
Porphyrin and chlorophyll metabolism					**Control**	**Azaserine**
Q7VE79	Uroporphyrin III synthase	1.98	0.0018	10	7.4 ± 4.2	4.42 ± 0.88
Sulfur metabolism					**Control**	**Azaserine**
Q7VEB8	3-phosphoadenosine 5´- phosphosulfate	1.63	0.036	10	13 ± 2.25	7.27 ± 2.93
Galactose metabolism					**Control**	**Azaserine**
Q7VAY9	UDP-glucose-4-epimerase	1.68	0.0399	12	16.6 ± 1	6.81 ± 2.22
Q7VB14	UDP-galactopyranose mutase	1.55	0.044	26	197.95 ± 63	85.17 ± 12.7
Streptomycin biosynthesis					**Control**	**Azasserine**
Q7VE98	Inositol monophosphatase family protein	3.195	0.0257	10	12.01 ± 0.19	0.094 ± 0.05
Biotin metabolism					**Control**	**Azaserine**
Q7VA42	ATP-dependent dethiobiotin synthetase	2.15	0.0385	4	3.49 ± 1.37	1.43 ± 0.43
Q7VA41	Adenosylmethionine-8-amino-7-oxononanoate aminotransferase	1.62	0.0395	4	11.85 ± 1.84	5.48 ± 0.58
RNA degradation					**Control**	**Azaserine**
Q7VA12	Ribonucleases G/E	1.593	0.0094	16	13.97 ± 3.2	8.4 ± 0.7
QYV9L8	Metallo-beta-lactamase superfamily	1.62	0.0032	25	31.69 ± 9.64	22.74 ± 8.78

Accession Number	Protein	Max Fold Change	Pvalue	Peptides used for quantification	Progenesis postprocessor (fmol/µL)	
Terpenoid backbone biosynthesis					**Control**	**Azaserine**
Q7TV99	tRNA-(Guanine-N1)-methyltransferase fused to 2-C-methyl-D-erythritol 2,4-cyclodiphosphate synthase	1.34	0.0301	12	3.49 ± 1.37	1.43 ± 0.43
DNA replication					**Control**	**Azaserine**
Q7V9J8	Replicative DNA helicase	1.64	0.036	8	25.69 ± 6.66	16.99 ± 4.24
Q7VEL1	DNA Polymerase III subunit beta	2.958	0.0035	13	50.98 ± 18.87	12.17 ± 1.89
Q7VCW1	DNA Helicase	1.779	0.00815	12	4.78 ± 0.89	2.42 ± 0.53
Protein metabolism					**Control**	**Azaserine**
Q7VC00	Peptidyl-prolyl-cis-trans isomerase	5.65	0.00084	10	38.7 ± 7.79	6.39 ± 5.41
Q7VEJ8	Peptide-methionine (R)-s-oxide reductase	1.88	0.0052	6	20.55 ± 6.44	7.74 ± 0.6
Q7VDL6	Putative translationl factor (SUA5)	2.2	0.008	7	12.37 ± 1.94	4.43 ± 0.13
Transcription					**Control**	**Azaserine**
Q7VE37	Transcriptional regulator, contains HTH motif	2.5	0.00619	4	17.83 ± 1.08	10.87 ± 0.41
Q7VD88	RNA polymerase sigma factor (SigA)	1.885	0.0068	12	41.94 ± 24.58	24.42 ± 4.84
Q7VA22	Transcription elongation factor NusA	2	0.0076	20	35.89 ± 8.14	12.55 ± 1.47
Q7VCX4	AbrB family transcriptional regultaor	1.84	0.0163	33	9.45 ± 2.05	3.76 ± 1.83
Q7VDY4	Transcription antitermination protein NusG	1.574	0.0279	8	32.29 ± 9.389	15.3 ± 3.39

Accession Number	Protein	Max Fold Change	Pvalue	Peptides used for quantification	Progenesis postprocessor (fmol/µL)	
Cell redox homeostasis					**Control**	**Azaserine**
Q7VE11	Glutaredoxin	2.29	0.0024	3	19.12 ± 6.31	4.15 ± 1.98
Q7VBK7	Glutaredoxin	2.473	0.0029	6	44.47 ± 4	17.77 ± 0.74
Two component system					**Control**	**Azaserine**
Q7VE57	Two component response regulator	2.448	0.0316	12	81.48 ± 24.94	22.2 ± 14.3
Q7V9P9	Two component response regulator	1.458	0.0087	16	66 ± 28.7	37.5 ± 9.6
Q7VE20	Two component response regulator	1.713	0.0141	18	110.37 ± 4.68	47.98 ± 3.72
DNA repair					**Control**	**Azaserine**
Q7VB64	DNA polymerase 3´-5´ exonuclease	1.47	0.00267	30	17.168 ± 0.66	6.17 ± 1.37
Q7V9F2	Uvr ABC system protein	1.83	0.0033	40	30.77 ± 5.77	15.2 ± 3.69
Q7VEA1	Exodeoxyribonuclease 7 small subunit	2.07	0.0066	7	4.38 ± 1.69	2 ± 0.5
Iron-sulfur cluster assembly					**Control**	**Azaserine**
Q7VEC7	ABC type transport system involved in Fe	2.645	0.0034	10	17.3 ± 4	8.98 ± 1.55
Q7VDF9	Thiorredoxin family protein	14.21	0.00124	5	9.77 ± 4.95	0.46 ± 0.27

Accession Number	Protein	Max Fold Change	Pvalue	Peptides used for quantification	Progenesis postprocessor (fmol/ µL)	
Transporters					**Control**	**Azaserine**
Q7VBN3	ABC-type Mn^{2+}/Zn^{2+} transport system ATPase	1.7475	0.0022	2		
Q7VAG1	Fe^{2+}/Zn^{2+} uptake regulation protein	1.3969	0.0125	5	83.47 ± 22.75	46.86 ± 9.41
Q7VEC8	ABC-type transport system involved in Fe-S	1.7	0.0314	8	5.56 ± 1.79	2.05 ± 1.33
Nitrogen metabolism regulator					**Control**	**Azaserine**
Q7VDI6	PII interaction protein X	1.584	0.0483	2	6.35 ± 1.1	3.16 ± 1.66
Sulfur relay system						
Q7VAV4	Sulfur transfer protein	2	0.0233	2		

Supplementary Table S3: Proteins from the extract of NtcA MIT9313 and possible candidates for protein-protein interaction. The samples were digested in solution and the data is from *Orbitrap Velos* (*Thermo Fisher*). These results are related with the figure 69 in chapter 1.

Accession	Description	Score Sample 1	Coverage Sample 1	MW [kDa]	calc. pI
A7ZSK9	50S ribosomal protein L3 OS=Escherichia coli O139:H28	840.67	74.16	22.23	9.91
P29283	Global nitrogen regulator OS=Syn. elongatus	1125.85	24.32	24.82	8.70
A7ZQ46;P0A7K6	50S ribosomal protein L19 OS=Escherichia coli O139:H28	386.47	61.74	13.13	10.62
P13645	Keratin, type I cytoskeletal 10 OS=Homo sapiens	357.80	30.82	58.79	5.21
C4ZUJ6;P02359	30S ribosomal protein S7 OS=Escherichia coli	491.60	63.13	20.01	10.36
P04264	Keratin, type II cytoskeletal 1 OS=Homo sapiens	375.19	21.43	66.00	8.12
A7ZSK6;P60422	50S ribosomal protein L2 OS=Escherichia coli O139:H28	399.79	61.17	29.84	10.93
P0A7T1;P0A7S9	30S ribosomal protein S13 OS=Escherichia coli O157:H7	310.54	67.80	13.09	10.78
P35908	Keratin, type II cytoskeletal 2 epidermal OS=Homo sapiens	290.88	19.87	65.39	8.00
A7ZSJ8;P60624	50S ribosomal protein L24 OS=Escherichia coli O139:H28	187.69	54.81	11.31	10.21
A7ZSK1	50S ribosomal protein L29 OS=Escherichia coli O139:H28	120.46	58.73	7.27	9.99
A7ZUJ7;P0A7L0	50S ribosomal protein L1 OS=Escherichia coli O139:H28	123.16	38.89	24.71	9.64
P35527	Keratin, type I cytoskeletal 9 OS=Homo sapiens	231.02	21.19	62.03	5.24
P21338	Ribonuclease I OS=Escherichia coli (strain K12)	109.04	42.16	29.60	8.57
A7ZUF1	50S ribosomal protein L31 OS=Escherichia coli O139:H28	167.28	41.43	7.87	9.32
A7ZSL0	30S ribosomal protein S10 OS=Escherichia coli O139:H28	188.78	51.46	11.73	9.69
A7ZSC5	50S ribosomal protein L13 OS=Escherichia coli O139:H28	76.32	47.89	16.01	9.91
A7ZSJ7;P62399	50S ribosomal protein L5 OS=Escherichia coli O139:H28	189.47	49.72	20.29	9.48
A7ZS62	30S ribosomal protein S15 OS=Escherichia coli O139:H28	104.53	68.54	10.26	10.40
P04259	Keratin, type II cytoskeletal 6B OS=Homo sapiens	192.55	17.20	60.03	8.00
P62593	Beta-lactamase TEM OS=Escherichia coli	63.15	20.63	31.50	6.04
O28132	Probable molybdenum cofactor biosynthesis protein	117.12	4.49	17.09	7.97
P0A9B1	Ferric uptake regulation protein OS=Escherichia coli O157:H7	79.67	18.92	16.78	6.11
A7ZSL7	30S ribosomal protein S12 OS=Escherichia coli O139:H28	77.85	51.61	13.73	10.87
A7ZS81	50S ribosomal protein L27 OS=Escherichia coli O139:H28	77.58	31.76	9.12	10.58
P0AGK6	RNA-binding protein YhbY OS=Escherichia coli O157:H7	73.11	37.11	10.78	9.38
A7ZHB2	30S ribosomal protein S20 OS=Escherichia coli O139:H28	55.91	22.99	9.68	11.18
A7ZSJ9	50S ribosomal protein L14 OS=Escherichia coli O139:H28	118.19	51.22	13.53	10.42
P02533	Keratin, type I cytoskeletal 14 OS=Homo sapiens	162.92	13.98	51.53	5.16
A7ZS83;P0AG48	50S ribosomal protein L21 OS=Escherichia coli O139:H28	73.59	52.43	11.56	9.85
A7ZSI3;P0AG44	50S ribosomal protein L17 OS=Escherichia coli O139:H28	33.21	7.87	14.36	11.05

Accession	Description	Score Sample 1	Coverage Sample 1	MW [kDa]	calc. pI
A7ZSJ4;P0AG55	50S ribosomal protein L6 OS=Escherichia coli O139:H28	99.77	27.68	18.89	9.70
Q14CN4	Keratin, type II cytoskeletal 72 OS=Homo sapiens	62.32	3.72	55.84	6.89
A7ZUJ6;P0A7J7	50S ribosomal protein L11 OS=Escherichia coli O139:H28	82.21	23.24	14.87	9.63
P02358	30S ribosomal protein S6 OS=Escherichia coli (strain K12)	75.03	48.89	15.69	5.00
P08779	Keratin, type I cytoskeletal 16 OS=Homo sapiens	121.39	12.68	51.24	5.05
A7ZUJ8;P0A7J3	50S ribosomal protein L10 OS=Escherichia coli O139:H28	92.63	31.52	17.70	8.98
A7ZQ60	SsrA-binding protein OS=Escherichia coli O139:H28	43.21	20.63	18.26	9.89
P37902	Glutamate/aspartate periplasmic-binding protein OS=Escherichia coli	87.84	5.30	33.40	8.53
A7ZUD3	Triosephosphate isomerase OS=Escherichia coli O139:H28	49.63	12.55	26.95	5.96
P0AC61	Glutaredoxin-2 OS=Escherichia coli O157:H7	43.36	5.58	24.33	7.96

Supplementary data for proteomics approach

METABOLISM UP-REGULATED

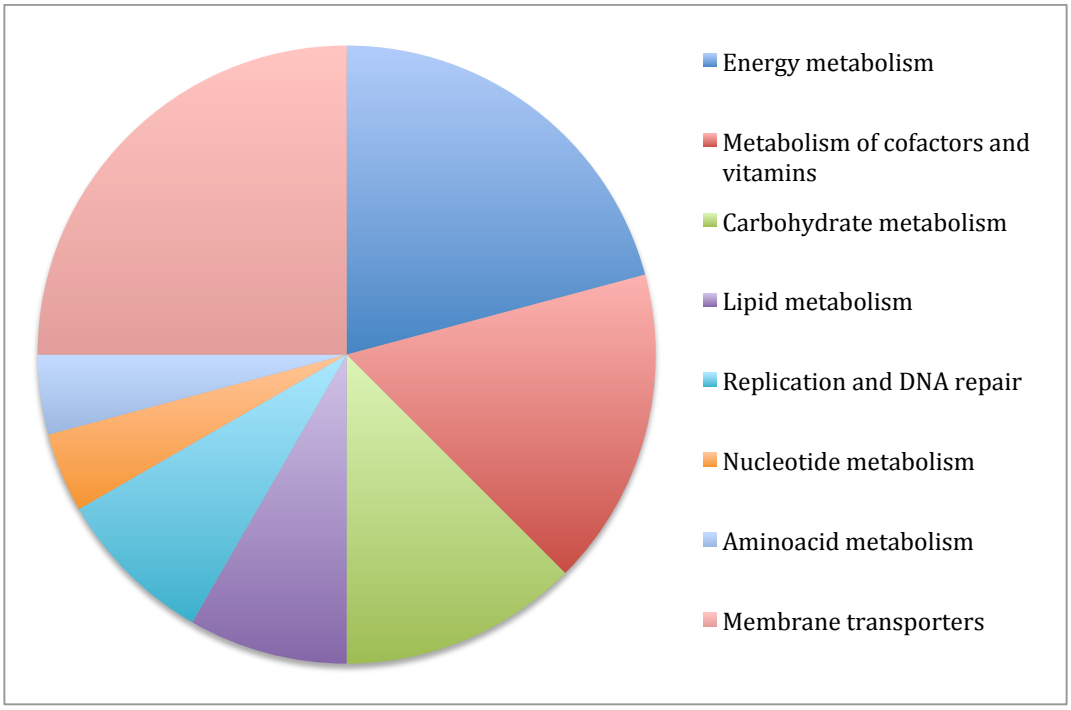

METABOLISM DOWN-REGULATED

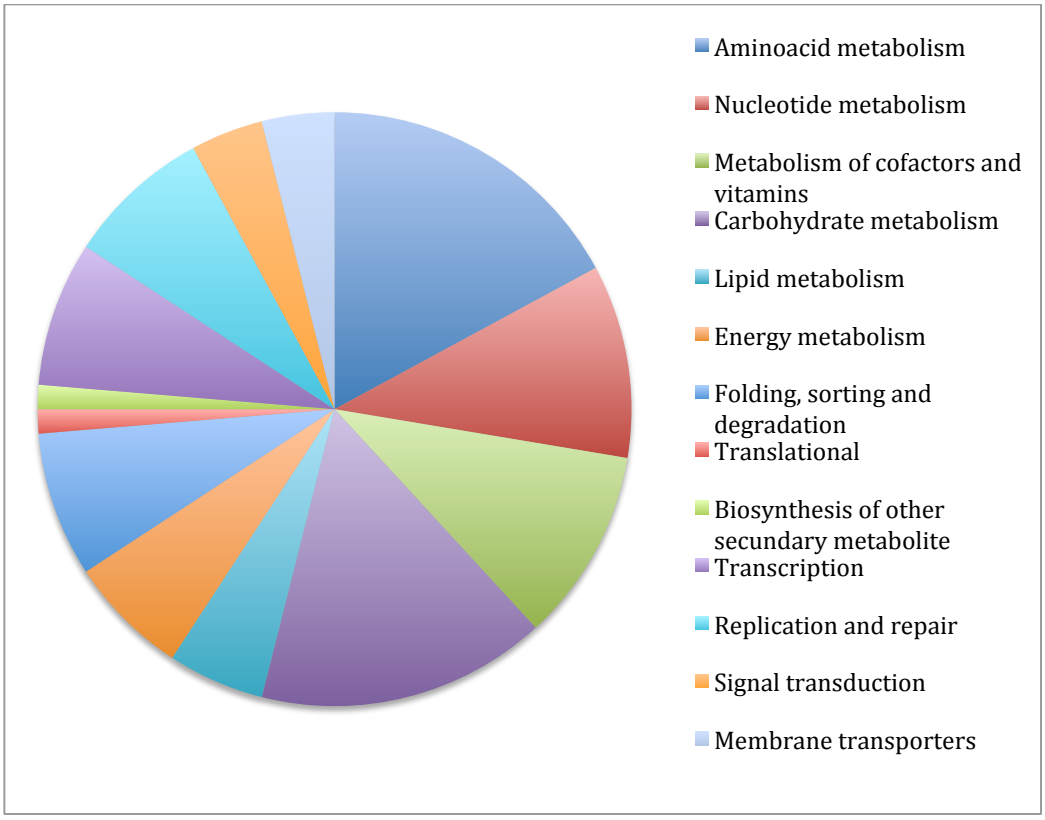

TÍTULO DE LA TESIS: Diversity of regulatory mechanisms in the C/N metabolism of the marine cyanobacteria *Prochlorococcus* and *Synechococcus*

DOCTORANDA: Mª Agustina Domínguez Martín

INFORME RAZONADO DE LOS DIRECTOR/ES DE LA TESIS

(se hará mención a la evolución y desarrollo de la tesis, así como a trabajos y publicaciones derivados de la misma).

El trabajo realizado por la doctoranda Mª Agustina Domínguez Martín para la obtención de su Tesis Doctoral se puede considerar excelente y de enorme complejidad. Su objetivo inicial se fue ampliando en base a los resultados obtenidos y se puede concretar en una importante aportación al conocimiento de la regulación de los metabolismo de carbono y nitrógeno en la cianobacteria marina *Prochlorococcus*, modelo ecológico de gran interés por ser el organismo fotosintetico más abundante de la tierra. Estos estudios se ampliaron además a su principal competidor en los oceanos, la cianobacteria *Synechococcus*, lo que ha permitido establecer comparaciones de gran interés que han abierto nuevas posibilidades de estudio. Durante su trabajo la doctorando ha utilizado una enorme variedad de técnicas de bioquímica y biología molecular, incluidas las de proteómica así como técnicas analíticas sofisticadas como la de *Surface Plasmon Resonance*. Durante estos años la doctoranda ha demostrado una enorme capacidad de trabajo, así como una gran ilusión y motivación que le han llevado a realizar un volumen de trabajo, de gran nivel, muy superior al necesario para desarrollar un Tesis doctoral de calidad. Su formación se ha completado con la lectura crítica de textos científicos, la escritura de los mismos, tanto en español como en inglés, así como su presentación (en ambos idiomas) mediante comunicaciones orales en diversos congresos. Debemos destacar por último, que a lo largo del trabajo ha realizado estancias en dos laboratorios de gran prestigio internacional: primero, en el equipo del Prof. A. Burkovski (Lehrstuhl für Mikrobiologie, Department Biologie, Friedrich-Alexander-Universität, Erlangen. Alemania) y luego en el equipo del Prof. R. J. Beynon (Centre for Proteome Research, Institute of Integrative Biology, University of Liverpool, Reino Unido).

La calidad del trabajo ha quedado demostrada mediante la publicación de parte de los resultados en revistas internacionales de alto prestigio, y están en preparación tres manuscritos adicionales:

McDonagh B, **Domínguez-Martín A**, Gómez-Baena G, López-Lozano A, Diez J, Bárcena JA & García-Fernández JM (2012) Nitrogen starvation induces extensive changes in the redox proteome of *Prochlorococcus* sp. strain SS120. *Environmental Microbiology Reports* 4(2): 257-267

Domínguez-Martín MA, López-Lozano A, Diez J, Gómez-Baena G, Rangel Zúñiga OA & García-Fernández JM (2014) Physiological regulation of isocitrate dehydrogenase and the role of 2-oxoglutarate in *Prochlorococcus* sp. strain PCC 9511. *PLoS ONE* 9 (7):e103380. DOI: 10.137/journal.pone.0103380

Gómez-Baena G, **Domínguez-Martín MA**, Donaldson R, García-Fernández JM & Diez J (2014) Nutrient starvation makes glutamine synthetase more sensitive to oxidative modification in *Prochlorococcus marinus* PCC 9511. Artículo invitado por la revista *Life*, para el número especial "*Cyanobacteria: Ecology, Physiology and Genetics*". En revisión.

Por todo ello, se autoriza la presentación de la tesis doctoral.

Córdoba, 11 de Noviembre de 2014

Firma de los directores

Fdo.:José Manuel García Fernández Fdo.: Jesús Diez Dapena